Chalcogenide semiconductor photocatalysis for the photocatalytic degradation of organic pollutants in water

By

Manishana Precious Sithole

Student Number: 62697153

Submitted in accordance with the requirements for the degree of

MAGISTER TECHNOLOGIAE

In

Chemical Engineering

At the

UNIVERSITY OF SOUTH AFRICA

Supervisor: Dr Alex T Kuvarega

Co-supervisor: Dr Lueta de Kock

: Dr Elvera Viljoen

Date submitted: 29 January 2020

DECLARATION

Name: Manishana Precious Sithole

Student number: 62697153

Degree: Magister Technologiae in Chemical Engineering

Chalcogenide semiconductor photocatalysis for the photodegradation of organic

I declare that the above dissertation/thesis is my own work and that all the sources that I have used or quoted have been indicated and acknowledged by means of complete references.

SIGNATURE

25 February 2020

DATE

Title of thesis: Chalcogenide semiconductor photocatalysis for the photocatalytic degradation of organic pollutants in water

Short description

This research work discusses the removal of organic pollutants specifically diclofenac and acid blue-25 using chalcogenide semiconductors. Semiconductors are materials that absorb light of specific energy and potentially degrade these organic pollutants into smaller compounds that are not toxic such as carbon dioxide and water.

KEY TERMS:

Photocatalysis, semiconductor, advanced oxidation process, photocatalytic degradation, pharmaceuticals, textile dyes, mineralization, organic pollutants, chalcogenide, ozonation, membrane, heterogeneous, homogenous.

DEDICATION

This is dedicated to my best friend and mother Esther Thabethe, for the love and amazing upbringing, prayers, support and, for being my pillar of strength and always being there to carry me when I fall. This would not have been possible if it was not for you Ngiyabonga.

To my dad who passed away in 2009, I wish you were still alive to see your nono grow up into this fine woman that you have moulded, to enjoy the fruits of your labour. May you Rest in Peace till we meet again. To my step dad, bab' Linus Dlamini for encouraging me to always better myself, for believing in me, supporting and loving me, you stepped in and played the role of a father, treated me like I am your own, I never lacked anything. Ngiyabonga may God bless you.

ACKNOWLEDGEMENTS

Firstly I would like to thank God for his undying love, strength and wisdom to complete this work.

To my supervisors, Dr Alex T Kuvarega, Dr Elvera Viljoen and Dr Lueta de Kock, thank you for the opportunity to do my masters under your excellent supervision, encouragement and support throughout the research years.

To my family, my mother Esther Thabethe, my brothers, Eddie Sithole, Obed Sithole, Mpho Sithole, and Bridget Sithole, My uncle Freddy Macaw and my Nephew Thato Masindi. I would like to take the opportunity to thank you for your love and support and prayers.

My heartfelt gratitude to the colleagues and members of the Photo/electrochemistry Group for the discussions we shared and assistance in improving my presentation skills.

To Kagiso for your excellent laboratory technician skills in assuring that my laboratory work goes smoothly and always being there whenever I needed anything.

To Dr Mkhize for allowing me to use your laboratory to conduct some of my experiments, your encouragement was highly appreciated.

My deepest appreciation to my best friend Lerato Monatisa for the love, support and encouragement.

Myra Nzaba and Potlako Mafa for always providing a helping hand towards my research through your busy schedule; I say thank you. The time you have given me was really appreciated.

To Tau Silvester Ntelane for giving a helping a hand with TGA and BET analysis, thank you for the time you have given me

And lastly to the Nanotechnology and Water Sustainability (NanoWS) Research Unit at the University of South Africa and National Research Foundation (NRF) for the financial support to conduct this research project.

PUBLICATIONS AND PRESENTATIONS:

Conference presentations

1. M. P. Sithole, L. de Kock, E. Viljoen and A. T. Kuvarega. **Chalcogenide based semiconductor photocatalysis for photodegradation of organic pollutants in water. Poster presentation** Catalysis society of South Africa 2019: from nanomaterials to industrial processes. Langebaan Club Mykonos (10-13 November 2019)

2. M. P. Sithole, L. de Kock, E. Viljoen and A. T. Kuvarega.g-C_3N_4/CdS photocatalysis for the photodegradation of AB-25 in water. The 8th University of South Africa (UNISA) research and innovation showcase. **Oral presentation**. UNISA sunny side campus (3-6 September 2019)

3. M. P. Sithole, L. de Kock, E. Viljoen and A. T. Kuvarega. **g-C_3N_4/CdS photocatalysis for the photodegradation of AB-25 in water. Poster presentation** US-Africa Forum Nanotechnology Convergence for sustainable Energy, Water and Environment UNISA Science Campus (11-15 August 2019).

Manuscripts under preparation for publication in peer journals

1. M. P. Sithole, L. de Kock, E. Viljoen and A. T. Kuvarega.g-C_3N_4/CdS photocatalysis for the photodegradation of AB-25 in water (submitted)

Awards

- Best Poster presentation at CATSA 2019 (Catalysis society of South a Afric2019) conference.
- Second runner up at the University of South Africa paper Innovation challenge (2019).
- Third place University of South Africa fame lab competition (2019).

ABSTRACT

Water is an essential and important resource to humans, and the environment. The quality and availability of clean water is compromised by the uncontrolled discharge of pollutants through anthropogenic activities associated with the quest for improved lifestyles. Over the past decades conventional water treatment methods such as coagulation, chlorination, flocculation and sedimentation have been reported not effective at completely removing organic pollutants and emerging pollutants such as organic dyes and pharmaceuticals. There is a need therefore for alternative technologies that can address the limitations of these traditional technologies.

Semiconductor photocatalysts have been widely applied for treatment of organic pollutants in water. Some of these semiconductor photocatalyst include chalcogenide semiconductors which are easy to prepare, are chemically and structurally stabile and are relatively cheap. However, they have the disadvantage of recombination of photo induced charge carriers. Many studies are currently focused on improving these properties so they can be applicable under solar light (sunlight) because it is abundant and relatively cheap. This can be achieved by coupling semiconductors with comparable band gaps that can absorb in the visible range and reduce recombination of electrons and holes and thus improve the photocatalytic activity of the resulting nanocomposite.

In this study, chalcogenide semiconductor cadmium sulphide (CdS) was synthesized for the photocatalytic degradation of organic pollutants. CdS has a small bandgap and can absorb visible light. However, it suffers from rapid recombination of photogenerated charge carriers. To improve its properties, g-C_3N_4 nanosheets were selected to improve the photocatalytic activity of CdS through formation of a heterojunction between the two materials. The two materials were synthesized separately through hydrothermal and chemical exfoliation and then combined to form a nanocomposite with different mass percentages of g-C_3N_4 nanosheets (10, 20 and 30%).

The nanocomposites were characterized using microscopic techniques such as high resolution scanning electron microscope (SEM), transmission electron microscope (TEM), energy dispersive x-ray (EDX), X-ray diffraction pattern, Brunauer Emmett teller (BET) and thermogravimetric analysis (TGA). The optical studies were performed using UV-Vis spectroscopy and photo luminescent spectrometry.

SEM and TEM confirmed the successful formation of g-C_3N_4 nanosheets, CdS microspheres and g-C_3N_4/CdS nanocomposites. SEM analysis also confirmed successful exfoliation of bulk g-C_3N_4, showing layer sheet-like morphology and with CdS dispersed on the surface of g-C_3N_4. The TEM results concurred with the results obtained from SEM and confirmed two morphologies of an almost transparent plate like material and black dark material on the surface ascribed to CdS microspheres showing formation of an interface between CdS and g-C_3N_4 (10%). BET analysis showed an increase in surface area of the g-C_3N_4 after exfoliation and increase in surface area of CdS after addition of g-C_3N_4 nanosheets. The TGA analysis showed a decrease in mass percentage of g-C_3N_4 after exfoliation and the increase in the amount of g-C_3N_4 nanosheets resulted in decreased thermal stability of the g-C_3N_4/CdS nanocomposite.

The UV-Vis analysis showed improved absorption of light by the g-C_3N_4 nanosheets towards shorter wavelength of the visible spectrum due to a reduced band gap. CdS showed an absorption edge in the visible range, as confirmed by its small band gap. The application studies confirmed that the photocatalytic activity of CdS was significantly improved and the nanocomposite with lowest g-C_3N_4 nanosheets load (10% g-C_3N_4/CdS) was the best photoactive nanocomposite which achieved 99.4% acid blue 25 dye removal. The increase in the amount of g-C_3N_4 nanosheets loaded in CdS resulted in a decrease in the photocatalytic efficiency of CdS. The effect of catalyst concentration and dye pH were also evaluated and the increase in catalyst concentration resulted in a decrease in the removal efficiency and the highest dye removal of 99.9% was achieved at pH 4.

The working composite (10% CNS/CdS) was further used for the photocatalytic degradation of diclofenac sodium (DFC) and a mixture of DFC and AB-25. The results showed that the nanocomposite was not very effective in degradation of

individual DFC and achieved only 65.8% removal efficiency at pH 6 and the removal efficiency increased to 77.2 at lower pH 4 and decreased significantly to 46.1% at higher pH 9. The increase in DFC concentration resulted in a decrease in the photocatalytic efficiency and higher catalyst loading resulted in high removal efficiency. In a pollutant mixture of DFC and AB-25, the photocatalytic efficiency of the nanocomposite decreased with increase in AB-25 concentration (5-20 ppm) from 66.7% to 28.9% and the efficiencies at different pH (2-8) resulted in different removal efficiencies. At lower pH (2) the removal efficiency of 88.9% was achieved, while for AB-25 only 39.7% removal was achieved.

The LC-MS results showed that DFC degradation resulted in low intensity and low molecular weight intermediates at 108m/z and 75 m/z after 180 min and this is associated with ring opening of the DFC to give by-products. The leaching studies showed that CdS in CdS/g-C_3N_4 nanocomposite was unstable and the amount of Cd^{2+} in DFC solution increased from 0.00116 mg/L to 0.00442 after 180 min which is insignificant.

Heterojunction chalcogenide photocatalysts are thus promising materials for visible light enhanced degradation of organic pollutants in water.

TABLE OF CONTENT

DEDICATION iii
ACKNOWLEDGEMENTS iv
PUBLICATIONS AND PRESENTATIONS v
ABSTRACT vii
LIST OF FIGURES xiv
List OF TABLES xvi
LIST OF ABBREVIATIONS xvii
CHAPTER 1 1
1.1 Background 1
1.2 Problem statement 2
1.3 Aim and Objectives 5
1.3.1 Aim 5
1.3.2 Objectives 5
1.4 Dissertation Statement 6
1.5 A brief overview of chapters 6
CHAPTER 2 35
2.1 Introduction 35
2.2 Organic pollutants 35
2.2.1 Dye pollutants 36
2.2.2 Emerging pollutants 39
2.3 Conventional Water treatment methods 42
2.3.1 Advanced oxidation processes (AOPs) 43
2.4 Semiconductor photocatalysis 45
2.4.1 TiO_2 semiconductor photocatalysis 45
2.4.2 Chalcogenide semiconductors 46
2.5 Graphitic carbon nitride g-C_3N_4 50
2.5.1 g-C_3N_4 nanostructures 51
2.5.2 Optical properties, crystalline structure and phase transition of g-C_3N_4 52
2.5.3 Advantages of g-C_3N_4 based photocatalysis 53
2.5.4 Application of g-C_3N_4 in photodegradation of organic pollutants 54
2.6 Synthetic techniques for CdS 55
2.6.1 Sonochemical methods 55

2.6.2 Solvothermal methods 56
2.6.3 Co-precipitation method 56
2.6.4 Hydrothermal Method 56
CHAPTER 3 85
3.1 Introduction 85
3.2 Material, reagents and solvents 85
3.3 Experimental procedure 85
3.3.1 Synthesis of g-C_3N_4 nanosheets 85
3.3.2 Synthesis of CdS 86
3.3.3 Synthesis of g-C_3N_4/CdS 86
3.4 Application procedure 86
3.4.1 Preparation of Acid blue 25 (AB-25) 86
3.4.2 Preparation of Diclofenac sodium (DFC) 87
3.4.3 Photocatalytic degradation studies 87
3.5 Instrumental techniques 88
3.5.1 Scanning Electron Microscopy (SEM) 88
3.5.2 Energy dispersive X-ray spectrometry (EDX) 89
3.5.3 Transmission Electron Microscopy 89
3.5.4 Fourier Transform Infra-red 90
3.5.5 X-Ray diffraction analysis 91
3.5.6 BET analysis 93
3.5.7 UV-Vis analysis 94
3.6 Photoluminescent spectrophotometry 97
3.7 Photoreactor 98
3.8 Inductively coupled plasma optical emission spectroscopy (ICP-OES) 99
3.9 Ultra-High Performance Liquid Chromatography 100
CHAPTER 4 131
4.1 Introduction 131
4.2 Results and discussion 131
4.2.1 X-Ray diffractometer (XRD) 131
4.2.2 Fourier transformation infra-red (FTIR) 132
4.2.3 Scanning Electron and Energy Dispersive Microscope 133
4.2.4 Transmission Electron Microscope (TEM) 134
4.2.5 BET analysis 135
4.2.6 Thermal gravimetric analysis 136

4.3 Optical properties 137
4.3.1 UV-Vis absorption spectroscopy 137
4.3.2 Photoluminescence spectroscopy 139
4.4 Photocatalytic degradation of AB-25 139
4.4.1 AB-25 Dye degradation absorption 139
4.4.2 Effect of exfoliation on CN for photocatalytic degradation of AB-25 ... 140
4.5 Reaction kinetics 141
4.6 Proposed mechanism 142
4.7 Conclusions 143
CHAPTER 5 171
5.1 Introduction 171
5.2 Results and discussion 171
5.2.1 X-Ray diffractometer (XRD) 171
5.2.2 Fourier transformation infra-red (FTIR) 173
5.2.3 Field Emission Scanning Electron Microscope and Energy Dispersive Microscope 174
5.2.4 5.1.4 Energy Dispersive Spectroscopy 175
5.2.5 Transmission Electron Microscope (TEM) 177
5.2.6 BET analysis 178
5.2.7 Thermogravimetric Analysis 180
5.3 Optical properties 181
5.3.1 UV-Vis absorption spectroscopy 181
5.4 Photocatalytic degradation of AB-25 evaluation 183
5.4.1 AB-25 Dye degradation absorption 183
5.4.2 Effect of CNS/CdS mass ratios on AB degradation efficiency 183
5.4.3 Effect of catalyst dosage 184
5.4.4 Effect of pH 186
5.5 Reaction kinetics 187
5.6 Photocatalytic stability and reusability 188
5.7 Reactive species 189
5.8 Proposed photodegradation of AB-25 mechanism 190
5.9 Conclusions 191
CHAPTER 6 220
6.1 Photocatalytic degradation of DFC 220
6.1.1 DFC degradation absorption 220

6.1.2 Effect of DFC concentration 221
6.1.3 Effect of 10% CNS/CdS catalyst dosage 222
6.1.4 Effect of pH 223
6.1.5 Reactive species 224
6.2 The effect of a mixture of pollutants (AB-25 and DFC) 225
6.2.1 DFC and AB-25 absorbance 226
6.2.2 The effect of AB-25 on DFC degradation 226
6.2.3 The effect of catalyst dosage 227
6.2.4 The effect of pH 228
6.2.5 Reaction kinetics 229
6.3 Proposed photodegradation of DFC mechanism 231
6.3.1 Degradation products of DFC 232
6.4 CdS leaching test studies 236
6.5 Conclusion 237
CHAPTER 7 265
7.1 Conclusion 265

LIST OF FIGURES

Figure 2.1.Chemical structure of Diclofenac [37]. 40
Figure 2.2.Entry pathways of DFC [34]. 41
Figure 2.3.Schematic diagram of photocatalysis mechanism [71]..... 44
Figure 2.4.Schematic diagram of (a) zinc blend and (b) hexagonal crystalline structure [93]. 47
Figure 2.5.Morphological structures of CdS [105] 48
Figure 2.6.Chemical structure of g-C_3N_4. 50
Figure 2.7. The stacked 2-D layer structure of g-C3N4 (a) s-triazine (b) tri-s-triazine (c) the primary block of g-C3N4 [117]..... 53
Figure 3.1. Schematic diagram of scanning electron Microscopy [5]. 88
Figure 3.2. Schematic diagram of TEM [7]. 90
Figure 3.3. Schematic diagram of FTIR [8]..... 91
Figure 3.4. Representation diagram of incident and diffraction rays [10]..... 92
Figure 3.5.Schematic diagram of BET analysis [12]..... 94
Figure 3.6. Schematic diagram of UV-Vis [14]. 97
Figure 3.7. Basic principle of PL [15]..... 98
Figure 3.8. Schematic diagram of the photocatalytic reactor..... 99
Figure 3.9.Schematic diagram of ICP-OES [13]..... 100
Figure 3.10. Schematic diagram of HPLC [196]. 101
Figure 4.1. XRD patterns of CN and CNS. 132
Figure 4.2. FTIR spectra of CN and CNS. 133
Figure 4.3.FESEM micrograms of (a) CN and (b) CNS. 134
Figure 4.4. EDX spectra of (a) CN and (b) CNS. 134
Figure 4.5.TEM images of (a) CNS and (b) SAED pattern of CNS. 135
Figure 4.6.BET analysis of (a) CN and (b) CNS. 136
Figure 4.7. TGA analysis of CN and CNS. 137
Figure 4.8. (a) UV-Vis spectra and (b) Tauc plots of prepared materials. 138
Figure 4.9. PL spectra of CN and CNS. 139
Figure 4.10. UV-Vis absorption for degradation of AB-25. 140
Figure 4.11. (a) UV-Vis absorption of AB-25 and (b) Effect of CN and CNS on AB-25. 141
Figure 4.12. Reaction rate constants of CN and CNS. 142
Figure 4.13. Proposed mechanism for CNS photodegradation of AB-25. 143
Figure 5.1. XRD pattern of CNS, CdS, 10%, 20% and 30% CNS/CdS. 172
Figure 5.2. HRSEM of CNS, 10%, 20% and 30% CNS/CdS. 174
Figure 5.3. FESEM micrograms of 10%, 20% 30% CNS/CdS (a-d). 175
Figure 5.4. EDS analysis of (a) CdS and 10%, 20% and 30%CNS/CdS (b-d). 176
Figure 5.5. EDS mapping images of 10% CNS/CdS (a-d). 177
Figure 5.6. TEM analysis of (a) CdS and (b) 10% CNS/CdS and (c) SAED for 10% CNS/CdS..... 178
Figure 5.7. BET analysis of CdS and 10% CNS/CdS. 180
Figure 5.8.TGA analysis of CdS, 10%, 20% and 30% CNS/CdS. 181
Figure 5.9. (a)UV-Vis spectra and (b) Tauc plots of prepared materials. 182
Figure 5.10. UV-Vis absorption spectra for degradation of AB-25. 183

Figure 5.11. Effect of CNS on CdS mass ratios for AB-25 degradation efficiency. 184
Figure 5.12. Effect of CNS mass ratios on CdS for AB-25 degradation. 185
Figure 5.13. The effect of AB-25 concentration. 186
Figure 5.14. The .effect of pH of AB-25. 187
Figure 5.15. Rate Constants for (a) photolysis, (b) CN, (c) CNS, (d) (CdS), (e) 30% CNS/CdS, (f) 20%CNS/CdS and (g) 10%CNS/CdS. 188
Figure 5.16. Stability of 10% CNS/CdS. 189
Figure 5.17.Determination of reactive species with different scavengers for photo-degradation of AB-25. 190
Figure 5.18.The proposed mechanism for photocatalytic degradation of AB-25. ... 191
Figure 6.1.UV-Vis absorption spectra of DFC. 221
Figure 6.2. The effect of DFC concentration. 222
Figure 6.3. Effect of catalysts dosage for DFC degradation. 223
Figure 6.4. Effect of pH on DFC degradation. 224
Figure 6.5.Determination of reactive species with different scavengers for photo-degradation of DFC. 225
Figure 6.6. UV-Vis absorption spectra of AB-25 and DFC mixture. 226
Figure 6.7. Photocatalytic degradation of AB-25 and DFC mixture. 227
Figure 6.8.The effect of catalyst dosage on degradation of a mixture of DFC and AB-25. 228
Figure 6.9.The effect of pH on DFC and AB-25 mixture degradation. 229
Figure 6.10. Rate Constants for (a) photolysis, (b) DFC (mixture), (c) individuals DFC, (d) AB-25 (mixture). 231
Figure 6.11. The proposed mechanism for photocatalytic degradation of DFC. 232
Figure 6.12. Mass spectra of UHPLC TOF-Ms during degradation of DFC at (a) 0 min, (b) 90 min and (c) 180 min. 234
Figure 6.13.Schematic diagram for the photocatalytic degradation pathway of DFC. 235
Figure 6.14.Leaching studies of Cd^{2+} of in degradation of DFC at pH 2. 236

List OF TABLES

Table 2.1.Chemical structure and categories of anthraquinone dyes [21]..... 37
Table 2.2. Detection of DFC in South Africa WWTWs and surface water [45]. 42
Table 2.3.Band gap positions of typical semiconductor photocatalyst [139]..... 54
Table 5.1.d spacing, crystalline size, and micro-strain of the as-prepared materials. 173
Table 5.2.Surface area and pore volume of the prepared materials. 179
Table 5.3.Reaction rate constants of the prepared materials. 187

LIST OF ABBREVIATIONS

CN	graphitic carbon nitride
CNS	graphitic carbon nitride nanosheets
CdS	Cadmium sulphide
PhAc	Pharmaceuticals
DFC	Diclofenac
AB-25	Acid blue 25
WWTP	Waste water treatment plants
(EU)	The European Union
(USEPA)	United States Environmental Protection Agency
(WFD)	Under the Framework Directive
PPCP	Pharmaceutical and personal care products
mg/L	Milligram per Litre
ng/L	Nano gram per Litre
SEM	Scanning Electron Microscopy
TEM	Transmission Electron Microscopy
TGA	Thermogravimetric analysis
FTIR	Fourier Transform Infrared
XRD	X-Ray diffractometer
UV-Vis	Ultra-violet visible
UHPLC	Ultra-High Performance Liquid Chromatography
IR	Infra-red
ECETOC	European Centre for Ecotoxicology and Toxicology of Chemical
WHO	World Health Organization
VS	Vinyl Sulfone
AC	Acid Orange
CT	Chlorotrainzine
TCP	Trichloropyrimidine
PR	Phenol Red
RB	Rose Bengal
EA	Environmental Agency

NF	Nanofiltration
RO	Reverse Osmosis
MF	Microfiltration
AOP	Advanced oxidation Process
VB	Valence Band
CB	Covalent Band
CNTs	Carbon nanotubes
AG-16	Acid Green
TMC	Transition Metal Chalcogenide
CdS	Cadmium sulphide
PVP	Polyvinylpyrrolidone
C_{60}	Fullerene
B (RhB)	Rhodamine
CQDs	Carbon quantum dots
UCN	Ultra-thin graphitic carbon nitride

CHAPTER 1

1.1 Background

Water is a vital and essential resource to all living forms of life. It is found in the natural environment and comprises the earth's oceans, seas, lakes, rivers and underground water sources [1,2]. Only 3% of the earth's total water supply is freshwater and only 0.06% can be accessed from the natural springs, rivers, wells and lakes. These sources are compromised as they are exposed to a variety of contaminants, which affect the human, animal and plant life [3]. There are more than 1 billion people who have no access to fresh water free of pathogens and contaminants. According to the World Health Organisation, the world's population growth is expected to double from 3.4 to 6.3 billion people by 2050 and thus increase the need for freshwater particularly for food production, as 70% of the world's freshwater withdrawals is for agricultural purposes [4–6]. Rapid industrialization, increased living standards and urbanization are also amongst the causes of fresh water declines and climate change aggravates the global water scarcity and predicted global warming of 2 ˚C above present temperatures [1,2].

Water scarcity remains a problem for both developed and developing countries having advanced treatment systems and quality water supplies [7–9]. South Africa is one the driest countries worldwide with recent reports on the water shortages faced in the country. These are due to factors such as limited and highly polluted water sources, low rainfall, increased population growths, high evaporation rates and also pollution caused by urbanization, mining industry, power generation and agriculture [10].

The major water pollutants include organic pollutants such as pharmaceuticals, personal care products, dyes, pesticides, surfactants, phenolic compounds, oil and phthalates. Some of these pollutants are classified as new emerging pollutants whose effects on human health and environment are not thoroughly understood [11,12].

About 10,000 textile dyes are produced globally in the textile industries and during the dyeing processes of the fabrics, not all of the dye is used on the fabrics. Some of

these dyes remain unfixed to the fabrics and are washed and released as coloured water. About 1.000-3.000 m^3 water containing dyes and chemicals are released into water bodies after the processing of the textiles per day. Some of these dyes and chemicals are non-biodegradable, very toxic and pose serious threat to health and the environmental [13].

Recently pharmaceutical drugs have raised increasing environmental and health concerns. They are readily seen as pollutants because they are used to improve human and animal health, to improve the living standards and also to help pursue the modern way of living. Pharmaceutical drugs are active compounds such as over the counter prescriptions, and therapeutic drugs used for prevention and treating of diseases in both humans and animals [14,15]. They have multiple functional groups and are biologically active at low concentrations and some are resistant to biodegradation. Once present in the environment, biological effects such as antibiotic resistance of microorganisms, endocrine disruption and chemo-sensitization can be induced [16–18].

WWTPs are the most common routes of entry of pharmaceuticals into the environment such as water, sediments and biota [19–22]. The European Union (EU) and United States Environmental Protection Agency (USEPA) developed a list of priority pollutants, identifying a number of chemicals in wastewaters and storm water runoff which pose a threat to surface water [22]. Under the Framework Directive (WFD) 2000/60/EC. Pharmaceuticals and personal care products (PPCPs) such as diclofenac, iopamidol, musk's and carbamazepine were identified as new emerging pollutants [23–26].

1.2 Problem statement

Organic pollutants including pharmaceuticals and textile dyes are bio-reactive compounds and are introduced into the environment as complex mixtures [27]. Pharmaceutical drugs are transformed into harmless by-products by the human body, so a combination of drug metabolites excreted by humans are discharged with household, industrial and hospital effluents to municipal (WWTPs) [28]. Though their effect is centred more on their environmental hygiene rather than their toxicology and pharmacology, recent research showed that they have negative biological effects in aquatic environment [29]. Some of these pharmaceuticals are endocrine disrupting

compounds, that interact with hormones systems and thus interfering with sexual development in humans and other organisms. The presence of complex mixtures of pharmaceuticals and other organic pollutants even at low concentrations may lead to synergistic interactions [30,31]. Pharmaceuticals have raised a concern worldwide as they have been detected in the environment across the world [32]. The centre for Drug Evaluation and Research.[32] European centre for Ecotoxicology and Toxicology of Chemicals (ECETOC) 2008 and World Health Organization (WHO 2011) developed regulations to evaluate the probable risks of pharmaceutical pollutants in the environment [14].

Textile dyes are a large group of organic compounds that are potential hazards to all life forms and the environment. Their effluents discharged into water bodies, which constitutes 80% of the total emissions produced in the textile industry [33]. During the dyeing process some the textile dyes do not remain attached on the fabrics and end up being released into the environment as textile effluents. Exposure to textile dyes can cause respiratory diseases due to the inhalation of dye particles even at lower concentrations. Some severe cases include respiratory sensitization with symptoms such as itching, watery eyes, sneezing, coughing and wheezing [33,34]. The color from the textile dyes causes aesthetic damage and also prevents light penetration through water and this leads to reduced rates of photosynthesis and lower dissolved oxygen levels and affect aquatic organisms. They are also toxic, mutagenic and carcinogenic agents [33].

The wastewater treatment techniques include physical (flocculation and coagulation), chemical (adsorption, coagulation, membrane filtration and advanced oxidation process) and biological techniques. Ozonation has been widely used for waste water treatment, though effective has been reported to result in formation of more harmful by-products. Physio-chemical treatment only transfer pollutants from one phase to another without eliminating them [34].The target compounds are not fully mineralized but merely transformed to other compounds requiring further treatment [35]. Recently treatment technologies such as membrane filtration, adsorption and advanced oxidation processes have attracted lot of attention. Adsorption has gained attention due to its simplicity and insensitivity to toxic pollutants however has the drawback sorption of desorption after absorption. Membrane technology is relatively

expensive but results in fouling which requires further treatment and is time consuming [34].

As an alternative advanced oxidation process techniques (semiconductor photocatalysis) have attracted attention to overcome the challenges of conventional techniques and the above mentioned techniques. These techniques are inexpensive, relatively simple, eco-friendly and capable of degrading organic pollutants in water. These processes include heterogeneous photocatalysis which is the speeding up of a reaction in the presence of catalyst (semiconductor) that absorbs light to degrade pollutants.

This work reports on relatively cheap, simple to use and effective semiconductor catalysts chalcogenide semiconductor (CdS) and g-C_3N_4 nanosheets coupled to produce an enhanced photocatalyst for the complete mineralization of Acid Blue-25 and Diclofenac sodium. Chalcogenide semiconductor CdS is a semiconductor that has attracted lots of attention due to its small bandgap for applications in the visible-light making it a promising material for water treatment. A lot of researchers have proved that CdS-based photocatalysts have good photocatalytic properties for waste water treatment [36]. It is unstable when illuminated with light energy and it is susceptible to corrosion and results in recombination of charge electrons and these are the limitations of a lot of semiconductors. A lot of studies have focused on eliminating this problem through coupling of two or more semiconductors with comparable bandgap gap energies to produce a highly photoactive catalyst [37].

In this work semiconductor g-C_3N_4 was used to enhance the photocatalytic activity of CdS. But g-C_3N_4 has the limitation of low visible-light response and regeneration of electron. To solve this researchers have reported on other g-C_3N_4 morphologies such g-C_3N_4 nanosheets, they have higher visible-light response than bulk g-C_3N_4 [38,39].

Recently g-C_3N_4/CdS based composites have been reported for a variety of applications including waste water treatment. However most of the research has been focused on the effect of CdS on g-C_3N_4 photocatalysis [40–42].

This work focuses on the effect of exfoliated g-C_3N_4 nanosheets on CdS photocatalysis and potentially eliminate some of the drawbacks of CdS to mineralize AB-25 and diclofenac sodium without producing secondary pollutants.

1.3 Aim and Objectives

1.3.1 Aim

The aim of this work was to develop a visible light active chalcogenide semiconductor g-C_3N_4 nanosheets-cadmium sulphide nanocomposites for photocatalytic degradation of organic pollutants, acid blue-25, diclofenac and mixture of acid blue-25 and diclofenac pollutants in water.

1.3.2 Objectives

The specific objectives of this study were to:

- Synthesize of g-C_3N_4 nanosheets through pyrolysis and chemical exfoliation method
- Fabrication of g-C_3N_4 nanosheets/CdS nanocomposites through an in-situ hydrothermal method
- Characterisation of the synthesized composites using techniques such as Fourier transform infra-red spectroscopy, scanning electron microscopy (SEM), energy dispersive x-ray spectroscopy (EDX), Brunauer-Emmett Teller (BET), X-ray diffraction spectroscopy, UV-Visible spectroscopy, Transmission electron microscopy (TEM).
- Evaluate the effect of different dosages of g-C_3N_4 nanosheets on the photocatalytic activity of CdS.
- Evaluate the photocatalytic performance of the g-C_3N_4 nanosheets/CdS nanocomposites in the degradation of Diclofenac and Acid blue-25 under visible light irradiation.
- Assess the possibility of Cd^{2+} leaching into the treated water using ICP-MS Characterization of the photodegradation by-products using LC-MS and to propose the degradation pathways and mechanisms

1.4 Dissertation Statement

CdS modified with g-C_3N_4 nanosheets should possess enhanced photocatalytic properties towards visible light photodegradation and complete mineralization of organic pollutants in water. By forming a heterojunction of the semiconductors could effectively result in a nanocomposite that is photoactive and absorb in the visible range because it is relatively safe, cheap and abundant.

1.5 A brief overview of chapters

This dissertation is divided into these chapters.

Chapter 1: Provides the background, problem statement, research motivation, dissertation statement, the aim and objectives of the study.

Chapter 2: Is the literature review of this research study, which gives classification of organic dyes, textile dyes and pharmaceuticals. It also provides information on the research approach of the study using semiconductor photocatalysis and provides information on the CdS and g-C_3N_4 photocatalysis.

Chapter 3: Provides details about the methodology and procedures followed to achieve the research objectives of the study. It also provides detailed lists of the materials used and information on the characterization techniques used in this study.

Chapter 4: Details on the characterization and application results of bulk g-C_3N_4 and g-C_3N_4 nanosheets.

Chapter 5: Details on the characterization and application of CdS, 10, 20 and 30% g-C_3N_4 nanosheets/CdS nanocomposites.

Chapter 6: Provides the photocalytic degradation results of diclofenac sodium by 10% g-C_3N_4 nanosheets/CdS (the working nanocomposite).

Chapter 7: This chapter is the conclusion and recommendations of the work.

References

[1] A. Azizullah, M.N.K. Khattak, P. Richter, D.P. Häder, Water pollution in Pakistan and its impact on public health - A review, Environ. Int. 37 (2011) 479–497. doi:10.1016/j.envint.2010.10.007.

[2] I. Gehrke, A. Somborn-schulz, Innovations in nanotechnology for water treatment, Nanotechnol. Sci. Appl. 8 (2015) 1–17.

[3] C.J.. ; G. Vorösmarty Pamela; ; Salisbury, Joseph; ; Lammers, Richard B., Global Water Resources: Vulnerability from Climate Change and Population Growth, Science (80-.). 289 (2000) 284–288. doi:10.1126/science.289.5477.284.

[4] J. Theron, T.E. Cloete, Emerging Waterborne Infections: Contributing Factors, Agents, and Detection Tools, Crit. Rev. Microbiol. 28 (2008) 1–26. doi:10.1080/1040-840291046669.

[5] K.K. Jain, Nanotechnology and Water, Contemp. Mater. 1 (2012) 26–30. doi:10.7251/122.

[6] F.W. Owa, Water pollution : Sources , Effects , Control and Management, Int. Lett. 3 (2014) 1–6.

[7] H. Zhou, D.W. Smith, Advanced technologies in water and wastewater treatment, in: 2002. doi:10.1139/S02-020.

[8] M. Wakil, M. Burhan, L. Ang, K. Choon, Energy-water-environment nexus underpinning future desalination sustainability, Desalination. 413 (2017) 52–64. doi:10.1016/j.desal.2017.03.009.

[9] M. Palaniappan, K. Address, Peak_Water_Talk.Pdf, in: Utah Am. Plan. Assoc. Annu. Conf., 2008: pp. 3–11.

[10] J.K. Bwapwa, Review on Main Issues Causing Deterioration of Water Quality and Water Scarcity: Case Study of South Africa, Environ. Manag. Sustain. Dev. 7 (2018) 14. doi:10.5296/emsd.v7i3.13156.

[11] J. Wang, S. Wang, Removal of pharmaceuticals and personal care products (PPCPs) from wastewater: A review, J. Environ. Manage. 182 (2016) 620–640.

doi:10.1016/j.jenvman.2016.07.049.

[12] G. Boczkaj, A. Fernandes, Wastewater treatment by means of advanced oxidation processes at basic pH conditions : A review, Chem. Eng. J. 320 (2017) 608–633. doi:10.1016/j.cej.2017.03.084.

[13] R. Ananthashankar, Treatment of textile effluent containing Reactive Red 120 dye using advanced oxidation, 2012.

[14] K. Klaus, Pharmaceuticals in the Environment, Annu Rev Env. Resour. 35 (2010) 57–75. doi:10.1146/annurev-environ-052809-161223.

[15] C. G. Daughton, Ternes. A. T, Pharmacueticals and Personal Care Products in the Environment; Agents of Subtle changes, 2001.

[16] A.B.A. Boxall, M.A. Rudd, B.W. Brooks, D.J. Caldwell, K. Choi, S. Hickmann, E. Innes, K. Ostapyk, J.P. Staveley, T. Verslycke, G.T. Ankley, K.F. Beazley, Review Pharmaceuticals and Personal Care Products in the Environment : What Are the Big Questions ?, 120 (2012) 1221–1229.

[17] G. Li, X. Nie, Y. Gao, T. An, Applied Catalysis B : Environmental Can environmental pharmaceuticals be photocatalytically degraded and completely mineralized in water using g-C_3N_4/TiO_2 under visible light irradiation ?— Implications of persistent toxic intermediates, "Applied Catal. B, Environ. 180 (2016) 726–732. doi:10.1016/j.apcatb.2015.07.014.

[18] B. Hoeger, B. Köllner, D.R. Dietrich, B. Hitzfeld, Water-borne diclofenac affects kidney and gill integrity and selected immune parameters in brown trout (Salmo trutta f. fario), Aquat. Toxicol. 75 (2005) 53–64. doi:10.1016/j.aquatox.2005.07.006.

[19] M. Lillenberg, S. Yurchenko, K. Kipper, K. Herodes, V. Pihl, R. Lõhmus, M. Ivask, A. Kuu, S. Kutti, S. V. Litvin, L. Nei, Presence of fluoroquinolones and sulfonamides in urban sewage sludge and their degradation as a result of composting, Int. J. Environ. Sci. Technol. 7 (2010) 307–312. doi:10.1007/BF03326140.

[20] S.K. Khetan, T.J. Collins, Human pharmaceuticals in the aquatic environment: A challenge to green chemisty, Chem. Rev. 107 (2007) 2319–2364.

doi:10.1021/cr020441w.

[21] A.M. Deegan, B. Shaik, K. Nolan, K. Urell, M. Oelgemöller, J. Tobin, A. Morrissey, Treatment options for wastewater effluents from pharmaceutical companies, Int. J. Environ. Sci. Technol. 8 (2011) 649–666. doi:10.1007/BF03326250.

[22] A.J. Ebele, M. Abou-Elwafa Abdallah, S. Harrad, Pharmaceuticals and personal care products (PPCPs) in the freshwater aquatic environment, Emerg. Contam. 3 (2017) 1–16. doi:10.1016/j.emcon.2016.12.004.

[23] B.D. Blair, J.P. Crago, C.J. Hedman, R.D. Klaper, Chemosphere Pharmaceuticals and personal care products found in the Great Lakes above concentrations of environmental concern, Chemosphere. 93 (2013) 2116–2123. doi:10.1016/j.chemosphere.2013.07.057.

[24] C.U. Meteyer, B.A. Rideout, M. Gilbert, H.L. Shivaprasad, L. Oaks, pathology and proposed pathophysiology of diclofenac poisoning in free-living and experimentally exposed oriental white backed vultures (Gyps bengalensis), J. Wildl. Dis. 41 (2005) 707–716.

[25] R. Triebskorn, H. Casper, V. Scheil, J. Schwaiger, Ultrastructural effects of pharmaceuticals (carbamazepine, clofibric acid, metoprolol, diclofenac) in rainbow trout (Oncorhynchus mykiss) and common carp (Cyprinus carpio), Anal. Bioanal. Chem. 387 (2007) 1405–1416. doi:10.1007/s00216-006-1033-x.

[26] J. Schwaiger, H. Ferling, U. Mallow, H. Wintermayr, R.D. Negele, Toxic effects of the non-steroidal anti-inflammatory drug diclofenac. Part I: Histopathological alterations and bioaccumulation in rainbow trout, Aquat. Toxicol. 68 (2004) 141–150. doi:10.1016/j.aquatox.2004.03.014.

[27] A.A.C. and Z.M. Dana Manuela Sirbu, Daniela Curseu, Monica Popa, Environmental Risks of Pharmaceuticals and Personal Care Products in Water, in: Tenth Int. Water Technol. Conf., 2006: pp. 1151–1162.

[28] E. Archer, G.M. Wolfaardt, J.H. van Wyk, Pharmaceutical and personal care products (PPCPs) as endocrine disrupting contaminants (EDCs) in South African surface waters, Water SA. 43 (2017) 684–706.

doi:10.4314/wsa.v43i4.16.

[29] O.A.H. Jones, N. Voulvoulis, J.N. Lester, Potential ecological and human health risks associated with the presence of pharmaceutically active compounds in the aquatic environment, Crit. Rev. Toxicol. 34 (2004) 335–350. doi:10.1080/10408440490464697.

[30] A.K. Karen, J.B. Paul, H.M. Kenneth, e P.P. Vinc, E.E. Robert, M.L. James, W.F. Robert, Disrupting Queer Incluslon, Pnas. 104 (2007) 8897–8901. doi:10.1073/pnas.0609568104.

[31] D.J. Caldwell, F. Mastrocco, T.H. Hutchinson, R. Länge, D. Heijerick, C. Janssen, P.D. Anderson, J.P. Sumpter, Derivation of an aquatic predicted no-effect concentration for the synthetic hormone, 17α-ethinyl estradiol, Environ. Sci. Technol. 42 (2008) 7046–7054. doi:10.1021/es800633q.

[32] M.F. Rahman, E.K. Yanful, S.Y. Jasim, Endocrine disrupting compounds (EDCs) and pharmaceuticals and personal care products (PPCPs) in the aquatic environment: Implications for the drinking water industry and global environmental health, J. Water Health. 7 (2009) 224–243. doi:10.2166/wh.2009.021.

[33] B. Lellis, C.Z. Fávaro-polonio, J.A. Pamphile, J.C. Polonio, Effects of textile dyes on health and the environment and bioremediation potential of living organisms, Biotecnol. Res. Innov. 3 (2019) 275–290. doi:10.1016/j.biori.2019.09.001.

[34] R. Paper, Decolorization of mixture of dyes : A critical review, Glob. J. Environ. Sci. Manag. Glob. J. Environ. Sci. Manag. 1 (2015) 71–94. doi:10.7508/gjesm.2015.01.007.

[35] A.M. Deegan, B. Shaik, K. Nolan, K. Urell, J. Tobin, A. Morrissey, Treatment options for wastewater effluents from pharmaceutical companies, 8 (2011) 649–666.

[36] L. Cheng, Q. Xiang, Y. Liao, H. Zhang, CdS-Based photocatalysts, Royal Society of Chemistry, 2018. doi:10.1039/c7ee03640j.

[37] H.L. Lee, A.M. Issam, M. Belmahi, M.B. Assouar, H. Rinnert, M. Alnot,

Synthesis and characterizations of bare cds nanocrystals using chemical precipitation method for photoluminescence application, J. Nanomater. 2009 (2009). doi:10.1155/2009/914501.

[38] S. Kumar, S. Karthikeyan, A.F. Lee, g-C_3N_4-based nanomaterials for visible light-driven photocatalysis, Catalysts. 8 (2018). doi:10.3390/catal8020074.

[39] S. Cao, J. Low, J. Yu, M. Jaroniec, Polymeric Photocatalysts Based on Graphitic Carbon Nitride, Adv. Mater. 27 (2015) 2150–2176. doi:10.1002/adma.201500033.

[40] Q.Y. Liu, Y.L. Qi, Y.F. Zheng, X.C. Song, Synthesis and enhanced photocatalytic activity of g-C_3N_4 hybridized CdS nanoparticles, Bull. Mater. Sci. 40 (2017) 1329–1333. doi:10.1007/s12034-017-1513-y.

[41] R.C. Pawar, V. Khare, C.S. Lee, Hybrid photocatalysts using graphitic carbon nitride/cadmium sulfide/reduced graphene oxide (g-C_3N_4/CdS/RGO) for superior photodegradation of organic pollutants under UV and visible light, Dalt. Trans. 43 (2014) 12514–12527. doi:10.1039/c4dt01278j.

[42] S.W. Cao, Y.P. Yuan, J. Fang, M.M. Shahjamali, F.Y.C. Boey, J. Barber, S.C. Joachim Loo, C. Xue, In-situ growth of CdS quantum dots on g-C_3N_4 nanosheets for highly efficient photocatalytic hydrogen generation under visible light irradiation, Int. J. Hydrogen Energy. 38 (2013) 1258–1266. doi:10.1016/j.ijhydene.2012.10.116.

[43] S. Rasalingam, R. Peng, R.T. Koodali, Removal of hazardous pollutants from wastewaters: Applications of TiO_2-SiO_2 mixed oxide materials, J. Nanomater. 2014 (2014). doi:10.1155/2014/617405.

[44] M.K. Hasan, A. Shahriar, K.U. Jim, Water pollution in Bangladesh and its impact on public health, Heliyon. 5 (2019) e02145. doi:10.1016/j.heliyon.2019.e02145.

[45] S. Rasalingam, R. Peng, R.T. Koodali, 617405.Pdf, 2014 (2014).

[46] U. Tahir, A. Yasmin, U.H. Khan, Phytoremediation: Potential flora for synthetic dyestuff metabolism, J. King Saud Univ. - Sci. 28 (2016) 119–130. doi:10.1016/j.jksus.2015.05.009.

[47] G. Dong, Y. Zhang, Q. Pan, J. Qiu, A fantastic graphitic carbon nitride (g-C_3N_4) material: Electronic structure, photocatalytic and photoelectronic properties, J. Photochem. Photobiol. C Photochem. Rev. 20 (2014) 33–50. doi:10.1016/j.jphotochemrev.2014.04.002.

[48] D.A. Yaseen, M. Scholz, Textile dye wastewater characteristics and constituents of synthetic effluents: a critical review, Springer Berlin Heidelberg, 2019. doi:10.1007/s13762-018-2130-z.

[49] T. Robinson, G. McMullan, R. Marchant, P. Nigam, Remediation of dyes in textile effluent: A critical review on current treatment technologies with a proposed alternative, Bioresour. Technol. 77 (2001) 247–255. doi:10.1016/S0960-8524(00)00080-8.

[50] G.S. Gupta, G. Prasad, V.N. Singh, Removal of chrome dye from aqueous solutions by mixed adsorbents: Fly ash and coal, Water Res. 24 (1990) 45–50. doi:10.1016/0043-1354(90)90063-C.

[51] N. Muhd Julkapli, S. Bagheri, S. Bee Abd Hamid, Recent advances in heterogeneous photocatalytic decolorization of synthetic dyes, Sci. World J. 2014 (2014) 25. doi:10.1155/2014/692307.

[52] Y. Fu, T. Viraraghavan, Fungal decolorization of dye wastewaters: A review, Bioresour. Technol. 79 (2001) 251–262. doi:10.1016/S0960-8524(01)00028-1.

[53] V.K. Gupta, S. Khamparia, I. Tyagi, D. Jaspal, A. Malviya, Decolorization of mixture of dyes: A critical review, Glob. J. Environ. Sci. Manag. Glob. J. Environ. Sci. Manag. 1 (2015) 71–94. doi:10.7508/gjesm.2015.01.007.

[54] Z. Aksu, Application of biosorption for the removal of organic pollutants: A review, Process Biochem. 40 (2005) 997–1026. doi:10.1016/j.procbio.2004.04.008.

[55] S. Sumathi, B.S. Manju, Uptake of reactive textile dyes by Aspergillus foetidus, Enzyme Microb. Technol. 27 (2000) 347–355. doi:10.1016/S0141-0229(00)00234-9.

[56] Z. Aksu, S. Tezer, Equilibrium and kinetic modelling of biosorption of Remazol black B by Rhizopus arrhizus in a batch system: Effect of temperature,

Process Biochem. 36 (2000) 431–439. doi:10.1016/S0032-9592(00)00233-8.

[57] T. O'Mahony, E. Guibal, J.M. Tobin, Reactive dye biosorption by Rhizopus arrhizus biomass, Enzyme Microb. Technol. 31 (2002) 456–463. doi:10.1016/S0141-0229(02)00110-2.

[58] B. Aruna, R.S. L, E. Shiva, A. Srinu, P. Roja, D. Vijayalakshmi, D.V.R. Prasad, Research Article Biodecolorization of Anthraquinone Textile (Acid Blue 25) Dye By Klebsiella Sp, 6 (2015) 3216–3222.

[59] M. Auta, B.H. Hameed, Preparation of waste tea activated carbon using potassium acetate as an activating agent for adsorption of Acid Blue 25 dye, Chem. Eng. J. 171 (2011) 502–509. doi:10.1016/j.cej.2011.04.017.

[60] C.A. Hsu, T.N. Wen, Y.C. Su, Z.B. Jiang, C.W. Chen, L.F. Shyur, Biological degradation of anthroquinone and azo dyes by a novel laccase from Lentinus sp., Environ. Sci. Technol. 46 (2012) 5109–5117. doi:10.1021/es2047014.

[61] H. hong Li, Y. tao Wang, Y. Wang, H. xia Wang, K. kai Sun, Z. mei Lu, Bacterial degradation of anthraquinone dyes, J. Zhejiang Univ. Sci. B. 20 (2019) 528–540. doi:10.1631/jzus.B1900165.

[62] M.E. Malefane, U. Feleni, A.T. Kuvarega, Tetraphenylporphyrin/WO_3/exfoliated graphite nanocomposite for photocatalytic degradation of an acid dye under visible light irradiation, New J. Chem. 10 (2019) 1–6. doi:10.1039/c9nj02747e.

[63] S. Benkhaya, S. El Harfi, A. El Harfi, Classifications , properties and applications of textile dyes : A review, Appl. J. Environ. Sci. 3 (2018) 311–320.

[64] D. Chakrabortty, S. Sen Gupta, Photo-catalytic decolourisation of toxic dye with N-doped titania: A case study with Acid Blue 25, J. Environ. Sci. (China). 25 (2013) 1034–1043. doi:10.1016/S1001-0742(12)60108-9.

[65] T. Deblonde, C. Cossu-Leguille, P. Hartemann, Emerging pollutants in wastewater: A review of the literature, Int. J. Hyg. Environ. Health. 214 (2011) 442–448. doi:10.1016/j.ijheh.2011.08.002.

[66] M. Clara, G. Windhofer, W. Hartl, K. Braun, M. Simon, O. Gans, C. Scheffknecht, A. Chovanec, Occurrence of phthalates in surface runoff, untreated and treated wastewater and fate during wastewater treatment,

Chemosphere. 78 (2010) 1078–1084. doi:10.1016/j.chemosphere.2009.12.052.

[67] M. la Farré, S. Pérez, L. Kantiani, D. Barceló, Fate and toxicity of emerging pollutants, their metabolites and transformation products in the aquatic environment, TrAC - Trends Anal. Chem. 27 (2008) 991–1007. doi:10.1016/j.trac.2008.09.010.

[68] A. Jennifer, M.A. Abdallah, S. Harrad, Pharmaceuticals and personal care products (PPCPs) in the freshwater aquatic environment, Emerg. Contam. 3 (2017) 1–16. doi:10.1016/j.emcon.2016.12.004.

[69] S.R. Hughes, P. Kay, L.E. Brown, Global synthesis and critical evaluation of pharmaceutical data sets collected from river systems, Environ. Sci. Technol. 47 (2013) 661–677. doi:10.1021/es3030148.

[70] D. Ashton, M. Hilton, K. V. Thomas, Investigating the environmental transport of human pharmaceuticals to streams in the United Kingdom, Sci. Total Environ. 333 (2004) 167–184. doi:10.1016/j.scitotenv.2004.04.062.

[71] S. Wiandt, H.J. Poremski, Selection and prioritisation procedure of hazardous substances for the marine environment within ospar/dynamec, Ecotoxicology. 11 (2002) 393–399. doi:10.1023/A:1020569608441.

[72] L. Lonappan, S.K. Brar, R.K. Das, M. Verma, R.Y. Surampalli, Diclofenac and its transformation products: Environmental occurrence and toxicity - A review, Environ. Int. 96 (2016) 127–138. doi:10.1016/j.envint.2016.09.014.

[73] Y. Zhang, S.U. Geißen, C. Gal, Carbamazepine and diclofenac: Removal in wastewater treatment plants and occurrence in water bodies, Chemosphere. 73 (2008) 1151–1161. doi:10.1016/j.chemosphere.2008.07.086.

[74] V. Acuña, A. Ginebreda, J.R. Mor, M. Petrovic, S. Sabater, J. Sumpter, D. Barceló, Balancing the health benefits and environmental risks of pharmaceuticals: Diclofenac as an example, Environ. Int. 85 (2015) 327–333. doi:10.1016/j.envint.2015.09.023.

[75] A.C. Johnson, E. Dumont, R.J. Williams, R. Oldenkamp, I. Cisowska, J.P. Sumpter, Do concentrations of ethinylestradiol, estradiol, and diclofenac in

European rivers exceed proposed EU environmental quality standards?, Environ. Sci. Technol. 47 (2013) 12297–12304. doi:10.1021/es4030035.

[76] A.Y. Shan, T.I.M. Ghazi, S.A. Rashid, Immobilisation of titanium dioxide onto supporting materials in heterogeneous photocatalysis: A review, Appl. Catal. A Gen. 389 (2010) 1–8. doi:10.1016/j.apcata.2010.08.053.

[77] Y. Mehmood, Index Academic Sciences Original Article Development and validation of UV-VIS spectroscopy method for the estimation of diclofenac sodium injections., Int. J. Pharm. Pract. Pharm. Sci. 2 (2015) 1–6.

[78] D. Chen, A.K. Ray, Photodegradation kinetics of 4-nitrophenol in TiO_2 suspension, Water Res. 32 (1998) 3223–3234. doi:10.1016/S0043-1354(98)00118-3.

[79] C. Martínez, M. Canle L., M.I. Fernández, J.A. Santaballa, J. Faria, Aqueous degradation of diclofenac by heterogeneous photocatalysis using nanostructured materials, Appl. Catal. B Environ. 107 (2011) 110–118. doi:10.1016/j.apcatb.2011.07.003.

[80] M. Letzel, G. Metzner, T. Letzel, Exposure assessment of the pharmaceutical diclofenac based on long-term measurements of the aquatic input, Environ. Int. 35 (2009) 363–368. doi:10.1016/j.envint.2008.09.002.

[81] C. Hao, R. Clement, P. Yang, Liquid chromatography-tandem mass spectrometry of bioactive pharmaceutical compounds in the aquatic environment-a decade's activities, Anal. Bioanal. Chem. 387 (2007) 1247–1257. doi:10.1007/s00216-006-0956-6.

[82] A.J. Sosiak, T. Hebben, A preliminary survey of pharmaceuticals and endocrine disrupting compounds in treated municipal wastewaters and receiving rivers of Alberta /, 2005. doi:10.5962/bhl.title.113982.

[83] M.J. Benotti, R.A. Trenholm, B.J. Vanderford, J.C. Holady, B.D. Stanford, S.A. Snyder, Pharmaceuticals and endocrine disrupting compounds in U.S. drinking water, Environ. Sci. Technol. 43 (2009) 597–603. doi:10.1021/es801845a.

[84] T. Heberer, Tracking persistent pharmaceutical residues from municipal sewage to drinking water, J. Hydrol. 266 (2002) 175–189. doi:10.1016/S0022-

1694(02)00165-8.

[85] F.O. Agunbiade, B. Moodley, Occurrence and distribution pattern of acidic pharmaceuticals in surface water, wastewater, and sediment of the Msunduzi River, Kwazulu-Natal, South Africa, Environ. Toxicol. Chem. 35 (2016) 36–46. doi:10.1002/etc.3144.

[86] M.T. Amin, A.A. Alazba, U. Manzoor, A Review of Removal of Pollutants from Water / Wastewater Using Different Types of Nanomaterials, 2014 (2014).

[87] M.R. Servos, D.T. Bennie, B.K. Burnison, A. Jurkovic, R. McInnis, T. Neheli, A. Schnell, P. Seto, S.A. Smyth, T.A. Ternes, Distribution of estrogens, 17β-estradiol and estrone, in Canadian municipal wastewater treatment plants, Sci. Total Environ. 336 (2005) 155–170. doi:10.1016/j.scitotenv.2004.05.025.

[88] T. Urase, T. Kikuta, Separate estimation of adsorption and degradation of pharmaceutical substances and estrogens in the activated sludge process, Water Res. 39 (2005) 1289–1300. doi:10.1016/j.watres.2005.01.015.

[89] N. Vieno, T. Tuhkanen, L. Kronberg, Removal of pharmaceuticals in drinking water treatment: Effect of chemical coagulation, Environ. Technol. 27 (2006) 183–192. doi:10.1080/09593332708618632.

[90] P. Westerhoff, Y. Yoon, S. Snyder, E. Wert, Fate of endocrine-disruptor, pharmaceutical, and personal care product chemicals during simulated drinking water treatment processes, Environ. Sci. Technol. 39 (2005) 6649–6663. doi:10.1021/es0484799.

[91] M. Petrovic, A. Diaz, F. Ventura, D. Barceló, Occurrence and removal of estrogenic short-chain ethoxy nonylphenolic compounds and their halogenated derivatives during drinking water production, Environ. Sci. Technol. 37 (2003) 4442–4448. doi:10.1021/es034139w.

[92] G. Becher, Drinking Water Chlorination and Health, Acta Hydrochim. Hydrobiol. 27 (1999) 100–102. doi:10.1002/(sici)1521-401x(199902)27:2<100::aid-aheh100>3.3.co;2-1.

[93] N. Bolong, A.F. Ismail, M.R. Salim, T. Matsuura, A review of the effects of emerging contaminants in wastewater and options for their removal,

Desalination. 239 (2009) 229–246. doi:10.1016/j.desal.2008.03.020.

[94] Y. Yoon, P. Westerhoff, S.A. Snyder, E.C. Wert, Nanofiltration and ultrafiltration of endocrine disrupting compounds, pharmaceuticals and personal care products, J. Memb. Sci. 270 (2006) 88–100. doi:10.1016/j.memsci.2005.06.045.

[95] L. Braeken, B. Bettens, K. Boussu, P. Van der Meeren, J. Cocquyt, J. Vermant, B. Van der Bruggen, Transport mechanisms of dissolved organic compounds in aqueous solution during nanofiltration, J. Memb. Sci. 279 (2006) 311–319. doi:10.1016/j.memsci.2005.12.024.

[96] J. Lu, T. Zhang, J. Ma, Z. Chen, Evaluation of disinfection by-products formation during chlorination and chloramination of dissolved natural organic matter fractions isolated from a filtered river water, J. Hazard. Mater. 162 (2009) 140–145. doi:10.1016/j.jhazmat.2008.05.058.

[97] M.N. Chong, B. Jin, C.W.K. Chow, C. Saint, Recent developments in photocatalytic water treatment technology: a review., Water Res. 44 (2010) 2997–3027. doi:10.1016/j.watres.2010.02.039.

[98] D.H. Bremner, R. Molina, F. Martínez, J.A. Melero, Y. Segura, Degradation of phenolic aqueous solutions by high frequency sono-Fenton systems (US-Fe_2O_3/SBA-15-H_2O_2), Appl. Catal. B Environ. 90 (2009) 380–388. doi:10.1016/j.apcatb.2009.03.028.

[99] G. Li, Z. Wang, M. Yu, Z. Quan, J. Lin, Fabrication and optical properties of core-shell structured spherical SiO_2@$GdVO_4$:Eu^{3+} phosphors via sol-gel process, J. Solid State Chem. 179 (2006) 2698–2706. doi:10.1016/j.jssc.2006.05.019.

[100] J. Zhang, G. Xiao, F.X. Xiao, B. Liu, Revisiting one-dimensional TiO_2 based hybrid heterostructures for heterogeneous photocatalysis: A critical review, Mater. Chem. Front. 1 (2017) 231–250. doi:10.1039/c6qm00141f.

[101] Y. Cui, In-situ synthesis of C_3N_4/CdS composites with enhanced photocatalytic properties, Cuihua Xuebao/Chinese J. Catal. 36 (2015) 372–379. doi:10.1016/S1872-2067(14)60237-0.

[102] V.S. Kosera, T.M. Cruz, E.S. Chaves, E.R.L. Tiburtius, Journal of Photochemistry and Photobiology A : Chemistry Triclosan degradation by heterogeneous photocatalysis using ZnO immobilized in biopolymer as catalyst, "Journal Photochem. Photobiol. A Chem. 344 (2017) 184–191. doi:10.1016/j.jphotochem.2017.05.014.

[103] M.R. Hoffmann, S.T. Martin, W. Choi, D.W. Bahnemann, Environmental Applications of Semiconductor Photocatalysis, Chem. Rev. 95 (1995) 69–96. doi:10.1021/cr00033a004.

[104] J.-M. Herrmann, Water Treatment By Heterogeneous Photocatalysis, in: 1999: pp. 171–194. doi:10.1142/9781848160613_0009.

[105] U.I. Gaya, A.H. Abdullah, Heterogeneous photocatalytic degradation of organic contaminants over titanium dioxide: A review of fundamentals, progress and problems, J. Photochem. Photobiol. C Photochem. Rev. 9 (2008) 1–12. doi:10.1016/j.jphotochemrev.2007.12.003.

[106] M. Ni, M.K.H. Leung, D.Y.C. Leung, K. Sumathy, A review and recent developments in photocatalytic water-splitting using TiO_2 for hydrogen production, Renew. Sustain. Energy Rev. 11 (2007) 401–425. doi:10.1016/j.rser.2005.01.009.

[107] M. Yasmina, K. Mourad, S.H. Mohammed, C. Khaoula, Treatment heterogeneous photocatalysis; Factors influencing the photocatalytic degradation by TiO_2, Energy Procedia. 50 (2014) 559–566. doi:10.1016/j.egypro.2014.06.068.

[108] L. Cheng, Q. Xiang, Y. Liao, CdS-based photocatalysts Energy and Environmental Science, (2018) 4–7. doi:10.1039/c7ee03640j.

[109] M. Wongaree, S. Chiarakorn, S. Chuangchote, Photocatalytic Improvement under Visible Light in TiO_2 Nanoparticles by Carbon Nanotube Incorporation, 2015 (2015).

[110] R.S. Singh, V.K. Rangari, S. Sanagapalli, V. Jayaraman, S. Mahendra, V.P. Singh, Nano-structured CdTe, CdS and TiO_2 for thin film solar cell applications, Sol. Energy Mater. Sol. Cells. 82 (2004) 315–330.

doi:10.1016/j.solmat.2004.02.006.

[111] S. Leong, A. Razmjou, K. Wang, K. Hapgood, X. Zhang, H. Wang, TiO_2 based photocatalytic membranes: A review, J. Memb. Sci. 472 (2014) 167–184. doi:10.1016/j.memsci.2014.08.016.

[112] Y. Yu, J.C. Yu, J.G. Yu, Y.C. Kwok, Y.K. Che, J.C. Zhao, L. Ding, W.K. Ge, P.K. Wong, Enhancement of photocatalytic activity of mesoporous TiO2 by using carbon nanotubes, Appl. Catal. A Gen. 289 (2005) 186–196. doi:10.1016/j.apcata.2005.04.057.

[113] R. Abe, K. Sayama, H. Arakawa, Significant effect of iodide addition on water splitting into H_2 and O_2 over Pt-loaded TiO_2 photocatalyst: Suppression of backward reaction, Chem. Phys. Lett. 371 (2003) 360–364. doi:10.1016/S0009-2614(03)00252-5.

[114] S. Sakthivel, M. V. Shankar, M. Palanichamy, B. Arabindoo, D.W. Bahnemann, V. Murugesan, Enhancement of photocatalytic activity by metal deposition: Characterisation and photonic efficiency of Pt, Au and Pd deposited on TiO_2 catalyst, Water Res. 38 (2004) 3001–3008. doi:10.1016/j.watres.2004.04.046.

[115] E. Szabó-Bárdos, H. Czili, A. Horváth, Photocatalytic oxidation of oxalic acid enhanced by silver deposition on a TiO_2 surface, J. Photochem. Photobiol. A Chem. 154 (2003) 195–201. doi:10.1016/S1010-6030(02)00330-1.

[116] N.L. Wu, M.S. Lee, Enhanced TiO_2 photocatalysis by Cu in hydrogen production from aqueous methanol solution, Int. J. Hydrogen Energy. 29 (2004) 1601–1605. doi:10.1016/j.ijhydene.2004.02.013.

[117] F. Haque, T. Daeneke, K. Kalantar-zadeh, J.Z. Ou, Two-Dimensional Transition Metal Oxide and Chalcogenide-Based Photocatalysts, Nano-Micro Lett. 10 (2018) 1–27. doi:10.1007/s40820-017-0176-y.

[118] A.H. Reshak, S. Auluck, Electronic and optical properties of the 1T phases of TiS_2, $TiSe_2$, and $TiTe_2$, Phys. Rev. B - Condens. Matter Mater. Phys. 68 (2003) 1–7. doi:10.1103/PhysRevB.68.245113.

[119] J.A. Wilson, A.D. Yoffe, The transition metal dichalcogenides discussion and interpretation of the observed optical, electrical and structural properties, Adv.

Phys. 18 (1969) 193–335. doi:10.1080/00018736900101307.

[120] L. Nie, Q. Zhang, Recent progress in crystalline metal chalcogenides as efficient photocatalysts for organic pollutant degradation, Inorg. Chem. Front. 4 (2017) 1953–1962. doi:10.1039/c7qi00651a.

[121] F. Li, X. Liu, Q. Zhang, T. Kong, H. Jin, Fabrication and photocatalytic property of CuO nanosheets via a facile solution route, Cryst. Res. Technol. 47 (2012) 1140–1147. doi:10.1002/crat.201200143.

[122] B. Peng, P.K. Ang, K.P. Loh, Two-dimensional dichalcogenides for light-harvesting applications, Nano Today. 10 (2015) 128–137. doi:10.1016/j.nantod.2015.01.007.

[123] D. Ke, S. Liu, K. Dai, J. Zhou, L. Zhang, T. Peng, CdS/regenerated cellulose nanocomposite films for highly efficient photocatalytic H_2 production under visible light irradiation, J. Phys. Chem. C. 113 (2009) 16021–16026. doi:10.1021/jp903378q.

[124] S. Xiong, B. Xi, Y. Qian, CdS hierarchical nanostructures with tunable morphologies: Preparation and photocatalytic properties, J. Phys. Chem. C. 114 (2010) 14029–14035. doi:10.1021/jp1049588.

[125] W.T. Yao, S.H. Yu, S.J. Liu, J.P. Chen, X.M. Liu, F.Q. Li, Architectural control syntheses of CdS and CdSe nanoflowers, branched nanowires, and nanotrees via a solvothermal approach in a mixed solution and their photocatalytic property, J. Phys. Chem. B. 110 (2006) 11704–11710. doi:10.1021/jp060164n.

[126] Q. Shen, J. Xue, A. Mi, H. Jia, X. Liu, B. Xu, The study on properties of CdS photocatalyst with different ratios of zinc-blende and wurtzite structure, RSC Adv. 3 (2013) 20930–20935. doi:10.1039/c3ra42179a.

[127] M. Liu, B. Wang, Y. Zheng, F. Xue, Y. Chen, L. Guo, Transformation of zincblende nanoparticles into wurtzite microrods by a dissolution-regrowth process: An intergrowth homojunction with enhanced photocatalytic activity, Catal. Sci. Technol. 6 (2016) 3371–3377. doi:10.1039/c6cy00298f.

[128] K. Wu, H. Zhu, T. Lian, Ultrafast Exciton Dynamics and Light-Driven H2 Evolution in Colloidal Semiconductor Nanorods and Pt-Tipped Nanorods, Acc.

Chem. Res. 48 (2015) 851–859. doi:10.1021/ar500398g.

[129] J. Yu, Y. Yu, P. Zhou, W. Xiao, B. Cheng, Morphology-dependent photocatalytic H_2-production activity of CdS, Appl. Catal. B Environ. 156–157 (2014) 184–191. doi:10.1016/j.apcatb.2014.03.013.

[130] B. Weng, S. Liu, N. Zhang, Z.R. Tang, Y.J. Xu, A simple yet efficient visible-light-driven CdS nanowires-carbon nanotube 1D-1D nanocomposite photocatalyst, J. Catal. 309 (2014) 146–155. doi:10.1016/j.jcat.2013.09.013.

[131] F. Caruso, X. Shi, R.A. Caruso, A. Susha, Hollow titania spheres from layered precursor deposition on sacrificial colloidal core particles, Adv. Mater. 13 (2001) 740–744. doi:10.1002/1521-4095(200105)13:10<740::AID-ADMA740>3.0.CO;2-6.

[132] C. Li, L. Han, R. Liu, H. Li, S. Zhang, G. Zhang, Controlled synthesis of CdS micro/nano leaves with (0001) facets exposed: Enhanced photocatalytic activity toward hydrogen evolution, J. Mater. Chem. 22 (2012) 23815–23820. doi:10.1039/c2jm35415b.

[133] T. Tsuzuki, P.G. McCormick, Synthesis of CdS quantum dots by mechanochemical reaction, Appl. Phys. A Mater. Sci. Process. 65 (1997) 607–609. doi:10.1007/s003390050629.

[134] A. Dumbrava, G. Prodan, D. Berger, M. Bica, Properties of PEG-capped CdS nanopowders synthesized under very mild conditions, Powder Technol. 270 (2015) 197–204. doi:10.1016/j.powtec.2014.10.012.

[135] A. Samadi-maybodi, F. Abbasi, R. Akhoondi, Aqueous synthesis and characterization of CdS quantum dots capped with some amino acids and investigations of their photocatalytic activities, Colloids Surfaces A Physicochem. Eng. Asp. 447 (2014) 111–119. doi:10.1016/j.colsurfa.2014.01.036.

[136] P. Chandran, P. Kumari, S. Sudheer Khan, Photocatalytic activation of CdS NPs under visible light for environmental cleanup and disinfection, Sol. Energy. 105 (2014) 542–547. doi:10.1016/j.solener.2014.04.028.

[137] M. Darwish, A. Mohammadi, N. Assi, Microwave-assisted polyol synthesis and

characterization of pvp-capped cds nanoparticles for the photocatalytic degradation of tartrazine, Mater. Res. Bull. 74 (2016) 387–396. doi:10.1016/j.materresbull.2015.11.002.

[138] R.A. Devi, M. Latha, S. Velumani, G. Oza, P. Reyes-Figueroa, M. Rohini, I.G. Becerril-Juarez, J.-H. Lee, J. Yi, Synthesis and Characterization of Cadmium Sulfide Nanoparticles by Chemical Precipitation Method, J. Nanosci. Nanotechnol. 15 (2015) 8434–8439. doi:10.1166/jnn.2015.11472.

[139] G.C. De, A.M. Roy, S.S. Bhattacharya, Photocatalytic production of hydrogen and concomitant cleavage of industrial waste hydrogen sulphide, Int. J. Hydrogen Energy. 20 (1995) 127–131. doi:10.1016/0360-3199(94)P3692-V.

[140] W. Li, D. Li, Z. Chen, H. Huang, M. Sun, Y. He, X. Fu, High-efficient degradation of dyes by $Zn_xCd_{1-x}S$ solid solutions under visible light irradiation, J. Phys. Chem. C. 112 (2008) 14943–14947. doi:10.1021/jp8049075.

[141] F. Yang, N.N. Yan, S. Huang, Q. Sun, L.Z. Zhang, Y. Yu, Zn-doped CdS nanoarchitectures prepared by hydrothermal synthesis: Mechanism for enhanced photocatalytic activity and stability under visible light, J. Phys. Chem. C. 116 (2012) 9078–9084. doi:10.1021/jp300939q.

[142] T.K. Jana, A. Pal, K. Chatterjee, Self assembled flower like CdS-ZnO nanocomposite and its photo catalytic activity, J. Alloys Compd. 583 (2014) 510–515. doi:10.1016/j.jallcom.2013.08.184.

[143] D. Wu, F. Wang, Y. Tan, C. Li, Facile synthesis of NiS/CdS nanocomposites for photocatalytic degradation of quinoline under visible-light irradiation, RSC Adv. 6 (2016) 73522–73526. doi:10.1039/c6ra13439d.

[144] P. Nyamukamba, M.J. Moloto, H. Mungondori, Visible light-active CdS/TiO_2 hybrid nanoparticles immobilized on polyacrylonitrile membranes for the photodegradation of dyes in water, J. Nanotechnol. 2019 (2019). doi:10.1155/2019/5135618.

[145] S. Ma, J. Xie, J. Wen, K. He, X. Li, W. Liu, X. Zhang, Constructing 2D layered hybrid CdS nanosheets/MoS_2 heterojunctions for enhanced visible-light photocatalytic H_2 generation, Appl. Surf. Sci. 391 (2017) 580–591.

doi:10.1016/j.apsusc.2016.07.067.

[146] Q. Cai, Z. Hu, Q. Zhang, B. Li, Z. Shen, Fullerene (C_{60})/CdS nanocomposite with enhanced photocatalytic activity and stability, Appl. Surf. Sci. 403 (2017) 151–158. doi:10.1016/j.apsusc.2017.01.135.

[147] K.A. Adegoke, M. Iqbal, H. Louis, O.S. Bello, Synthesis, characterization and application of CdS/ZnO nanorod heterostructure for the photodegradation of Rhodamine B dye, Mater. Sci. Energy Technol. 2 (2019) 329–336. doi:10.1016/j.mset.2019.02.008.

[148] S. Cao, J. Yu, G-C_3N_4-based photocatalysts for hydrogen generation, J. Phys. Chem. Lett. 5 (2014) 2101–2107. doi:10.1021/jz500546b.

[149] J. Wen, J. Xie, X. Chen, X. Li, A review on g-C_3N_4 -based photocatalysts, Appl. Surf. Sci. 391 (2017) 72–123. doi:10.1016/j.apsusc.2016.07.030.

[150] E.A. Weiss, Designing the surfaces of semiconductor quantum dots for colloidal photocatalysis, ACS Energy Lett. 2 (2017) 1005–1013. doi:10.1021/acsenergylett.7b00061.

[151] K.R. Reddy, C.V. Reddy, M.N. Nadagouda, N.P. Shetti, S. Jaesool, T.M. Aminabhavi, Polymeric graphitic carbon nitride (g-C_3N_4)-based semiconducting nanostructured materials: Synthesis methods, properties and photocatalytic applications, J. Environ. Manage. 238 (2019) 25–40. doi:10.1016/j.jenvman.2019.02.075.

[152] S. Wang, C. Li, T. Wang, P. Zhang, A. Li, J. Gong, Controllable synthesis of nanotube-type graphitic C_3N_4 and their visible-light photocatalytic and fluorescent properties, J. Mater. Chem. A. 2 (2014) 2885–2890. doi:10.1039/c3ta14576j.

[153] B. Weng, S. Liu, Z. Tang, Y. Xu, RSC Advances One-dimensional nanostructure based materials for versatile photocatalytic applications, (2014) 12685–12700. doi:10.1039/c3ra47910b.

[154] J. Zhang, Y. Chen, X. Wang, Two-dimensional covalent carbon nitride nanosheets: Synthesis, functionalization, and applications, Energy Environ. Sci. 8 (2015) 3092–3108. doi:10.1039/c5ee01895a.

[155] X. Bai, L. Wang, R. Zong, Y. Zhu, Photocatalytic activity enhanced via g-C_3N_4 nanoplates to nanorods, J. Phys. Chem. C. 117 (2013) 9952–9961. doi:10.1021/jp402062d.

[156] Q. Han, B. Wang, J. Gao, Z. Cheng, Y. Zhao, Z. Zhang, L. Qu, Atomically Thin Mesoporous Nanomesh of Graphitic C_3N_4 for High-Efficiency Photocatalytic Hydrogen Evolution, ACS Nano. 10 (2016) 2745–2751. doi:10.1021/acsnano.5b07831.

[157] X. Zhang, X. Xie, H. Wang, J. Zhang, B. Pan, Y. Xie, Enhanced photoresponsive ultrathin graphitic-phase C_3N_4 nanosheets for bioimaging, J. Am. Chem. Soc. 135 (2013) 18–21. doi:10.1021/ja308249k.

[158] J. Senker, K. Schwinghammer, B. V. Lotsch, C. Ziegler, M.B. Mesch, V. Duppel, Crystalline Carbon Nitride Nanosheets for Improved Visible-Light Hydrogen Evolution, J. Am. Chem. Soc. 136 (2014) 1730–1733. doi:10.1021/ja411321s.

[159] B. Luo, G. Liu, L. Wang, Recent advances in 2D materials for photocatalysis, Nanoscale. 8 (2016) 6904–6920. doi:10.1039/c6nr00546b.

[160] P. Niu, L. Zhang, G. Liu, H.M. Cheng, Graphene-like carbon nitride nanosheets for improved photocatalytic activities, Adv. Funct. Mater. 22 (2012) 4763–4770. doi:10.1002/adfm.201200922.

[161] Q. Liu, T. Chen, Y. Guo, Z. Zhang, X. Fang, Ultrathin g-C_3N_4 nanosheets coupled with carbon nanodots as 2D/0D composites for efficient photocatalytic H2 evolution, Appl. Catal. B Environ. 193 (2016) 248–258. doi:10.1016/j.apcatb.2016.04.034.

[162] Y. Xu, S.P. Gao, Band gap of C_3N_4 in the GW approximation, Int. J. Hydrogen Energy. 37 (2012) 11072–11080. doi:10.1016/j.ijhydene.2012.04.138.

[163] K. Maeda, X. Wang, Y. Nishihara, D. Lu, M. Antonietti, K. Domen, Photocatalytic activities of graphitic carbon nitride powder for water reduction and oxidation under visible light, J. Phys. Chem. C. 113 (2009) 4940–4947. doi:10.1021/jp809119m.

[164] A.H. Reshak, AA- and ABA-stacked carbon nitride (C_3N_4): Novel photocatalytic

water splitting solar-to-hydrogen energy conversion, Phys. Chem. Chem. Phys. 20 (2018) 22972–22979. doi:10.1039/c8cp02898b.

[165] A.Y. Liu, M.L. Cohen, Prediction of new low compressibility solids, Science (80-.). 245 (1989) 841–842. doi:10.1126/science.245.4920.841.

[166] B. Jürgens, E. Irran, J. Senker, P. Kroll, H. Müller, W. Schnick, Melem (2,5,8-triamino-tri-s-triazine), an important intermediate during condensation of melamine rings to graphitic carbon nitride: Synthesis, structure determination by x-ray powder diffractometry, solid-state NMR, and theoretical studies, J. Am. Chem. Soc. 125 (2003) 10288–10300. doi:10.1021/ja0357689.

[167] J. Sehnert, K. Baerwinkel, J. Senker, Ab initio calculation of solid-state NMR spectra for different triazine and heptazine based structure proposals of g-C_3N_4, J. Phys. Chem. B. 111 (2007) 10671–10680. doi:10.1021/jp072001k.

[168] A. Thomas, A. Fischer, F. Goettmann, M. Antonietti, J.O. Müller, R. Schlögl, J.M. Carlsson, Graphitic carbon nitride materials: Variation of structure and morphology and their use as metal-free catalysts, J. Mater. Chem. 18 (2008) 4893–4908. doi:10.1039/b800274f.

[169] Y. Wang, J. Hong, W. Zhang, R. Xu, Carbon nitride nanosheets for photocatalytic hydrogen evolution: Remarkably enhanced activity by dye sensitization, Catal. Sci. Technol. 3 (2013) 1703–1711. doi:10.1039/c3cy20836b.

[170] H. Luo, Z. Zeng, G. Zeng, C. Zhang, R. Xiao, C. Zhou, H. Wang, Y. Zhou, S. Tian, Recent progress on metal-organic frameworks based- and derived-photocatalysts for water splitting, Chem. Eng. J. (2019) 123196. doi:10.1016/j.cej.2019.123196.

[171] D. Zheng, C. Pang, Y. Liu, X. Wang, Shell-engineering of hollow g-C_3N_4 nanospheres via copolymerization for photocatalytic hydrogen evolution , Chem. Commun. 51 (2015) 9706–9709. doi:10.1039/c5cc03143e.

[172] S.W. Bian, Z. Ma, W.G. Song, Preparation and characterization of carbon nitride nanotubes and their applications as catalyst supporter, J. Phys. Chem. C. 113 (2009) 8668–8672. doi:10.1021/jp810630k.

[173] L. Xu, J. Xia, L. Wang, H. Ji, J. Qian, H. Xu, K. Wang, H. Li, Graphitic carbon nitride nanorods for photoelectrochemical sensing of trace copper(II) ions, Eur. J. Inorg. Chem. (2014) 3665–3673. doi:10.1002/ejic.201402051.

[174] S. Hu, R. Jin, G. Lu, D. Liu, J. Gui, The properties and photocatalytic performance comparison of Fe^{3+}-doped g-C_3N_4 and Fe_2O_3/g-C_3N_4 composite catalysts, RSC Adv. 4 (2014) 24863–24869. doi:10.1039/c4ra03290j.

[175] Y. Wang, Y. Wang, Y. Li, H. Shi, Y. Xu, H. Qin, X. Li, Y. Zuo, S. Kang, L. Cui, Simple synthesis of Zr-doped graphitic carbon nitride towards enhanced photocatalytic performance under simulated solar light irradiation, Catal. Commun. 72 (2015) 24–28. doi:10.1016/j.catcom.2015.08.022.

[176] P. Fageria, R. Nazir, S. Gangopadhyay, H.C. Barshilia, S. Pande, Graphitic-carbon nitride support for the synthesis of shape-dependent ZnO and their application in visible light photocatalysts, RSC Adv. 5 (2015) 80397–80409. doi:10.1039/c5ra12463h.

[177] H. Yu, F. Chen, F. Chen, X. Wang, Applied Surface Science In situ self-transformation synthesis of g-C_3N_4 -modified CdS heterostructure with enhanced photocatalytic activity, Appl. Surf. Sci. 358 (2015) 385–392. doi:10.1016/j.apsusc.2015.06.074.

[178] F. Jiang, T. Yan, H. Chen, A. Sun, C. Xu, X. Wang, Applied Surface Science A g-C_3N_4 – CdS composite catalyst with high visible-light-driven catalytic activity and photostability for methylene blue degradation, Appl. Surf. Sci. 295 (2014) 164–172. doi:10.1016/j.apsusc.2014.01.022.

[179] Y. Guo, J. Wang, Z. Tao, F. Dong, K. Wang, X. Ma, P. Yang, P. Hu, Y. Xu, L. Yang, Facile synthesis of mesoporous CdS nanospheres and their application in photocatalytic degradation and adsorption of organic dyes, CrystEngComm. 14 (2012) 1185–1188. doi:10.1039/c2ce06172d.

[180] H.M. Xiong, D.G. Shchukin, H. Möhwald, Y. Xu, Y.Y. Xia, Sonochemical synthesis of highly luminescent zinc oxide nanoparticles doped with magnesium(II), Angew. Chemie - Int. Ed. 48 (2009) 2727–2731. doi:10.1002/anie.200805590.

[181] Z.R. Tang, X. Yin, Y. Zhang, Y.J. Xu, Synthesis of titanate nanotube-CdS nanocomposites with enhanced visible light photocatalytic activity, Inorg. Chem. 52 (2013) 11758–11766. doi:10.1021/ic4010483.

[182] Y. Li, L. Tang, S. Peng, Z. Li, G. Lu, Phosphate-assisted hydrothermal synthesis of hexagonal CdS for efficient photocatalytic hydrogen evolution, Cryst Eng Comm. 14 (2012) 6974–6982. doi:10.1039/c2ce25838b.

[183] M. Salavati-Niasari, M.R. Loghman-Estarki, F. Davar, Controllable synthesis of nanocrystalline CdS with different morphologies by hydrothermal process in the presence of thioglycolic acid, Chem. Eng. J. 145 (2008) 346–350. doi:10.1016/j.cej.2008.08.040.

[184] L.R. Zou, G.F. Huang, D.F. Li, J.H. Liu, A.L. Pan, W.Q. Huang, A facile and rapid route for synthesis of g-C_3N_4 nanosheets with high adsorption capacity and photocatalytic activity, RSC Adv. 6 (2016) 86688–86694. doi:10.1039/c6ra20514c.

[185] N. Chidhambaram, K. Ravichandran, Fabrication of ZnO/g-C_3N_4 nanocomposites for enhanced visible light driven photocatalytic activity Fabrication of ZnO/g-C_3N_4 nanocomposites for enhanced visible light driven photocatalytic activity, (n.d.).

[186] M. Iqbal, A. Ali, N.A. Nahyoon, A. Majeed, R. Pothu, S. Phulpoto, K.H. Thebo, Photocatalytic degradation of organic pollutant with nanosized cadmium sulfide, Mater. Sci. Energy Technol. 2 (2018) 41–45. doi:10.1016/j.mset.2018.09.002.

[187] S. Vadivel, D. Maruthamani, B. Paul, S.S. Dhar, K. Selvam, Facile synthesis of novel $CaFe_2O_4$/g-C_3N_4 nanocomposites for degradation of methylene blue under visible-light irradiation Journal of Colloid and Interface Science Facile synthesis of novel $CaFe_2O_4$/g-C_3N_4 nanocomposites for degradation of methyle, J. Colloid Interface Sci. 480 (2016) 126–136. doi:10.1016/j.jcis.2016.07.012.

[188] Z.X. Han, Z. Zhu, D.D. Wu, J. Wu, Y.R. Liu, Adsorption Kinetics and Thermodynamics of Acid Blue 25 and methylene blue dye solutions on natural sepiolite, Synth. React. Inorganic, Met. Nano-Metal Chem. 44 (2014) 140–147.

doi:10.1080/15533174.2013.770755.

[189] S. Kaur, A brief review on photocatalytic activity of ZnS and CQDs nanoparticles, Int. J. Eng. Appl. Sci. Technol. 2 (2017) 75–82. http://www.ijeast.com.

[190] M. Joshi, A. Bhattacharyya, S.W. Ali, Characterization techniques for nanotechnology applications in textiles, Indian J. Fibre Text. Res. 33 (2008) 304–317.

[191] R. Kohli, Methods for Monitoring and Measuring Cleanliness of Surfaces, in: Dev. Surf. Contam. Clean. - Detect. Charact. Anal. Contam., Elsevier, 2012: pp. 107–178. doi:10.1016/B978-1-4377-7883-0.00003-1.

[192] G. ZHANG, Master Thesis, University of Illinois at Urbana-Champaign, 2013, 2013.

[193] P.J. Mafa, A.T. Kuvarega, B.B. Mamba, B. Ntsendwana, Photoelectrocatalytic degradation of sulfamethoxazole on g-C_3N_4/BiOI/EG p-n heterojunction photoanode under visible light irradiation, Appl. Surf. Sci. 483 (2019) 506–520. doi:10.1016/j.apsusc.2019.03.281.

[194] M. Izadifard, G. Achari, C.H. Langford, Application of photocatalysts and LED light sources in drinking water treatment, Catalysts. 3 (2013) 726–743. doi:10.3390/catal3030726.

[195] C.G. Young, an Inductively Coupled Plasma Atomic Emission Spectrometer for the Detection of Nonmetals in the Vacuum Ultraviolet, 2011.

[196] A.M. Sabir, M. Moloy, P.S. Bhasin, Hplc Method Development and Validation: $_2$a Review, Int. Res. J. Pharm. 4 (2016) 39–46. doi:10.7897/2230-8407.04407.

[197] F. Jiang, T. Yan, H. Chen, A. Sun, C. Xu, X. Wang, A g-C_3N_4 -CdS composite catalyst with high visible-light-driven catalytic activity and photostability for methylene blue degradation, Appl. Surf. Sci. 295 (2014) 164–172. doi:10.1016/j.apsusc.2014.01.022.

[198] Z. Zhang, J. Huang, M. Zhang, Q. Yuan, B. Dong, Ultrathin hexagonal SnS nanosheets coupled with g-C_3N_4 nanosheets as 2D/2D heterojunction photocatalysts toward high photocatalytic activity, Appl. Catal. B Environ. 163

(2015) 298–305. doi:10.1016/j.apcatb.2014.08.013.

[199] A. Akhundi, A. Habibi-yangjeh, Novel magnetically separable g-C_3N_4/AgBr/Fe_3O_4 nanocomposites as visible-light-driven photocatalysts with highly enhanced activities, Ceram. Int. 41 (2015) 5634–5643. doi:10.1016/j.ceramint.2014.12.145.

[200] L.J. Cote, F. Kim, J. Huang, Langmuir-blodgett assembly of graphite oxide single layers, J. Am. Chem. Soc. 131 (2009) 1043–1049. doi:10.1021/ja806262m.

[201] Z. Zhou, J. Wang, J. Yu, Y. Shen, Y. Li, A. Liu, S. Liu, Y. Zhang, Dissolution and liquid crystals phase of 2D polymeric carbon nitride, J. Am. Chem. Soc. 137 (2015) 2179–2182. doi:10.1021/ja512179x.

[202] J. Xu, L. Zhang, R. Shi, Y. Zhu, Chemical exfoliation of graphitic carbon nitride for efficient heterogeneous photocatalysis, J. Mater. Chem. A. 1 (2013) 14766–14772. doi:10.1039/c3ta13188b.

[203] F. Dong, Z. Wang, Y. Sun, W.K. Ho, H. Zhang, Engineering the nanoarchitecture and texture of polymeric carbon nitride semiconductor for enhanced visible light photocatalytic activity, J. Colloid Interface Sci. 401 (2013) 70–79. doi:10.1016/j.jcis.2013.03.034.

[204] C. Li, Z. Sun, W. Huang, S. Zheng, Facile synthesis of g-C_3N_4/montmorillonite composite with enhanced visible light photodegradation of rhodamine B and tetracycline, J. Taiwan Inst. Chem. Eng. 66 (2016) 363–371. doi:10.1016/j.jtice.2016.06.014.

[205] J. Tong, L. Zhang, F. Li, K. Wang, L. Han, S. Cao, Rapid and high-yield production of g-C_3N_4 nanosheets via chemical exfoliation for photocatalytic H_2 evolution, RSC Adv. 5 (2015) 88149–88153. doi:10.1039/c5ra16988g.

[206] J. Zhu, P. Xiao, H. Li, S.A.C. Carabineiro, Graphitic carbon nitride: Synthesis, properties, and applications in catalysis, ACS Appl. Mater. Interfaces. 6 (2014) 16449–16465. doi:10.1021/am502925j.

[207] Y. Chen, X. Wang, Template-Free Synthesis of Hollow G-C_3N_4 Polymer with Vesicle Structure for Enhanced Photocatalytic Water Splitting, (2018).

doi:10.1021/acs.jpcc.7b12496.

[208] H.B. Tao, H. Bin Yang, J. Chen, J. Miao, B. Liu, Biomolecule-assisted synthesis of carbon nitride and sulfur-doped carbon nitride heterojunction nanosheets: An efficient heterojunction photocatalyst for photoelectrochemical applications, Beilstein J. Nanotechnol. 5 (2014) 770–777. doi:10.3762/bjnano.5.89.

[209] J. Tong, L. Zhang, F. Li, K. Wang, L. Han, S. Cao, Rapid and high-yield production of g-C_3N_4 nanosheets via chemical exfoliation for photocatalytic H_2 evolution, RSC Adv. 5 (2015) 88149–88153. doi:10.1039/c5ra16988g.

[210] S. Asadzadeh-khaneghah, A. Habibi-yangjeh, S. Vadivel, Journal of the Taiwan Institute of Chemical Engineers Fabrication of novel g-C_3N_4 nanosheet/carbon dots/$Ag_6Si_2O_7$ nanocomposites with high stability and enhanced visible-light photocatalytic activity, J. Taiwan Inst. Chem. Eng. 103 (2019) 94–109. doi:10.1016/j.jtice.2019.07.018.

[211] G. Mamba, A.K. Mishra, Applied Catalysis B : Environmental Graphitic carbon nitride (g-C_3N_4) nanocomposites : A new and exciting generation of visible light driven photocatalysts for environmental pollution remediation, "Applied Catal. B, Environ. 198 (2016) 347–377. doi:10.1016/j.apcatb.2016.05.052.

[212] J. Jin, J. Yu, G. Liu, P.K. Wong, Single crystal CdS nanowires with high visible-light photocatalytic H_2-production performance, J. Mater. Chem. A. 1 (2013) 10927–10934. doi:10.1039/c3ta12301d.

[213] S. Rengaraj, A. Ferancova, S.H. Jee, S. Venkataraj, Y. Kim, J. Labuda, M. Sillanpää, Physical and electrochemical characterization of CdS hollow microspheres prepared by a novel template free solution phase method, Electrochim. Acta. 56 (2010) 501–509. doi:10.1016/j.electacta.2010.09.019.

[214] J. Fu, B. Chang, Y. Tian, F. Xi, X. Dong, Novel C_3N_4-CdS composite photocatalysts with organic-inorganic heterojunctions: In situ synthesis, exceptional activity, high stability and photocatalytic mechanism, J. Mater. Chem. A. 1 (2013) 3083–3090. doi:10.1039/c2ta00672c.

[215] Q. Li, B. Guo, J. Yu, J. Ran, B. Zhang, H. Yan, J.R. Gong, Highly efficient

visible-light-driven photocatalytic hydrogen production of CdS-cluster-decorated graphene nanosheets, J. Am. Chem. Soc. 133 (2011) 10878–10884. doi:10.1021/ja2025454.

[216] V. Mohanraj, R. Jayaprakash, R. Robert, J. Balavijayalakshmi, S. Gopi, Effect of particle size on optical and electrical properties in mixed CdS and NiS nanoparticles synthesis by ultrasonic wave irradiation method, Mater. Sci. Semicond. Process. 56 (2016) 394–402. doi:10.1016/j.mssp.2016.08.014.

[217] N.H. Patel, M.P. Deshpande, S.H. Chaki, H.R. Keharia, Tuning of optical, thermal and antimicrobial capabilities of CdS nanoparticles with incorporated Mn prepared by chemical method, J. Mater. Sci. Mater. Electron. 28 (2017) 10866–10876. doi:10.1007/s10854-017-6865-y.

[218] A. Modwi, M.A. Ghanem, A.M. Al-Mayouf, A. Houas, Lowering energy band gap and enhancing photocatalytic properties of Cu/ZnO composite decorated by transition metals, J. Mol. Struct. 1173 (2018) 1–6. doi:10.1016/j.molstruc.2018.06.082.

[219] Q. Tang, C. Zhou, X. Yuan, Q. Jing, Y. Mu, A. Du, Facile Synthesis of g-C_3N_4 Nanosheets/ZnO Nanocomposites with Enhanced Photocatalytic Activity in Reduction of Aqueous Chromium(VI) under Visible Light, Nanomaterials. 6 (2016) 173. doi:10.3390/nano6090173.

[220] D. Wang, Z. Xu, Q. Luo, X. Li, J. An, R. Yin, C. Bao, Preparation and visible-light photocatalytic performances of g-C_3N_4 surface hybridized with a small amount of CdS nanoparticles, J. Mater. Sci. 51 (2016) 893–902. doi:10.1007/s10853-015-9417-y.

[221] A. Kumar, A Review on the Factors Affecting the Photocatalytic Degradation of Hazardous Materials, Mater. Sci. Eng. Int. J. 1 (2017) 1–10. doi:10.15406/mseij.2017.01.00018.

[222] S. Talebi, N. Chaibakhsh, Z. Moradi-Shoeili, Application of nanoscale ZnS/TiO_2 composite for optimized photocatalytic decolorization of a textile dye, J. Appl. Res. Technol. 15 (2017) 378–385. doi:10.1016/j.jart.2017.03.007.

[223] Y.S. Al-Degs, M.I. El-Barghouthi, A.H. El-Sheikh, G.M. Walker, Effect of

solution pH, ionic strength, and temperature on adsorption behavior of reactive dyes on activated carbon, Dye. Pigment. 77 (2008) 16–23. doi:10.1016/j.dyepig.2007.03.001.

[224] E.T. Helmy, A. El Nemr, M. Mousa, E. Arafa, S. Eldafrawy, Photocatalytic degradation of organic dyes pollutants in the industrial textile wastewater by using synthesized TiO_2, C-doped TiO_2, S-doped TiO_2 and C,S co-doped TiO_2 nanoparticles, J. Water Environ. Nanotechnol. 3 (2018) 116–127. doi:10.22090/JWENT.2018.02.003.

[225] E. Mugunthan, M.B. Saidutta, P.E. Jagadeeshbabu, Visible light assisted photocatalytic degradation of diclofenac using TiO_2-WO_3 mixed oxide catalysts, Environ. Nanotechnology, Monit. Manag. 10 (2018) 322–330. doi:10.1016/j.enmm.2018.07.012.

[226] S. Iguchi, K. Teramura, S. Hosokawa, T. Tanaka, Effect of the chloride ion as a hole scavenger on the photocatalytic conversion of CO_2 in an aqueous solution over Ni-Al layered double hydroxides, Phys. Chem. Chem. Phys. 17 (2015) 17995–18003. doi:10.1039/c5cp02724a.

[227] L. Das, S.K. Barodia, S. Sengupta, J.K. Basu, Aqueous degradation kinetics of pharmaceutical drug diclofenac by photocatalysis using nanostructured titania–zirconia composite catalyst, Int. J. Environ. Sci. Technol. 12 (2015) 317–326. doi:10.1007/s13762-013-0466-y.

[228] J.M. Monteagudo, H. El-taliawy, A. Durán, G. Caro, K. Bester, Sono-activated persulfate oxidation of diclofenac: Degradation, kinetics, pathway and contribution of the different radicals involved, J. Hazard. Mater. 357 (2018) 457–465. doi:10.1016/j.jhazmat.2018.06.031.

[229] T. Huang, G. Zhang, S. Chong, Y. Liu, N. Zhang, S. Fang, J. Zhu, Effects and mechanism of diclofenac degradation in aqueous solution by US/Zn0, Ultrason. Sonochem. 37 (2017) 676–685. doi:10.1016/j.ultsonch.2017.02.032.

[230] M. V. Bagal, P.R. Gogate, Degradation of diclofenac sodium using combined processes based on hydrodynamic cavitation and heterogeneous photocatalysis, Ultrason. Sonochem. 21 (2014) 1035–1043. doi:10.1016/j.ultsonch.2013.10.020.

[231] P. Sathishkumar, R.A.A. Meena, T. Palanisami, V. Ashokkumar, T. Palvannan, F.L. Gu, Occurrence, interactive effects and ecological risk of diclofenac in environmental compartments and biota - a review, Sci. Total Environ. 698 (2020) 134057. doi:10.1016/j.scitotenv.2019.134057.

[232] R.R. Giri, H. Ozaki, S. Ota, R. Takanami, S. Taniguchi, Degradation of common pharmaceuticals and personal care products in mixed solutions by advanced oxidation techniques, Int. J. Environ. Sci. Tech. 7 (2010) 251–260. doi:10.1007/BF03326135.

[233] S. Sébastien, Les soignants face à la mort, Rev. Infirm. 1 (2012) 39–41.

[234] H. Xu, L. Wu, L. Jin, K. Wu, Combination Mechanism and Enhanced Visible-Light Photocatalytic Activity and Stability of CdS/g-C_3N_4 Heterojunctions, J. Mater. Sci. Technol. 33 (2017) 30–38. doi:10.1016/j.jmst.2016.04.008.

[235] I.W. As, M.C. Level, P.H. Effects, T. Methods, I. Exchange, R. Osmosis, WQA Technical Fact Sheet: Cadmium health effects treatment methods Residential Point-of-Entry Point-of-Use, 2013. http://www.epa.gov/safewater/pdfs/factsheets/ioc/cadmium.pdf.

CHAPTER 2
LITERATURE REVIEW

2.1 Introduction

Fresh water supply is declining slowly [2]. Population growth, rapid industrialization, increased living standards and urbanization are some of the contributing factors to the decline. Manufacturing industries have been identified as posing a threat to fresh water availability water as they discharge large volumes of toxic effluents. Water is a vital resource with important application in agriculture, fishing, energy production, transportation, tourism and is also important in the growth and sustenance of the economy. Clean water is important for a healthy lifestyle and everyone has the right to access safe drinking water. However, this vital resource is compromised daily due to pollution from human activities [43,44]. Therefore, there is a growing need for water reuse. There is a growing need for the development of water treatment technologies capable of completely removing pollutants in water specifically organic pollutants such as textile dyes and pharmaceuticals and possibly save human life and the ecosystem [45].

This chapter provides details on dye pollutants and emerging pollutants and their impacts on water quality. Advanced oxidation processes and details on heterogeneous catalysis are highlighted. Synthetic approaches that have been used to develop some of the semiconductors photocatalyst

2.2 Organic pollutants

Organic pollutants include dyes, humic substances, phenolic compounds, petroleum surfactants and new emerging pollutants (pesticides, pharmaceuticals and personal care products). These pollutants are mainly from industries or improper disposal from households through flushing down the toilet or through the drain. These organic pollutants are toxic to the environment and living organisms and tend to bio-accumulate once released into the environment even in trace quantities. Their toxicity is not limited to the current generation but maybe passed to the next generation thus potentially causing gene mutations, birth defects and inherited diseases. They also tend to result in more toxic by-products during disinfection and

therefore the need for the development of treatment technologies that will reduce pollutant load in water and also result in sustainable treatment of the polluted water.

2.2.1 Dye pollutants

Synthetic dyes are widely used in the textile, leather, plastic, pharmaceuticals, cosmetic, food and many other industries [13,46]. There are over 100000 dyes commercially available producing over 7 x 10^5 metric tons per year [47,48]. The textile industry is responsible for two-thirds of the dying industry and about 2-5% of the dyes remain unused and end up in wastewater effluents [48–50]. The synthetic dyes are discharged directly from the industries into the environment and their effluents have been identified as one of the toughest wastewaters to be treated, affecting the aesthetic merit, water limpidness, and gas solubility of the water bodies [51,52]. They are toxic to human health causing skin ulceration, nausea and dermatitis and have a high chemical, and biological oxygen demand, suspended solids, and intense colour which makes dyes difficult to treat [53]. They also have big aromatic molecular structures making them more stable and hard to degrade [54]. Their presence in water also reduces light penetration and thus affecting the photosynthesis activity of aquatic life [49]. Dyes can either: be anionic (direct) acid and reactive dyes, cationic (basic) or non-ionic dispersive. Anionic and non-ionic dyes are mainly classified as azo and anthraquinone dyes. Reactive dyes have reactive groups and examples include vinyl sulfone (VS), chlorotrainzine (CT), trichloropyrimidine (TCP), Difluorochloropyrimidine (DFCP), acid orange (AO), acid blue 25 (AB-25), phenol red (PR) and rose bengal (RB). In textile dying, they bind to the fibres by their reactive groups through covalent bonding. Most of these dyes are also water soluble and exist in their hydrolysed forms [55–57]. After the dyeing process, approximately 50% of the unbound reactive dyes remain in wastewater. While anthraquinone dyes vary from red to green-blue dyes, the simple anthraquinone dyes are very bright. They are the second most used dyes after the azo dyes as they are cheap and easily accessible. Anthraquinone dyes are relatively stable under dyeing conditions, they have combined aromatic structures and their colour remains in wastewater for a long time which makes them hard to degrade [58–60]. Different anthraquinone dyes are obtained by changing the substituent groups such as amino, hydroxyl, halogen and sulfonic acid. The electron donating

and electron accepting nature of the anthraquinone dye can affect the color of the dyes, for example electron donating amino groups or substituted amino groups can result in change in the color of the dye from yellow to red, purple or blue [61]. Table 2.1 shows the different anthraquinone dyes and their structures [60].

Table 2.1. Chemical structure and categories of anthraquinone dyes [21].

Dye	Structure	Category
Anthraquinone Yellow(AY)	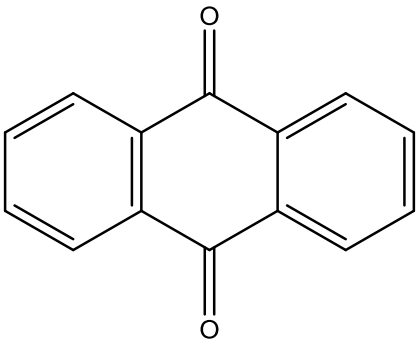	Anthraquinone derivatives
1-Amino-4-(Methyl amino) anthracene-9,10-dione blue	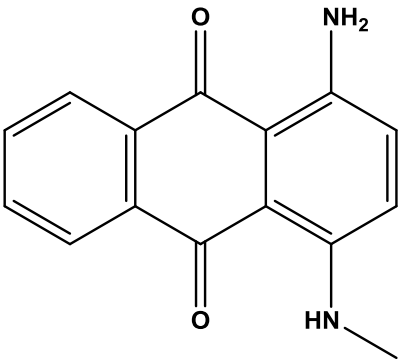	Anthraquinone derivatives
Dispersive Red 3B	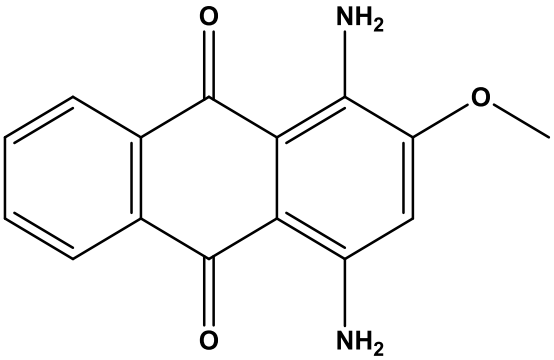	Anthraquinone

Vat Yellow 28	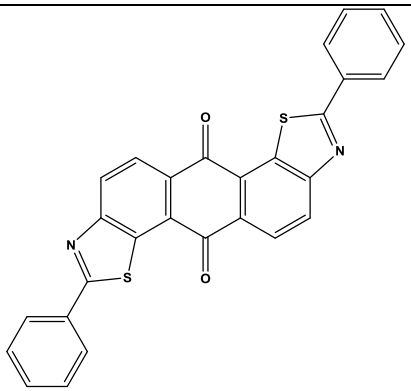	Heterocyclic anthraquinone
Vat green 1	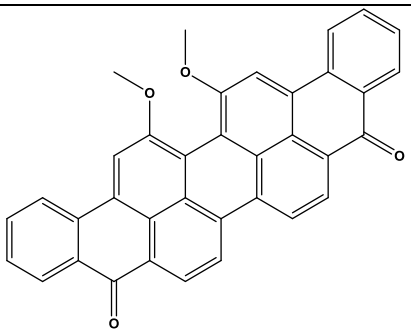	Fused ring Anthrone
Acid blue 25	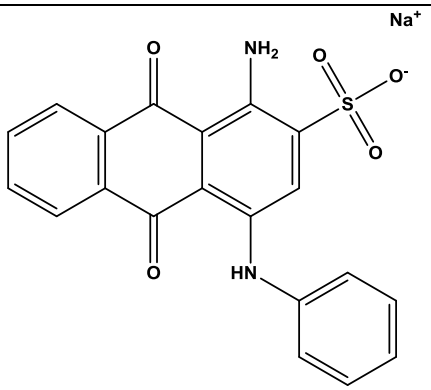	Anthraquinone

2.2.1.1 Acid blue 25

Among the many anthraquinone dyes, Acid Blue 25 (sodium; 1-amino-4-anilino-9, 10-dioxoanthracene-2-sulfonate) has a widespread applications in a number of industries. It is used for dying of wools, nylon, silk, paper, ink, aluminium, detergents, wood, cosmetics and biologicals [62]. Like most Acid dyes it is applied on fabrics at pH range 3-7 [63] and it is generally used as a model compound for removal of anthraquinone dyes from aqueous solutions.

2.2.1.2 Acid blue in the environment

The long-time exposure of AB-25 is toxic to human health as it may cause respiratory problems caused by inhalation of the dye particles skin and eye irritation.

It may also affect the immune system of humans hence its selection as a model organic compound in the current study [64].

2.2.2 Emerging pollutants

Emerging pollutants are chemical pollutants that have been identified to have potential toxicity to the environment and human health. The EU water framework directive 2000/06/CE identifies 33 substances as potential emerging pollutants. These include pesticides, pharmaceuticals, phthalates and personal care products. The major problem with emerging pollutants is the lack of knowledge on their short term or long term effect on the aquatic environment and human health [65]. They are discharged into the environment by different activities such as disposal through municipal, industrial and agricultural waste. They are often present in wastewater treatment plants (WWTPs), surface, ground and drinking water suppliers [66,67]. Among the above-mentioned pollutants, pharmaceuticals (PhACs) are the most recently studied emerging pollutants to date. They are defined as prescription, therapeutic and non-prescribed drugs used to treat and prevent diseases in animals and humans [68].They are highly used and their demand continues to increase as new diseases emerge and are thus continuously released into the environment [22]. They are often discharged to the environment through incorrect disposal and excretion as metabolites through WWTPs [23]. The Environmental Agency (EA) of England and Wales introduced a ranking system of PhACs and personal care products (PCPs) to reduce the potential risks to the aquatic environment. Most of these PhACs are detected in very low concentrations in fresh water however, many are biologically active and affect non-target aquatic organisms [69,70].

Drugs such as Ibuprofen, iopamidol, and carbamazepine have been identified as the most widely used pharmaceuticals and are priority pollutants as they cannot be easily degraded due to their complex structures [71].

2.2.2.1 Diclofenac sodium

Diclofenac (DFC) (sodium: 2-(2, 6-dichloranilino) phenyl acetate (Fig. 2.1) is an anti-inflammatory drug and most widely used pharmaceuticals (PhACs) around the world. It is produced in large quantities (100 tons annually) and is used in the form of

tablets, capsules, suppositories, ointments and gels for dermal applications, Palmer., 2012 reported that diclofenac is the 12th bestselling generic molecule globally [72].The Intercontinental Market Services (IMS) estimated that 940 tons of DFC are consumed globally annually [73]. In 2007 alone about 877 tons of DFC were sold in countries including European countries and believed to account for 96% of the D FC global pharmaceutical market [73]. Recently it was reported on the Intercontinental Marketing Statistical (IMS) health data (serving 82% of the global population) which included 86 countries estimating that an average of 1443 tons of DFC is consumed globally [74]. This is an indication of how much of DFC is consumed globally and the potential effects it has on the environment in terms of production.

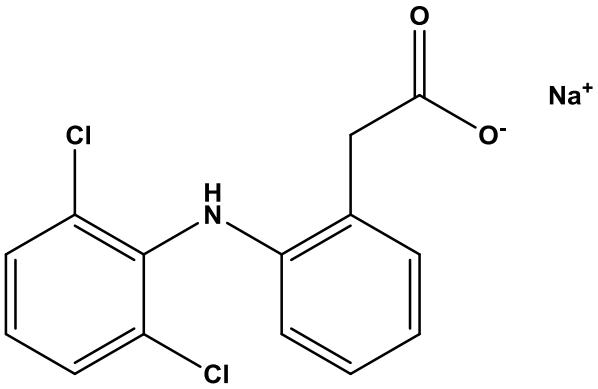

Figure 2.1.Chemical structure of Diclofenac [37].

In 2013 DFC was included in the watch list of the EU Waster Frame Directive to determine the risk management measurements. Few countries imposed regulatory measures for the use of DFC. However there are no strict legislations or laws in place to govern the production and consumption of DFC, since DFC recently raised environmental concerns [75].

2.2.2.2 Diclofenac in the Environment

The source of DFC is from the pharmaceutical industry and is used for human and veterinary purposes and excreted as diclofenac and its metabolites. They are then released to the wastewater treatment plants (WWTP) or landfills [76]. Because the conventional treatment technologies are not effective, the untreated DFC and other pollutants are then released to surface water and into drinking water supplies and other water bodies (Figure. 2.3.) Low concentrations of 0.42 μgL^{-1} and 5.45 μgL^{-1} have been detected in both surface water and WWTPs respectively [77,78].

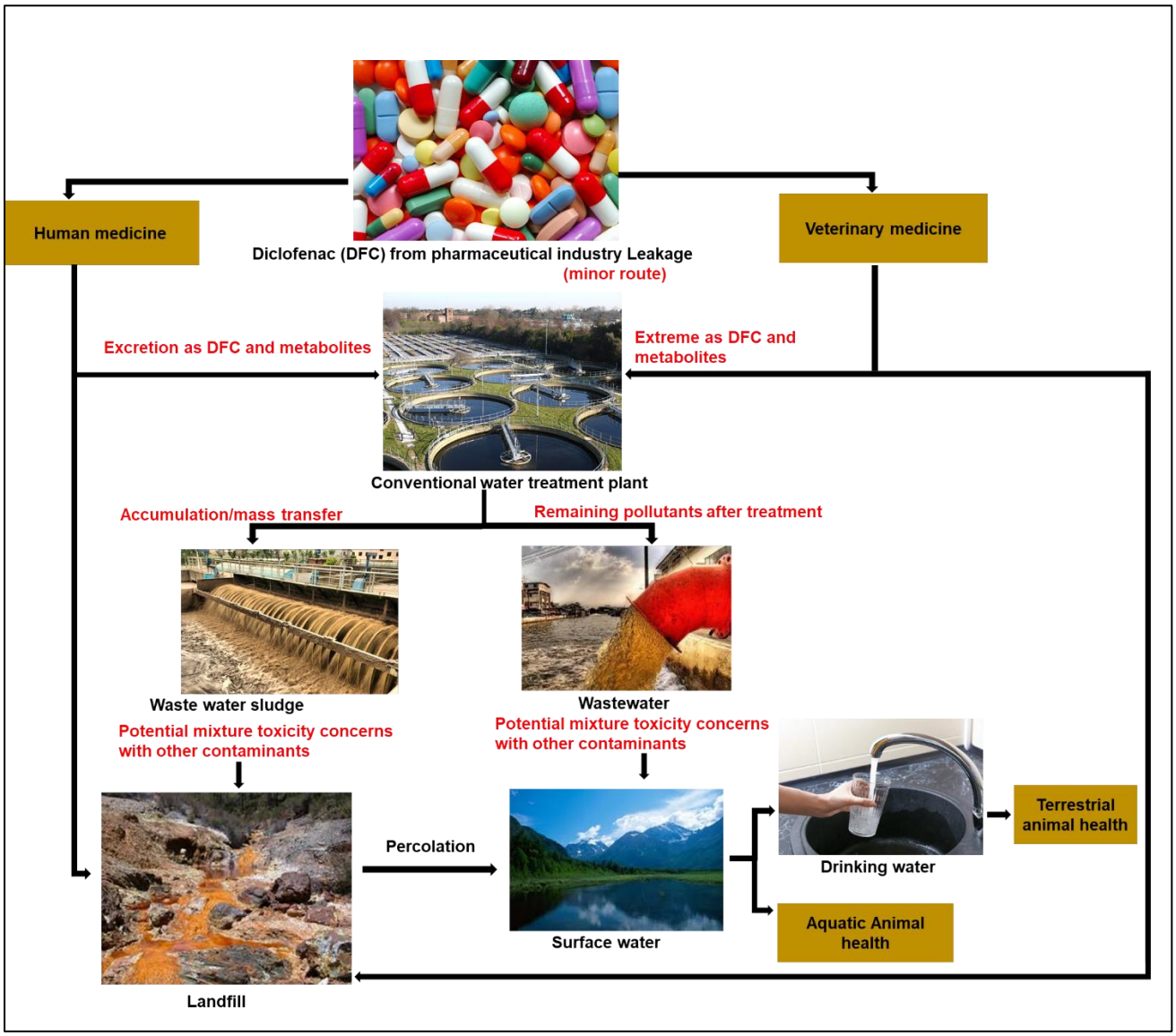

Figure 2.2.Entry pathways of DFC [34].

Although DFC is detected in low concentrations (from ng to μgL^{-1}), it has been reported to cause a decline in vulture populations in Western Asia [79]. It was also reported that ng/L sub-chronic exposure of DFC could interfere with the biochemical functions of species and also cause tissue damage of fish [79]. The long term exposure of DFC with concentrations (10-20 µg) could induce cytological alterations of rainbow trout [18]. Letzel et al. reported that DFC at relatively low concentrations of ngL^{-1} may cause chronic effects on fish [80]. DFC concentration of 4 mg L^{-1} was reported to alter the gene expression of Vitellogenin (VTG) in the liver of laptides fish, thereby showing estrogenic effects [28,81]. DFC has been detected globally and has raised concerns globally. However most of the reports and detection of DFC has

been reported from EU countries and North America, while in Asia the reported data is low to predict the environment concentrations because there was no systematic reported annual data [82]. Other countries that have reported on the presence of DFC in WWTP are Canada, Germany and America where it was even detected in drinking water [83,84]. In South Africa there are few reports on the detection of DFC with concentration in the range of f1.1 to 15.6 µg L^{-1} in the WWTP effluent in Kwazulu-Natal Province river systems [85]. Archer et al., 2017 reported on DFC in the Gauteng Province surface water and WWTW [28]. Table .2.1 shows the summary on detection of DFC in South Africa.

Table 2.2. Detection of DFC in South Africa WWTWs and surface water [45].

Concentration (µg/L	**Province**	**Sources**	**References**
1.1-15.6	Kwazulu-Natal	Surface water	Agunbiade and Moodley, 2014
222.7	Kwazulu-Natal	WWTW effluent	Agunbiade and Moodley, 2016
123.7	Kwazulu-Natal	WWTW effluent	Agunbiade and Moodley, 2016
0.6-8.2	Kwazulu-Natal	Surface water	Agunbiade and Moodley, 2016
2.7-5.6	Gauteng	WWTW effluent	Archer et al, 2017a
2.2-2.5	Gauteng	WWTW effluent	Archer et al.,2017a
0.3-2.2	Gauteng	Surface water	Archer et al.,2017a

2.3 Conventional Water treatment methods

The conventional waste water treatment plants have been proven not to be effective in treating and complete removal of organic pollutants such as organic dyes, and emerging pollutants in polluted water. Traditional treatment technologies such as use of activated carbon, oxidation, biological methods, nanofiltration (NF) and reverse osmosis RO) membranes result in secondary pollution and are energy intensive in addition to expertise engineering requirements [86]. Biological processes are not able to remove complex pollutants such as emerging pollutants as they are resistant

to biological oxidation. [87,88]. Physiochemical treatment methods including coagulation, flocculation and lime softening are not effective in removal of pharmaceuticals and endocrine disruptors [89–91]. Chlorination kills bacteria and pathogens but results in undesirable taste and odour [92]. Ozonation is an expensive treatment method and has a short life span. Membrane processes which include microfiltration (MF), ultrafiltration (UF), NF and RO have proved to be successful in removal of many organic pollutants in water however they are expensive and energy intensive and often tend to foul over time [93–95].

2.3.1 Advanced oxidation processes (AOPs)

Advanced oxidation processes (AOPs) are alternative treatment technologies for wastewater treatment. They are inexpensive, eco-friendly and effective for removal of organic pollutants in water [96]. Types of AOPs include Fenton reactions, sonolysis, ozonation and heterogeneous photocatalysis [97,98]. Photocatalysis is a sub-class of AOPs based on the generation of highly reactive and non-selective chemical oxidants (i.e. $^{\bullet}OH$, $^{\bullet}O_2^-$ O_2) which are strongly oxidizing and can degrade pollutants into nontoxic products such as carbon dioxide and water [12]. [7]

2.3.1.1 Heterogeneous photocatalysis

Heterogeneous photocatalysis is the acceleration of a reaction in the existence of light and a catalyst to effectively degrade organic pollutants such as pharmaceuticals, personal care products, pesticides and organic dyes [99]. It has advantages that include (i) ambient temperature operation, (ii) complete mineralization of pollutants without producing secondary pollutants and (iii) cost effectiveness which are feasible in waste water treatment [100] . However photocatalysis has limitations of photostability of the semiconductor catalyst under operational conditions, which often results in corrosion of the semiconductor [101–104].

The important aspect in heterogeneous photocatalysis mechanism is the generation of active species which are hydroxyl radicals ($^{\bullet}OH$) and superoxide radicals ($^{\bullet}O_2$), hydrogen peroxide (H_2O_2) and oxygen (O_2) all known as reactive oxygen species

(ROS). However the •O_2 and •OH play important roles in the photocatalytic process compared to the H_2O_2 and O_2 as they are readily produced (Figure. 2.3).

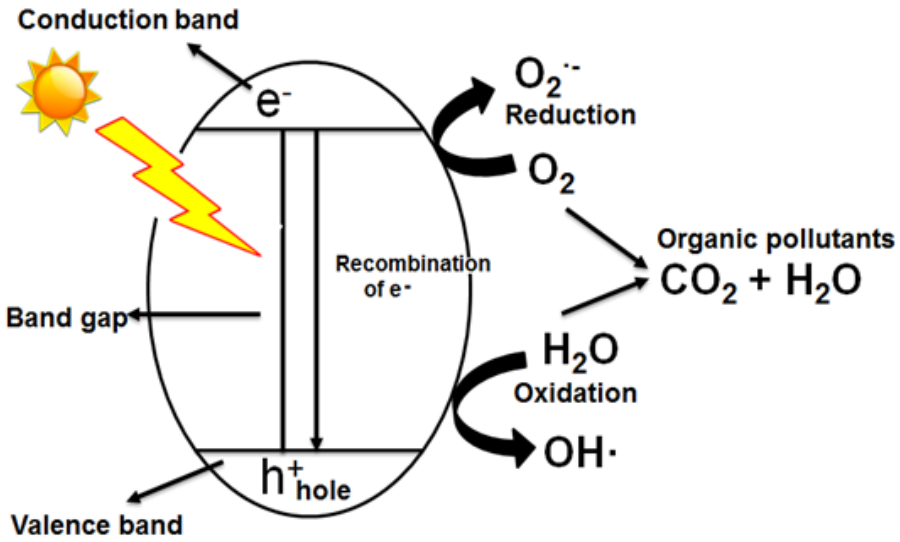

Figure 2.3.Schematic diagram of photocatalysis mechanism [71]

During photocatalysis, a semiconductor is absorbs light of certain energy equal to or higher than the semiconductor energy gap, this causes electrons to move from the valence band (VB) to the conduction band (CB) and leaves holes on the valence band which migrate to the surface and scavenge hydroxyl and water molecules to form hydroxyl radicals which are strong oxidizing and initiate degradation of pollutants. The excited electrons then react with dissolved oxygen at the conduction band and result in formation of super peroxide ions and result in redox reactions.

Catalyst activation by light

$$\text{Semiconductor} + hv \rightarrow \text{Semiconductor}\ (e^-_{CB} + h^+_{VB})$$

Oxidation process: The generated positive holes migrate to the surface of the catalyst and react with oxygen or water to form free radicals. The radicals degrade the pollutants which can accept or donate electrons. The photocatalysis process is divided in the following 4 stages[105–107]:

$$\text{Semiconductor}\ (h^+_{VB}) + H_2O \rightarrow \text{Semiconductor} + H^+ + OH^\bullet$$

$$\text{Semiconductor}\ (h^+_{VB}) + OH^- \rightarrow \text{Semiconductor} + OH^\bullet$$

Reduction Process: the excited electrons react with dissolved oxygen to form super peroxide ions and result in a series of redox reactions

$$\text{Semiconductor } (e^-_{CB}) + O_2 \rightarrow \text{Semiconductor} + O^{\bullet -}_2$$

$$O^{\bullet -}_2 + H+ \rightarrow HO^{\bullet}_2$$

$$HO^{\bullet}_2 + HO^{\bullet}_2 \rightarrow H_2O_2 + O_2$$

$$H_2O_2 + O^{\bullet -} \rightarrow OH^{\bullet} + OH^- + O_2$$

$$\text{Pollutant} + OH^{\bullet} \rightarrow \text{Degradation products}$$

The degradation capacity of the semiconductor catalyst depends on the nature and power of the light source, the amount of active sites of the semiconductor catalysts that are present in the reaction medium, the amount of water to produce the hydroxyl radicals and the concentration of the pollutants.

2.4 Semiconductor photocatalysis

2.4.1 TiO_2 semiconductor photocatalysis

There are a variety of semiconductors that have been used for water treatment. TiO_2 is one of the most widely studied semiconductor catalyst due to its superior properties such as inexpensive, durability, low toxicity, super hydrophilicity, chemical and photochemical stability [108]. However it has the disadvantage of recombination of electron hole pairs and it can only absorb UV light having a wavelength smaller than 387 nm which accounts for about 3-5% of the solar spectrum, this is due to its narrow energy gap of (3.2eV) and hence the application of TiO_2 under visible light (sunlight) is restricted [109–111].

The use of UV radiation to activate TiO_2 can be expensive and hence much effort has been focused on improving the properties of TiO_2 to make it an ideal material in water treatment applications. The most common modification strategies include doping with dye sensitizers, coupling with short bandgap semiconductors, and doping with transition metals [97]. In one study TiO_2 was coupled with carbon nanotubes (CNTs) to enhance its photocatalytic activity, the nanocomposite resulted in prolonged lifetime of electron-hole pairs through capturing the electron within the

CNTs structure [112]. Dye sensitizers help provide additional electrons to the conduction band and enhance the formation of electron-holes [106]. The photocatalytic efficiency of TiO_2 has been widely enhanced through the use of metals such as Pt, Au, Rh, Ni, Cu, and Ag and have effectively transferred electrons from the conduction band of TiO_2 to the metal particles deposited on the TiO_2 surface, they reduced the recombination of electron hole pairs and increased photocatalytic activity [113–116]. A study was reported on the enhancement of the photocatalytic activity of TiO_2 by deposition of metals such as Pt, Au and Pd for the photo-excitation of acid green 16 (AG-16) in aqueous solution and the noble metals enhanced the photocatalytic efficiency of TiO_2 and inhibited recombination of electron-hole pairs and complete removal of (AG-16) was achieved within 30 min [114]

2.4.2 Chalcogenide semiconductors

Chalcogenide semiconductors contain elements in the groups 16 or VI. Metal chalcogenides contain at least one chalcogen anion, and one electropositive metal element. Most elements from group VI_A are referred to as chalcogens. However, metal chalcogenides refers to compounds containing sulphides, selenides and tellurides. [117]. The metallic character of these elements increase in descending order of the group VI_A elements of the periodic table Some examples of chalcogenide metal compounds include Na_2S, CaTe, Ti_2S, Cu_2Se, $CsBiTe_6$ and $AgBiSe_2$, CdS, CdTe, CdSe. Transition metal chalcogenide are one class of metal chalcogenides that have been widely studied due to their narrow bandgap and visible light absorption capabilities. They have wide applications including energy storage, energy conversion, solar control coating, microelectronic devices, photocatalysis and sensors [118,119]. In photocatalysis transition metal chalcogenides that contain sulphur include simple sulphides such as Sb_2S_3, In_2S_3, ZnS and CdS and complex sulphides such as $ZnIn_2S_4$, $Zn_xCdS_{1-x}S$ and $AgIn_5S_8$ [120]. CdS is one of the most reported transition metal chalcogenide (TMC) which has high visible light absorption compared to many other TMC [117,121,122].

2.4.2.1 CdS Photocatalysis

Chalcogenide materials have good properties such as superior optical, photosensitization, photoluminescence and photocatalytic properties [123–125], it is an n-type semiconductor with a bandgap of 2.4 eV and a promising material for

wastewater remediation under visible light. Recently it has been widely reported for water purification applications and H_2 production [123]. However, more research is required to understand the physical and chemical properties of CdS nanostructures to develop novel materials for photocatalytic applications.

2.4.2.2 Optical properties, crystalline structure and phase transition of CdS

The CdS photocatalyst consist of two crystalline structures which are cubic (zinc blend) and hexagonal (Wurtzite). The cubic crystalline structure shows a tetrahedral structure which belongs to the equated system type with a facial structure and the hexagonal CdS crystalline structure shows a hexagonal cone structure (Fig. 2.4). The crystalline structures have different stability at different temperature and altering the atoms of the material can result in change of the phase structure. In a study a mixture of zinc blende and wurtzite CdS were synthesized by a simple sonolysis method and by varying the Cd/S ratios, the morphology and phase composition of CdS nanostructures were altered [126]. In another study zinc blend CdS nanoparticles were successfully transformed to wurtzite micro rods through a dissolution-regrowth process [127].

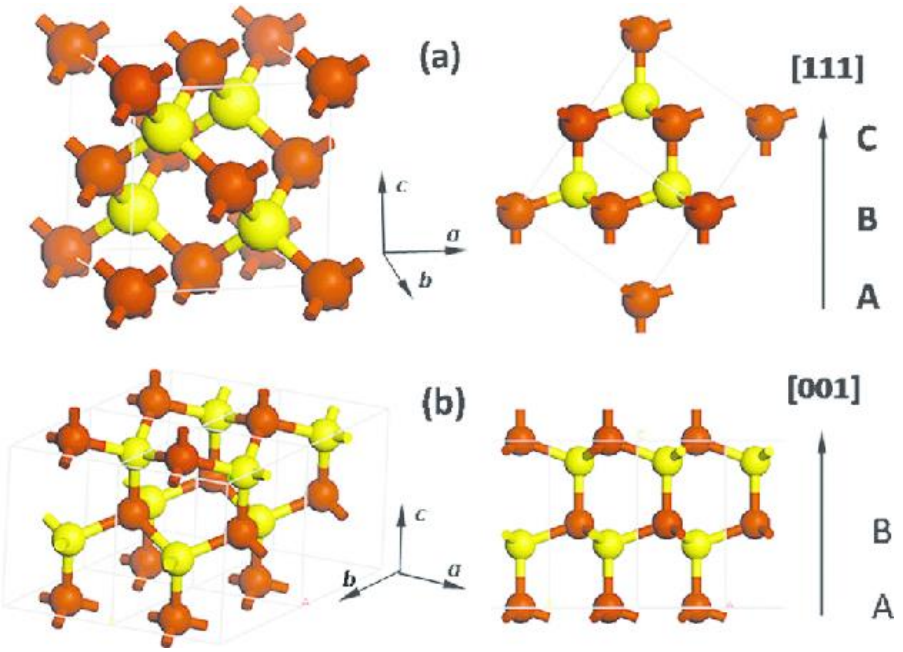

Figure 2.4.Schematic diagram of (a) zinc blend and (b) hexagonal crystalline structure [93].

2.4.2.3 CdS morphologies

The morphological structure of semiconductors play a significant role in the photocatalytic properties of the semiconductor photocatalyst. The nanostructures of CdS include 0-dimensional (0-D) which are generally spherical in shape, 1-dimensional (1-D) which have rod like structures [128–130], 2-dimensional (2-D) have sheet like structures, and 3-dimensional (3-D) include hollow spheres [131], porous CdS nanosheets-assembles flowers [132] and hierarchical CdS [132] (Fig. 2.5).

Zero dimensional (0-D) structures generally have spherical shape and have the advantage of high surface area compared to the other dimensional structures [133]. They can be obtained through methods such as combustion method, complex thermolysis, sonochemical method, solvothermal method and chemical precipitation [134,135]. The type of precursor also play a significant role in the shapes and morphologies of the resulting materials. Polyvinylpyrrolidone (PVP) has been reported as a capping agent in the synthesis of uniform sized spherical CdS [136]. In a study it was reported that PVP can be used as a raw material for the synthesis of O-D PVP capped CdS and the synthesized nanoparticles were smaller in size and less agglomerated compared to the uncapped CdS [137].

Figure 2.5.Morphological structures of CdS [105]

2.4.2.4 Application of CdS based photocatalyst in pollutants degradation

CdS has high photocatalytic activity at wavelengths shorter than 516 nm ,which is attributed to its good carrier transportation capacity and thus enabling efficient mobility of photo-generated electrons and holes [138]. However pure CdS is unstable when illuminated with light and is susceptible to photo-corrosion or photo-dissolution where the sulphide ions are oxidized by photogenerated holes [139,140] and thus resulting in recombination of electron hole pairs which is the main disadvantage of most semiconductor photocatalysts and hence research has focused on modifying CdS through metal doping [141] and coupling with other semiconductor photocatalysts [142,143] to overcome these drawbacks and enhance the photocatalytic properties of CdS.

2.4.2.5 Modification of CdS

A lot of researches focused on enhancing the photocatalytic activity of CdS and to reduce the drawbacks associated with CdS photocatalysis. These include doping with metals and coupling with other semiconductors.

In a previous study, Ag_2S/CdS heterojunction photocatalyst was reported for the photocatalytic removal of methylene orange (MO) and RhB. The results demonstrated that the Ag_2S/CdS composite exhibited a wide absorption ranging from ultraviolet (UV) to near-infrared (NIR), demonstrating its potential for solar energy utilization. The photocatalytic efficiency increased and 100% removal of RhB and MO was achieved [144]. In another study CdS/TiO_2 hybrid nanoparticles immobilized on polyacrylonitrile membrane were reported for the simultaneous filtration and photodegradation of methylene blue (MB) in water. In the study TiO_2 acted as a barrier reducing Cd^{2+} ions from leaching and also enhanced the photocatalytic activity of CdS and 66.29% of MB was removed [144].

In another report on the 2-D layer hybrid CdS nanosheets/MoS_2 heterojunction synthesized via a two-step hydrothermal and ultrasonic treatment technique for the photocatalytic generation of H_2, MoS_2 enhanced the photocatalytic efficiency of pristine CdS and 1.7 mmol g^{-1} h^{-1} H_2 was successfully generated due to effective promotion, separation and transportation of charge carriers [145].

Cai et al., 2017 reported on fullerene (C_{60})/CdS nanocomposite synthesized for the photocatalytic removal of rhodamine B (RhB). The composite was synthesized using hydrothermal method and results showed that C_{60} efficiently accelerated the separation and transfer of charge carriers and reduced CdS photo corrosion and thereby improving the photocatalytic activity of CdS and reducing the photo corrosion of CdS. Up to 97% removal of RhB was achieved [146].

CdS was also reported on improving the photocatalytic activity of other semiconductors. Adegoke et al., 2018 reported on the synthesis, characterization and application of CdS/ZnO nanorods heterostructure prepared by hydrothermal and photochemical method for the photocatalytic removal of Rhodamine B dye. CdS significantly enhanced the photocatalytic activity of ZnO and 85% of RhB removal was achieved [147].

In this study g-C_3N_4 nanosheets will be used as a support material to improve the photocatalytic properties of CdS.

2.5 Graphitic carbon nitride g-C_3N_4

Graphitic carbon nitride (g-C_3N_4) is widely studied metal free, visible-light active catalyst with a band gap of 2.7 eV. It is a 2-D π-conjugated polymeric structure composed of only carbon (C) and nitrogen (N_2). Its structure is similar to that of graphene and been widely studied for the synthetic photosynthesis and environmental remediation, such as waste water treatment, and air purification (Fig. 2.6) [148].

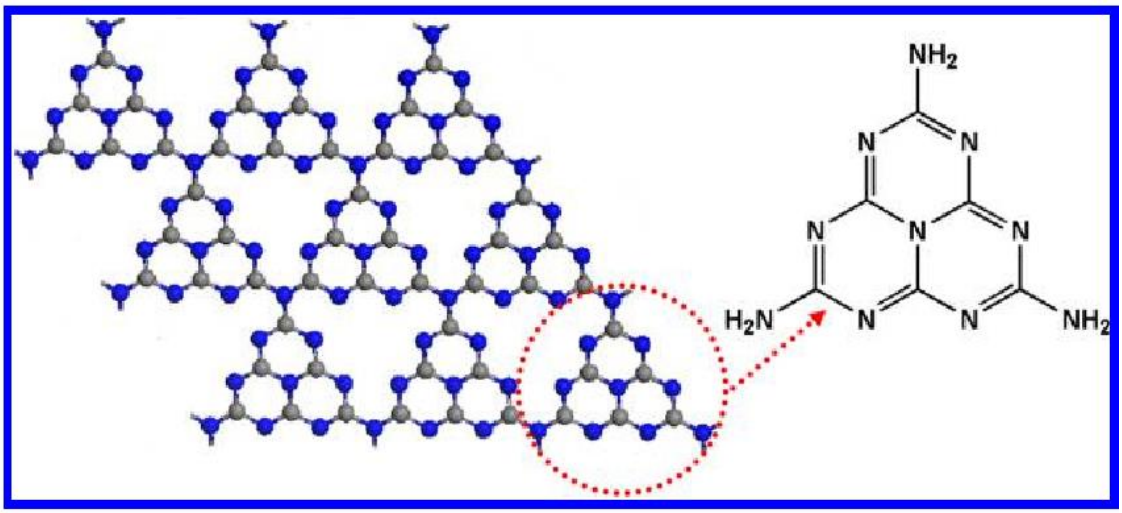

Figure 2.6.Chemical structure of g-C_3N_4.

g-C_3N_4 also known as “melon” is one of the most stable allotrope compared to many carbon nitride based semiconductors. It is easy to synthesize, cheap, stable, easily scalable and is an outstanding photocatalyst hence it is one of the most favoured semiconductor catalyst. Some of its large applications are in water splitting, and energy conversion. It has been widely used in H_2 generation because of its rich hydrogen absorption locations and tuneable band structures [148].

2.5.1 g-C_3N_4 nanostructures

Different types of nanostructures of g-C_3N_4 including nanoparticles, nanorods, nanowires, nanotubes, nanospheres and nanosheets; have attracted lot of research attention for their excellent properties such as solar radiation adsorption ability, effective charge carrier separation, high surface area and presence of more active sites [149].

Zero dimensional (0-D) g-C_3N_4 nanostructures such as quantum dots, have the ability to convert Near Infra-Red (NIR) to visible light making them a promising material for transfer of energy in photocatalytic systems and to absorb high wavelength solar energy [150]. They are soluble and stable in water and have applications in water splitting and water treatment [151]. A study was reported on the synthesis of g-C_3N_4 quantum dots from bulk g-C_3N_4 through thermochemical etching and intense fluorescent quantum dots were obtained which indicated their potential applications as blue light fluorescent materials and they also exhibit good visible-light photocatalytic activity [152]

One dimensional g-C_3N_4 structures have rod and ribbon like structures and have attracted lots of research due their unique morphology and physical properties in photocatalysis applications [153,154]. They also display high photocatalytic efficiency compared to a variety of g-C_3N_4 nanostructures. In a study, g-C_3N_4 nanorods were reported for the photocatalytic removal of MB and the g-C_3N_4 nanorods photocurrent response was 50-100% greater than the g-C_3N_4 nanoplates from which they were obtained [155]. Mesoporous g-C_3N_4 is a porous type of g-C_3N_4. It has a large surface that results in enhanced mass transfer and thus high quantum efficiency properties. Their internal scattering of incident light ability can be used for light harvesting applications [156–158].

Two dimensional g-C_3N_4 these include nanosheets, or sheet like structures. They have high surface area providing abundant reactive sites, good crystallinity, excellent photocatalytic properties resulting from their charge-carrier separation probability and result in reduced recombination of charge carries [159]. They have the advantage of narrow bandgap and can alter the photo physical behaviour of photoexcited charge carriers due to quantum confinement effect [38,157,160]. In a study ultrathin g-C_3N_4 nanosheets synthesized by a green liquid exfoliation method were reported for bio-imaging applications and they displayed enhanced photo absorption and photoresponse, which induced their high PL quantum yield up to 19.6%. Ultrathin g-C_3N_4 nanosheets (UCN) coupled with carbon dots (CQDs) via hydrothermal method were also reported for the efficient photocatalytic evolution of H_2. The results displayed that the carbon nanorods uniformly dispersed on the nanosheets surface through the $\pi - \pi$ interactions. The 0.2% CQDs/UCN composite provided 88.1 µmol/h H_2 evolution [161].

2.5.2 Optical properties, crystalline structure and phase transition of g-C_3N_4

The crystalline structure, surface physicochemical stability, optical, adsorption capability, electronic and photo electrochemical properties play important roles in the photocatalytic efficiency of semiconductor catalysts.

The phase structure of g-C_3N_4 include α-C_3N_4,β-C_3N_4, cubic C_3N_4, pseudo cubic C_3N_4, g-h-triazine, h-heptazine and g-o-triazine with bandgaps of 5.49, 4.85, 4.30, 4.13, 2.97, 2.88 and 0.93 eV respectively [162]. All the other phases except for g-h-triazine phases and pseudo cubic have indirect bandgaps in their bulk structures [163,164]. β-C_3N_4 is a super hard crystal phase form of g-C_3N_4 and its hardness is similar to that of a diamond [165]. The g-h-triazine and g-h-triazine units can absorb in the visible region of the solar spectrum and thus have applications in a variety of photocatalytic fields. g-C_3N_4 is made up of a 2-D layered strong covalently linked, sp^2 hybridized carbon and nitrogen atoms [164] (Fig. 2.7a) and has two main types of structural polymorphs consisting of condensed s-triazine units (Fig. 2.7b) with a periodic array of single carbon vacancies and tri-s-triazine (tri-ring C_6N_7) subunits couples through planar tertiary amino groups and has greater vacancies in the lattice (Fig. 2.8c) [166]. The energetically tri-s-triazine-based g-C_3N_4 are 30 kJ mol-1 more stable than triazine based g-C_3N_4 and therefore the tri-s-triazine based g-C_3N_4 is the most accepted unit of the g-C_3N_4 networks [167].

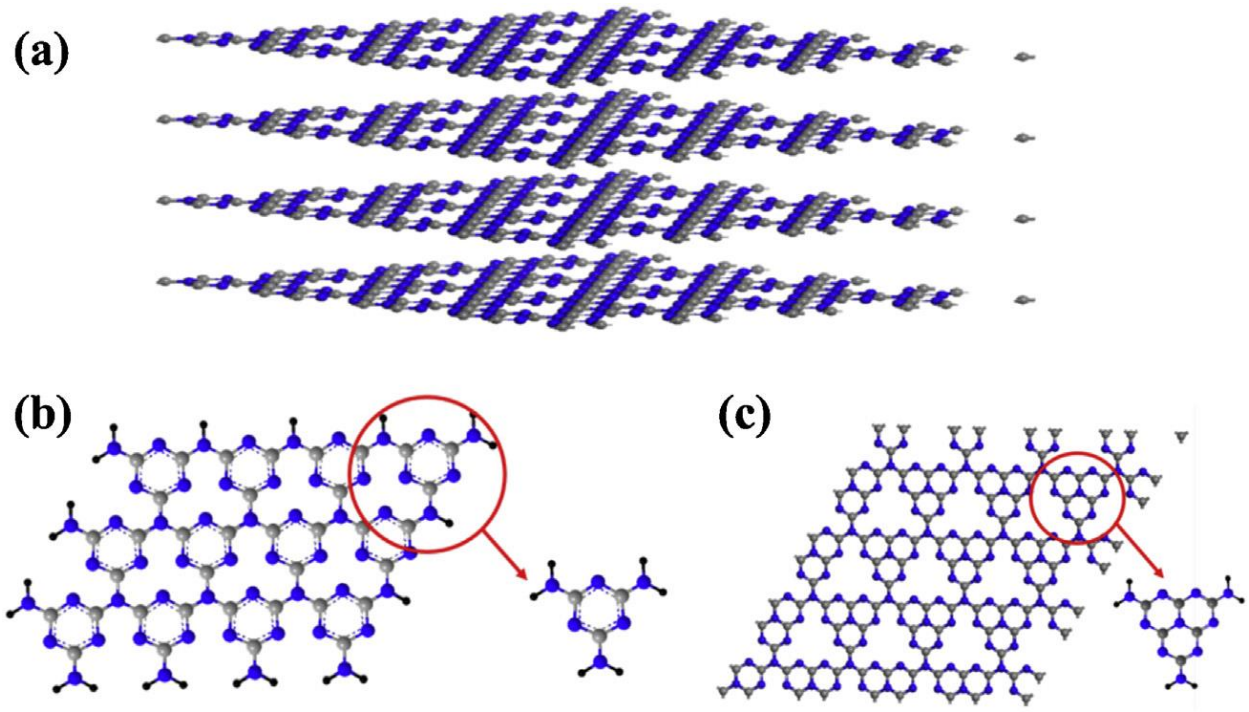

Figure 2.7. The stacked 2-D layer structure of g-C3N4 (a) s-triazine (b) tri-s-triazine (c) the primary block of g-C3N4 [117].

2.5.3 Advantages of g-C_3N_4 based photocatalysis

The photocatalytic applications of g-C_3N_4 is one field that has been widely studied due to a number of advantages that the material possesses that are important in the photocatalytic process such as nontoxicity, readily available, good stability, it possesses a stacked 2-D layer structure made of a single-layer nitrogen heteroatom and carbon atoms and both C and N are abundant elements, thus it can easily be fabricated making it cost effective. The position of the conduction band of g-C_3N_4 makes it suitable for a number of reduction reactions because it is more negative than most semiconductors (Table 3). The potentials of H_2-evolution [157], CO_2-reduction and O_2-reduction reactions are also much smaller than these semiconductors which suggests that the g-C_3N_4 photo-generated electrons have a high thermodynamic driving force to reduce various kinds of small molecules such as H_2O, CO_2 and O_2 and thus making g-C_3N_4 an ideal material for various applications including photocatalytic degradation of pollutants, organic synthesis, photocatalytic water splitting and CO_2 reduction. It can easily be obtained through a simple thermal

condensation of cheap and readily available precursors such as urea, thiourea, melamine, dicyandiamide, cyanimide and guanidine hydrochloride [39,168].

Table 2.3.Band gap positions of typical semiconductor photocatalyst [139].

Semiconductor	CB	VB	Egg/eV
g-C_3N_4	-1.30	1.40	2.70
TiO_2	-0.50	2.70	3.20
WO_3	-0.10	2.70	2.80
Ag_3PO_4	0.040	2.49	2.45
$BiVO_4$	-0.30	2.10	2.40

2.5.4 Application of g-C_3N_4 in photodegradation of organic pollutants

g-C_3N_4 has a small energy gap of 2.7 eV which corresponds to wavelengths of 450 nm and it is thus suitable for visible light harvesting [169] and thus many researchers reported on the modification of g-C_3N_4 to enhance its photocatalytic efficiency and reduce the recombination probability of photo-generation electron-hole pairs [170–173].

Some modifications of g-C_3N_4 include metal, non-metal doping, and coupling with low bandgap semiconductors. Metal doping involves introducing metals into g-C_3N_4. In a study Fe (III) doped g-C_3N_4 (Fe^{3+} g-C_3N_4) synthesized by in-situ method was reported for the photocatalytic degradation of RhB and the Fe enhanced the photocatalytic efficiency of g-C_3N_4 which was 2.5 and 1.8 times higher than that of the pure g-C_3N_4. The increase in the efficiency was ascribed to the efficient inhibition of charge carrier recombination [174]. Wang et al. also reported on Zr-doped g-C_3N_4 synthesized via a pyrolysis method for the photocatalytic degradation of RhB and g-C_3N_4 that displayed improved photocatalytic efficiency and nearly 100% removal of RhB was achieved compare to pure g-C_3N_4 which achieved only 70% RhB removal [175].

By coupling with other semiconductors to form heterojunctions may result in efficient separation of photogenerated charge carries and improved photocatalytic efficiency. In a study, g-C_3N_4 was used as a support for the synthesis for the synthesis of shape dependent ZnO and their application in MB degradation. The synthesized dumbbell

and coned g-C_3N_4/ZnO heterostructure displayed enhanced photocatalytic efficiencies and 99% MB degradation was achieved [176].

A lot of research on CdS/g-C_3N_4 based heterostructure have been reported where CdS was used to enhance the photocatalytic properties of g-C_3N_4. In a study the photocatalytic activity of g-C_3N_4 hybridized CdS nanoparticles was reported for the photocatalytic degradation of RhB, the g-C_3N_4 hybridized CdS was synthesized via successive calcination and hydrothermal process and the photocatalytic efficiency of the obtained heterostructure was much higher compared to pure CdS and g-C_3N_4 which may have been due to the efficient separation of electron-hole pairs [40].

Recently a heterostructure g-C_3N_4/CdS synthesized via in-situ high temperature self-transformation method was reported for the photocatalytic generation of H_2. The g-C_3N_4 nanoparticles homogeneously grafted on the surface of CdS with closely contacted interfaces. The optimal photocatalytic activity was achieved with 1wt% g-C_3N_4/CdS and achieved 5303 µmol h^{-1} g^{-1} with apparent quantum efficiency of 3.61% at 420nm [177]. Jiang et al. 2014 reported on g-C_3N_4-CdS composite, possessing high photocalytic activity and photostability for the degradation of methylene blue. The CdS enhanced the photocatalytic activity of g-C_3N_4 where 90.45% MB removal was achieved within 180 min [178].

In this study the effect of g-C_3N_4 nanosheets on the photocatalytic efficiency of CdS for the degradation of Acid Blue 25 and Diclofenac was investigated. The g-C_3N_4 was used as a support for the CdS and the nanocomposite was synthesized via a hydrothermal method.

2.6 Synthetic techniques for CdS

The synthetic strategy of CdS play an important role in achieving the photocatalysts. The synthetic approaches can result in different morphologies, sizes and structures which can affect photocatalytic performance of photocatalysts [179]. There are many synthetic approaches for CdS based photocatalysts.

2.6.1 Sonochemical methods

Sonochemical methods are methods that uses ultrasonic energy to cause a chemical reaction. The process occurs by the change in cavitation such as liquid cavities, oscillation, growth contraction, physical and chemical changes [179,180]. During the synthesis, heat, pressure, heating and cooling rates of approximately 5000 k, 1000

atm and >10_9 K S^{-1} can be produced respectively in a short time [180]. It has been reported to result in reduced energy consumption, increase surface area and adsorption capacity. However it is difficult to operate in a scale and because of the vibration cavities produced during the reaction, few meters of working space should be established.

2.6.2 Solvothermal methods

The solvothermal method involves the use organic solvent for synthesis of photocatalysts. During the synthesis process, reactants are dispersed in the solvent and heated at a specific temperature. It is similar to hydrothermal method, the difference between the two, is that in hydrothermal method synthesis water is used as a solvent while solvothermal uses organic solvents. Solvothermal method results in easy controlled size, phase and shape of nanomaterials [36].

2.6.3 Co-precipitation method

Co-precipitation method involves the occurrence of growth, nucleation, coarsening and or agglomeration processes simultaneously. It is a simple and rapid of synthesis, easy to control the particle size and energy efficient and has been widely used for synthesis of many photocatalysts including CdS, however is susceptible to impurities in the final product and batch to batch results not reproducible [181].

2.6.4 Hydrothermal Method

Hydrothermal method involves synthesis of nanomaterials in aqueous solutions at high temperatures above the boiling point of water in a steel autoclave. It has been widely reported for CdS and CdS based photocatalysts and resulted in high purity, good dispersion and high crystallinity photocatalyst. CdS based photocatalysts can be obtained via in-situ, which is a single step method of synthesis and highly explored in the production of photocalyst composites. Recently CdS/TNTs composite was reported and synthesized via hydrothermal method and resulted in enhanced photocatalytic activity and stability of CdS [181]. 2-dimesional CdS nanosheets were also reported with well-defined morphology and good photocatalytic efficiency towards H_2 evolution [182]. Masoud et al 2008, reported on monocrystalline CdS synthesis with different morphologies in the presence of thioglycolic acid, by

changing the ratio of the reactants, reaction time and temperature, different morphologies of CdS and particle sizes were obtained [183].

References

[1] A. Azizullah, M.N.K. Khattak, P. Richter, D.P. Häder, Water pollution in Pakistan and its impact on public health - A review, Environ. Int. 37 (2011) 479–497. doi:10.1016/j.envint.2010.10.007.

[2] I. Gehrke, A. Somborn-schulz, Innovations in nanotechnology for water treatment, Nanotechnol. Sci. Appl. 8 (2015) 1–17.

[3] C.J.. ; G. Vorösmarty Pamela; ; Salisbury, Joseph; ; Lammers, Richard B., Global Water Resources: Vulnerability from Climate Change and Population Growth, Science (80-.). 289 (2000) 284–288. doi:10.1126/science.289.5477.284.

[4] J. Theron, T.E. Cloete, Emerging Waterborne Infections: Contributing Factors, Agents, and Detection Tools, Crit. Rev. Microbiol. 28 (2008) 1–26. doi:10.1080/1040-840291046669.

[5] K.K. Jain, Nanotechnology and Water, Contemp. Mater. 1 (2012) 26–30. doi:10.7251/122.

[6] F.W. Owa, Water pollution : sources , effects , control and management, Int. Lett. 3 (2014) 1–6.

[7] H. Zhou, D.W. Smith, Advanced technologies in water and wastewater treatment, in: 2002. doi:10.1139/S02-020.

[8] M. Wakil, M. Burhan, L. Ang, K. Choon, Energy-water-environment nexus underpinning future desalination sustainability, Desalination. 413 (2017) 52–64. doi:10.1016/j.desal.2017.03.009.

[9] M. Palaniappan, K. Address, Peak_Water_Talk.Pdf, in: Utah Am. Plan. Assoc. Annu. Conf., 2008: pp. 3–11.

[10] J.K. Bwapwa, Review on Main Issues Causing Deterioration of Water Quality and Water Scarcity: Case Study of South Africa, Environ. Manag. Sustain. Dev. 7 (2018) 14. doi:10.5296/emsd.v7i3.13156.

[11] J. Wang, S. Wang, Removal of pharmaceuticals and personal care products (PPCPs) from wastewater: A review, J. Environ. Manage. 182 (2016) 620–640.

doi:10.1016/j.jenvman.2016.07.049.

[12] G. Boczkaj, A. Fernandes, Wastewater treatment by means of advanced oxidation processes at basic pH conditions : A review, Chem. Eng. J. 320 (2017) 608–633. doi:10.1016/j.cej.2017.03.084.

[13] R. Ananthashankar, Treatment of textile effluent containing Reactive Red 120 dye using advanced oxidation, 2012.

[14] K. Klaus, Pharmaceuticals in the Environment, Annu Rev Env. Resour. 35 (2010) 57–75. doi:10.1146/annurev-environ-052809-161223.

[15] G. Kjosavik, Subtle changes, 2001.

[16] A.B.A. Boxall, M.A. Rudd, B.W. Brooks, D.J. Caldwell, K. Choi, S. Hickmann, E. Innes, K. Ostapyk, J.P. Staveley, T. Verslycke, G.T. Ankley, K.F. Beazley, Review Pharmaceuticals and Personal Care Products in the Environment : What Are the Big Questions ?, 120 (2012) 1221–1229.

[17] G. Li, X. Nie, Y. Gao, T. An, Applied Catalysis B : Environmental Can environmental pharmaceuticals be photocatalytically degraded and completely mineralized in water using g-C_3N_4/TiO_2 under visible light irradiation ?— Implications of persistent toxic intermediates, "Applied Catal. B, Environ. 180 (2016) 726–732. doi:10.1016/j.apcatb.2015.07.014.

[18] B. Hoeger, B. Köllner, D.R. Dietrich, B. Hitzfeld, Water-borne diclofenac affects kidney and gill integrity and selected immune parameters in brown trout (Salmo trutta f. fario), Aquat. Toxicol. 75 (2005) 53–64. doi:10.1016/j.aquatox.2005.07.006.

[19] M. Lillenberg, S. Yurchenko, K. Kipper, K. Herodes, V. Pihl, R. Lõhmus, M. Ivask, A. Kuu, S. Kutti, S. V. Litvin, L. Nei, Presence of fluoroquinolones and sulfonamides in urban sewage sludge and their degradation as a result of composting, Int. J. Environ. Sci. Technol. 7 (2010) 307–312. doi:10.1007/BF03326140.

[20] S.K. Khetan, T.J. Collins, Human pharmaceuticals in the aquatic environment: A challenge to green chemisty, Chem. Rev. 107 (2007) 2319–2364. doi:10.1021/cr020441w.

[21] A.M. Deegan, B. Shaik, K. Nolan, K. Urell, M. Oelgemöller, J. Tobin, A. Morrissey, Treatment options for wastewater effluents from pharmaceutical companies, Int. J. Environ. Sci. Technol. 8 (2011) 649–666. doi:10.1007/BF03326250.

[22] A.J. Ebele, M. Abou-Elwafa Abdallah, S. Harrad, Pharmaceuticals and personal care products (PPCPs) in the freshwater aquatic environment, Emerg. Contam. 3 (2017) 1–16. doi:10.1016/j.emcon.2016.12.004.

[23] B.D. Blair, J.P. Crago, C.J. Hedman, R.D. Klaper, Chemosphere Pharmaceuticals and personal care products found in the Great Lakes above concentrations of environmental concern, Chemosphere. 93 (2013) 2116–2123. doi:10.1016/j.chemosphere.2013.07.057.

[24] C.U. Meteyer, B.A. Rideout, M. Gilbert, H.L. Shivaprasad, L. Oaks, Pathology and proposed pathophysiology of diclofenac poisoning in free living and experimentally exposed oriental white backed vultures (Gyps bengalensis), J. Wildl. Dis. 41 (2005) 707–716.

[25] R. Triebskorn, H. Casper, V. Scheil, J. Schwaiger, Ultrastructural effects of pharmaceuticals (carbamazepine, clofibric acid, metoprolol, diclofenac) in rainbow trout (Oncorhynchus mykiss) and common carp (Cyprinus carpio), Anal. Bioanal. Chem. 387 (2007) 1405–1416. doi:10.1007/s00216-006-1033-x.

[26] J. Schwaiger, H. Ferling, U. Mallow, H. Wintermayr, R.D. Negele, Toxic effects of the non-steroidal anti-inflammatory drug diclofenac. Part I: Histopathological alterations and bioaccumulation in rainbow trout, Aquat. Toxicol. 68 (2004) 141–150. doi:10.1016/j.aquatox.2004.03.014.

[27] A.A.C. and Z.M. Dana Manuela Sirbu, Daniela Curseu, Monica Popa, Environmental Risks of Pharmaceuticals and Personal Care Products in Water, in: Tenth Int. Water Technol. Conf., 2006: pp. 1151–1162.

[28] E. Archer, G.M. Wolfaardt, J.H. van Wyk, Pharmaceutical and personal care products (PPCPs) as endocrine disrupting contaminants (EDCs) in South African surface waters, Water SA. 43 (2017) 684–706. doi:10.4314/wsa.v43i4.16.

[29] O.A.H. Jones, N. Voulvoulis, J.N. Lester, Potential ecological and human health risks associated with the presence of pharmaceutically active compounds in the aquatic environment, Crit. Rev. Toxicol. 34 (2004) 335–350. doi:10.1080/10408440490464697.

[30] A.K. Karen, J.B. Paul, H.M. Kenneth, e P.P. Vinc, E.E. Robert, M.L. James, W.F. Robert, Disrupting Queer Incluslon, Pnas. 104 (2007) 8897–8901. doi:10.1073/pnas.0609568104.

[31] D.J. Caldwell, F. Mastrocco, T.H. Hutchinson, R. Länge, D. Heijerick, C. Janssen, P.D. Anderson, J.P. Sumpter, Derivation of an aquatic predicted no-effect concentration for the synthetic hormone, 17α-ethinyl estradiol, Environ. Sci. Technol. 42 (2008) 7046–7054. doi:10.1021/es800633q.

[32] M.F. Rahman, E.K. Yanful, S.Y. Jasim, Endocrine disrupting compounds (EDCs) and pharmaceuticals and personal care products (PPCPs) in the aquatic environment: Implications for the drinking water industry and global environmental health, J. Water Health. 7 (2009) 224–243. doi:10.2166/wh.2009.021.

[33] B. Lellis, C.Z. Fávaro-polonio, J.A. Pamphile, J.C. Polonio, Effects of textile dyes on health and the environment and bioremediation potential of living organisms, Biotecnol. Res. Innov. 3 (2019) 275–290. doi:10.1016/j.biori.2019.09.001.

[34] R. Paper, Decolorization of mixture of dyes : A critical review, Glob. J. Environ. Sci. Manag. Glob. J. Environ. Sci. Manag. 1 (2015) 71–94. doi:10.7508/gjesm.2015.01.007.

[35] A.M. Deegan, B. Shaik, K. Nolan, K. Urell, J. Tobin, A. Morrissey, Treatment options for wastewater effluents from pharmaceutical companies, 8 (2011) 649–666.

[36] L. Cheng, Q. Xiang, Y. Liao, H. Zhang, CdS-Based photocatalysts, Royal Society of Chemistry, 2018. doi:10.1039/c7ee03640j.

[37] H.L. Lee, A.M. Issam, M. Belmahi, M.B. Assouar, H. Rinnert, M. Alnot, Synthesis and characterizations of bare cds nanocrystals using chemical

precipitation method for photoluminescence application, J. Nanomater. 2009 (2009). doi:10.1155/2009/914501.

[38] S. Kumar, S. Karthikeyan, A.F. Lee, g-C_3N_4-based nanomaterials for visible light-driven photocatalysis, Catalysts. 8 (2018). doi:10.3390/catal8020074.

[39] S. Cao, J. Low, J. Yu, M. Jaroniec, Polymeric Photocatalysts Based on Graphitic Carbon Nitride, Adv. Mater. 27 (2015) 2150–2176. doi:10.1002/adma.201500033.

[40] Q.Y. Liu, Y.L. Qi, Y.F. Zheng, X.C. Song, Synthesis and enhanced photocatalytic activity of g-C_3N_4 hybridized CdS nanoparticles, Bull. Mater. Sci. 40 (2017) 1329–1333. doi:10.1007/s12034-017-1513-y.

[41] R.C. Pawar, V. Khare, C.S. Lee, Hybrid photocatalysts using graphitic carbon nitride/cadmium sulfide/reduced graphene oxide (g-C_3N_4/CdS/RGO) for superior photodegradation of organic pollutants under UV and visible light, Dalt. Trans. 43 (2014) 12514–12527. doi:10.1039/c4dt01278j.

[42] S.W. Cao, Y.P. Yuan, J. Fang, M.M. Shahjamali, F.Y.C. Boey, J. Barber, S.C. Joachim Loo, C. Xue, In-situ growth of CdS quantum dots on g-C_3N_4 nanosheets for highly efficient photocatalytic hydrogen generation under visible light irradiation, Int. J. Hydrogen Energy. 38 (2013) 1258–1266. doi:10.1016/j.ijhydene.2012.10.116.

[43] S. Rasalingam, R. Peng, R.T. Koodali, Removal of hazardous pollutants from wastewaters: Applications of TiO_2-SiO_2 mixed oxide materials, J. Nanomater. 2014 (2014). doi:10.1155/2014/617405.

[44] M.K. Hasan, A. Shahriar, K.U. Jim, Water pollution in Bangladesh and its impact on public health, Heliyon. 5 (2019) e02145. doi:10.1016/j.heliyon.2019.e02145.

[45] S. Rasalingam, R. Peng, R.T. Koodali, 617405.Pdf, 2014 (2014).

[46] U. Tahir, A. Yasmin, U.H. Khan, Phytoremediation: Potential flora for synthetic dyestuff metabolism, J. King Saud Univ. - Sci. 28 (2016) 119–130. doi:10.1016/j.jksus.2015.05.009.

[47] G. Dong, Y. Zhang, Q. Pan, J. Qiu, A fantastic graphitic carbon nitride (g-C_3N_4)

material: Electronic structure, photocatalytic and photoelectronic properties, J. Photochem. Photobiol. C Photochem. Rev. 20 (2014) 33–50. doi:10.1016/j.jphotochemrev.2014.04.002.

[48] D.A. Yaseen, M. Scholz, Textile dye wastewater characteristics and constituents of synthetic effluents: a critical review, Springer Berlin Heidelberg, 2019. doi:10.1007/s13762-018-2130-z.

[49] T. Robinson, G. McMullan, R. Marchant, P. Nigam, Remediation of dyes in textile effluent: A critical review on current treatment technologies with a proposed alternative, Bioresour. Technol. 77 (2001) 247–255. doi:10.1016/S0960-8524(00)00080-8.

[50] G.S. Gupta, G. Prasad, V.N. Singh, Removal of chrome dye from aqueous solutions by mixed adsorbents: Fly ash and coal, Water Res. 24 (1990) 45–50. doi:10.1016/0043-1354(90)90063-C.

[51] N. Muhd Julkapli, S. Bagheri, S. Bee Abd Hamid, Recent advances in heterogeneous photocatalytic decolorization of synthetic dyes, Sci. World J. 2014 (2014) 25. doi:10.1155/2014/692307.

[52] Y. Fu, T. Viraraghavan, Fungal decolorization of dye wastewaters: A review, Bioresour. Technol. 79 (2001) 251–262. doi:10.1016/S0960-8524(01)00028-1.

[53] V.K. Gupta, S. Khamparia, I. Tyagi, D. Jaspal, A. Malviya, Decolorization of mixture of dyes: A critical review, Glob. J. Environ. Sci. Manag. Glob. J. Environ. Sci. Manag. 1 (2015) 71–94. doi:10.7508/gjesm.2015.01.007.

[54] Z. Aksu, Application of biosorption for the removal of organic pollutants: A review, Process Biochem. 40 (2005) 997–1026. doi:10.1016/j.procbio.2004.04.008.

[55] S. Sumathi, B.S. Manju, Uptake of reactive textile dyes by Aspergillus foetidus, Enzyme Microb. Technol. 27 (2000) 347–355. doi:10.1016/S0141-0229(00)00234-9.

[56] Z. Aksu, S. Tezer, Equilibrium and kinetic modelling of biosorption of Remazol black B by Rhizopus arrhizus in a batch system: Effect of temperature, Process Biochem. 36 (2000) 431–439. doi:10.1016/S0032-9592(00)00233-8.

[57] T. O'Mahony, E. Guibal, J.M. Tobin, Reactive dye biosorption by Rhizopus arrhizus biomass, Enzyme Microb. Technol. 31 (2002) 456–463. doi:10.1016/S0141-0229(02)00110-2.

[58] B. Aruna, R.S. L, E. Shiva, A. Srinu, P. Roja, D. Vijayalakshmi, D.V.R. Prasad, Research Article Biodecolorization of Anthraquinone Textile (Acid Blue 25) Dye By Klebsiella Sp, 6 (2015) 3216–3222.

[59] M. Auta, B.H. Hameed, Preparation of waste tea activated carbon using potassium acetate as an activating agent for adsorption of Acid Blue 25 dye, Chem. Eng. J. 171 (2011) 502–509. doi:10.1016/j.cej.2011.04.017.

[60] C.A. Hsu, T.N. Wen, Y.C. Su, Z.B. Jiang, C.W. Chen, L.F. Shyur, Biological degradation of anthroquinone and azo dyes by a novel laccase from Lentinus sp., Environ. Sci. Technol. 46 (2012) 5109–5117. doi:10.1021/es2047014.

[61] H. hong Li, Y. tao Wang, Y. Wang, H. xia Wang, K. kai Sun, Z. mei Lu, Bacterial degradation of anthraquinone dyes, J. Zhejiang Univ. Sci. B. 20 (2019) 528–540. doi:10.1631/jzus.B1900165.

[62] M.E. Malefane, U. Feleni, A.T. Kuvarega, Tetraphenylporphyrin/WO_3/exfoliated graphite nanocomposite for photocatalytic degradation of an acid dye under visible light irradiation, New J. Chem. 10 (2019) 1–6. doi:10.1039/c9nj02747e.

[63] S. Benkhaya, S. El Harfi, A. El Harfi, Classifications , properties and applications of textile dyes : A review, Appl. J. Environ. Sci. 3 (2018) 311–320.

[64] D. Chakrabortty, S. Sen Gupta, Photo-catalytic decolourisation of toxic dye with N-doped titania: A case study with Acid Blue 25, J. Environ. Sci. (China). 25 (2013) 1034–1043. doi:10.1016/S1001-0742(12)60108-9.

[65] T. Deblonde, C. Cossu-Leguille, P. Hartemann, Emerging pollutants in wastewater: A review of the literature, Int. J. Hyg. Environ. Health. 214 (2011) 442–448. doi:10.1016/j.ijheh.2011.08.002.

[66] M. Clara, G. Windhofer, W. Hartl, K. Braun, M. Simon, O. Gans, C. Scheffknecht, A. Chovanec, Occurrence of phthalates in surface runoff, untreated and treated wastewater and fate during wastewater treatment, Chemosphere. 78 (2010) 1078–1084.

doi:10.1016/j.chemosphere.2009.12.052.

[67] M. la Farré, S. Pérez, L. Kantiani, D. Barceló, Fate and toxicity of emerging pollutants, their metabolites and transformation products in the aquatic environment, TrAC - Trends Anal. Chem. 27 (2008) 991–1007. doi:10.1016/j.trac.2008.09.010.

[68] A. Jennifer, M.A. Abdallah, S. Harrad, Pharmaceuticals and personal care products (PPCPs) in the freshwater aquatic environment, Emerg. Contam. 3 (2017) 1–16. doi:10.1016/j.emcon.2016.12.004.

[69] S.R. Hughes, P. Kay, L.E. Brown, Global synthesis and critical evaluation of pharmaceutical data sets collected from river systems, Environ. Sci. Technol. 47 (2013) 661–677. doi:10.1021/es3030148.

[70] D. Ashton, M. Hilton, K. V. Thomas, Investigating the environmental transport of human pharmaceuticals to streams in the United Kingdom, Sci. Total Environ. 333 (2004) 167–184. doi:10.1016/j.scitotenv.2004.04.062.

[71] S. Wiandt, H.J. Poremski, Selection and prioritisation procedure of hazardous substances for the marine environment within Ospar/dynamec, Ecotoxicology. 11 (2002) 393–399. doi:10.1023/A:1020569608441.

[72] L. Lonappan, S.K. Brar, R.K. Das, M. Verma, R.Y. Surampalli, Diclofenac and its transformation products: Environmental occurrence and toxicity - A review, Environ. Int. 96 (2016) 127–138. doi:10.1016/j.envint.2016.09.014.

[73] Y. Zhang, S.U. Geißen, C. Gal, Carbamazepine and diclofenac: Removal in wastewater treatment plants and occurrence in water bodies, Chemosphere. 73 (2008) 1151–1161. doi:10.1016/j.chemosphere.2008.07.086.

[74] V. Acuña, A. Ginebreda, J.R. Mor, M. Petrovic, S. Sabater, J. Sumpter, D. Barceló, Balancing the health benefits and environmental risks of pharmaceuticals: Diclofenac as an example, Environ. Int. 85 (2015) 327–333. doi:10.1016/j.envint.2015.09.023.

[75] A.C. Johnson, E. Dumont, R.J. Williams, R. Oldenkamp, I. Cisowska, J.P. Sumpter, Do concentrations of ethinylestradiol, estradiol, and diclofenac in European rivers exceed proposed EU environmental quality standards?,

Environ. Sci. Technol. 47 (2013) 12297–12304. doi:10.1021/es4030035.

[76] A.Y. Shan, T.I.M. Ghazi, S.A. Rashid, Immobilisation of titanium dioxide onto supporting materials in heterogeneous photocatalysis: A review, Appl. Catal. A Gen. 389 (2010) 1–8. doi:10.1016/j.apcata.2010.08.053.

[77] Y. Mehmood, Index Academic Sciences Original Article development and validation of UV-Vis spectrophotometric method for the estimation of diclofenac sodium injections., Int. J. Pharm. Pract. Pharm. Sci. 2 (2015) 1–6.

[78] D. Chen, A.K. Ray, Photodegradation kinetics of 4-nitrophenol in TiO_2 suspension, Water Res. 32 (1998) 3223–3234. doi:10.1016/S0043-1354(98)00118-3.

[79] C. Martínez, M. Canle L., M.I. Fernández, J.A. Santaballa, J. Faria, Aqueous degradation of diclofenac by heterogeneous photocatalysis using nanostructured materials, Appl. Catal. B Environ. 107 (2011) 110–118. doi:10.1016/j.apcatb.2011.07.003.

[80] M. Letzel, G. Metzner, T. Letzel, Exposure assessment of the pharmaceutical diclofenac based on long-term measurements of the aquatic input, Environ. Int. 35 (2009) 363–368. doi:10.1016/j.envint.2008.09.002.

[81] C. Hao, R. Clement, P. Yang, Liquid chromatography-tandem mass spectrometry of bioactive pharmaceutical compounds in the aquatic environment-a decade's activities, Anal. Bioanal. Chem. 387 (2007) 1247–1257. doi:10.1007/s00216-006-0956-6.

[82] A.J. Sosiak, T. Hebben, A preliminary survey of pharmaceuticals and endocrine disrupting compounds in treated municipal wastewaters and receiving rivers of Alberta /, 2005. doi:10.5962/bhl.title.113982.

[83] M.J. Benotti, R.A. Trenholm, B.J. Vanderford, J.C. Holady, B.D. Stanford, S.A. Snyder, Pharmaceuticals and endocrine disrupting compounds in U.S. drinking water, Environ. Sci. Technol. 43 (2009) 597–603. doi:10.1021/es801845a.

[84] T. Heberer, Tracking persistent pharmaceutical residues from municipal sewage to drinking water, J. Hydrol. 266 (2002) 175–189. doi:10.1016/S0022-1694(02)00165-8.

[85] F.O. Agunbiade, B. Moodley, Occurrence and distribution pattern of acidic pharmaceuticals in surface water, wastewater, and sediment of the Msunduzi River, Kwazulu-Natal, South Africa, Environ. Toxicol. Chem. 35 (2016) 36–46. doi:10.1002/etc.3144.

[86] M.T. Amin, A.A. Alazba, U. Manzoor, A Review of Removal of Pollutants from Water / Wastewater Using Different Types of Nanomaterials, 2014 (2014).

[87] M.R. Servos, D.T. Bennie, B.K. Burnison, A. Jurkovic, R. McInnis, T. Neheli, A. Schnell, P. Seto, S.A. Smyth, T.A. Ternes, Distribution of estrogens, 17β-estradiol and estrone, in Canadian municipal wastewater treatment plants, Sci. Total Environ. 336 (2005) 155–170. doi:10.1016/j.scitotenv.2004.05.025.

[88] T. Urase, T. Kikuta, Separate estimation of adsorption and degradation of pharmaceutical substances and estrogens in the activated sludge process, Water Res. 39 (2005) 1289–1300. doi:10.1016/j.watres.2005.01.015.

[89] N. Vieno, T. Tuhkanen, L. Kronberg, Removal of pharmaceuticals in drinking water treatment: Effect of chemical coagulation, Environ. Technol. 27 (2006) 183–192. doi:10.1080/09593332708618632.

[90] P. Westerhoff, Y. Yoon, S. Snyder, E. Wert, Fate of endocrine-disruptor, pharmaceutical, and personal care product chemicals during simulated drinking water treatment processes, Environ. Sci. Technol. 39 (2005) 6649–6663. doi:10.1021/es0484799.

[91] M. Petrovic, A. Diaz, F. Ventura, D. Barceló, Occurrence and removal of estrogenic short-chain ethoxy nonylphenolic compounds and their halogenated derivatives during drinking water production, Environ. Sci. Technol. 37 (2003) 4442–4448. doi:10.1021/es034139w.

[92] G. Becher, Drinking Water Chlorination and Health, Acta Hydrochim. Hydrobiol. 27 (1999) 100–102. doi:10.1002/(sici)1521-401x(199902)27:2<100::aid-aheh100>3.3.co;2-1.

[93] N. Bolong, A.F. Ismail, M.R. Salim, T. Matsuura, A review of the effects of emerging contaminants in wastewater and options for their removal, Desalination. 239 (2009) 229–246. doi:10.1016/j.desal.2008.03.020.

[94] Y. Yoon, P. Westerhoff, S.A. Snyder, E.C. Wert, Nanofiltration and ultrafiltration of endocrine disrupting compounds, pharmaceuticals and personal care products, J. Memb. Sci. 270 (2006) 88–100. doi:10.1016/j.memsci.2005.06.045.

[95] L. Braeken, B. Bettens, K. Boussu, P. Van der Meeren, J. Cocquyt, J. Vermant, B. Van der Bruggen, Transport mechanisms of dissolved organic compounds in aqueous solution during nanofiltration, J. Memb. Sci. 279 (2006) 311–319. doi:10.1016/j.memsci.2005.12.024.

[96] J. Lu, T. Zhang, J. Ma, Z. Chen, Evaluation of disinfection by-products formation during chlorination and chloramination of dissolved natural organic matter fractions isolated from a filtered river water, J. Hazard. Mater. 162 (2009) 140–145. doi:10.1016/j.jhazmat.2008.05.058.

[97] M.N. Chong, B. Jin, C.W.K. Chow, C. Saint, Recent developments in photocatalytic water treatment technology: a review., Water Res. 44 (2010) 2997–3027. doi:10.1016/j.watres.2010.02.039.

[98] D.H. Bremner, R. Molina, F. Martínez, J.A. Melero, Y. Segura, Degradation of phenolic aqueous solutions by high frequency sono-Fenton systems (US-Fe_2O_3/SBA-15-H_2O_2), Appl. Catal. B Environ. 90 (2009) 380–388. doi:10.1016/j.apcatb.2009.03.028.

[99] G. Li, Z. Wang, M. Yu, Z. Quan, J. Lin, Fabrication and optical properties of core-shell structured spherical SiO_2@$GdVO_4$:Eu^{3+} phosphors via sol-gel process, J. Solid State Chem. 179 (2006) 2698–2706. doi:10.1016/j.jssc.2006.05.019.

[100] J. Zhang, G. Xiao, F.X. Xiao, B. Liu, Revisiting one-dimensional TiO_2 based hybrid heterostructures for heterogeneous photocatalysis: A critical review, Mater. Chem. Front. 1 (2017) 231–250. doi:10.1039/c6qm00141f.

[101] Y. Cui, In-situ synthesis of C_3N_4/CdS composites with enhanced photocatalytic properties, Cuihua Xuebao/Chinese J. Catal. 36 (2015) 372–379. doi:10.1016/S1872-2067(14)60237-0.

[102] V.S. Kosera, T.M. Cruz, E.S. Chaves, E.R.L. Tiburtius, Journal of

Photochemistry and Photobiology A : Chemistry Triclosan degradation by heterogeneous photocatalysis using ZnO immobilized in biopolymer as catalyst, "Journal Photochem. Photobiol. A Chem. 344 (2017) 184–191. doi:10.1016/j.jphotochem.2017.05.014.

[103] M.R. Hoffmann, S.T. Martin, W. Choi, D.W. Bahnemann, Environmental Applications of Semiconductor Photocatalysis, Chem. Rev. 95 (1995) 69–96. doi:10.1021/cr00033a004.

[104] J.-M. Hermann, Water Treatment By Heterogeneous Photocatalysis, in: 1999: pp. 171–194. doi:10.1142/9781848160613_0009.

[105] U.I. Gaya, A.H. Abdullah, Heterogeneous photocatalytic degradation of organic contaminants over titanium dioxide: A review of fundamentals, progress and problems, J. Photochem. Photobiol. C Photochem. Rev. 9 (2008) 1–12. doi:10.1016/j.jphotochemrev.2007.12.003.

[106] M. Ni, M.K.H. Leung, D.Y.C. Leung, K. Sumathy, A review and recent developments in photocatalytic water-splitting using TiO_2 for hydrogen production, Renew. Sustain. Energy Rev. 11 (2007) 401–425. doi:10.1016/j.rser.2005.01.009.

[107] M. Yasmina, K. Mourad, S.H. Mohammed, C. Khaoula, Treatment heterogeneous photocatalysis; Factors influencing the photocatalytic degradation by TiO_2, Energy Procedia. 50 (2014) 559–566. doi:10.1016/j.egypro.2014.06.068.

[108] L. Cheng, Q. Xiang, Y. Liao, Environmental Science, (2018) 4–7. doi:10.1039/c7ee03640j.

[109] M. Wongaree, S. Chiarakorn, S. Chuangchote, Photocatalytic Improvement under Visible Light in TiO_2 Nanoparticles by Carbon Nanotube Incorporation, 2015 (2015).

[110] R.S. Singh, V.K. Rangari, S. Sanagapalli, V. Jayaraman, S. Mahendra, V.P. Singh, Nano-structured CdTe, CdS and TiO_2 for thin film solar cell applications, Sol. Energy Mater. Sol. Cells. 82 (2004) 315–330. doi:10.1016/j.solmat.2004.02.006.

[111] S. Leong, A. Razmjou, K. Wang, K. Hapgood, X. Zhang, H. Wang, TiO_2 based photocatalytic membranes: A review, J. Memb. Sci. 472 (2014) 167–184. doi:10.1016/j.memsci.2014.08.016.

[112] Y. Yu, J.C. Yu, J.G. Yu, Y.C. Kwok, Y.K. Che, J.C. Zhao, L. Ding, W.K. Ge, P.K. Wong, Enhancement of photocatalytic activity of mesoporous TiO_2 by using carbon nanotubes, Appl. Catal. A Gen. 289 (2005) 186–196. doi:10.1016/j.apcata.2005.04.057.

[113] R. Abe, K. Sayama, H. Arakawa, Significant effect of iodide addition on water splitting into H_2 and O_2 over Pt-loaded TiO_2 photocatalyst: Suppression of backward reaction, Chem. Phys. Lett. 371 (2003) 360–364. doi:10.1016/S0009-2614(03)00252-5.

[114] S. Sakthivel, M. V. Shankar, M. Palanichamy, B. Arabindoo, D.W. Bahnemann, V. Murugesan, Enhancement of photocatalytic activity by metal deposition: Characterisation and photonic efficiency of Pt, Au and Pd deposited on TiO_2 catalyst, Water Res. 38 (2004) 3001–3008. doi:10.1016/j.watres.2004.04.046.

[115] E. Szabó-Bárdos, H. Czili, A. Horváth, Photocatalytic oxidation of oxalic acid enhanced by silver deposition on a TiO_2 surface, J. Photochem. Photobiol. A Chem. 154 (2003) 195–201. doi:10.1016/S1010-6030(02)00330-1.

[116] N.L. Wu, M.S. Lee, Enhanced TiO2 photocatalysis by Cu in hydrogen production from aqueous methanol solution, Int. J. Hydrogen Energy. 29 (2004) 1601–1605. doi:10.1016/j.ijhydene.2004.02.013.

[117] F. Haque, T. Daeneke, K. Kalantar-zadeh, J.Z. Ou, Two-Dimensional Transition Metal Oxide and Chalcogenide-Based Photocatalysts, Nano-Micro Lett. 10 (2018) 1–27. doi:10.1007/s40820-017-0176-y.

[118] A.H. Reshak, S. Auluck, Electronic and optical properties of the 1T phases of TiS_2, $TiSe_2$, and $TiTe_2$, Phys. Rev. B - Condens. Matter Mater. Phys. 68 (2003) 1–7. doi:10.1103/PhysRevB.68.245113.

[119] J.A. Wilson, A.D. Yoffe, The transition metal dichalcogenides discussion and interpretation of the observed optical, electrical and structural properties, Adv. Phys. 18 (1969) 193–335. doi:10.1080/00018736900101307.

[120] L. Nie, Q. Zhang, Recent progress in crystalline metal chalcogenides as efficient photocatalysts for organic pollutant degradation, Inorg. Chem. Front. 4 (2017) 1953–1962. doi:10.1039/c7qi00651a.

[121] F. Li, X. Liu, Q. Zhang, T. Kong, H. Jin, Fabrication and photocatalytic property of CuO nanosheets via a facile solution route, Cryst. Res. Technol. 47 (2012) 1140–1147. doi:10.1002/crat.201200143.

[122] B. Peng, P.K. Ang, K.P. Loh, Two-dimensional dichalcogenides for light-harvesting applications, Nano Today. 10 (2015) 128–137. doi:10.1016/j.nantod.2015.01.007.

[123] D. Ke, S. Liu, K. Dai, J. Zhou, L. Zhang, T. Peng, CdS/regenerated cellulose nanocomposite films for highly efficient photocatalytic H_2 production under visible light irradiation, J. Phys. Chem. C. 113 (2009) 16021–16026. doi:10.1021/jp903378q.

[124] S. Xiong, B. Xi, Y. Qian, CdS hierarchical nanostructures with tunable morphologies: Preparation and photocatalytic properties, J. Phys. Chem. C. 114 (2010) 14029–14035. doi:10.1021/jp1049588.

[125] W.T. Yao, S.H. Yu, S.J. Liu, J.P. Chen, X.M. Liu, F.Q. Li, Architectural control syntheses of CdS and CdSe nanoflowers, branched nanowires, and nanotrees via a solvothermal approach in a mixed solution and their photocatalytic property, J. Phys. Chem. B. 110 (2006) 11704–11710. doi:10.1021/jp060164n.

[126] Q. Shen, J. Xue, A. Mi, H. Jia, X. Liu, B. Xu, The study on properties of CdS photocatalyst with different ratios of zinc-blende and wurtzite structure, RSC Adv. 3 (2013) 20930–20935. doi:10.1039/c3ra42179a.

[127] M. Liu, B. Wang, Y. Zheng, F. Xue, Y. Chen, L. Guo, Transformation of zincblende nanoparticles into wurtzite microrods by a dissolution-regrowth process: An intergrowth homojunction with enhanced photocatalytic activity, Catal. Sci. Technol. 6 (2016) 3371–3377. doi:10.1039/c6cy00298f.

[128] K. Wu, H. Zhu, T. Lian, Ultrafast Exciton Dynamics and Light-Driven H_2 Evolution in Colloidal Semiconductor Nanorods and Pt-Tipped Nanorods, Acc. Chem. Res. 48 (2015) 851–859. doi:10.1021/ar500398g.

[129] J. Yu, Y. Yu, P. Zhou, W. Xiao, B. Cheng, Morphology-dependent photocatalytic H_2-production activity of CdS, Appl. Catal. B Environ. 156–157 (2014) 184–191. doi:10.1016/j.apcatb.2014.03.013.

[130] B. Weng, S. Liu, N. Zhang, Z.R. Tang, Y.J. Xu, A simple yet efficient visible-light-driven CdS nanowires-carbon nanotube 1D-1D nanocomposite photocatalyst, J. Catal. 309 (2014) 146–155. doi:10.1016/j.jcat.2013.09.013.

[131] F. Caruso, X. Shi, R.A. Caruso, A. Susha, Hollow titania spheres from layered precursor deposition on sacrificial colloidal core particles, Adv. Mater. 13 (2001) 740–744. doi:10.1002/1521-4095(200105)13:10<740::AID-ADMA740>3.0.CO;2-6.

[132] C. Li, L. Han, R. Liu, H. Li, S. Zhang, G. Zhang, Controlled synthesis of CdS micro/nano leaves with (0001) facets exposed: Enhanced photocatalytic activity toward hydrogen evolution, J. Mater. Chem. 22 (2012) 23815–23820. doi:10.1039/c2jm35415b.

[133] T. Tsuzuki, P.G. McCormick, Synthesis of CdS quantum dots by mechanochemical reaction, Appl. Phys. A Mater. Sci. Process. 65 (1997) 607–609. doi:10.1007/s003390050629.

[134] A. Dumbrava, G. Prodan, D. Berger, M. Bica, Properties of PEG-capped CdS nanopowders synthesized under very mild conditions, Powder Technol. 270 (2015) 197–204. doi:10.1016/j.powtec.2014.10.012.

[135] A. Samadi-maybodi, F. Abbasi, R. Akhoondi, Aqueous synthesis and characterization of CdS quantum dots capped with some amino acids and investigations of their photocatalytic activities, Colloids Surfaces A Physicochem. Eng. Asp. 447 (2014) 111–119. doi:10.1016/j.colsurfa.2014.01.036.

[136] P. Chandran, P. Kumari, S. Sudheer Khan, Photocatalytic activation of CdS NPs under visible light for environmental cleanup and disinfection, Sol. Energy. 105 (2014) 542–547. doi:10.1016/j.solener.2014.04.028.

[137] M. Darwish, A. Mohammadi, N. Assi, Microwave-assisted polyol synthesis and characterization of pvp-capped cds nanoparticles for the photocatalytic

degradation of tartrazine, Mater. Res. Bull. 74 (2016) 387–396. doi:10.1016/j.materresbull.2015.11.002.

[138] R.A. Devi, M. Latha, S. Velumani, G. Oza, P. Reyes-Figueroa, M. Rohini, I.G. Becerril-Juarez, J.-H. Lee, J. Yi, Synthesis and Characterization of Cadmium Sulfide Nanoparticles by Chemical Precipitation Method, J. Nanosci. Nanotechnol. 15 (2015) 8434–8439. doi:10.1166/jnn.2015.11472.

[139] G.C. De, A.M. Roy, S.S. Bhattacharya, Photocatalytic production of hydrogen and concomitant cleavage of industrial waste hydrogen sulphide, Int. J. Hydrogen Energy. 20 (1995) 127–131. doi:10.1016/0360-3199(94)P3692-V.

[140] W. Li, D. Li, Z. Chen, H. Huang, M. Sun, Y. He, X. Fu, High-efficient degradation of dyes by ZnxCd1-xS solid solutions under visible light irradiation, J. Phys. Chem. C. 112 (2008) 14943–14947. doi:10.1021/jp8049075.

[141] F. Yang, N.N. Yan, S. Huang, Q. Sun, L.Z. Zhang, Y. Yu, Zn-doped CdS nanoarchitectures prepared by hydrothermal synthesis: Mechanism for enhanced photocatalytic activity and stability under visible light, J. Phys. Chem. C. 116 (2012) 9078–9084. doi:10.1021/jp300939q.

[142] T.K. Jana, A. Pal, K. Chatterjee, Self assembled flower like CdS-ZnO nanocomposite and its photo catalytic activity, J. Alloys Compd. 583 (2014) 510–515. doi:10.1016/j.jallcom.2013.08.184.

[143] D. Wu, F. Wang, Y. Tan, C. Li, Facile synthesis of NiS/CdS nanocomposites for photocatalytic degradation of quinoline under visible-light irradiation, RSC Adv. 6 (2016) 73522–73526. doi:10.1039/c6ra13439d.

[144] P. Nyamukamba, M.J. Moloto, H. Mungondori, Visible light-active CdS/TiO_2 hybrid nanoparticles immobilized on polyacrylonitrile membranes for the photodegradation of dyes in water, J. Nanotechnol. 2019 (2019). doi:10.1155/2019/5135618.

[145] S. Ma, J. Xie, J. Wen, K. He, X. Li, W. Liu, X. Zhang, Constructing 2D layered hybrid CdS nanosheets/MoS 2 heterojunctions for enhanced visible-light photocatalytic H 2 generation, Appl. Surf. Sci. 391 (2017) 580–591. doi:10.1016/j.apsusc.2016.07.067.

[146] Q. Cai, Z. Hu, Q. Zhang, B. Li, Z. Shen, Fullerene (C 60)/CdS nanocomposite with enhanced photocatalytic activity and stability, Appl. Surf. Sci. 403 (2017) 151–158. doi:10.1016/j.apsusc.2017.01.135.

[147] K.A. Adegoke, M. Iqbal, H. Louis, O.S. Bello, Synthesis, characterization and application of CdS/ZnO nanorod heterostructure for the photodegradation of Rhodamine B dye, Mater. Sci. Energy Technol. 2 (2019) 329–336. doi:10.1016/j.mset.2019.02.008.

[148] S. Cao, J. Yu, G-C3N4-based photocatalysts for hydrogen generation, J. Phys. Chem. Lett. 5 (2014) 2101–2107. doi:10.1021/jz500546b.

[149] J. Wen, J. Xie, X. Chen, X. Li, A review on g-C 3 N 4 -based photocatalysts, Appl. Surf. Sci. 391 (2017) 72–123. doi:10.1016/j.apsusc.2016.07.030.

[150] E.A. Weiss, Designing the surfaces of semiconductor quantum dots for colloidal photocatalysis, ACS Energy Lett. 2 (2017) 1005–1013. doi:10.1021/acsenergylett.7b00061.

[151] K.R. Reddy, C.V. Reddy, M.N. Nadagouda, N.P. Shetti, S. Jaesool, T.M. Aminabhavi, Polymeric graphitic carbon nitride (g-C_3N_4)-based semiconducting nanostructured materials: Synthesis methods, properties and photocatalytic applications, J. Environ. Manage. 238 (2019) 25–40. doi:10.1016/j.jenvman.2019.02.075.

[152] S. Wang, C. Li, T. Wang, P. Zhang, A. Li, J. Gong, Controllable synthesis of nanotube-type graphitic C_3N_4 and their visible-light photocatalytic and fluorescent properties, J. Mater. Chem. A. 2 (2014) 2885–2890. doi:10.1039/c3ta14576j.

[153] B. Weng, S. Liu, Z. Tang, Y. Xu, RSC Advances One-dimensional nanostructure based materials for versatile photocatalytic applications, (2014) 12685–12700. doi:10.1039/c3ra47910b.

[154] J. Zhang, Y. Chen, X. Wang, Two-dimensional covalent carbon nitride nanosheets: Synthesis, functionalization, and applications, Energy Environ. Sci. 8 (2015) 3092–3108. doi:10.1039/c5ee01895a.

[155] X. Bai, L. Wang, R. Zong, Y. Zhu, Photocatalytic activity enhanced via g-C_3N_4

nanoplates to nanorods, J. Phys. Chem. C. 117 (2013) 9952–9961. doi:10.1021/jp402062d.

[156] Q. Han, B. Wang, J. Gao, Z. Cheng, Y. Zhao, Z. Zhang, L. Qu, Atomically Thin Mesoporous Nanomesh of Graphitic C_3N_4 for High-Efficiency Photocatalytic Hydrogen Evolution, ACS Nano. 10 (2016) 2745–2751. doi:10.1021/acsnano.5b07831.

[157] X. Zhang, X. Xie, H. Wang, J. Zhang, B. Pan, Y. Xie, Enhanced photoresponsive ultrathin graphitic-phase C_3N_4 nanosheets for bioimaging, J. Am. Chem. Soc. 135 (2013) 18–21. doi:10.1021/ja308249k.

[158] J. Senker, K. Schwinghammer, B. V. Lotsch, C. Ziegler, M.B. Mesch, V. Duppel, Crystalline Carbon Nitride Nanosheets for Improved Visible-Light Hydrogen Evolution, J. Am. Chem. Soc. 136 (2014) 1730–1733. doi:10.1021/ja411321s.

[159] B. Luo, G. Liu, L. Wang, Recent advances in 2D materials for photocatalysis, Nanoscale. 8 (2016) 6904–6920. doi:10.1039/c6nr00546b.

[160] P. Niu, L. Zhang, G. Liu, H.M. Cheng, Graphene-like carbon nitride nanosheets for improved photocatalytic activities, Adv. Funct. Mater. 22 (2012) 4763–4770. doi:10.1002/adfm.201200922.

[161] Q. Liu, T. Chen, Y. Guo, Z. Zhang, X. Fang, Ultrathin g-C_3N_4 nanosheets coupled with carbon nanodots as 2D/0D composites for efficient photocatalytic H2 evolution, Appl. Catal. B Environ. 193 (2016) 248–258. doi:10.1016/j.apcatb.2016.04.034.

[162] Y. Xu, S.P. Gao, Band gap of C_3N_4 in the GW approximation, Int. J. Hydrogen Energy. 37 (2012) 11072–11080. doi:10.1016/j.ijhydene.2012.04.138.

[163] K. Maeda, X. Wang, Y. Nishihara, D. Lu, M. Antonietti, K. Domen, Photocatalytic activities of graphitic carbon nitride powder for water reduction and oxidation under visible light, J. Phys. Chem. C. 113 (2009) 4940–4947. doi:10.1021/jp809119m.

[164] A.H. Reshak, AA- and ABA-stacked carbon nitride (C_3N_4): Novel photocatalytic water splitting solar-to-hydrogen energy conversion, Phys. Chem. Chem.

Phys. 20 (2018) 22972–22979. doi:10.1039/c8cp02898b.

[165] A.Y. Liu, M.L. Cohen, Prediction of new low compressibility solids, Science (80-.). 245 (1989) 841–842. doi:10.1126/science.245.4920.841.

[166] B. Jürgens, E. Irran, J. Senker, P. Kroll, H. Müller, W. Schnick, Melem (2,5,8-triamino-tri-s-triazine), an important intermediate during condensation of melamine rings to graphitic carbon nitride: Synthesis, structure determination by x-ray powder diffractometry, solid-state NMR, and theoretical studies, J. Am. Chem. Soc. 125 (2003) 10288–10300. doi:10.1021/ja0357689.

[167] J. Sehnert, K. Baerwinkel, J. Senker, Ab initio calculation of solid-state NMR spectra for different triazine and heptazine based structure proposals of g-C_3N_4, J. Phys. Chem. B. 111 (2007) 10671–10680. doi:10.1021/jp072001k.

[168] A. Thomas, A. Fischer, F. Goettmann, M. Antonietti, J.O. Müller, R. Schlögl, J.M. Carlsson, Graphitic carbon nitride materials: Variation of structure and morphology and their use as metal-free catalysts, J. Mater. Chem. 18 (2008) 4893–4908. doi:10.1039/b800274f.

[169] Y. Wang, J. Hong, W. Zhang, R. Xu, Carbon nitride nanosheets for photocatalytic hydrogen evolution: Remarkably enhanced activity by dye sensitization, Catal. Sci. Technol. 3 (2013) 1703–1711. doi:10.1039/c3cy20836b.

[170] H. Luo, Z. Zeng, G. Zeng, C. Zhang, R. Xiao, C. Zhou, H. Wang, Y. Zhou, S. Tian, Recent progress on metal-organic frameworks based- and derived-photocatalysts for water splitting, Chem. Eng. J. (2019) 123196. doi:10.1016/j.cej.2019.123196.

[171] D. Zheng, C. Pang, Y. Liu, X. Wang, Shell-engineering of hollow g-C_3N_4 nanospheres via copolymerization for photocatalytic hydrogen evolution , Chem. Commun. 51 (2015) 9706–9709. doi:10.1039/c5cc03143e.

[172] S.W. Bian, Z. Ma, W.G. Song, Preparation and characterization of carbon nitride nanotubes and their applications as catalyst supporter, J. Phys. Chem. C. 113 (2009) 8668–8672. doi:10.1021/jp810630k.

[173] L. Xu, J. Xia, L. Wang, H. Ji, J. Qian, H. Xu, K. Wang, H. Li, Graphitic carbon

nitride nanorods for photoelectrochemical sensing of trace copper(II) ions, Eur. J. Inorg. Chem. (2014) 3665–3673. doi:10.1002/ejic.201402051.

[174] S. Hu, R. Jin, G. Lu, D. Liu, J. Gui, The properties and photocatalytic performance comparison of Fe^{3+}-doped g-C_3N_4 and Fe_2O_3/g-C_3N_4 composite catalysts, RSC Adv. 4 (2014) 24863–24869. doi:10.1039/c4ra03290j.

[175] Y. Wang, Y. Wang, Y. Li, H. Shi, Y. Xu, H. Qin, X. Li, Y. Zuo, S. Kang, L. Cui, Simple synthesis of Zr-doped graphitic carbon nitride towards enhanced photocatalytic performance under simulated solar light irradiation, Catal. Commun. 72 (2015) 24–28. doi:10.1016/j.catcom.2015.08.022.

[176] P. Fageria, R. Nazir, S. Gangopadhyay, H.C. Barshilia, S. Pande, Graphitic-carbon nitride support for the synthesis of shape-dependent ZnO and their application in visible light photocatalysts, RSC Adv. 5 (2015) 80397–80409. doi:10.1039/c5ra12463h.

[177] H. Yu, F. Chen, F. Chen, X. Wang, Applied Surface Science In situ self-transformation synthesis of g-C_3N_4 -modified CdS heterostructure with enhanced photocatalytic activity, Appl. Surf. Sci. 358 (2015) 385–392. doi:10.1016/j.apsusc.2015.06.074.

[178] F. Jiang, T. Yan, H. Chen, A. Sun, C. Xu, X. Wang, Applied Surface Science A g-C_3N_4 – CdS composite catalyst with high visible-light-driven catalytic activity and photostability for methylene blue degradation, Appl. Surf. Sci. 295 (2014) 164–172. doi:10.1016/j.apsusc.2014.01.022.

[179] Y. Guo, J. Wang, Z. Tao, F. Dong, K. Wang, X. Ma, P. Yang, P. Hu, Y. Xu, L. Yang, Facile synthesis of mesoporous CdS nanospheres and their application in photocatalytic degradation and adsorption of organic dyes, CrystEngComm. 14 (2012) 1185–1188. doi:10.1039/c2ce06172d.

[180] H.M. Xiong, D.G. Shchukin, H. Möhwald, Y. Xu, Y.Y. Xia, Sonochemical synthesis of highly luminescent zinc oxide nanoparticles doped with magnesium(II), Angew. Chemie - Int. Ed. 48 (2009) 2727–2731. doi:10.1002/anie.200805590.

[181] Z.R. Tang, X. Yin, Y. Zhang, Y.J. Xu, Synthesis of titanate nanotube-CdS

nanocomposites with enhanced visible light photocatalytic activity, Inorg. Chem. 52 (2013) 11758–11766. doi:10.1021/ic4010483.

[182] Y. Li, L. Tang, S. Peng, Z. Li, G. Lu, Phosphate-assisted hydrothermal synthesis of hexagonal CdS for efficient photocatalytic hydrogen evolution, CrystEngComm. 14 (2012) 6974–6982. doi:10.1039/c2ce25838b.

[183] M. Salavati-Niasari, M.R. Loghman-Estarki, F. Davar, Controllable synthesis of nanocrystalline CdS with different morphologies by hydrothermal process in the presence of thioglycolic acid, Chem. Eng. J. 145 (2008) 346–350. doi:10.1016/j.cej.2008.08.040.

[184] L.R. Zou, G.F. Huang, D.F. Li, J.H. Liu, A.L. Pan, W.Q. Huang, A facile and rapid route for synthesis of g-C_3N_4 nanosheets with high adsorption capacity and photocatalytic activity, RSC Adv. 6 (2016) 86688–86694. doi:10.1039/c6ra20514c.

[185] N. Chidhambaram, K. Ravichandran, Fabrication of ZnO/g-C_3N_4 nanocomposites for enhanced visible light driven photocatalytic activity Fabrication of ZnO/g-C_3N_4 nanocomposites for enhanced visible light driven photocatalytic activity, (n.d.).

[186] M. Iqbal, A. Ali, N.A. Nahyoon, A. Majeed, R. Pothu, S. Phulpoto, K.H. Thebo, Photocatalytic degradation of organic pollutant with nanosized cadmium sulfide, Mater. Sci. Energy Technol. 2 (2018) 41–45. doi:10.1016/j.mset.2018.09.002.

[187] S. Vadivel, D. Maruthamani, B. Paul, S.S. Dhar, K. Selvam, Facile synthesis of novel $CaFe_2O_4$/g-C_3N_4 nanocomposites for degradation of methylene blue under visible-light irradiation Journal of Colloid and Interface Science Facile synthesis of novel $CaFe_2O_4$/g-C_3N_4 nanocomposites for degradation of methyle, J. Colloid Interface Sci. 480 (2016) 126–136. doi:10.1016/j.jcis.2016.07.012.

[188] Z.X. Han, Z. Zhu, D.D. Wu, J. Wu, Y.R. Liu, Adsorption Kinetics and Thermodynamics of Acid Blue 25 and methylene blue dye solutions on natural sepiolite, Synth. React. Inorganic, Met. Nano-Metal Chem. 44 (2014) 140–147. doi:10.1080/15533174.2013.770755.

[189] S. Kaur, A brief review on photocatalytic activity of ZnS and CQDs nanoparticles, Int. J. Eng. Appl. Sci. Technol. 2 (2017) 75–82. http://www.ijeast.com.

[190] M. Joshi, A. Bhattacharyya, S.W. Ali, Characterization techniques for nanotechnology applications in textiles, Indian J. Fibre Text. Res. 33 (2008) 304–317.

[191] R. Kohli, Methods for Monitoring and Measuring Cleanliness of Surfaces, in: Dev. Surf. Contam. Clean. - Detect. Charact. Anal. Contam., Elsevier, 2012: pp. 107–178. doi:10.1016/B978-1-4377-7883-0.00003-1.

[192] G. Zhang, Master Thesis, University of Illinois at Urbana-Champaign, 2013, 2013.

[193] P.J. Mafa, A.T. Kuvarega, B.B. Mamba, B. Ntsendwana, Photoelectrocatalytic degradation of sulfamethoxazole on g-C_3N_4/BiOI/EG p-n heterojunction photoanode under visible light irradiation, Appl. Surf. Sci. 483 (2019) 506–520. doi:10.1016/j.apsusc.2019.03.281.

[194] M. Izadifard, G. Achari, C.H. Langford, Application of photocatalysts and LED light sources in drinking water treatment, Catalysts. 3 (2013) 726–743. doi:10.3390/catal3030726.

[195] C.G. Young, an Inductively Coupled Plasma Atomic Emission Spectrometer for the Detection of Nonmetals in the Vacuum Ultraviolet, 2011.

[196] A.M. Sabir, M. Moloy, P.S. Bhasin, Hplc Method Development and Validation: a Review, Int. Res. J. Pharm. 4 (2016) 39–46. doi:10.7897/2230-8407.04407.

[197] F. Jiang, T. Yan, H. Chen, A. Sun, C. Xu, X. Wang, A g-C_3N_4 -CdS composite catalyst with high visible-light-driven catalytic activity and photostability for methylene blue degradation, Appl. Surf. Sci. 295 (2014) 164–172. doi:10.1016/j.apsusc.2014.01.022.

[198] Z. Zhang, J. Huang, M. Zhang, Q. Yuan, B. Dong, Ultrathin hexagonal SnS_2 nanosheets coupled with g-C_3N_4 nanosheets as 2D/2D heterojunction photocatalysts toward high photocatalytic activity, Appl. Catal. B Environ. 163 (2015) 298–305. doi:10.1016/j.apcatb.2014.08.013.

[199] A. Akhundi, A. Habibi-yangjeh, Novel magnetically separable g-C_3N_4/AgBr /Fe_3O_4 nanocomposites as visible-light-driven photocatalysts with highly enhanced activities, Ceram. Int. 41 (2015) 5634–5643. doi:10.1016/j.ceramint.2014.12.145.

[200] L.J. Cote, F. Kim, J. Huang, Langmuir-blodgett assembly of graphite oxide single layers, J. Am. Chem. Soc. 131 (2009) 1043–1049. doi:10.1021/ja806262m.

[201] Z. Zhou, J. Wang, J. Yu, Y. Shen, Y. Li, A. Liu, S. Liu, Y. Zhang, Dissolution and liquid crystals phase of 2D polymeric carbon nitride, J. Am. Chem. Soc. 137 (2015) 2179–2182. doi:10.1021/ja512179x.

[202] J. Xu, L. Zhang, R. Shi, Y. Zhu, Chemical exfoliation of graphitic carbon nitride for efficient heterogeneous photocatalysis, J. Mater. Chem. A. 1 (2013) 14766–14772. doi:10.1039/c3ta13188b.

[203] F. Dong, Z. Wang, Y. Sun, W.K. Ho, H. Zhang, Engineering the nanoarchitecture and texture of polymeric carbon nitride semiconductor for enhanced visible light photocatalytic activity, J. Colloid Interface Sci. 401 (2013) 70–79. doi:10.1016/j.jcis.2013.03.034.

[204] C. Li, Z. Sun, W. Huang, S. Zheng, Facile synthesis of g-C_3N_4/montmorillonite composite with enhanced visible light photodegradation of rhodamine B and tetracycline, J. Taiwan Inst. Chem. Eng. 66 (2016) 363–371. doi:10.1016/j.jtice.2016.06.014.

[205] J. Tong, L. Zhang, F. Li, K. Wang, L. Han, S. Cao, Rapid and high-yield production of g-C_3N_4 nanosheets via chemical exfoliation for photocatalytic H_2 evolution, RSC Adv. 5 (2015) 88149–88153. doi:10.1039/c5ra16988g.

[206] J. Zhu, P. Xiao, H. Li, S.A.C. Carabineiro, Graphitic carbon nitride: Synthesis, properties, and applications in catalysis, ACS Appl. Mater. Interfaces. 6 (2014) 16449–16465. doi:10.1021/am502925j.

[207] Y. Chen, X. Wang, Template-Free Synthesis of Hollow G-C_3N_4 Polymer with Vesicle Structure for Enhanced Photocatalytic Water Splitting, (2018). doi:10.1021/acs.jpcc.7b12496.

[208] H.B. Tao, H. Bin Yang, J. Chen, J. Miao, B. Liu, Biomolecule-assisted synthesis of carbon nitride and sulfur-doped carbon nitride heterojunction nanosheets: An efficient heterojunction photocatalyst for photoelectrochemical applications, Beilstein J. Nanotechnol. 5 (2014) 770–777. doi:10.3762/bjnano.5.89.

[209] J. Tong, L. Zhang, F. Li, K. Wang, L. Han, S. Cao, Rapid and high-yield production of g-C_3N_4 nanosheets via chemical exfoliation for photocatalytic H_2 evolution, RSC Adv. 5 (2015) 88149–88153. doi:10.1039/c5ra16988g.

[210] S. Asadzadeh-khaneghah, A. Habibi-yangjeh, S. Vadivel, Journal of the Taiwan Institute of Chemical Engineers Fabrication of novel g-C_3N_4 nanosheet /carbon dots/$Ag_6Si_2O_7$ nanocomposites with high stability and enhanced visible-light photocatalytic activity, J. Taiwan Inst. Chem. Eng. 103 (2019) 94–109. doi:10.1016/j.jtice.2019.07.018.

[211] G. Mamba, A.K. Mishra, Applied Catalysis B : Environmental Graphitic carbon nitride (g-C_3N_4) nanocomposites : A new and exciting generation of visible light driven photocatalysts for environmental pollution remediation, "Applied Catal. B, Environ. 198 (2016) 347–377. doi:10.1016/j.apcatb.2016.05.052.

[212] J. Jin, J. Yu, G. Liu, P.K. Wong, Single crystal CdS nanowires with high visible-light photocatalytic H_2-production performance, J. Mater. Chem. A. 1 (2013) 10927–10934. doi:10.1039/c3ta12301d.

[213] S. Rengaraj, A. Ferancova, S.H. Jee, S. Venkataraj, Y. Kim, J. Labuda, M. Sillanpää, Physical and electrochemical characterization of CdS hollow microspheres prepared by a novel template free solution phase method, Electrochim. Acta. 56 (2010) 501–509. doi:10.1016/j.electacta.2010.09.019.

[214] J. Fu, B. Chang, Y. Tian, F. Xi, X. Dong, Novel C_3N_4-CdS composite photocatalysts with organic-inorganic heterojunctions: In situ synthesis, exceptional activity, high stability and photocatalytic mechanism, J. Mater. Chem. A. 1 (2013) 3083–3090. doi:10.1039/c2ta00672c.

[215] Q. Li, B. Guo, J. Yu, J. Ran, B. Zhang, H. Yan, J.R. Gong, Highly efficient visible-light-driven photocatalytic hydrogen production of CdS-cluster-decorated graphene nanosheets, J. Am. Chem. Soc. 133 (2011) 10878–

10884. doi:10.1021/ja2025454.

[216] V. Mohanraj, R. Jayaprakash, R. Robert, J. Balavijayalakshmi, S. Gopi, Effect of particle size on optical and electrical properties in mixed CdS and NiS nanoparticles synthesis by ultrasonic wave irradiation method, Mater. Sci. Semicond. Process. 56 (2016) 394–402. doi:10.1016/j.mssp.2016.08.014.

[217] N.H. Patel, M.P. Deshpande, S.H. Chaki, H.R. Keharia, Tuning of optical, thermal and antimicrobial capabilities of CdS nanoparticles with incorporated Mn prepared by chemical method, J. Mater. Sci. Mater. Electron. 28 (2017) 10866–10876. doi:10.1007/s10854-017-6865-y.

[218] A. Modwi, M.A. Ghanem, A.M. Al-Mayouf, A. Houas, Lowering energy band gap and enhancing photocatalytic properties of Cu/ZnO composite decorated by transition metals, J. Mol. Struct. 1173 (2018) 1–6. doi:10.1016/j.molstruc.2018.06.082.

[219] Q. Tang, C. Zhou, X. Yuan, Q. Jing, Y. Mu, A. Du, Facile Synthesis of g-C_3N_4 Nanosheets/ZnO Nanocomposites with Enhanced Photocatalytic Activity in Reduction of Aqueous Chromium(VI) under Visible Light, Nanomaterials. 6 (2016) 173. doi:10.3390/nano6090173.

[220] D. Wang, Z. Xu, Q. Luo, X. Li, J. An, R. Yin, C. Bao, Preparation and visible-light photocatalytic performances of g-C_3N_4 surface hybridized with a small amount of CdS nanoparticles, J. Mater. Sci. 51 (2016) 893–902. doi:10.1007/s10853-015-9417-y.

[221] A. Kumar, A Review on the Factors Affecting the Photocatalytic Degradation of Hazardous Materials, Mater. Sci. Eng. Int. J. 1 (2017) 1–10. doi:10.15406/mseij.2017.01.00018.

[222] S. Talebi, N. Chaibakhsh, Z. Moradi-Shoeili, Application of nanoscale ZnS/TiO_2 composite for optimized photocatalytic decolorization of a textile dye, J. Appl. Res. Technol. 15 (2017) 378–385. doi:10.1016/j.jart.2017.03.007.

[223] Y.S. Al-Degs, M.I. El-Barghouthi, A.H. El-Sheikh, G.M. Walker, Effect of solution pH, ionic strength, and temperature on adsorption behavior of reactive dyes on activated carbon, Dye. Pigment. 77 (2008) 16–23.

doi:10.1016/j.dyepig.2007.03.001.

[224] E.T. Helmy, A. El Nemr, M. Mousa, E. Arafa, S. Eldafrawy, Photocatalytic degradation of organic dyes pollutants in the industrial textile wastewater by using synthesized TiO_2, C-doped TiO_2, S-doped TiO2 and C,S co-doped TiO_2 nanoparticles, J. Water Environ. Nanotechnol. 3 (2018) 116–127. doi:10.22090/JWENT.2018.02.003.

[225] E. Mugunthan, M.B. Saidutta, P.E. Jagadeeshbabu, Visible light assisted photocatalytic degradation of diclofenac using TiO_2-WO_3 mixed oxide catalysts, Environ. Nanotechnology, Monit. Manag. 10 (2018) 322–330. doi:10.1016/j.enmm.2018.07.012.

[226] S. Iguchi, K. Teramura, S. Hosokawa, T. Tanaka, Effect of the chloride ion as a hole scavenger on the photocatalytic conversion of CO_2 in an aqueous solution over Ni-Al layered double hydroxides, Phys. Chem. Chem. Phys. 17 (2015) 17995–18003. doi:10.1039/c5cp02724a.

[227] L. Das, S.K. Barodia, S. Sengupta, J.K. Basu, Aqueous degradation kinetics of pharmaceutical drug diclofenac by photocatalysis using nanostructured titania–zirconia composite catalyst, Int. J. Environ. Sci. Technol. 12 (2015) 317–326. doi:10.1007/s13762-013-0466-y.

[228] J.M. Monteagudo, H. El-taliawy, A. Durán, G. Caro, K. Bester, Sono-activated persulfate oxidation of diclofenac: Degradation, kinetics, pathway and contribution of the different radicals involved, J. Hazard. Mater. 357 (2018) 457–465. doi:10.1016/j.jhazmat.2018.06.031.

[229] T. Huang, G. Zhang, S. Chong, Y. Liu, N. Zhang, S. Fang, J. Zhu, Effects and mechanism of diclofenac degradation in aqueous solution by US/Zn0, Ultrason. Sonochem. 37 (2017) 676–685. doi:10.1016/j.ultsonch.2017.02.032.

[230] M. V. Bagal, P.R. Gogate, Degradation of diclofenac sodium using combined processes based on hydrodynamic cavitation and heterogeneous photocatalysis, Ultrason. Sonochem. 21 (2014) 1035–1043. doi:10.1016/j.ultsonch.2013.10.020.

[231] P. Sathishkumar, R.A.A. Meena, T. Palanisami, V. Ashokkumar, T. Palvannan,

F.L. Gu, Occurrence, interactive effects and ecological risk of diclofenac in environmental compartments and biota - a review, Sci. Total Environ. 698 (2020) 134057. doi:10.1016/j.scitotenv.2019.134057.

[232] R.R. Giri, H. Ozaki, S. Ota, R. Takanami, S. Taniguchi, Degradation of common pharmaceuticals and personal care products in mixed solutions by advanced oxidation techniques, Int. J. Environ. Sci. Tech. 7 (2010) 251–260. doi:10.1007/BF03326135.

[233] S. Sébastien, Les soignants face à la mort, Rev. Infirm. 1 (2012) 39–41.

[234] H. Xu, L. Wu, L. Jin, K. Wu, Combination Mechanism and Enhanced Visible-Light Photocatalytic Activity and Stability of CdS/g-C_3N_4 Heterojunctions, J. Mater. Sci. Technol. 33 (2017) 30–38. doi:10.1016/j.jmst.2016.04.008.

[235] I.W. As, M.C. Level, P.H. Effects, T. Methods, I. Exchange, R. Osmosis, WQA Technical Fact Sheet: Cadmium health effects treatment methods Residential Point-of-Entry Point-of-Use, 2013. http://www.epa.gov/safewater/pdfs/factsheets/ioc/cadmium.pdf.

CHAPTER 3
RESEARCH METHODOLOGY

3.1 Introduction

This chapter provides details of the chemicals used and details the procedures followed to achieve the aims of this research and it also includes spectroscopic and microscopic characterization techniques employed in this research.

The techniques used to study the surface morphology and optical studies of the synthesized samples, thermal stability and optical properties include scanning electron microscopy (SEM), energy dispersive X-ray spectroscopy (EDX), Fourier transform infra-red (FTIR), X-ray diffraction (XRD), ultraviolet-visible spectroscopy (UV-Vis), thermogravimetric analysis (TGA), Photoluminescence spectroscopy (PL) , Inductively coupled plasma optical emission spectroscopy (ICP-OES) and High performance liquid chromatography (HPLC).

3.2 Material, reagents and solvents

Cadmium acetate dihydrate ($Cd(CH_3COO)_2 \cdot 2H_2O$), thiourea ($CH_4N_2S$) ,melamine, sulfuric acid (H_2SO_4) 98%, sodium hydroxide (NaOH), hydrochloric acid (HCl), ethanol (C_2H_2O), benzoquinone ($C_6H_4O_2$), propanol (C_3H_8O), ethylenediamine ($C_{10}H_{16}N_2O_8$), Acid blue-25 ($C_{20}H_{12}N_2NaO_5S$) and diclofenac sodium ($C_{14}H_{11}Cl_2NNaO_2$) were purchased from Sigma-Aldrich South Africa and were used without further purification. A 0.45 µm PVDF syringe membrane was purchased from sigma Aldrich (SA). Deionized water was used throughout this research.

3.3 Experimental procedure

3.3.1 Synthesis of g-C_3N_4 nanosheets

The g-C_3N_4 nanosheets were synthesized using the method reported in literature [184]. The g-C_3N_4 nanosheets were prepared by firstly preparing bulk g-C_3N_4 (CN) which was prepared by polymerization of melamine at 550 °C at a heating rate of 10°C min^{-1} for 6 hours in a furnace. The resultant yellow agglomerate was crushed into fine powder. The bulk g-C_3N_4 (0.5 g) was mixed with 15 mL concentrated H_2SO_4 (98 wt. %) in a 200 mL beaker and stirred for 10 min. 10 mL deionized water was

added rapidly to the yellow suspension with vigorous stirring until it turned into colourless transparent solution. 150 mL ethanol was then added to form a white precipitate. The precipitate was centrifuged and washed using ethanol and deionized water to remove the excess H_2SO_4, then dried at 60 °C for 24 hours and calcined at 400 °C for 1h [185].

3.3.2 Synthesis of CdS

The CdS nanoparticles were synthesized using the method reported in literature [186] Cadmium sulphide nanoparticles were synthesized using hydrothermal method where 2.3 g of cadmium acetate and 0.36 g of thiourea were dissolved in 60 ml deionized water and admixed together, then stirred for 1 hour to allow homogeneity thereafter the solution was transferred into a 100 ml steel autoclave and then heated at 180 ^oC for 24 hours. The obtained precipitate was washed using ethanol and deionized water to remove any impurities thereafter dried at 60 ^oC for 6 hours [186].

3.3.3 Synthesis of g-C_3N_4/CdS

The g-C_3N_4/CdS nanocomposites were synthesized using the modified method reported in literature [187]. CN/CdS nanocomposites were synthesized using the in-situ hydrothermal method where 2.3 g of cadmium acetate and 0.36 g of thiourea were dissolved in 60 ml deionized water and stirred for 1 hour, then 10, 20 and 30% CNS were added to the solution then stirred for 24 hours to achieve a homogeneous suspension, the resulting solution was transferred into a steel autoclave and then heated at 180 ^oC for 24hours thereafter washed using ethanol and deionized water and dried at 60 ^oC for 6 hours.

3.4 Application procedure

3.4.1 Preparation of Acid blue 25 (AB-25)

A stock solution with a concentration of 100 mg/L AB-25 was prepared by weighing 20 mg of 40% AB-25 and dissolving with 500 mL deionized water in a 500 mL volumetric flask. From the stock solution, standard solutions with concentrations (10, 20, 30 and 50 mg/L) in 100mL volumetric flask were prepared by dilution method. The 10, 20 and 50 mg/L standards were used to optimise the concentration of AB-25 and g-C_3N_4/CdS composites for the photocatalytic degradation studies.

3.4.2 Preparation of Diclofenac sodium (DFC)

A 50 mg/L stock solution of DFC was prepared by weight 50 mg of DFC and dissolving with 500 mL deionized water in a 500 mL volumetric flask. From the stock solution 5, 10, 15, 20, 30, 35 and 40 mg/L of the stock solution were pipetted into 100mL volumetric flask and diluted to obtain the calibration curve and the working standard.

The removal efficiency of the pollutants were calculated using the equation:

$$(\%)Removal\ efficiency\ = \frac{C_o - C_f}{C_o} \quad (3.4)$$

Where C_o is the initial concentration of sample and C_f is the final concentration of the solution. The 10, 20, and 40 mL of the standards were used throughout the experimental procedure for the photocatalytic degradation studies.

3.4.3 Photocatalytic degradation studies

Parameters such as, catalyst dosage/concentration, pH of solution, volume of the pollutants and reusability test were studied to determine the photocatalytic efficiency of the nanocomposites.

3.4.3.1 Effect of catalyst dosage

To determine the optimum amount of catalyst needed to carry the photocatalytic studies, the catalyst dosage in the range 10-40 mg of photocatalyst were used to carry the photocatalytic degradation studies of AB-25 and DFC. 10, 20 and 40 mg of Catalyst were weighed and added into volume of AB-25 and DFC, stirred in the dark for 30 min to allow homogeneity.

3.4.3.2 pH of the pollutant solution

The effect of pH of the pollutants were evaluated during the photocatalytic degradation studies,3 M HCL and 1M NaOH were prepared and used to adjust the pH of AB-25 and DFC to 3-9 and 2-10 respectively [188].

3.4.3.3 Volume of the pollutants

The effect of pollutant concentration was evaluated and concentrations of acid blue 25 dye were selected according to the effluent discharges. The volumes for AB-25 and DFC, 10-50 mL and 5 -15 mL were evaluated respectively [189].

3.4.3.4 Reusability Studies

The 10% CNS/CdS nanocomposite was filtered and washed with deionized water to remove any adsorbed pollutants of the surface of the photocatalyst and dried at 60 ^{o}C for 6 h after each photocatalytic cycle [62]

3.5 Instrumental techniques

3.5.1 Scanning Electron Microscopy (SEM)

Scanning Electron Microscopy (SEM) is a type of electron microscopy that is used to determine the surface of a material. The sample is placed in a raster pattern containing an electron beam. The SEM contains an electron gun, where a beam of electrons are generated in a column and onto a series of electromagnetic lenses which are tune wrapped in coil referred to as solenoids. The coils are adjustable and focus the electron beam on the sample and thus cause fluctuations in the voltage which may increase or decrease the speed in which the electrons interact with the material surface. When the electrons of the instrument interact with the electrons in the sample, electrons are released in the form of a signal from the surface of the sample containing information about the surface, shape, texture and composition of the sample and image is generated. Fig. 3.1 shows the schematic diagram of scanning electron microscope.

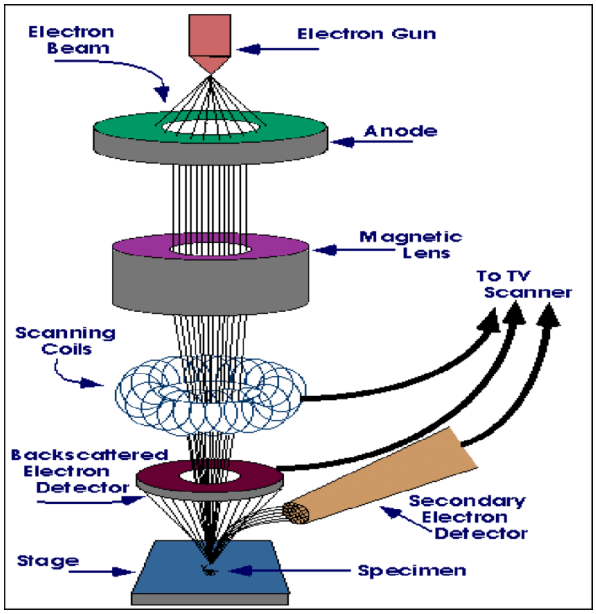

Figure 3.1. Schematic diagram of scanning electron Microscopy [5].

SEM has found applications in the field of science, biology, forensic science gemmology, and medicine. It is also one of the most important imaging instruments for structural analysis of nanoparticles. It can provide information about the microstructures of samples, reveal spatial vibrations and identify the crystalline structures [190].

The surface morphology and elemental composition of bulk g-C_3N_4 (CN), g-C_3N_4 nanosheets (CNS), CdS, CNS/CdS nanocomposites was determined using the scanning electron microscopy (SEM)-JOEL (JSM-IT 300 series) coupled to EDX (Oxford X-MAX 50) The prepared samples were placed on a double sided carbon tape adhesive mounted on a aluminium stub holder. The samples were then gold coated by a cathodic sputtering to improve visibility of the samples and enhance the surface conductivity.

3.5.2 Energy dispersive X-ray spectrometry (EDX)

Energy dispersive X-ray spectroscopy (EDS) is a technique used for quantitative and qualitative analysis of materials and is commonly used together with SEM and TEM as an attachment, it gives information about the elemental surface composition of the materials.

3.5.3 Transmission Electron Microscopy

Transmission electron microscopy (TEM) provides the morphology, composition and crystallography information of the sample. Fig. 3.2 shows the schematic diagram of TEM analysis. In a typical TEM, air is pumped out of the vacuum chamber which creates a space for electrons to move. The electrons pass through multiple electromagnetic lenses. Solenoids which are tubes with a coil wrapped around them where a beam of electrons pass through them and down the column and make contact with the screen where the electrons are converted to light and form an Image. The voltage gun in the instrument is adjusted to increase or decrease the speed of electrons and also change the electromagnetic wavelength through the solenoids. During transmission, the electrons are directly proportional to the wavelength of the electrons, where the faster the electrons move, the shorter the wavelength of the electrons. Shorter wavelengths result in high quality and more detailed images. The images are obtained as dark and light areas, where the light area of the image represents the places where a large number of the electrons were

able to pass through the sample and the dark areas represents the dense are of the sample. These areas contain the information on the structure, texture, shape and size of the sample.

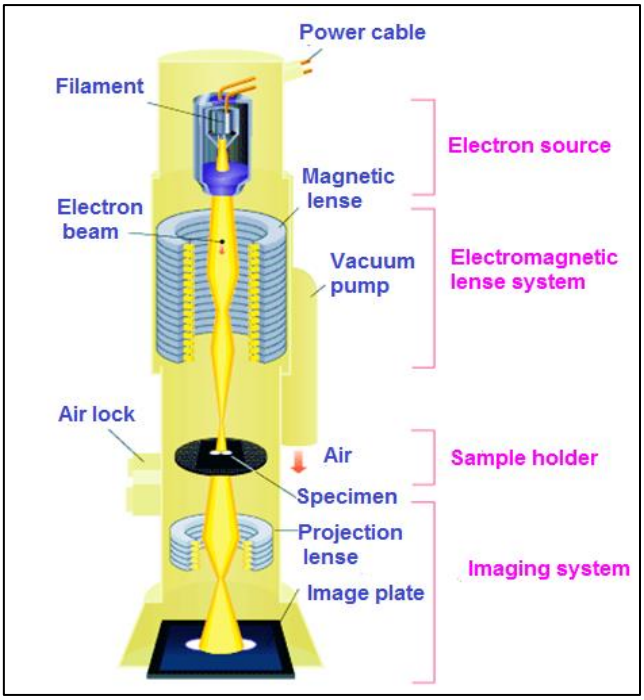

Figure 3.2. Schematic diagram of TEM [7].

In this study the TEM analysis was carried on a Tecnai G2F2O X-Twin MAT (Eindhoven, Netherlands) operating at 200 kV. During the analysis the sample was dispersed in ethanol, sonicated for 2 hours, air dried and placed on copper coated grid and thereafter the dried sample placed in the instrument.

3.5.4 Fourier Transform Infra-red

Fourier transform-infrared spectroscopy (FTIR) is an instrument used to determine the structure and functional groups of samples. A typical FTIR consist of two beams from the IR-source which pass through the sample and reference chambers as independent beams (Fig. 3.3). The optical chopper focuses the reference and sample beams. One beam passes through the sample and the second beam passes through a reference sample for analytical comparison of transmitted photon wave front information. Once the incident radiation passed through the sample, a wave front of radiation is dispersed by gratings and slits into the instrument frequencies. Different slit sizes have different impact on the results obtained. Narrow slits result in better resolution and the to distinguish the spaced frequencies of radiation and wider

slits allow more light to pass through the sample and reach the detector, providing good system sensitivity. The emitted wave front beam strike the detector and generates an electrical signal as a response where they processed by the computer using mathematical algorithm to give the final spectrum.

.

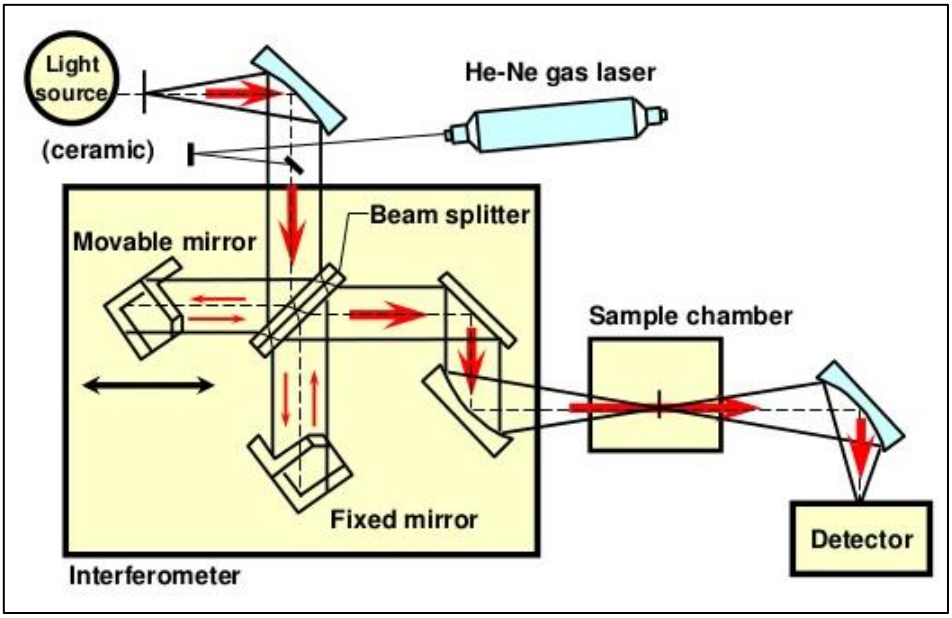

Figure 3.3. Schematic diagram of FTIR [8].

A PerkinElmer FTIR spectrometer Frontier (spectrum 100 spectrometer) in the range of 400-4500 cm^{-1} and 2 cm^{-1} using the pallet presser method was used to determine the functional groups of the prepared samples. The samples were prepared in KBr under vacuum using the pellet presser (international Crystal laboratories, New Jersey, USA). The instrument was set for analysis in the spectral range with optimal resolution from (400-4500 cm^{-1}).

3.5.5 X-Ray diffraction analysis

X-Ray diffraction is a technique used to determine the crystallinity, phase structure lattice properties, structural identification and texture of a sample [191]. During the analysis, X-rays are generated by a cathode ray tube, which are filtered to produce monochromatic radiation and are then collimated to concentrated and directed towards the sample (Fig. 3.5). When the sample interacts with the incident rays, constructive interference and diffraction array occurs following the Bragg's Law:

$$(n\lambda = 2d\ sin\theta) \tag{3.5}$$

n is an integer

λ is the wavelength of the X-rays measured in angstrom

d is the interplanar spacing that generates the diffraction in angstrom and θ is the angle of diffraction.

It is a relation of the wavelength of the electromagnetic radiation to the diffraction angle and the lattice spacing in a crystalline sample. The diffracted X-rays are the sent to the detector, where they are processed and counted.

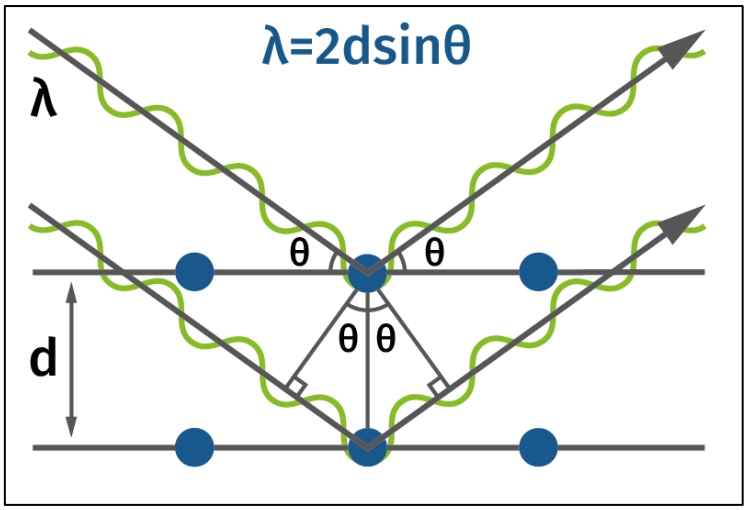

Figure 3.4. Representation diagram of incident and diffraction rays [10].

The crystalline size and micro strain of the samples can also be obtained using the XRD. Profile widths also provide determine domain and crystalline size. The peak width profile increase of the diffraction beam increases with decreasing crystalline size and micro-strain of the samples are estimated using by the Debye-Scherrer relation, equation (3.6) and micro-strain equation (3.7):

$$D = \frac{k\lambda}{\beta cos\theta} \tag{3.6}$$

$$\varepsilon = \beta/4\ tan\,\theta \tag{3.7}$$

D is the crystalline size

λ is the wavelength of the x-rays

K is the dimensionless constant,

θ is the Bragg angle

B is the full width at half-maximum (FWHM) of the peak in radians corrected for instrumental broadening and is equal to 0.154059 nm [11].

The XRD, Rigaku SmartLab X-Ray Diffractometer at room temperature using the Cu-Kα (λ=0.154059 nm) source operated at 45 kV and 200 mA with 2θ range of 5^o to 90^o and scan speed of 2^o/min was used to determine the crystallinity and micro strain of the samples. The sample was placed on the XRD sample holder then placed in the instrument.

3.5.6 BET analysis

The Brunauer Emmett teller (BET) is generally used to evaluate the surface area and porosity of solid samples. During surface area analysis, gas is adsorbed on the surface of the sample, the amount of gas adsorbed which corresponds to a monomolecular layer on the sample surface is calculated (Fig. 3.8). The calculation is carried in the presence of liquid nitrogen (N_2) and is measured using the adsorption isotherm:

$$\frac{1}{V_a\left(\frac{P_a}{P}-1\right)} = \frac{C-1}{V_m C}\, X\, \frac{P}{P_0} + \frac{1}{V_m C} \qquad (3.8)$$

P is the equilibrium partial vapour pressure of the adsorbed gas at 77.4 K in Pascal's.

P_0 is the saturated pressure of adsorbed gas in pressure

V_a is the volume of gas adsorbed at STP to produce an apparent monolayer on the sample surface in millilitres.

V_m is the volume of the gas adsorbed at the standard temperature and pressure (STP) (ml).

C is a constant with no dimensions, it is related to the enthalpy of adsorption of the adsorbate gas on the solid sample.

V_a value is measured at each but not less than 3 values of P/P_0, therefore the value of BET is:

$$\frac{1}{V_a\left(\frac{Pa}{P}-1\right)} \qquad (3.9)$$

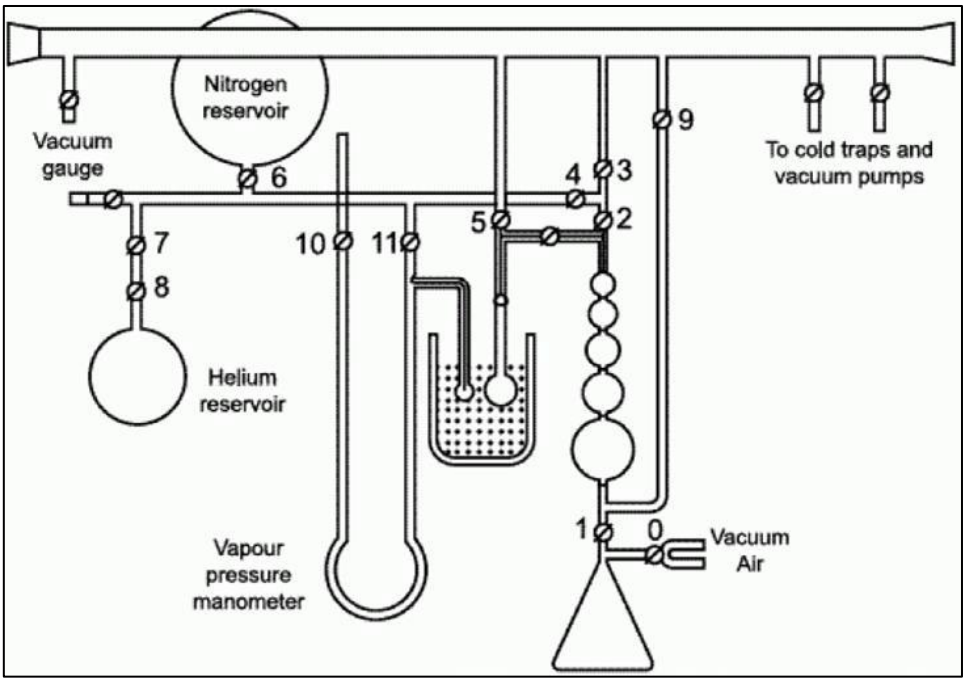

Figure 3.5.Schematic diagram of BET analysis [12].

The Emmett-Teller (BET) TriStar surface and porosity analyser was used to find the surface area of the prepared sample and during the analysis. The sample was prepared overnight in a micrometrics Flow Prep 060 samples degassed system at 180 ^oC prior to analysis to remove gases and vapours adsorbed on the surface of the sample during the sample preparation, treatment, sample handling and storage.

3.5.7 UV-Vis analysis

UV-Vis is an instrument used to conduct the optical studies of both solid and liquid samples. Generally in a UV-Vis, a beam of light with wavelength in the range of 180-

1100 nm passes through the moochromator which then passes through a cuvette carrying the sample. The samples absorbs the ultra violet or visible light irradiation. The amount of light the sample absorbs depends on the concentration, the path length of light passing through the sample and how well the sample absorbs the light with certain wavelength. The amount of absorption by the samples is related to the concentration of the samples and is given by the relation Lambert-Beer's law equation (3.10). Fig. 3.8 shows the schematic diagram of UV-Vis.

$$A = \varepsilon lc \tag{3.10}$$

A is the absorbance

ε is the molar absorption coefficient

l is the path length in centimetres (cm)

c is the concentration of the sample in mol per litter (mol-L^{-1})

The bandgaps of the materials can be estimated from the absorption spectra using the equation (3.11):

$$hv = \frac{hc}{\lambda} = \frac{1239.8}{\lambda} \tag{3.11}$$

Where hv is the energy bandgap, h is the Planck's constant and c is the speed of light.

The path length of light through the sample. It is equal to the thickness of the sample for solid samples and related to the equation (3.12):

$$\alpha(cm^{-1}) = \frac{lin(10)^{*}A}{\iota(cm)} = lin(10)\varepsilon l \tag{3.12}$$

Where A is the absorbance, α is the absorbance coefficient and l is the path length.

According to the Davis-Mott relationship for which the values of α are above 104 cm^{-1} the data follows the Tauc equation (3.13):

$$\alpha hv = A(hv - E^{opt}{}_{g})^{n} \tag{3.13}$$

The absorbance (A) depends on the transition probability, α is the absorption coefficient, E^{opt}_g is the optical band gap and n is the number with transition processes and the values of 2, 2/3, ½ or 1/3 can be either direct (allowed), direct (forbidden), indirect (allowed) and indirect (forbidden) respectively [62].

Tauc plot with relation $(\alpha hv)^n$ vs *hv* can be used to determine the energy gap of the materials and extrapolated to fit the baseline at y=0.

The degradation rate of pollutants can evaluated by presenting the degradation data using the Langmuir-Hinshelwood first order kinetics using the equation (3.14.):

$$r = -dC/dt = \kappa_r KC/(1+KC) \quad (3.14.)$$

κ_r is the rate constant and K is the equilibrium coefficient. When $K \ll 1$ the concentration of the analyst is small due to the dilution and thus the reaction kinetics order is pseudo-first order as K_{app} is the reaction rate constant with equation:

$$lnC_0/C_t = \kappa_r Kt = kt \quad (3.15)$$

C_0 and C_t are the concentrations of AB-25 at reaction time t. The rate constant is determined from the slopes of the lnC_0/C_t vs t graphs and the slope is the rate of photocatalytic degradation (min^{-1}).

The obtained band edge potentials can be used to determine the separation of charge, the band edge potentials at the conduction band (CB) and valence band (VB) of materials using the Equations (3.15) and (3.16):

$$E_{vb} = X - E^e + 0.5Eg \quad (3.16)$$

$$E_{CB} = E_{CB} - Eg \quad (3.17)$$

X is the mean of the electronegativity of the atoms, E^e is the free electrons energy on the hydrogen scale and it is approx. 4.5 eV, Eg is the band gap of the semiconductor, E_{CB} and E_{vb} are the CB and VB potentials respectively [193]

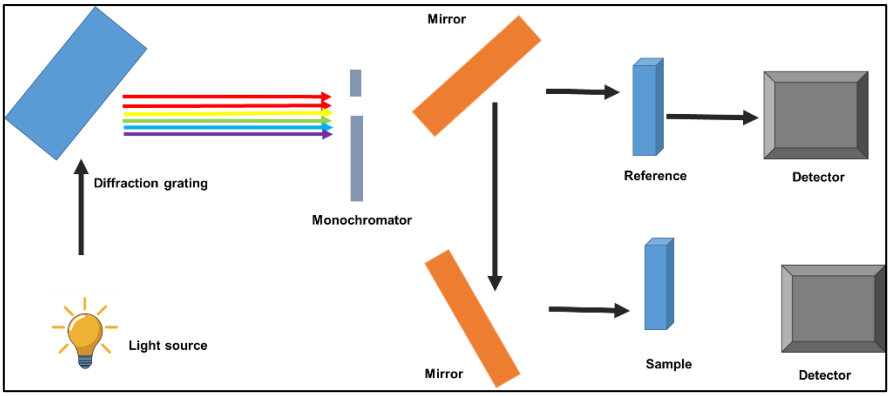

Figure 3.6. Schematic diagram of UV-Vis [14].

The optical properties of the samples were determined using UV-Vis absorption spectrophotometry on a PerkinElmer UV/Vis/NIR spectrometer Lambda 1050 where the standards for Acid blue-25 and Diclofenac sodium were prepared to obtain a calibration curve, thereafter the concentrations of the samples were analyzed quantitatively analyzed in the instrument set in the range (800-250).

3.6 Photoluminescent spectrophotometry

Photoluminescence spectroscopy (PL) is an instrument that determines the optical properties of a sample and is related to UV-vis. During sample analysis, light passes through the sample and is absorbed, and photons on the surface of the sample are excited to higher electronic state and release energy of photons. When the energy of photons relax, they fall to a lower energy level, the excess energy is then emitted (luminescence) and therefore the word photoluminescence (Fig. 3.9).

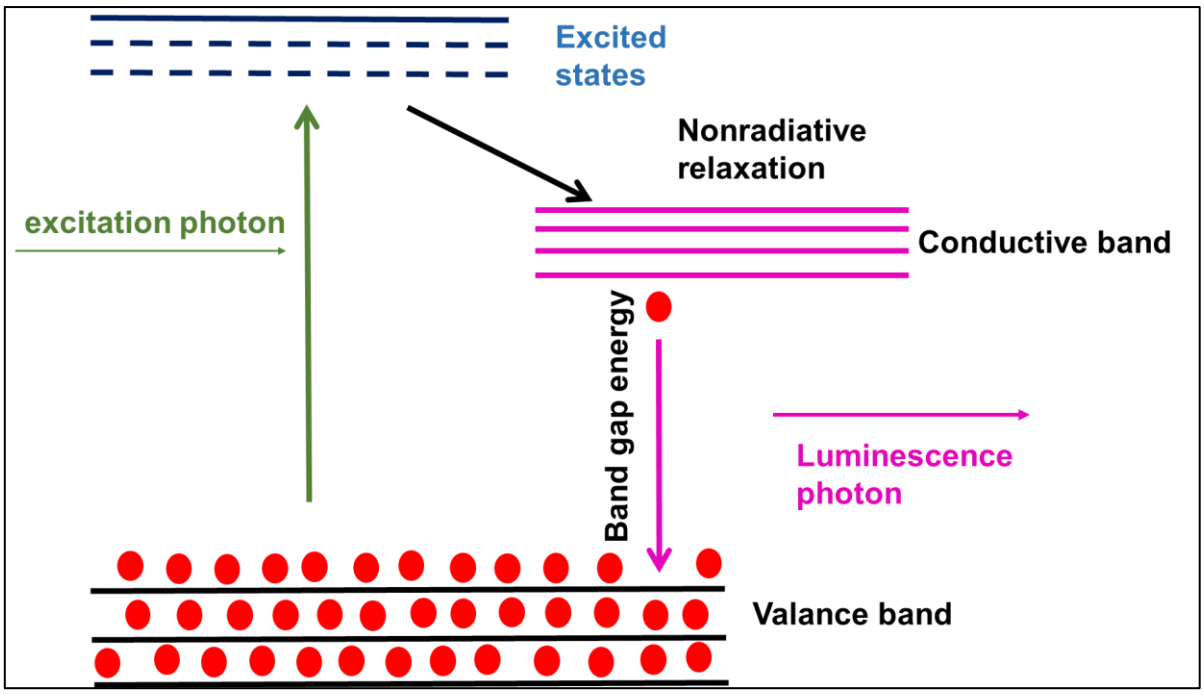

Figure 3.7. Basic principle of PL [15].

The PL spectra in this study was obtained using the HORIBA Fluorolog 3 (FL-1057) with 450 W tungsten xenon lamps. The excitation wavelength of g-C_3N_4 and CdS were 350 nm and 372 nm respectively. The S1-PMT detector was from 300 to 800 nm. The samples were placed in PL sample holder, thereafter placed in the instrument. The data was collected and analyzed.

3.7 Photoreactor

The application of semiconductor nanoparticles in photocatalysis requires excitation with light energy at wavelength exceeding the band gap of the semiconductor. This light source includes UV and visible light. UV represents only 5%-8% of the solar spectrums at sea level and hence only a limited amount of light of the required artificial illumination of the catalyst for degradation of the organic pollutants to occur and it is hazardous to use. Different types of light sources have been reported towards water purification applications. These include LEDs (light emitting diodes) light sources. They are reliable, cheap and have high current to light conversion efficiency and produce less heat making them more efficient compared to conventional light sources that produce mercury [194]. LED light sources with selected wavelength can easily be designed.

In this study the photocatalytic degradation of the chosen pollutants discussed in the previous chapter was carried out under visible light irradiation using a 24V RGB LED light source. The reactor consists of a glass beaker (v=2L) wrapped up by the 5 m LED strip (white color, 12W.m^{-2} power rating) externally coated by aluminium foil for the control of external light as shown on (Fig. 3.10).

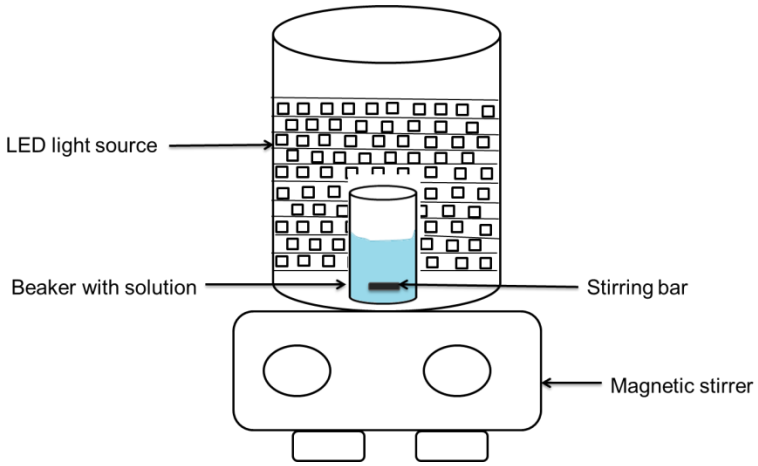

Figure 3.8. Schematic diagram of the photocatalytic reactor.

3.8 Inductively coupled plasma optical emission spectroscopy (ICP-OES)

The Inductively coupled plasma optical emission spectroscopy (ICP-OES) is an instrument that is mostly used for determining trace metal of samples. The sample is injected into the instrument, converted into to aerosol and passed through to a central channel and led into an argon plasma. The aerosols are vaporized at a temperature of 10 000 K where the elements of the samples are liberated as gaseous free atoms and are excited by energy produced through collisional excitation. Wavelengths from their original sources converted it to a signal, amplified, processed through the detector, displayed and collected on a computer (Fig. 3.7) [195].

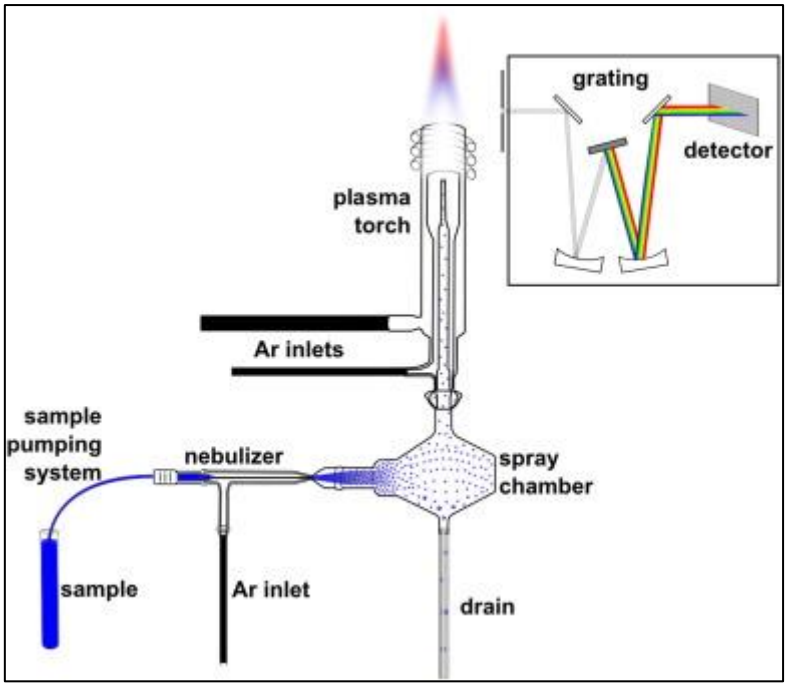

Figure 3.9.Schematic diagram of ICP-OES [13].

The amount of Cd leached into the solutions were estimated using Agilent technologies 700 series ICP-OES. The Cadmium standards of concentration 2-40 mgL^{-1} were prepared prior to analysis, thereafter 1 mL of the degraded samples were injected into tube vials then placed into instrument for analysis.

3.9 Ultra-High Performance Liquid Chromatography

High Performance Liquid Chromatography is an instruments used for the separation of different compounds. It consist of two components which is the stationary phase (packing material of the column) and the mobile phase (eluent). The molecules of the analyte retarded as they pass through the stationary phase. The samples are eluted at different times due to the intermolecular interactions between the molecules of a sample and the packing material and this determines their time in the column which is the component of the instrument responsible for adequate separation of the sample. Thereby, the separation of the sample ingredients is achieved. After leaving the column, a detector unit is used to recognize the analyte. The signals are converted and by a data management system or a computer and shown in a chromatogram. The mobile face is injected to the additional detector unit, a fractional collected unit or waste. Thereby, the separation of the sample ingredients is achieved. The solvent is delivered by the pump at high pressure and constant speed through the system. Components such as the drift, noise of the detected signal

should be kept as low as possible by controlling the flow from pump. The sample is provided to the eluent by the injection valve [196].

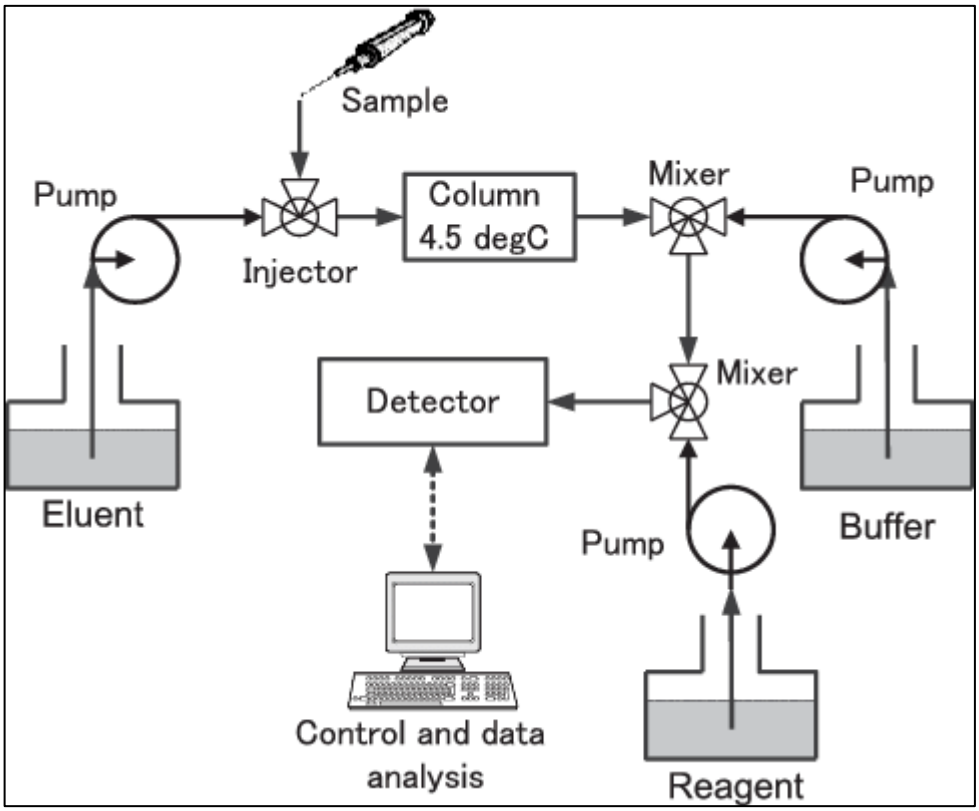

Figure 3.10. Schematic diagram of HPLC [196].

The degradation by-products were determined on a Dionex ultimate 3000 ultra-high performance liquid chromatography (UHPLC), (Thermal scientific, Massachusetts, United States) system equipped with a binary pump, an online degasser, column oven and an auto sampler coupled to impact II Quadrupole time of flight (QTOF) tandem mass spectrometer (Bruker, Germany) with electrospray ionization (ESI), Chromatographic separation was achieved using Acquity BEH C_{18} column (2.1 x 100 mm x 1.7 µm) supplied by Waters Corporation (Milford, MA, USA), ultrapure water (A) and acetonitrile (B), both containing 0.1% formic acid, were used as mobile phases applying gradient elution. The elution gradient started with 40% of eluent B, increasing to 100% in 7 min, holding at 100% for 2 min and then, back to 40% within 1 min. The flow rate for mobile phase was 0.3 mL min^{-1}, injection volume of 5 µL and column temperature at 35 ºC was used. The MS parameters for the analysis were the following: drying gas (N_2 generated by Peak Scientific Genius nitrogen generator) flow rate was 8 min L^{-1}, drying gas temperature was set at 200 ºC, nebulizer gas (N2) was 1.8 bar, and the capillary voltage was 4500 V. The mass

spectra were recorded across the range of m/z 50-1600 in full scan. The compounds were analysed in positive mode.

References

[1] A. Azizullah, M.N.K. Khattak, P. Richter, D.P. Häder, Water pollution in Pakistan and its impact on public health - A review, Environ. Int. 37 (2011) 479–497. doi:10.1016/j.envint.2010.10.007.

[2] I. Gehrke, A. Somborn-schulz, Innovations in nanotechnology for water treatment, Nanotechnol. Sci. Appl. 8 (2015) 1–17.

[3] C.J.. ; G. Vorösmarty Pamela; ; Salisbury, Joseph; ; Lammers, Richard B., Global Water Resources: Vulnerability from Climate Change and Population Growth, Science (80-.). 289 (2000) 284–288. doi:10.1126/science.289.5477.284.

[4] J. Theron, T.E. Cloete, Emerging Waterborne Infections: Contributing Factors, Agents, and Detection Tools, Crit. Rev. Microbiol. 28 (2008) 1–26. doi:10.1080/1040-840291046669.

[5] K.K. Jain, Nanotechnology and Water, Contemp. Mater. 1 (2012) 26–30. doi:10.7251/122.

[6] F.W. Owa, Water pollution : sources , effects , control and management, Int. Lett. 3 (2014) 1–6.

[7] H. Zhou, D.W. Smith, Advanced technologies in water and wastewater treatment, in: 2002. doi:10.1139/S02-020.

[8] M. Wakil, M. Burhan, L. Ang, K. Choon, Energy-water-environment nexus underpinning future desalination sustainability, Desalination. 413 (2017) 52–64. doi:10.1016/j.desal.2017.03.009.

[9] M. Palaniappan, K. Address, Peak_Water_Talk.Pdf, in: Utah Am. Plan. Assoc. Annu. Conf., 2008: pp. 3–11.

[10] J.K. Bwapwa, Review on Main Issues Causing Deterioration of Water Quality and Water Scarcity: Case Study of South Africa, Environ. Manag. Sustain. Dev. 7 (2018) 14. doi:10.5296/emsd.v7i3.13156.

[11] J. Wang, S. Wang, Removal of pharmaceuticals and personal care products (PPCPs) from wastewater: A review, J. Environ. Manage. 182 (2016) 620–640. doi:10.1016/j.jenvman.2016.07.049.

[12] G. Boczkaj, A. Fernandes, Wastewater treatment by means of advanced oxidation processes at basic pH conditions : A review, Chem. Eng. J. 320 (2017) 608–633. doi:10.1016/j.cej.2017.03.084.

[13] R. Ananthashankar, Treatment of textile effluent containing Reactive Red 120 dye using advanced oxidation, 2012.

[14] K. Klaus, Pharmaceuticals in the Environment, Annu Rev Env. Resour. 35 (2010) 57–75. doi:10.1146/annurev-environ-052809-161223.

[15] G. Kjosavik, Subtle changes, 2001.

[16] A.B.A. Boxall, M.A. Rudd, B.W. Brooks, D.J. Caldwell, K. Choi, S. Hickmann, E. Innes, K. Ostapyk, J.P. Staveley, T. Verslycke, G.T. Ankley, K.F. Beazley, Review Pharmaceuticals and Personal Care Products in the Environment : What Are the Big Questions ?, 120 (2012) 1221–1229.

[17] G. Li, X. Nie, Y. Gao, T. An, Applied Catalysis B : Environmental Can environmental pharmaceuticals be photocatalytically degraded and completely mineralized in water using g-C_3N_4/TiO_2 under visible light irradiation ?— Implications of persistent toxic intermediates, "Applied Catal. B, Environ. 180 (2016) 726–732. doi:10.1016/j.apcatb.2015.07.014.

[18] B. Hoeger, B. Köllner, D.R. Dietrich, B. Hitzfeld, Water-borne diclofenac affects kidney and gill integrity and selected immune parameters in brown trout (Salmo trutta f. fario), Aquat. Toxicol. 75 (2005) 53–64. doi:10.1016/j.aquatox.2005.07.006.

[19] M. Lillenberg, S. Yurchenko, K. Kipper, K. Herodes, V. Pihl, R. Lõhmus, M. Ivask, A. Kuu, S. Kutti, S. V. Litvin, L. Nei, Presence of fluoroquinolones and sulfonamides in urban sewage sludge and their degradation as a result of composting, Int. J. Environ. Sci. Technol. 7 (2010) 307–312. doi:10.1007/BF03326140.

[20] S.K. Khetan, T.J. Collins, Human pharmaceuticals in the aquatic environment: A challenge to green chemisty, Chem. Rev. 107 (2007) 2319–2364. doi:10.1021/cr020441w.

[21] A.M. Deegan, B. Shaik, K. Nolan, K. Urell, M. Oelgemöller, J. Tobin, A. Morrissey, Treatment options for wastewater effluents from pharmaceutical companies, Int. J. Environ. Sci. Technol. 8 (2011) 649–666. doi:10.1007/BF03326250.

[22] A.J. Ebele, M. Abou-Elwafa Abdallah, S. Harrad, Pharmaceuticals and personal care products (PPCPs) in the freshwater aquatic environment, Emerg. Contam. 3 (2017) 1–16. doi:10.1016/j.emcon.2016.12.004.

[23] B.D. Blair, J.P. Crago, C.J. Hedman, R.D. Klaper, Chemosphere Pharmaceuticals and personal care products found in the Great Lakes above concentrations of environmental concern, Chemosphere. 93 (2013) 2116–2123. doi:10.1016/j.chemosphere.2013.07.057.

[24] C.U. Meteyer, B.A. Rideout, M. Gilbert, H.L. Shivaprasad, L. Oaks, Phathology and proposed pathology of diclofenac in free living and experimentally expeosd oriental white backed vultures (Gypas bengalensis), J. Wildl. Dis. 41 (2005) 707–716.

[25] R. Triebskorn, H. Casper, V. Scheil, J. Schwaiger, Ultrastructural effects of pharmaceuticals (carbamazepine, clofibric acid, metoprolol, diclofenac) in rainbow trout (Oncorhynchus mykiss) and common carp (Cyprinus carpio), Anal. Bioanal. Chem. 387 (2007) 1405–1416. doi:10.1007/s00216-006-1033-x.

[26] J. Schwaiger, H. Ferling, U. Mallow, H. Wintermayr, R.D. Negele, Toxic effects of the non-steroidal anti-inflammatory drug diclofenac. Part I: Histopathological alterations and bioaccumulation in rainbow trout, Aquat. Toxicol. 68 (2004) 141–150. doi:10.1016/j.aquatox.2004.03.014.

[27] A.A.C. and Z.M. Dana Manuela Sirbu, Daniela Curseu, Monica Popa, Environmental Risks of Pharmaceuticals and Personal Care Products in Water, in: Tenth Int. Water Technol. Conf., 2006: pp. 1151–1162.

[28] E. Archer, G.M. Wolfaardt, J.H. van Wyk, Pharmaceutical and personal care products (PPCPs) as endocrine disrupting contaminants (EDCs) in South African surface waters, Water SA. 43 (2017) 684–706. doi:10.4314/wsa.v43i4.16.

[29] O.A.H. Jones, N. Voulvoulis, J.N. Lester, Potential ecological and human health risks associated with the presence of pharmaceutically active compounds in the aquatic environment, Crit. Rev. Toxicol. 34 (2004) 335–350. doi:10.1080/10408440490464697.

[30] A.K. Karen, J.B. Paul, H.M. Kenneth, e P.P. Vinc, E.E. Robert, M.L. James, W.F. Robert, Disrupting Queer Incluslon, Pnas. 104 (2007) 8897–8901. doi:10.1073/pnas.0609568104.

[31] D.J. Caldwell, F. Mastrocco, T.H. Hutchinson, R. Länge, D. Heijerick, C. Janssen, P.D. Anderson, J.P. Sumpter, Derivation of an aquatic predicted no-effect concentration for the synthetic hormone, 17α-ethinyl estradiol, Environ. Sci. Technol. 42 (2008) 7046–7054. doi:10.1021/es800633q.

[32] M.F. Rahman, E.K. Yanful, S.Y. Jasim, Endocrine disrupting compounds (EDCs) and pharmaceuticals and personal care products (PPCPs) in the aquatic environment: Implications for the drinking water industry and global environmental health, J. Water Health. 7 (2009) 224–243. doi:10.2166/wh.2009.021.

[33] B. Lellis, C.Z. Fávaro-polonio, J.A. Pamphile, J.C. Polonio, Effects of textile dyes on health and the environment and bioremediation potential of living organisms, Biotecnol. Res. Innov. 3 (2019) 275–290. doi:10.1016/j.biori.2019.09.001.

[34] R. Paper, Decolorization of mixture of dyes : A critical review, Glob. J. Environ. Sci. Manag. Glob. J. Environ. Sci. Manag. 1 (2015) 71–94. doi:10.7508/gjesm.2015.01.007.

[35] A.M. Deegan, B. Shaik, K. Nolan, K. Urell, J. Tobin, A. Morrissey, Treatment options for wastewater effluents from pharmaceutical companies, 8 (2011)

649–666.

[36] L. Cheng, Q. Xiang, Y. Liao, H. Zhang, CdS-Based photocatalysts, Royal Society of Chemistry, 2018. doi:10.1039/c7ee03640j.

[37] H.L. Lee, A.M. Issam, M. Belmahi, M.B. Assouar, H. Rinnert, M. Alnot, Synthesis and characterizations of bare cds nanocrystals using chemical precipitation method for photoluminescence application, J. Nanomater. 2009 (2009). doi:10.1155/2009/914501.

[38] S. Kumar, S. Karthikeyan, A.F. Lee, g-C_3N_4-based nanomaterials for visible light-driven photocatalysis, Catalysts. 8 (2018). doi:10.3390/catal8020074.

[39] S. Cao, J. Low, J. Yu, M. Jaroniec, Polymeric Photocatalysts Based on Graphitic Carbon Nitride, Adv. Mater. 27 (2015) 2150–2176. doi:10.1002/adma.201500033.

[40] Q.Y. Liu, Y.L. Qi, Y.F. Zheng, X.C. Song, Synthesis and enhanced photocatalytic activity of g-C_3N_4 hybridized CdS nanoparticles, Bull. Mater. Sci. 40 (2017) 1329–1333. doi:10.1007/s12034-017-1513-y.

[41] R.C. Pawar, V. Khare, C.S. Lee, Hybrid photocatalysts using graphitic carbon nitride/cadmium sulfide/reduced graphene oxide (g-C_3N_4/CdS/RGO) for superior photodegradation of organic pollutants under UV and visible light, Dalt. Trans. 43 (2014) 12514–12527. doi:10.1039/c4dt01278j.

[42] S.W. Cao, Y.P. Yuan, J. Fang, M.M. Shahjamali, F.Y.C. Boey, J. Barber, S.C. Joachim Loo, C. Xue, In-situ growth of CdS quantum dots on g-C_3N_4 nanosheets for highly efficient photocatalytic hydrogen generation under visible light irradiation, Int. J. Hydrogen Energy. 38 (2013) 1258–1266. doi:10.1016/j.ijhydene.2012.10.116.

[43] S. Rasalingam, R. Peng, R.T. Koodali, Removal of hazardous pollutants from wastewaters: Applications of TiO_2-SiO_2 mixed oxide materials, J. Nanomater. 2014 (2014). doi:10.1155/2014/617405.

[44] M.K. Hasan, A. Shahriar, K.U. Jim, Water pollution in Bangladesh and its

impact on public health, Heliyon. 5 (2019) e02145. doi:10.1016/j.heliyon.2019.e02145.

[45] S. Rasalingam, R. Peng, R.T. Koodali, 617405.Pdf, 2014 (2014).

[46] U. Tahir, A. Yasmin, U.H. Khan, Phytoremediation: Potential flora for synthetic dyestuff metabolism, J. King Saud Univ. - Sci. 28 (2016) 119–130. doi:10.1016/j.jksus.2015.05.009.

[47] G. Dong, Y. Zhang, Q. Pan, J. Qiu, A fantastic graphitic carbon nitride (g-C3N4) material: Electronic structure, photocatalytic and photoelectronic properties, J. Photochem. Photobiol. C Photochem. Rev. 20 (2014) 33–50. doi:10.1016/j.jphotochemrev.2014.04.002.

[48] D.A. Yaseen, M. Scholz, Textile dye wastewater characteristics and constituents of synthetic effluents: a critical review, Springer Berlin Heidelberg, 2019. doi:10.1007/s13762-018-2130-z.

[49] T. Robinson, G. McMullan, R. Marchant, P. Nigam, Remediation of dyes in textile effluent: A critical review on current treatment technologies with a proposed alternative, Bioresour. Technol. 77 (2001) 247–255. doi:10.1016/S0960-8524(00)00080-8.

[50] G.S. Gupta, G. Prasad, V.N. Singh, Removal of chrome dye from aqueous solutions by mixed adsorbents: Fly ash and coal, Water Res. 24 (1990) 45–50. doi:10.1016/0043-1354(90)90063-C.

[51] N. Muhd Julkapli, S. Bagheri, S. Bee Abd Hamid, Recent advances in heterogeneous photocatalytic decolorization of synthetic dyes, Sci. World J. 2014 (2014) 25. doi:10.1155/2014/692307.

[52] Y. Fu, T. Viraraghavan, Fungal decolorization of dye wastewaters: A review, Bioresour. Technol. 79 (2001) 251–262. doi:10.1016/S0960-8524(01)00028-1.

[53] V.K. Gupta, S. Khamparia, I. Tyagi, D. Jaspal, A. Malviya, Decolorization of mixture of dyes: A critical review, Glob. J. Environ. Sci. Manag. Glob. J. Environ. Sci. Manag. 1 (2015) 71–94. doi:10.7508/gjesm.2015.01.007.

[54] Z. Aksu, Application of biosorption for the removal of organic pollutants: A review, Process Biochem. 40 (2005) 997–1026. doi:10.1016/j.procbio.2004.04.008.

[55] S. Sumathi, B.S. Manju, Uptake of reactive textile dyes by Aspergillus foetidus, Enzyme Microb. Technol. 27 (2000) 347–355. doi:10.1016/S0141-0229(00)00234-9.

[56] Z. Aksu, S. Tezer, Equilibrium and kinetic modelling of biosorption of Remazol black B by Rhizopus arrhizus in a batch system: Effect of temperature, Process Biochem. 36 (2000) 431–439. doi:10.1016/S0032-9592(00)00233-8.

[57] T. O'Mahony, E. Guibal, J.M. Tobin, Reactive dye biosorption by Rhizopus arrhizus biomass, Enzyme Microb. Technol. 31 (2002) 456–463. doi:10.1016/S0141-0229(02)00110-2.

[58] B. Aruna, R.S. L, E. Shiva, A. Srinu, P. Roja, D. Vijayalakshmi, D.V.R. Prasad, Research Article Biodecolorization of Anthraquinone Textile (Acid Blue 25) Dye By Klebsiella Sp, 6 (2015) 3216–3222.

[59] M. Auta, B.H. Hameed, Preparation of waste tea activated carbon using potassium acetate as an activating agent for adsorption of Acid Blue 25 dye, Chem. Eng. J. 171 (2011) 502–509. doi:10.1016/j.cej.2011.04.017.

[60] C.A. Hsu, T.N. Wen, Y.C. Su, Z.B. Jiang, C.W. Chen, L.F. Shyur, Biological degradation of anthroquinone and azo dyes by a novel laccase from Lentinus sp., Environ. Sci. Technol. 46 (2012) 5109–5117. doi:10.1021/es2047014.

[61] H. hong Li, Y. tao Wang, Y. Wang, H. xia Wang, K. kai Sun, Z. mei Lu, Bacterial degradation of anthraquinone dyes, J. Zhejiang Univ. Sci. B. 20 (2019) 528–540. doi:10.1631/jzus.B1900165.

[62] M.E. Malefane, U. Feleni, A.T. Kuvarega, Tetraphenylporphyrin/WO_3/exfoliated graphite nanocomposite for photocatalytic degradation of an acid dye under visible light irradiation, New J. Chem. 10 (2019) 1–6. doi:10.1039/c9nj02747e.

[63] S. Benkhaya, S. El Harfi, A. El Harfi, Classifications , properties and

applications of textile dyes : A review, Appl. J. Environ. Sci. 3 (2018) 311–320.

[64] D. Chakrabortty, S. Sen Gupta, Photo-catalytic decolourisation of toxic dye with N-doped titania: A case study with Acid Blue 25, J. Environ. Sci. (China). 25 (2013) 1034–1043. doi:10.1016/S1001-0742(12)60108-9.

[65] T. Deblonde, C. Cossu-Leguille, P. Hartemann, Emerging pollutants in wastewater: A review of the literature, Int. J. Hyg. Environ. Health. 214 (2011) 442–448. doi:10.1016/j.ijheh.2011.08.002.

[66] M. Clara, G. Windhofer, W. Hartl, K. Braun, M. Simon, O. Gans, C. Scheffknecht, A. Chovanec, Occurrence of phthalates in surface runoff, untreated and treated wastewater and fate during wastewater treatment, Chemosphere. 78 (2010) 1078–1084. doi:10.1016/j.chemosphere.2009.12.052.

[67] M. la Farré, S. Pérez, L. Kantiani, D. Barceló, Fate and toxicity of emerging pollutants, their metabolites and transformation products in the aquatic environment, TrAC - Trends Anal. Chem. 27 (2008) 991–1007. doi:10.1016/j.trac.2008.09.010.

[68] A. Jennifer, M.A. Abdallah, S. Harrad, Pharmaceuticals and personal care products (PPCPs) in the freshwater aquatic environment, Emerg. Contam. 3 (2017) 1–16. doi:10.1016/j.emcon.2016.12.004.

[69] S.R. Hughes, P. Kay, L.E. Brown, Global synthesis and critical evaluation of pharmaceutical data sets collected from river systems, Environ. Sci. Technol. 47 (2013) 661–677. doi:10.1021/es3030148.

[70] D. Ashton, M. Hilton, K. V. Thomas, Investigating the environmental transport of human pharmaceuticals to streams in the United Kingdom, Sci. Total Environ. 333 (2004) 167–184. doi:10.1016/j.scitotenv.2004.04.062.

[71] S. Wiandt, H.J. Poremski, Selection and prioritisation procedure of hazardous substances for the marine environment within ospar/dynamec, Ecotoxicology. 11 (2002) 393–399. doi:10.1023/A:1020569608441.

[72] L. Lonappan, S.K. Brar, R.K. Das, M. Verma, R.Y. Surampalli, Diclofenac and its transformation products: Environmental occurrence and toxicity - A review, Environ. Int. 96 (2016) 127–138. doi:10.1016/j.envint.2016.09.014.

[73] Y. Zhang, S.U. Geißen, C. Gal, Carbamazepine and diclofenac: Removal in wastewater treatment plants and occurrence in water bodies, Chemosphere. 73 (2008) 1151–1161. doi:10.1016/j.chemosphere.2008.07.086.

[74] V. Acuña, A. Ginebreda, J.R. Mor, M. Petrovic, S. Sabater, J. Sumpter, D. Barceló, Balancing the health benefits and environmental risks of pharmaceuticals: Diclofenac as an example, Environ. Int. 85 (2015) 327–333. doi:10.1016/j.envint.2015.09.023.

[75] A.C. Johnson, E. Dumont, R.J. Williams, R. Oldenkamp, I. Cisowska, J.P. Sumpter, Do concentrations of ethinylestradiol, estradiol, and diclofenac in European rivers exceed proposed EU environmental quality standards?, Environ. Sci. Technol. 47 (2013) 12297–12304. doi:10.1021/es4030035.

[76] A.Y. Shan, T.I.M. Ghazi, S.A. Rashid, Immobilisation of titanium dioxide onto supporting materials in heterogeneous photocatalysis: A review, Appl. Catal. A Gen. 389 (2010) 1–8. doi:10.1016/j.apcata.2010.08.053.

[77] Y. Mehmood, Index Academic Sciences Original Article development and validation of UV-Vis spectrophtometric method for the estimation of diclofenac sodium injections., Int. J. Pharm. Pract. Pharm. Sci. 2 (2015) 1–6.

[78] D. Chen, A.K. Ray, Photodegradation kinetics of 4-nitrophenol in TiO2 suspension, Water Res. 32 (1998) 3223–3234. doi:10.1016/S0043-1354(98)00118-3.

[79] C. Martínez, M. Canle L., M.I. Fernández, J.A. Santaballa, J. Faria, Aqueous degradation of diclofenac by heterogeneous photocatalysis using nanostructured materials, Appl. Catal. B Environ. 107 (2011) 110–118. doi:10.1016/j.apcatb.2011.07.003.

[80] M. Letzel, G. Metzner, T. Letzel, Exposure assessment of the pharmaceutical diclofenac based on long-term measurements of the aquatic input, Environ. Int.

35 (2009) 363–368. doi:10.1016/j.envint.2008.09.002.

[81] C. Hao, R. Clement, P. Yang, Liquid chromatography-tandem mass spectrometry of bioactive pharmaceutical compounds in the aquatic environment-a decade's activities, Anal. Bioanal. Chem. 387 (2007) 1247–1257. doi:10.1007/s00216-006-0956-6.

[82] A.J. Sosiak, T. Hebben, A preliminary survey of pharmaceuticals and endocrine disrupting compounds in treated municipal wastewaters and receiving rivers of Alberta /, 2005. doi:10.5962/bhl.title.113982.

[83] M.J. Benotti, R.A. Trenholm, B.J. Vanderford, J.C. Holady, B.D. Stanford, S.A. Snyder, Pharmaceuticals and endocrine disrupting compounds in U.S. drinking water, Environ. Sci. Technol. 43 (2009) 597–603. doi:10.1021/es801845a.

[84] T. Heberer, Tracking persistent pharmaceutical residues from municipal sewage to drinking water, J. Hydrol. 266 (2002) 175–189. doi:10.1016/S0022-1694(02)00165-8.

[85] F.O. Agunbiade, B. Moodley, Occurrence and distribution pattern of acidic pharmaceuticals in surface water, wastewater, and sediment of the Msunduzi River, Kwazulu-Natal, South Africa, Environ. Toxicol. Chem. 35 (2016) 36–46. doi:10.1002/etc.3144.

[86] M.T. Amin, A.A. Alazba, U. Manzoor, A Review of Removal of Pollutants from Water / Wastewater Using Different Types of Nanomaterials, 2014 (2014).

[87] M.R. Servos, D.T. Bennie, B.K. Burnison, A. Jurkovic, R. McInnis, T. Neheli, A. Schnell, P. Seto, S.A. Smyth, T.A. Ternes, Distribution of estrogens, 17β-estradiol and estrone, in Canadian municipal wastewater treatment plants, Sci. Total Environ. 336 (2005) 155–170. doi:10.1016/j.scitotenv.2004.05.025.

[88] T. Urase, T. Kikuta, Separate estimation of adsorption and degradation of pharmaceutical substances and estrogens in the activated sludge process, Water Res. 39 (2005) 1289–1300. doi:10.1016/j.watres.2005.01.015.

[89] N. Vieno, T. Tuhkanen, L. Kronberg, Removal of pharmaceuticals in drinking

water treatment: Effect of chemical coagulation, Environ. Technol. 27 (2006) 183–192. doi:10.1080/09593332708618632.

[90] P. Westerhoff, Y. Yoon, S. Snyder, E. Wert, Fate of endocrine-disruptor, pharmaceutical, and personal care product chemicals during simulated drinking water treatment processes, Environ. Sci. Technol. 39 (2005) 6649–6663. doi:10.1021/es0484799.

[91] M. Petrovic, A. Diaz, F. Ventura, D. Barceló, Occurrence and removal of estrogenic short-chain ethoxy nonylphenolic compounds and their halogenated derivatives during drinking water production, Environ. Sci. Technol. 37 (2003) 4442–4448. doi:10.1021/es034139w.

[92] G. Becher, Drinking Water Chlorination and Health, Acta Hydrochim. Hydrobiol. 27 (1999) 100–102. doi:10.1002/(sici)1521-401x(199902)27:2<100::aid-aheh100>3.3.co;2-1.

[93] N. Bolong, A.F. Ismail, M.R. Salim, T. Matsuura, A review of the effects of emerging contaminants in wastewater and options for their removal, Desalination. 239 (2009) 229–246. doi:10.1016/j.desal.2008.03.020.

[94] Y. Yoon, P. Westerhoff, S.A. Snyder, E.C. Wert, Nanofiltration and ultrafiltration of endocrine disrupting compounds, pharmaceuticals and personal care products, J. Memb. Sci. 270 (2006) 88–100. doi:10.1016/j.memsci.2005.06.045.

[95] L. Braeken, B. Bettens, K. Boussu, P. Van der Meeren, J. Cocquyt, J. Vermant, B. Van der Bruggen, Transport mechanisms of dissolved organic compounds in aqueous solution during nanofiltration, J. Memb. Sci. 279 (2006) 311–319. doi:10.1016/j.memsci.2005.12.024.

[96] J. Lu, T. Zhang, J. Ma, Z. Chen, Evaluation of disinfection by-products formation during chlorination and chloramination of dissolved natural organic matter fractions isolated from a filtered river water, J. Hazard. Mater. 162 (2009) 140–145. doi:10.1016/j.jhazmat.2008.05.058.

[97] M.N. Chong, B. Jin, C.W.K. Chow, C. Saint, Recent developments in

photocatalytic water treatment technology: a review., Water Res. 44 (2010) 2997–3027. doi:10.1016/j.watres.2010.02.039.

[98] D.H. Bremner, R. Molina, F. Martínez, J.A. Melero, Y. Segura, Degradation of phenolic aqueous solutions by high frequency sono-Fenton systems (US-Fe_2O_3/SBA-15-H_2O_2), Appl. Catal. B Environ. 90 (2009) 380–388. doi:10.1016/j.apcatb.2009.03.028.

[99] G. Li, Z. Wang, M. Yu, Z. Quan, J. Lin, Fabrication and optical properties of core-shell structured spherical SiO_2@$GdVO_4$:Eu^{3+} phosphors via sol-gel process, J. Solid State Chem. 179 (2006) 2698–2706. doi:10.1016/j.jssc.2006.05.019.

[100] J. Zhang, G. Xiao, F.X. Xiao, B. Liu, Revisiting one-dimensional TiO_2 based hybrid heterostructures for heterogeneous photocatalysis: A critical review, Mater. Chem. Front. 1 (2017) 231–250. doi:10.1039/c6qm00141f.

[101] Y. Cui, In-situ synthesis of C_3N_4/CdS composites with enhanced photocatalytic properties, Cuihua Xuebao/Chinese J. Catal. 36 (2015) 372–379. doi:10.1016/S1872-2067(14)60237-0.

[102] V.S. Kosera, T.M. Cruz, E.S. Chaves, E.R.L. Tiburtius, Journal of Photochemistry and Photobiology A : Chemistry Triclosan degradation by heterogeneous photocatalysis using ZnO immobilized in biopolymer as catalyst, "Journal Photochem. Photobiol. A Chem. 344 (2017) 184–191. doi:10.1016/j.jphotochem.2017.05.014.

[103] M.R. Hoffmann, S.T. Martin, W. Choi, D.W. Bahnemann, Environmental Applications of Semiconductor Photocatalysis, Chem. Rev. 95 (1995) 69–96. doi:10.1021/cr00033a004.

[104] J.-M. Herrmann, Water Treatment By Heterogeneous Photocatalysis, in: 1999: pp. 171–194. doi:10.1142/9781848160613_0009.

[105] U.I. Gaya, A.H. Abdullah, Heterogeneous photocatalytic degradation of organic contaminants over titanium dioxide: A review of fundamentals, progress and problems, J. Photochem. Photobiol. C Photochem. Rev. 9 (2008) 1–12.

doi:10.1016/j.jphotochemrev.2007.12.003.

[106] M. Ni, M.K.H. Leung, D.Y.C. Leung, K. Sumathy, A review and recent developments in photocatalytic water-splitting using TiO_2 for hydrogen production, Renew. Sustain. Energy Rev. 11 (2007) 401–425. doi:10.1016/j.rser.2005.01.009.

[107] M. Yasmina, K. Mourad, S.H. Mohammed, C. Khaoula, Treatment heterogeneous photocatalysis; Factors influencing the photocatalytic degradation by TiO_2, Energy Procedia. 50 (2014) 559–566. doi:10.1016/j.egypro.2014.06.068.

[108] L. Cheng, Q. Xiang, Y. Liao, Morphology-dependent photocatalytic H_2-production activity of CdS Environmental Science, (2018) 4–7. doi:10.1039/c7ee03640j.

[109] M. Wongaree, S. Chiarakorn, S. Chuangchote, Photocatalytic Improvement under Visible Light in TiO_2 Nanoparticles by Carbon Nanotube Incorporation, 2015 (2015).

[110] R.S. Singh, V.K. Rangari, S. Sanagapalli, V. Jayaraman, S. Mahendra, V.P. Singh, Nano-structured CdTe, CdS and TiO_2 for thin film solar cell applications, Sol. Energy Mater. Sol. Cells. 82 (2004) 315–330. doi:10.1016/j.solmat.2004.02.006.

[111] S. Leong, A. Razmjou, K. Wang, K. Hapgood, X. Zhang, H. Wang, TiO_2 based photocatalytic membranes: A review, J. Memb. Sci. 472 (2014) 167–184. doi:10.1016/j.memsci.2014.08.016.

[112] Y. Yu, J.C. Yu, J.G. Yu, Y.C. Kwok, Y.K. Che, J.C. Zhao, L. Ding, W.K. Ge, P.K. Wong, Enhancement of photocatalytic activity of mesoporous TiO_2 by using carbon nanotubes, Appl. Catal. A Gen. 289 (2005) 186–196. doi:10.1016/j.apcata.2005.04.057.

[113] R. Abe, K. Sayama, H. Arakawa, Significant effect of iodide addition on water splitting into H_2 and O_2 over Pt-loaded TiO_2 photocatalyst: Suppression of backward reaction, Chem. Phys. Lett. 371 (2003) 360–364.

doi:10.1016/S0009-2614(03)00252-5.

[114] S. Sakthivel, M. V. Shankar, M. Palanichamy, B. Arabindoo, D.W. Bahnemann, V. Murugesan, Enhancement of photocatalytic activity by metal deposition: Characterisation and photonic efficiency of Pt, Au and Pd deposited on TiO_2 catalyst, Water Res. 38 (2004) 3001–3008. doi:10.1016/j.watres.2004.04.046.

[115] E. Szabó-Bárdos, H. Czili, A. Horváth, Photocatalytic oxidation of oxalic acid enhanced by silver deposition on a TiO_2 surface, J. Photochem. Photobiol. A Chem. 154 (2003) 195–201. doi:10.1016/S1010-6030(02)00330-1.

[116] N.L. Wu, M.S. Lee, Enhanced TiO_2 photocatalysis by Cu in hydrogen production from aqueous methanol solution, Int. J. Hydrogen Energy. 29 (2004) 1601–1605. doi:10.1016/j.ijhydene.2004.02.013.

[117] F. Haque, T. Daeneke, K. Kalantar-zadeh, J.Z. Ou, Two-Dimensional Transition Metal Oxide and Chalcogenide-Based Photocatalysts, Nano-Micro Lett. 10 (2018) 1–27. doi:10.1007/s40820-017-0176-y.

[118] A.H. Reshak, S. Auluck, Electronic and optical properties of the 1T phases of TiS_2, $TiSe_2$, and $TiTe_2$, Phys. Rev. B - Condens. Matter Mater. Phys. 68 (2003) 1–7. doi:10.1103/PhysRevB.68.245113.

[119] J.A. Wilson, A.D. Yoffe, The transition metal dichalcogenides discussion and interpretation of the observed optical, electrical and structural properties, Adv. Phys. 18 (1969) 193–335. doi:10.1080/00018736900101307.

[120] L. Nie, Q. Zhang, Recent progress in crystalline metal chalcogenides as efficient photocatalysts for organic pollutant degradation, Inorg. Chem. Front. 4 (2017) 1953–1962. doi:10.1039/c7qi00651a.

[121] F. Li, X. Liu, Q. Zhang, T. Kong, H. Jin, Fabrication and photocatalytic property of CuO nanosheets via a facile solution route, Cryst. Res. Technol. 47 (2012) 1140–1147. doi:10.1002/crat.201200143.

[122] B. Peng, P.K. Ang, K.P. Loh, Two-dimensional dichalcogenides for light-harvesting applications, Nano Today. 10 (2015) 128–137.

doi:10.1016/j.nantod.2015.01.007.

[123] D. Ke, S. Liu, K. Dai, J. Zhou, L. Zhang, T. Peng, CdS/regenerated cellulose nanocomposite films for highly efficient photocatalytic H_2 production under visible light irradiation, J. Phys. Chem. C. 113 (2009) 16021–16026. doi:10.1021/jp903378q.

[124] S. Xiong, B. Xi, Y. Qian, CdS hierarchical nanostructures with tunable morphologies: Preparation and photocatalytic properties, J. Phys. Chem. C. 114 (2010) 14029–14035. doi:10.1021/jp1049588.

[125] W.T. Yao, S.H. Yu, S.J. Liu, J.P. Chen, X.M. Liu, F.Q. Li, Architectural control syntheses of CdS and CdSe nanoflowers, branched nanowires, and nanotrees via a solvothermal approach in a mixed solution and their photocatalytic property, J. Phys. Chem. B. 110 (2006) 11704–11710. doi:10.1021/jp060164n.

[126] Q. Shen, J. Xue, A. Mi, H. Jia, X. Liu, B. Xu, The study on properties of CdS photocatalyst with different ratios of zinc-blende and wurtzite structure, RSC Adv. 3 (2013) 20930–20935. doi:10.1039/c3ra42179a.

[127] M. Liu, B. Wang, Y. Zheng, F. Xue, Y. Chen, L. Guo, Transformation of zincblende nanoparticles into wurtzite microrods by a dissolution-regrowth process: An intergrowth homojunction with enhanced photocatalytic activity, Catal. Sci. Technol. 6 (2016) 3371–3377. doi:10.1039/c6cy00298f.

[128] K. Wu, H. Zhu, T. Lian, Ultrafast Exciton Dynamics and Light-Driven H2 Evolution in Colloidal Semiconductor Nanorods and Pt-Tipped Nanorods, Acc. Chem. Res. 48 (2015) 851–859. doi:10.1021/ar500398g.

[129] J. Yu, Y. Yu, P. Zhou, W. Xiao, B. Cheng, Morphology-dependent photocatalytic H2-production activity of CdS, Appl. Catal. B Environ. 156–157 (2014) 184–191. doi:10.1016/j.apcatb.2014.03.013.

[130] B. Weng, S. Liu, N. Zhang, Z.R. Tang, Y.J. Xu, A simple yet efficient visible-light-driven CdS nanowires-carbon nanotube 1D-1D nanocomposite photocatalyst, J. Catal. 309 (2014) 146–155. doi:10.1016/j.jcat.2013.09.013.

[131] F. Caruso, X. Shi, R.A. Caruso, A. Susha, Hollow titania spheres from layered precursor deposition on sacrificial colloidal core particles, Adv. Mater. 13 (2001) 740–744. doi:10.1002/1521-4095(200105)13:10<740::AID-ADMA740>3.0.CO;2-6.

[132] C. Li, L. Han, R. Liu, H. Li, S. Zhang, G. Zhang, Controlled synthesis of CdS micro/nano leaves with (0001) facets exposed: Enhanced photocatalytic activity toward hydrogen evolution, J. Mater. Chem. 22 (2012) 23815–23820. doi:10.1039/c2jm35415b.

[133] T. Tsuzuki, P.G. McCormick, Synthesis of CdS quantum dots by mechanochemical reaction, Appl. Phys. A Mater. Sci. Process. 65 (1997) 607–609. doi:10.1007/s003390050629.

[134] A. Dumbrava, G. Prodan, D. Berger, M. Bica, Properties of PEG-capped CdS nanopowders synthesized under very mild conditions, Powder Technol. 270 (2015) 197–204. doi:10.1016/j.powtec.2014.10.012.

[135] A. Samadi-maybodi, F. Abbasi, R. Akhoondi, Aqueous synthesis and characterization of CdS quantum dots capped with some amino acids and investigations of their photocatalytic activities, Colloids Surfaces A Physicochem. Eng. Asp. 447 (2014) 111–119. doi:10.1016/j.colsurfa.2014.01.036.

[136] P. Chandran, P. Kumari, S. Sudheer Khan, Photocatalytic activation of CdS NPs under visible light for environmental cleanup and disinfection, Sol. Energy. 105 (2014) 542–547. doi:10.1016/j.solener.2014.04.028.

[137] M. Darwish, A. Mohammadi, N. Assi, Microwave-assisted polyol synthesis and characterization of pvp-capped cds nanoparticles for the photocatalytic degradation of tartrazine, Mater. Res. Bull. 74 (2016) 387–396. doi:10.1016/j.materresbull.2015.11.002.

[138] R.A. Devi, M. Latha, S. Velumani, G. Oza, P. Reyes-Figueroa, M. Rohini, I.G. Becerril-Juarez, J.-H. Lee, J. Yi, Synthesis and Characterization of Cadmium Sulfide Nanoparticles by Chemical Precipitation Method, J. Nanosci.

Nanotechnol. 15 (2015) 8434–8439. doi:10.1166/jnn.2015.11472.

[139] G.C. De, A.M. Roy, S.S. Bhattacharya, Photocatalytic production of hydrogen and concomitant cleavage of industrial waste hydrogen sulphide, Int. J. Hydrogen Energy. 20 (1995) 127–131. doi:10.1016/0360-3199(94)P3692-V.

[140] W. Li, D. Li, Z. Chen, H. Huang, M. Sun, Y. He, X. Fu, High-efficient degradation of dyes by ZnxCd1-xS solid solutions under visible light irradiation, J. Phys. Chem. C. 112 (2008) 14943–14947. doi:10.1021/jp8049075.

[141] F. Yang, N.N. Yan, S. Huang, Q. Sun, L.Z. Zhang, Y. Yu, Zn-doped CdS nanoarchitectures prepared by hydrothermal synthesis: Mechanism for enhanced photocatalytic activity and stability under visible light, J. Phys. Chem. C. 116 (2012) 9078–9084. doi:10.1021/jp300939q.

[142] T.K. Jana, A. Pal, K. Chatterjee, Self assembled flower like CdS-ZnO nanocomposite and its photo catalytic activity, J. Alloys Compd. 583 (2014) 510–515. doi:10.1016/j.jallcom.2013.08.184.

[143] D. Wu, F. Wang, Y. Tan, C. Li, Facile synthesis of NiS/CdS nanocomposites for photocatalytic degradation of quinoline under visible-light irradiation, RSC Adv. 6 (2016) 73522–73526. doi:10.1039/c6ra13439d.

[144] P. Nyamukamba, M.J. Moloto, H. Mungondori, Visible light-active CdS/TiO_2 hybrid nanoparticles immobilized on polyacrylonitrile membranes for the photodegradation of dyes in water, J. Nanotechnol. 2019 (2019). doi:10.1155/2019/5135618.

[145] S. Ma, J. Xie, J. Wen, K. He, X. Li, W. Liu, X. Zhang, Constructing 2D layered hybrid CdS nanosheets/MoS_2 heterojunctions for enhanced visible-light photocatalytic H_2 generation, Appl. Surf. Sci. 391 (2017) 580–591. doi:10.1016/j.apsusc.2016.07.067.

[146] Q. Cai, Z. Hu, Q. Zhang, B. Li, Z. Shen, Fullerene (C_{60})/CdS nanocomposite with enhanced photocatalytic activity and stability, Appl. Surf. Sci. 403 (2017) 151–158. doi:10.1016/j.apsusc.2017.01.135.

[147] K.A. Adegoke, M. Iqbal, H. Louis, O.S. Bello, Synthesis, characterization and application of CdS/ZnO nanorod heterostructure for the photodegradation of Rhodamine B dye, Mater. Sci. Energy Technol. 2 (2019) 329–336. doi:10.1016/j.mset.2019.02.008.

[148] S. Cao, J. Yu, G-C_3N_4-based photocatalysts for hydrogen generation, J. Phys. Chem. Lett. 5 (2014) 2101–2107. doi:10.1021/jz500546b.

[149] J. Wen, J. Xie, X. Chen, X. Li, A review on g-C_3N_4 -based photocatalysts, Appl. Surf. Sci. 391 (2017) 72–123. doi:10.1016/j.apsusc.2016.07.030.

[150] E.A. Weiss, Designing the surfaces of semiconductor quantum dots for colloidal photocatalysis, ACS Energy Lett. 2 (2017) 1005–1013. doi:10.1021/acsenergylett.7b00061.

[151] K.R. Reddy, C.V. Reddy, M.N. Nadagouda, N.P. Shetti, S. Jaesool, T.M. Aminabhavi, Polymeric graphitic carbon nitride (g-C_3N_4)-based semiconducting nanostructured materials: Synthesis methods, properties and photocatalytic applications, J. Environ. Manage. 238 (2019) 25–40. doi:10.1016/j.jenvman.2019.02.075.

[152] S. Wang, C. Li, T. Wang, P. Zhang, A. Li, J. Gong, Controllable synthesis of nanotube-type graphitic C_3N_4 and their visible-light photocatalytic and fluorescent properties, J. Mater. Chem. A. 2 (2014) 2885–2890. doi:10.1039/c3ta14576j.

[153] B. Weng, S. Liu, Z. Tang, Y. Xu, RSC Advances One-dimensional nanostructure based materials for versatile photocatalytic applications, (2014) 12685–12700. doi:10.1039/c3ra47910b.

[154] J. Zhang, Y. Chen, X. Wang, Two-dimensional covalent carbon nitride nanosheets: Synthesis, functionalization, and applications, Energy Environ. Sci. 8 (2015) 3092–3108. doi:10.1039/c5ee01895a.

[155] X. Bai, L. Wang, R. Zong, Y. Zhu, Photocatalytic activity enhanced via g-C_3N_4 nanoplates to nanorods, J. Phys. Chem. C. 117 (2013) 9952–9961. doi:10.1021/jp402062d.

[156] Q. Han, B. Wang, J. Gao, Z. Cheng, Y. Zhao, Z. Zhang, L. Qu, Atomically Thin Mesoporous Nanomesh of Graphitic C_3N_4 for High-Efficiency Photocatalytic Hydrogen Evolution, ACS Nano. 10 (2016) 2745–2751. doi:10.1021/acsnano.5b07831.

[157] X. Zhang, X. Xie, H. Wang, J. Zhang, B. Pan, Y. Xie, Enhanced photoresponsive ultrathin graphitic-phase C_3N_4 nanosheets for bioimaging, J. Am. Chem. Soc. 135 (2013) 18–21. doi:10.1021/ja308249k.

[158] J. Senker, K. Schwinghammer, B. V. Lotsch, C. Ziegler, M.B. Mesch, V. Duppel, Crystalline Carbon Nitride Nanosheets for Improved Visible-Light Hydrogen Evolution, J. Am. Chem. Soc. 136 (2014) 1730–1733. doi:10.1021/ja411321s.

[159] B. Luo, G. Liu, L. Wang, Recent advances in 2D materials for photocatalysis, Nanoscale. 8 (2016) 6904–6920. doi:10.1039/c6nr00546b.

[160] P. Niu, L. Zhang, G. Liu, H.M. Cheng, Graphene-like carbon nitride nanosheets for improved photocatalytic activities, Adv. Funct. Mater. 22 (2012) 4763–4770. doi:10.1002/adfm.201200922.

[161] Q. Liu, T. Chen, Y. Guo, Z. Zhang, X. Fang, Ultrathin g-C_3N_4 nanosheets coupled with carbon nanodots as 2D/0D composites for efficient photocatalytic H_2 evolution, Appl. Catal. B Environ. 193 (2016) 248–258. doi:10.1016/j.apcatb.2016.04.034.

[162] Y. Xu, S.P. Gao, Band gap of C_3N_4 in the GW approximation, Int. J. Hydrogen Energy. 37 (2012) 11072–11080. doi:10.1016/j.ijhydene.2012.04.138.

[163] K. Maeda, X. Wang, Y. Nishihara, D. Lu, M. Antonietti, K. Domen, Photocatalytic activities of graphitic carbon nitride powder for water reduction and oxidation under visible light, J. Phys. Chem. C. 113 (2009) 4940–4947. doi:10.1021/jp809119m.

[164] A.H. Reshak, AA- and ABA-stacked carbon nitride (C_3N_4): Novel photocatalytic water splitting solar-to-hydrogen energy conversion, Phys. Chem. Chem. Phys. 20 (2018) 22972–22979. doi:10.1039/c8cp02898b.

[165] A.Y. Liu, M.L. Cohen, Prediction of new low compressibility solids, Science (80-.). 245 (1989) 841–842. doi:10.1126/science.245.4920.841.

[166] B. Jürgens, E. Irran, J. Senker, P. Kroll, H. Müller, W. Schnick, Melem (2,5,8-triamino-tri-s-triazine), an important intermediate during condensation of melamine rings to graphitic carbon nitride: Synthesis, structure determination by x-ray powder diffractometry, solid-state NMR, and theoretical studies, J. Am. Chem. Soc. 125 (2003) 10288–10300. doi:10.1021/ja0357689.

[167] J. Sehnert, K. Baerwinkel, J. Senker, Ab initio calculation of solid-state NMR spectra for different triazine and heptazine based structure proposals of g-C3N4, J. Phys. Chem. B. 111 (2007) 10671–10680. doi:10.1021/jp072001k.

[168] A. Thomas, A. Fischer, F. Goettmann, M. Antonietti, J.O. Müller, R. Schlögl, J.M. Carlsson, Graphitic carbon nitride materials: Variation of structure and morphology and their use as metal-free catalysts, J. Mater. Chem. 18 (2008) 4893–4908. doi:10.1039/b800274f.

[169] Y. Wang, J. Hong, W. Zhang, R. Xu, Carbon nitride nanosheets for photocatalytic hydrogen evolution: Remarkably enhanced activity by dye sensitization, Catal. Sci. Technol. 3 (2013) 1703–1711. doi:10.1039/c3cy20836b.

[170] H. Luo, Z. Zeng, G. Zeng, C. Zhang, R. Xiao, C. Zhou, H. Wang, Y. Zhou, S. Tian, Recent progress on metal-organic frameworks based- and derived-photocatalysts for water splitting, Chem. Eng. J. (2019) 123196. doi:10.1016/j.cej.2019.123196.

[171] D. Zheng, C. Pang, Y. Liu, X. Wang, Shell-engineering of hollow g-C_3N_4 nanospheres via copolymerization for photocatalytic hydrogen evolution , Chem. Commun. 51 (2015) 9706–9709. doi:10.1039/c5cc03143e.

[172] S.W. Bian, Z. Ma, W.G. Song, Preparation and characterization of carbon nitride nanotubes and their applications as catalyst supporter, J. Phys. Chem. C. 113 (2009) 8668–8672. doi:10.1021/jp810630k.

[173] L. Xu, J. Xia, L. Wang, H. Ji, J. Qian, H. Xu, K. Wang, H. Li, Graphitic carbon

nitride nanorods for photoelectrochemical sensing of trace copper(II) ions, Eur. J. Inorg. Chem. (2014) 3665–3673. doi:10.1002/ejic.201402051.

[174] S. Hu, R. Jin, G. Lu, D. Liu, J. Gui, The properties and photocatalytic performance comparison of Fe^{3+}-doped g-C_3N_4 and Fe_2O_3/g-C_3N_4 composite catalysts, RSC Adv. 4 (2014) 24863–24869. doi:10.1039/c4ra03290j.

[175] Y. Wang, Y. Wang, Y. Li, H. Shi, Y. Xu, H. Qin, X. Li, Y. Zuo, S. Kang, L. Cui, Simple synthesis of Zr-doped graphitic carbon nitride towards enhanced photocatalytic performance under simulated solar light irradiation, Catal. Commun. 72 (2015) 24–28. doi:10.1016/j.catcom.2015.08.022.

[176] P. Fageria, R. Nazir, S. Gangopadhyay, H.C. Barshilia, S. Pande, Graphitic-carbon nitride support for the synthesis of shape-dependent ZnO and their application in visible light photocatalysts, RSC Adv. 5 (2015) 80397–80409. doi:10.1039/c5ra12463h.

[177] H. Yu, F. Chen, F. Chen, X. Wang, Applied Surface Science In situ self-transformation synthesis of g-C_3N_4 -modified CdS heterostructure with enhanced photocatalytic activity, Appl. Surf. Sci. 358 (2015) 385–392. doi:10.1016/j.apsusc.2015.06.074.

[178] F. Jiang, T. Yan, H. Chen, A. Sun, C. Xu, X. Wang, Applied Surface Science A g-C_3N_4 – CdS composite catalyst with high visible-light-driven catalytic activity and photostability for methylene blue degradation, Appl. Surf. Sci. 295 (2014) 164–172. doi:10.1016/j.apsusc.2014.01.022.

[179] Y. Guo, J. Wang, Z. Tao, F. Dong, K. Wang, X. Ma, P. Yang, P. Hu, Y. Xu, L. Yang, Facile synthesis of mesoporous CdS nanospheres and their application in photocatalytic degradation and adsorption of organic dyes, CrystEngComm. 14 (2012) 1185–1188. doi:10.1039/c2ce06172d.

[180] H.M. Xiong, D.G. Shchukin, H. Möhwald, Y. Xu, Y.Y. Xia, Sonochemical synthesis of highly luminescent zinc oxide nanoparticles doped with magnesium(II), Angew. Chemie - Int. Ed. 48 (2009) 2727–2731. doi:10.1002/anie.200805590.

[181] Z.R. Tang, X. Yin, Y. Zhang, Y.J. Xu, Synthesis of titanate nanotube-CdS nanocomposites with enhanced visible light photocatalytic activity, Inorg. Chem. 52 (2013) 11758–11766. doi:10.1021/ic4010483.

[182] Y. Li, L. Tang, S. Peng, Z. Li, G. Lu, Phosphate-assisted hydrothermal synthesis of hexagonal CdS for efficient photocatalytic hydrogen evolution, CrystEngComm. 14 (2012) 6974–6982. doi:10.1039/c2ce25838b.

[183] M. Salavati-Niasari, M.R. Loghman-Estarki, F. Davar, Controllable synthesis of nanocrystalline CdS with different morphologies by hydrothermal process in the presence of thioglycolic acid, Chem. Eng. J. 145 (2008) 346–350. doi:10.1016/j.cej.2008.08.040.

[184] L.R. Zou, G.F. Huang, D.F. Li, J.H. Liu, A.L. Pan, W.Q. Huang, A facile and rapid route for synthesis of g-C_3N_4 nanosheets with high adsorption capacity and photocatalytic activity, RSC Adv. 6 (2016) 86688–86694. doi:10.1039/c6ra20514c.

[185] N. Chidhambaram, K. Ravichandran, Fabrication of ZnO/g-C_3N_4 nanocomposites for enhanced visible light driven photocatalytic activity Fabrication of ZnO/g-C_3N_4 nanocomposites for enhanced visible light driven photocatalytic activity, (n.d.).

[186] M. Iqbal, A. Ali, N.A. Nahyoon, A. Majeed, R. Pothu, S. Phulpoto, K.H. Thebo, Photocatalytic degradation of organic pollutant with nanosized cadmium sulfide, Mater. Sci. Energy Technol. 2 (2018) 41–45. doi:10.1016/j.mset.2018.09.002.

[187] S. Vadivel, D. Maruthamani, B. Paul, S.S. Dhar, K. Selvam, Facile synthesis of novel $CaFe_2O_4$ / g-C_3N_4 nanocomposites for degradation of methylene blue under visible-light irradiation Journal of Colloid and Interface Science Facile synthesis of novel $CaFe_2O_4$/g-C_3N_4 nanocomposites for degradation of methyle, J. Colloid Interface Sci. 480 (2016) 126–136. doi:10.1016/j.jcis.2016.07.012.

[188] Z.X. Han, Z. Zhu, D.D. Wu, J. Wu, Y.R. Liu, Adsorption Kinetics and

Thermodynamics of Acid Blue 25 and methylene blue dye solutions on natural sepiolite, Synth. React. Inorganic, Met. Nano-Metal Chem. 44 (2014) 140–147. doi:10.1080/15533174.2013.770755.

[189] S. Kaur, A brief overview on photocatalytic activity of ZnS and CQDs nanopartilces, Int. J. Eng. Appl. Sci. Technol. 2 (2017) 75–82. http://www.ijeast.com.

[190] M. Joshi, A. Bhattacharyya, S.W. Ali, Characterization techniques for nanotechnology applications in textiles, Indian J. Fibre Text. Res. 33 (2008) 304–317.

[191] R. Kohli, Methods for Monitoring and Measuring Cleanliness of Surfaces, in: Dev. Surf. Contam. Clean. - Detect. Charact. Anal. Contam., Elsevier, 2012: pp. 107–178. doi:10.1016/B978-1-4377-7883-0.00003-1.

[192] G. ZHANG, Master Thesis, University of Illinois at Urbana-Champaign, 2013, 2013.

[193] P.J. Mafa, A.T. Kuvarega, B.B. Mamba, B. Ntsendwana, Photoelectrocatalytic degradation of sulfamethoxazole on g-C_3N_4/BiOI/EG p-n heterojunction photoanode under visible light irradiation, Appl. Surf. Sci. 483 (2019) 506–520. doi:10.1016/j.apsusc.2019.03.281.

[194] M. Izadifard, G. Achari, C.H. Langford, Application of photocatalysts and LED light sources in drinking water treatment, Catalysts. 3 (2013) 726–743. doi:10.3390/catal3030726.

[195] C.G. Young, an Inductively Coupled Plasma Atomic Emission Spectrometer for the Detection of Nonmetals in the Vacuum Ultraviolet, 2011.

[196] A.M. Sabir, M. Moloy, P.S. Bhasin, Hplc Method Development and Validation: a Review, Int. Res. J. Pharm. 4 (2016) 39–46. doi:10.7897/2230-8407.04407.

[197] F. Jiang, T. Yan, H. Chen, A. Sun, C. Xu, X. Wang, A g-C_3N_4 -CdS composite catalyst with high visible-light-driven catalytic activity and photostability for methylene blue degradation, Appl. Surf. Sci. 295 (2014) 164–172.

doi:10.1016/j.apsusc.2014.01.022.

[198] Z. Zhang, J. Huang, M. Zhang, Q. Yuan, B. Dong, Ultrathin hexagonal SnS_2 nanosheets coupled with g-C_3N_4 nanosheets as 2D/2D heterojunction photocatalysts toward high photocatalytic activity, Appl. Catal. B Environ. 163 (2015) 298–305. doi:10.1016/j.apcatb.2014.08.013.

[199] A. Akhundi, A. Habibi-yangjeh, Novel magnetically separable g-C_3N_4/AgBr / Fe_3O_4 nanocomposites as visible-light-driven photocatalysts with highly enhanced activities, Ceram. Int. 41 (2015) 5634–5643. doi:10.1016/j.ceramint.2014.12.145.

[200] L.J. Cote, F. Kim, J. Huang, Langmuir-blodgett assembly of graphite oxide single layers, J. Am. Chem. Soc. 131 (2009) 1043–1049. doi:10.1021/ja806262m.

[201] Z. Zhou, J. Wang, J. Yu, Y. Shen, Y. Li, A. Liu, S. Liu, Y. Zhang, Dissolution and liquid crystals phase of 2D polymeric carbon nitride, J. Am. Chem. Soc. 137 (2015) 2179–2182. doi:10.1021/ja512179x.

[202] J. Xu, L. Zhang, R. Shi, Y. Zhu, Chemical exfoliation of graphitic carbon nitride for efficient heterogeneous photocatalysis, J. Mater. Chem. A. 1 (2013) 14766–14772. doi:10.1039/c3ta13188b.

[203] F. Dong, Z. Wang, Y. Sun, W.K. Ho, H. Zhang, Engineering the nanoarchitecture and texture of polymeric carbon nitride semiconductor for enhanced visible light photocatalytic activity, J. Colloid Interface Sci. 401 (2013) 70–79. doi:10.1016/j.jcis.2013.03.034.

[204] C. Li, Z. Sun, W. Huang, S. Zheng, Facile synthesis of g-C_3N_4/montmorillonite composite with enhanced visible light photodegradation of rhodamine B and tetracycline, J. Taiwan Inst. Chem. Eng. 66 (2016) 363–371. doi:10.1016/j.jtice.2016.06.014.

[205] J. Tong, L. Zhang, F. Li, K. Wang, L. Han, S. Cao, Rapid and high-yield production of g-C_3N_4 nanosheets via chemical exfoliation for photocatalytic H2 evolution, RSC Adv. 5 (2015) 88149–88153. doi:10.1039/c5ra16988g.

[206] J. Zhu, P. Xiao, H. Li, S.A.C. Carabineiro, Graphitic carbon nitride: Synthesis, properties, and applications in catalysis, ACS Appl. Mater. Interfaces. 6 (2014) 16449–16465. doi:10.1021/am502925j.

[207] Y. Chen, X. Wang, Template-Free Synthesis of Hollow G‐C_3N_4 Polymer with Vesicle Structure for Enhanced Photocatalytic Water Splitting, (2018). doi:10.1021/acs.jpcc.7b12496.

[208] H.B. Tao, H. Bin Yang, J. Chen, J. Miao, B. Liu, Biomolecule-assisted synthesis of carbon nitride and sulfur-doped carbon nitride heterojunction nanosheets: An efficient heterojunction photocatalyst for photoelectrochemical applications, Beilstein J. Nanotechnol. 5 (2014) 770–777. doi:10.3762/bjnano.5.89.

[209] J. Tong, L. Zhang, F. Li, K. Wang, L. Han, S. Cao, Rapid and high-yield production of g-C_3N_4 nanosheets via chemical exfoliation for photocatalytic H2 evolution, RSC Adv. 5 (2015) 88149–88153. doi:10.1039/c5ra16988g.

[210] S. Asadzadeh-khaneghah, A. Habibi-yangjeh, S. Vadivel, Journal of the Taiwan Institute of Chemical Engineers Fabrication of novel g-C_3N_4 nanosheet / carbon dots / $Ag_6Si_2O_7$ nanocomposites with high stability and enhanced visible-light photocatalytic activity, J. Taiwan Inst. Chem. Eng. 103 (2019) 94–109. doi:10.1016/j.jtice.2019.07.018.

[211] G. Mamba, A.K. Mishra, Applied Catalysis B : Environmental Graphitic carbon nitride (g-C_3N_4) nanocomposites : A new and exciting generation of visible light driven photocatalysts for environmental pollution remediation, "Applied Catal. B, Environ. 198 (2016) 347–377. doi:10.1016/j.apcatb.2016.05.052.

[212] J. Jin, J. Yu, G. Liu, P.K. Wong, Single crystal CdS nanowires with high visible-light photocatalytic H_2-production performance, J. Mater. Chem. A. 1 (2013) 10927–10934. doi:10.1039/c3ta12301d.

[213] S. Rengaraj, A. Ferancova, S.H. Jee, S. Venkataraj, Y. Kim, J. Labuda, M. Sillanpää, Physical and electrochemical characterization of CdS hollow microspheres prepared by a novel template free solution phase method,

Electrochim. Acta. 56 (2010) 501–509. doi:10.1016/j.electacta.2010.09.019.

[214] J. Fu, B. Chang, Y. Tian, F. Xi, X. Dong, Novel C_3N_4-CdS composite photocatalysts with organic-inorganic heterojunctions: In situ synthesis, exceptional activity, high stability and photocatalytic mechanism, J. Mater. Chem. A. 1 (2013) 3083–3090. doi:10.1039/c2ta00672c.

[215] Q. Li, B. Guo, J. Yu, J. Ran, B. Zhang, H. Yan, J.R. Gong, Highly efficient visible-light-driven photocatalytic hydrogen production of CdS-cluster-decorated graphene nanosheets, J. Am. Chem. Soc. 133 (2011) 10878–10884. doi:10.1021/ja2025454.

[216] V. Mohanraj, R. Jayaprakash, R. Robert, J. Balavijayalakshmi, S. Gopi, Effect of particle size on optical and electrical properties in mixed CdS and NiS nanoparticles synthesis by ultrasonic wave irradiation method, Mater. Sci. Semicond. Process. 56 (2016) 394–402. doi:10.1016/j.mssp.2016.08.014.

[217] N.H. Patel, M.P. Deshpande, S.H. Chaki, H.R. Keharia, Tuning of optical, thermal and antimicrobial capabilities of CdS nanoparticles with incorporated Mn prepared by chemical method, J. Mater. Sci. Mater. Electron. 28 (2017) 10866–10876. doi:10.1007/s10854-017-6865-y.

[218] A. Modwi, M.A. Ghanem, A.M. Al-Mayouf, A. Houas, Lowering energy band gap and enhancing photocatalytic properties of Cu/ZnO composite decorated by transition metals, J. Mol. Struct. 1173 (2018) 1–6. doi:10.1016/j.molstruc.2018.06.082.

[219] Q. Tang, C. Zhou, X. Yuan, Q. Jing, Y. Mu, A. Du, Facile Synthesis of g-C_3N_4 Nanosheets/ZnO Nanocomposites with Enhanced Photocatalytic Activity in Reduction of Aqueous Chromium(VI) under Visible Light, Nanomaterials. 6 (2016) 173. doi:10.3390/nano6090173.

[220] D. Wang, Z. Xu, Q. Luo, X. Li, J. An, R. Yin, C. Bao, Preparation and visible-light photocatalytic performances of g-C_3N_4 surface hybridized with a small amount of CdS nanoparticles, J. Mater. Sci. 51 (2016) 893–902. doi:10.1007/s10853-015-9417-y.

[221] A. Kumar, A Review on the Factors Affecting the Photocatalytic Degradation of Hazardous Materials, Mater. Sci. Eng. Int. J. 1 (2017) 1–10. doi:10.15406/mseij.2017.01.00018.

[222] S. Talebi, N. Chaibakhsh, Z. Moradi-Shoeili, Application of nanoscale ZnS/TiO2 composite for optimized photocatalytic decolorization of a textile dye, J. Appl. Res. Technol. 15 (2017) 378–385. doi:10.1016/j.jart.2017.03.007.

[223] Y.S. Al-Degs, M.I. El-Barghouthi, A.H. El-Sheikh, G.M. Walker, Effect of solution pH, ionic strength, and temperature on adsorption behavior of reactive dyes on activated carbon, Dye. Pigment. 77 (2008) 16–23. doi:10.1016/j.dyepig.2007.03.001.

[224] E.T. Helmy, A. El Nemr, M. Mousa, E. Arafa, S. Eldafrawy, Photocatalytic degradation of organic dyes pollutants in the industrial textile wastewater by using synthesized TiO_2, C-doped TiO_2, S-doped TiO_2 and C,S co-doped TiO_2 nanoparticles, J. Water Environ. Nanotechnol. 3 (2018) 116–127. doi:10.22090/JWENT.2018.02.003.

[225] E. Mugunthan, M.B. Saidutta, P.E. Jagadeeshbabu, Visible light assisted photocatalytic degradation of diclofenac using TiO_2-WO_3 mixed oxide catalysts, Environ. Nanotechnology, Monit. Manag. 10 (2018) 322–330. doi:10.1016/j.enmm.2018.07.012.

[226] S. Iguchi, K. Teramura, S. Hosokawa, T. Tanaka, Effect of the chloride ion as a hole scavenger on the photocatalytic conversion of CO_2 in an aqueous solution over Ni-Al layered double hydroxides, Phys. Chem. Chem. Phys. 17 (2015) 17995–18003. doi:10.1039/c5cp02724a.

[227] L. Das, S.K. Barodia, S. Sengupta, J.K. Basu, Aqueous degradation kinetics of pharmaceutical drug diclofenac by photocatalysis using nanostructured titania–zirconia composite catalyst, Int. J. Environ. Sci. Technol. 12 (2015) 317–326. doi:10.1007/s13762-013-0466-y.

[228] J.M. Monteagudo, H. El-taliawy, A. Durán, G. Caro, K. Bester, Sono-activated persulfate oxidation of diclofenac: Degradation, kinetics, pathway and

contribution of the different radicals involved, J. Hazard. Mater. 357 (2018) 457–465. doi:10.1016/j.jhazmat.2018.06.031.

[229] T. Huang, G. Zhang, S. Chong, Y. Liu, N. Zhang, S. Fang, J. Zhu, Effects and mechanism of diclofenac degradation in aqueous solution by US/Zn0, Ultrason. Sonochem. 37 (2017) 676–685. doi:10.1016/j.ultsonch.2017.02.032.

[230] M. V. Bagal, P.R. Gogate, Degradation of diclofenac sodium using combined processes based on hydrodynamic cavitation and heterogeneous photocatalysis, Ultrason. Sonochem. 21 (2014) 1035–1043. doi:10.1016/j.ultsonch.2013.10.020.

[231] P. Sathishkumar, R.A.A. Meena, T. Palanisami, V. Ashokkumar, T. Palvannan, F.L. Gu, Occurrence, interactive effects and ecological risk of diclofenac in environmental compartments and biota - a review, Sci. Total Environ. 698 (2020) 134057. doi:10.1016/j.scitotenv.2019.134057.

[232] R.R. Giri, H. Ozaki, S. Ota, R. Takanami, S. Taniguchi, Degradation of common pharmaceuticals and personal care products in mixed solutions by advanced oxidation techniques, Int. J. Environ. Sci. Tech. 7 (2010) 251–260. doi:10.1007/BF03326135.

[233] S. Sébastien, Les soignants face à la mort, Rev. Infirm. 1 (2012) 39–41.

[234] H. Xu, L. Wu, L. Jin, K. Wu, Combination Mechanism and Enhanced Visible-Light Photocatalytic Activity and Stability of CdS/g-C_3N_4 Heterojunctions, J. Mater. Sci. Technol. 33 (2017) 30–38. doi:10.1016/j.jmst.2016.04.008.

[235] I.W. As, M.C. Level, P.H. Effects, T. Methods, I. Exchange, R. Osmosis, WQA Technical Fact Sheet: Cadmium health effects treatments methods Residential Point-of-Entry Point-of-Use, 2013. http://www.epa.gov/safewater/pdfs/factsheets/ioc/cadmium.pdf.

CHAPTER 4

SYNTHESIS, CHARACTERIZATION AND APPLICATION OF GRAPHITIC CARBON NITRIDE NANOSHEETS

4.1 Introduction

This chapter demonstrates the characterization and application of exfoliated graphitic carbon nitride for the photocatalytic degradation of AB-25. Bulk graphitic carbon nitride was exfoliated to form graphitic carbon nitride nanosheets (section 3.1). The application of AB-25 was carried at the initial dye pH of 5. This was done to confirm the improved photocatalytic efficiency of exfoliated g-C_3N_4 (nanosheets).

4.2 Results and discussion

4.2.1 X-Ray diffractometer (XRD)

The crystalline phases and purity of CN and CNS were characterized using XRD analysis (Fig. 4.1). Two characteristic peaks of CN were identified at 2Θ = 13.7°, 27.5 and for CNS were identified at 13.9° and 27.7° and were indexed to (100), (002) respectively as indexed in JCDPS 87-1526. The lattice planes indicate that the natural crystalline structure of CN was maintained in CNS with small changes. The peak at 27.5º was characteristic of the (002) planar due to the interlayer stacking of aromatic systems of graphitic materials and the weak diffraction peak at 12.8° was characteristic of the (100) planar due to the interplanar stacking which significantly weakened after exfoliation [187,197].

The crystallite sizes (d) and micro-strain (ε) values of the synthesized materials were estimated using Scherrer equation (3.6) and micro-strain equation (3.7);

The micro-strain values of CN and CNS were determined to be 0.00196 and 0.00261 respectively. The increase in micro-strain and crystalline broadening resulted in the broadening of XRD profiles.

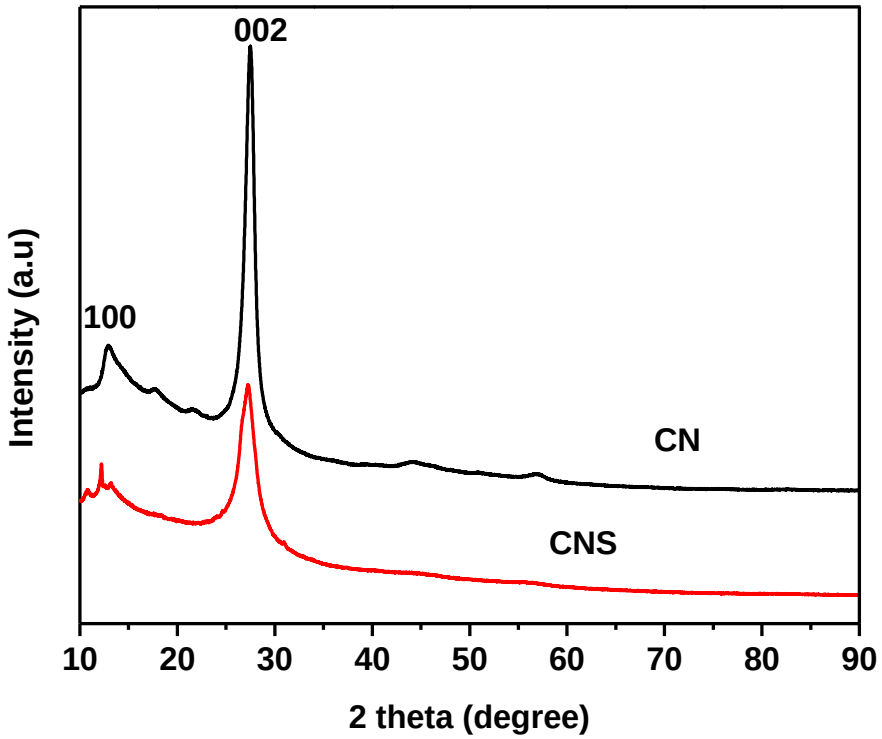

Figure 4.1. XRD patterns of CN and CNS.

4.2.2 Fourier transformation infra-red (FTIR)

The functional groups of the prepared materials were determined using FTIR analysis (Fig. 4.2). The characteristic FTIR analysis CN and CNS were similar. The peaks at 806 cm^{-1} are ascribed to tri-s-triazine ring, the peak in the range 1200-1700 cm^{-1} is ascribed to the aromatic CN stretching modes which maybe either trigonal $N(-C)_3$ or bridging C-NH-C units [198,199]. The peaks at 1641, 1565, 1465, and 1417 cm^{-1} are due to the stretching modes of heptazine derived units which were characteristic of the FTIR spectrum of g-C_3N_4. The broad band at 3000-3500 cm^{-1} is ascribed to the uncondensed terminal amino groups and the peak intensity in the range 1200-1700 cm^{-1} for g-C_3N_4 nanosheets slightly shifted which may be due to the protonation and disintegration of CN [184,200,201].

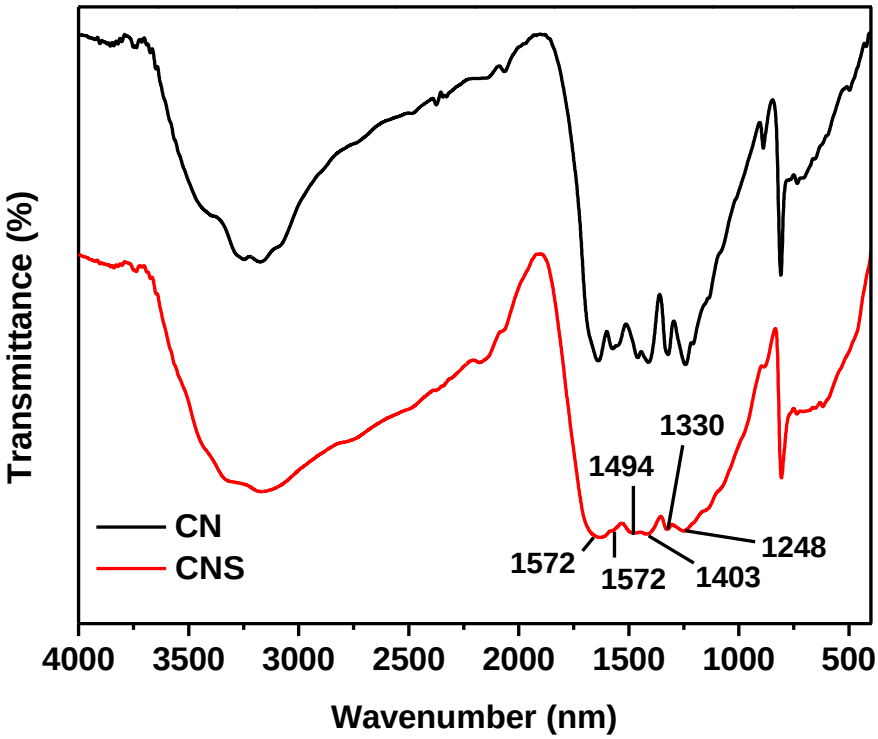

Figure 4.2. FTIR spectra of CN and CNS.

4.2.3 Scanning Electron and Energy Dispersive Microscope

The surface morphology of CN and CNS were determined with FESEM (Fig. 4.3a and b). The FESEM image shows the irregular micrometer size block of CN (Fig. 4.3.a) [187,202–204]. Furthermore, the layered sheet like morphology of CNS was observed (Fig. 4.3b). Moreover some aggregates of CN remained in CNS suggesting the CN was not fully exfoliated which may be due to the insufficient H_2SO_4 to C_2H_2OH ratio to achieve full adequate CN exfoliation.

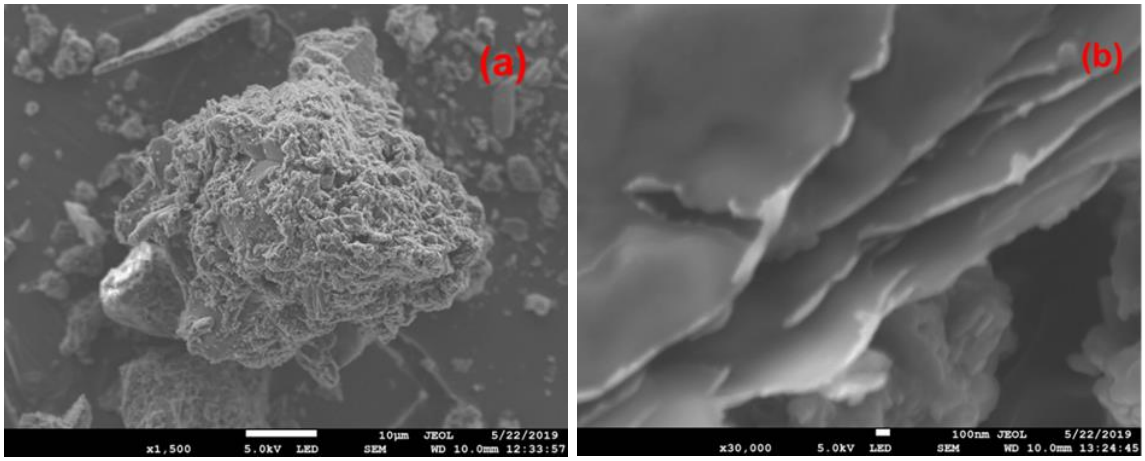

Figure 4.3.FESEM micrograms of (a) CN and (b) CNS.

The elemental composition of CN and CNS were determined EDS (Fig. 4.4a and b). The EDS of CN showed the presence of C, O, and N. The elements C and N were consistent with the heterocycle group of g-C_3N_4 (Fig. 4.4). Furthermore, the EDS for CNS showed the presence of C, O, N and S. The small S peak was due to residual H_2SO_4 used for exfoliation of CN (Fig. 4.4b).

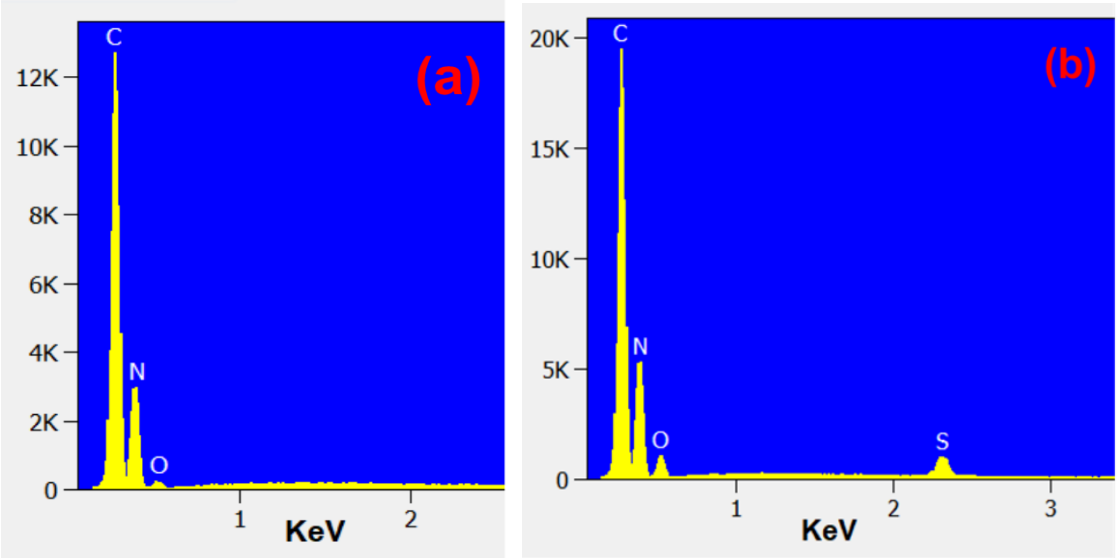

Figure 4.4. EDX spectra of (a) CN and (b) CNS.

4.2.4 Transmission Electron Microscope (TEM)

The morphology and structure of CN were determined using TEM (Fig. 4.5). The TEM image shows an almost transparent ultra-thick morphology of CNS. The image demonstrated that the CNS were stacked on each other and concurs with the morphology observed on SEM micrographs (Fig. 4.5a). The SAED (Selected Area

Electron Diffraction) was used to determine crystalline structure of CN and suggests that the CN is polycrystalline structure which was observed on the SEM images (Fig. 4.3b) showing different morphologies of both CN and CNS (Fig.4.5b).

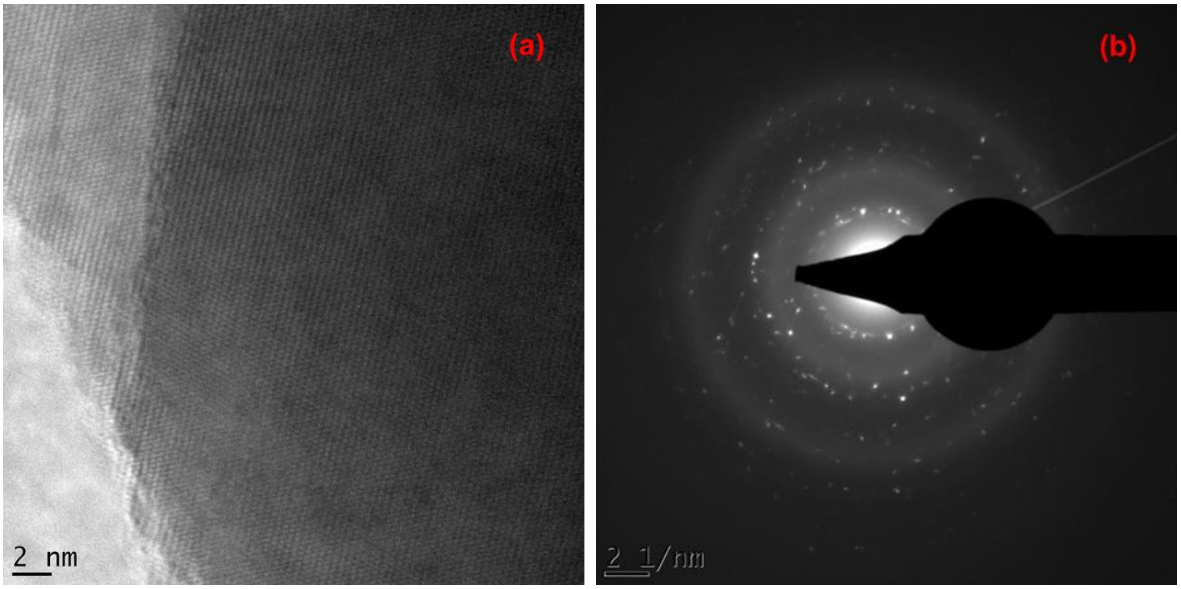

Figure 4.5.TEM images of (a) CNS and (b) SAED pattern of CNS.

4.2.5 BET analysis

The nitrogen adsorption/desorption isotherm of CN and CNS are shown in (Fig. 4.6). The N_2 adsorption/desorption isotherms exhibit a type H3 hysteresis loop, indicating the formation of sheet like morphology supported by the TEM analysis. The BET analysis shows a significant increase in surface area of CN from 3.04 to 11 $m^2 g^{-1}$. The increased surface area should be beneficial for photocatalytic activity of the material because there are more active sites for photodegradation [205].

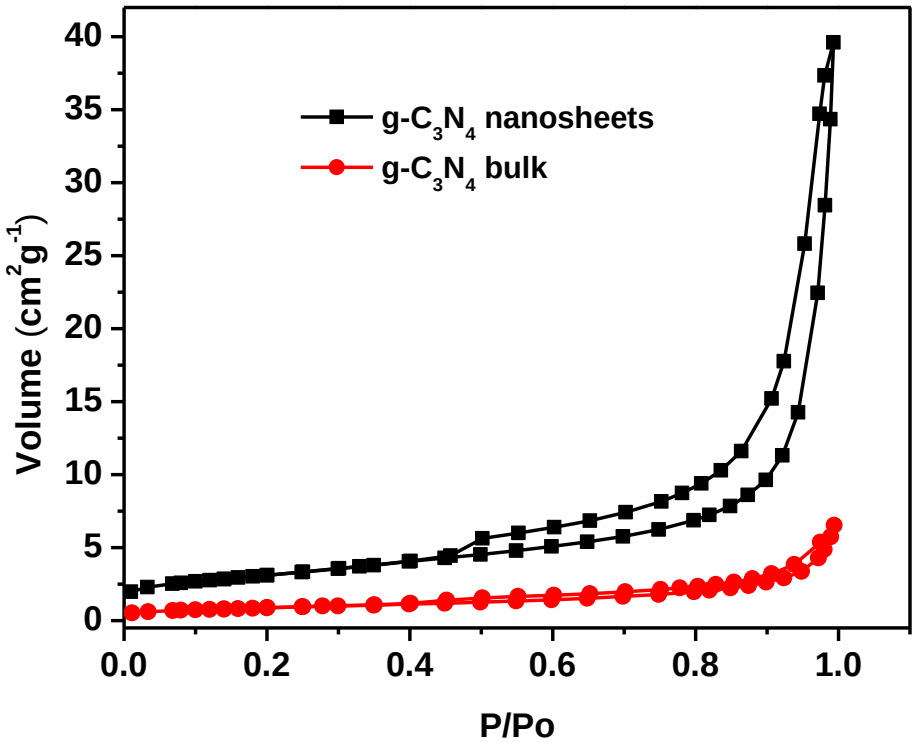

Figure 4.6.BET analysis of (a) CN and (b) CNS.

4.2.6 Thermal gravimetric analysis

The thermal stability of the synthesized materials were determined using thermal graphitic analysis (Fig. 4.7). The small weight loss below 550 ^{o}C was due to the dehydration of the sample where water was lost. Major weight loss of 94.1% for CN was observed from 563 to 738 ^{o}C which was due to thermal decomposition its self and also shows robustness and thermal stability after 758 ^{o}C [206]. Furthermore compared to CN, the CNS had two major weightless at of (10%) from 92.1 to 231 ^{o}C and 88.2% from 453 to 646 ^{o}C after exfoliation. The 10% weight loss is ascribed to increase in surface area due to H_2O molecule and other substances adsorbed on the CNS surface [207].

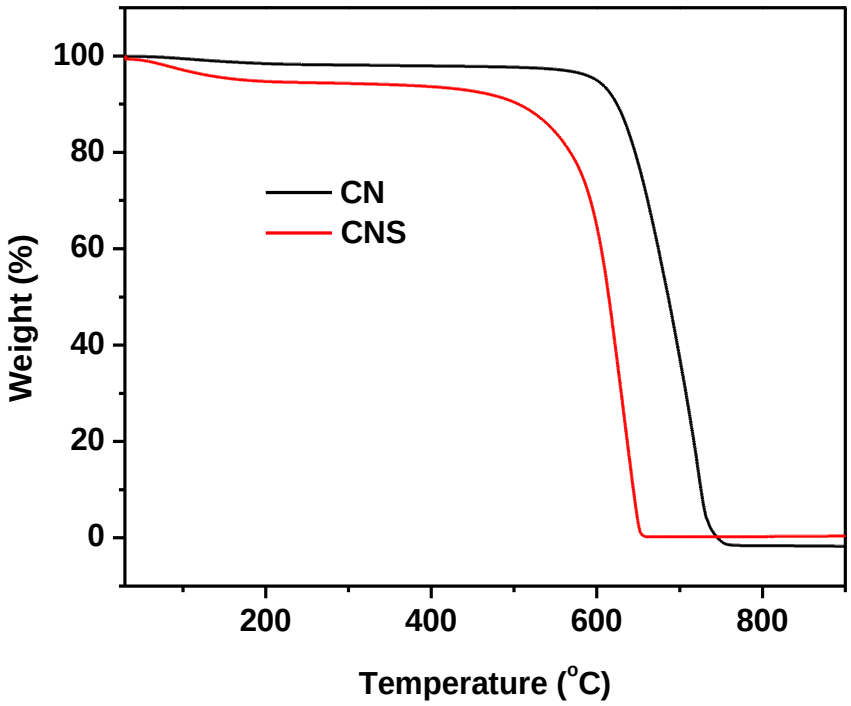

Figure 4.7. TGA analysis of CN and CNS.

4.3 Optical properties

4.3.1 UV-Vis absorption spectroscopy

The optical properties of CN and CN were determined with UV-Vis spectroscopy (Fig. 4.8a). The CN and CNS displayed UV-Vis absorption in the visible region with wavelength edges of 445 nm and 417 nm respectively. A blue shift with respect to CN was observed and is ascribed to the decrease in the conjugation length of CNS and the quantum confinement effect associated with the single layer structure of CNS [184]. The bandgaps of the materials were estimated from the absorption spectra using the equation (3.11) to (3.12).

Tauc plot with relation equation (3.13) were determined using the energy gap of the materials and extrapolated to fit the baseline at y=0 and related to and the best fit for CN and CNS was for indirect (allowed) transition and obtained bandgap of 2.58 and 2.62 eV respectively (Fig. 4.7b) [152,208]. The larger bandgap of CNS is ascribed to

the acidification effect, which reduced the electron density of the single layers of CNS [184,205]

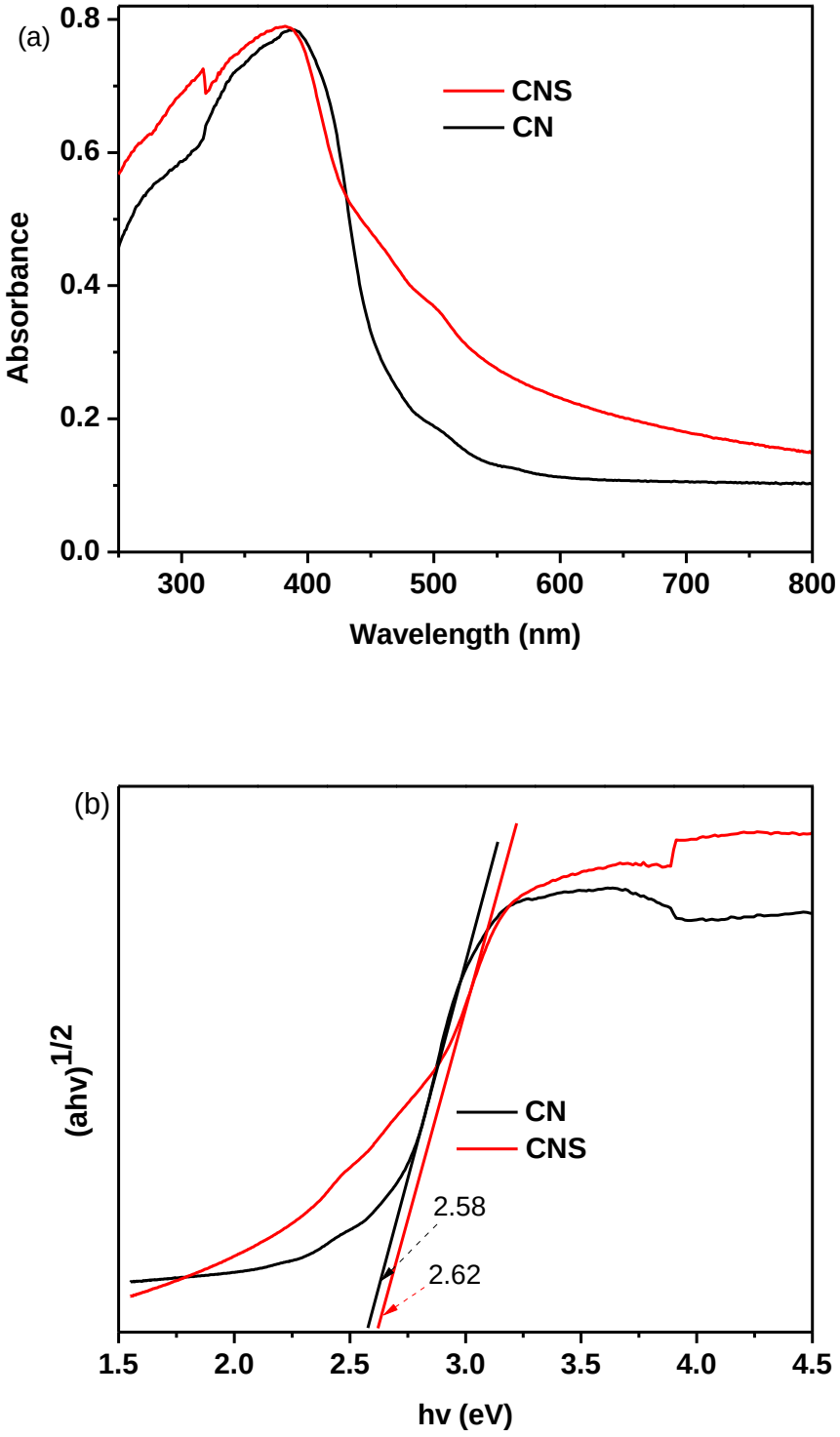

Figure 4.8. (a) UV-Vis spectra and (b) Tauc plots of prepared materials.

4.3.2 Photoluminescence spectroscopy

The emission peaks of CN and CNS were evaluated using PL (Fig. 4.9). The emission peaks of CN is located at 463 nm and blue shifted to 434 nm for CNS. Furthermore, the emission intensity of CNS was lower than that of CN suggesting that the CNS had lower recombination rate of electrons and holes, which may result in improved photocatalytic performance of CN under light irradiation [157,184,209].

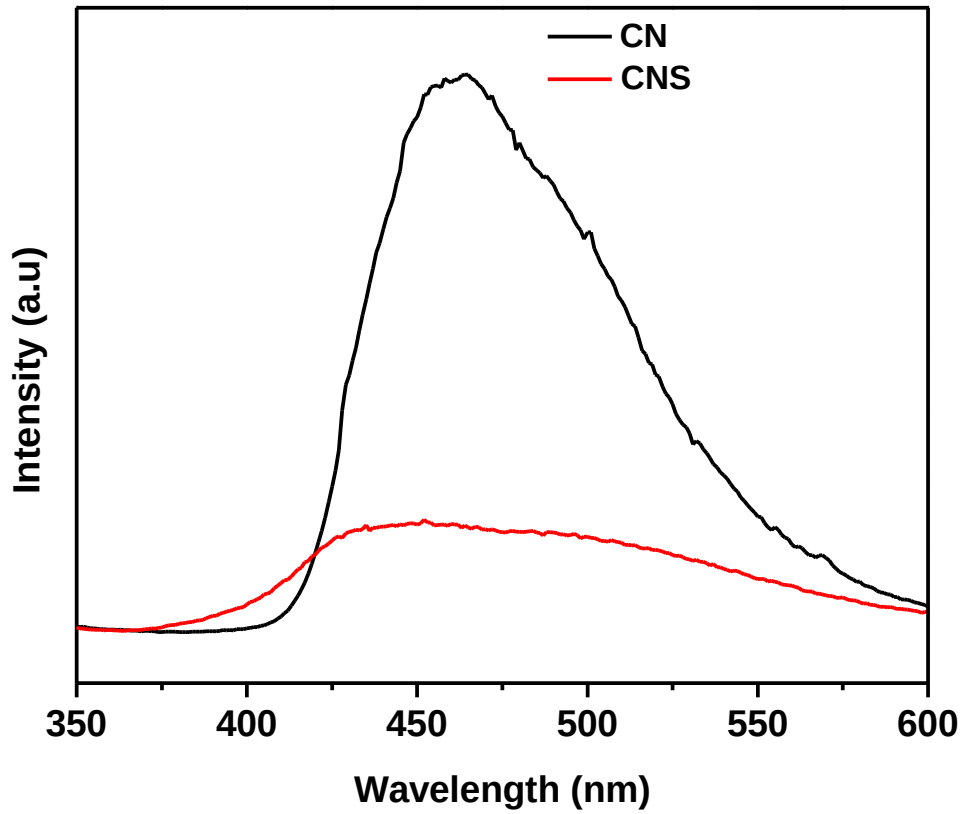

Figure 4.9. PL spectra of CN and CNS.

4.4 Photocatalytic degradation of AB-25

4.4.1 AB-25 Dye degradation absorption

The photocatalytic degradation of AB 25 was followed using UV-Vis spectrophotometry at a maximum wavelength of (λ_{max}= 603 nm). The photocatalytic degradation of AB-25 at a concentration of 20 mg L^{-1} (50 mL), pH 5 was evaluated

using 20 mg L^{-1} of catalyst. The results showed that the dye absorbance decreased with decreasing time showing that the chromophore of the dye after 180 min was not completely degraded (Fig.4.10).

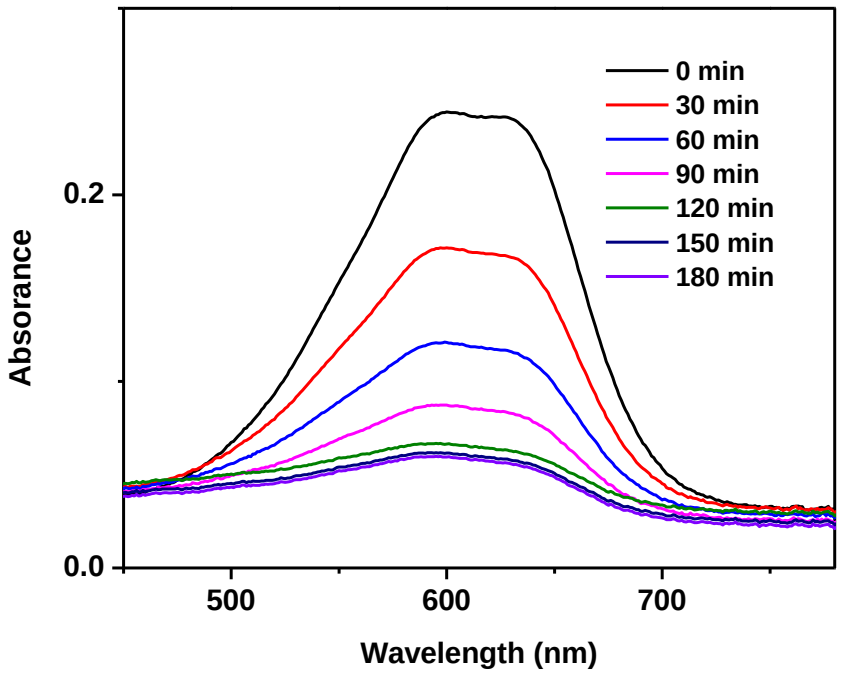

Figure 4.10. UV-Vis absorption for degradation of AB-25.

4.4.2 Effect of exfoliation on CN for photocatalytic degradation of AB-25

The photocatalytic efficiency of exfoliated CN for AB-25 degradation was evaluated using the equation (3.4) (Fig.4.11). The degradation in the absence of the catalyst (photolysis) the concentration of the dye remained the same therefore the dye was not decolorized. Furthermore, the photocatalytic efficiency of CN and CNS significantly increased from 23% to 61% respectively, suggesting that the photocatalytic activity of CN was successfully improved through exfoliation. However the chromophore of the dye was not completely after 180 min decolorized as 39% of the dye still remained.

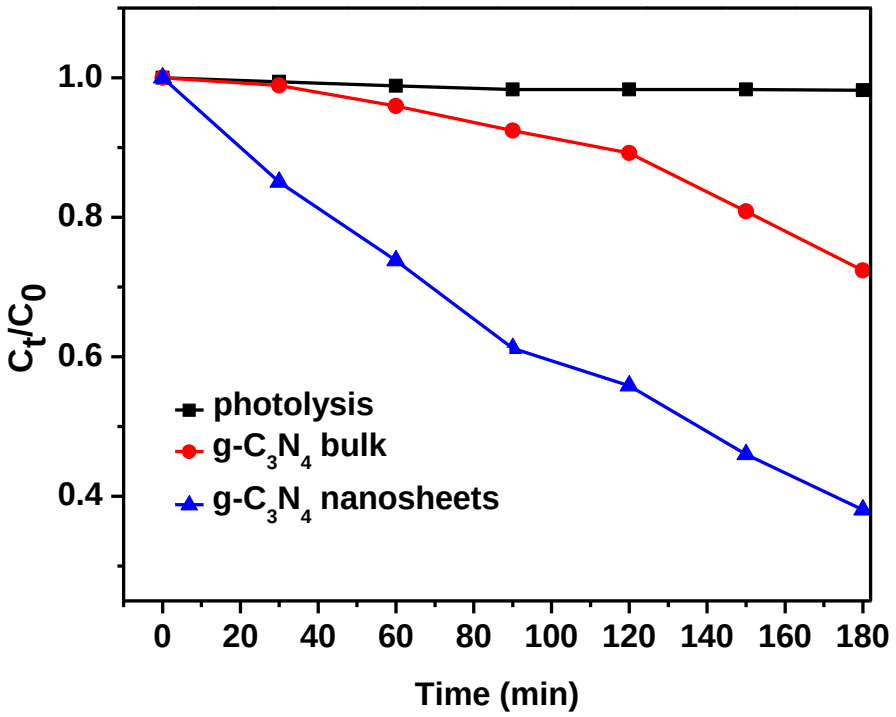

Figure 4.11. (a) UV-Vis absorption of AB-25 and (b) Effect of CN and CNS on AB-25.

4.5 Reaction kinetics

The degradation rate of AB-25 was evaluated by presenting the degradation data using the Langmuir-Hinshelwood first order kinetics using the equation (3.13) and (3.14).

The reaction rate of photolysis was slow 0.0001 min^{-1}. Furthermore the reaction rate for CN and CNS were 0.0009 and 0.0050 min^{-1}, respectively, showing that the reaction rate for CN was slower than CNS and is due to the improved photocatalytic efficiency of CN. The fast reaction rate are ascribed to the low recombination of photo-induces charge carriers. Moreover, the photodegradation of AB-25 followed the pseudo-first order model (Fig. 4.12).

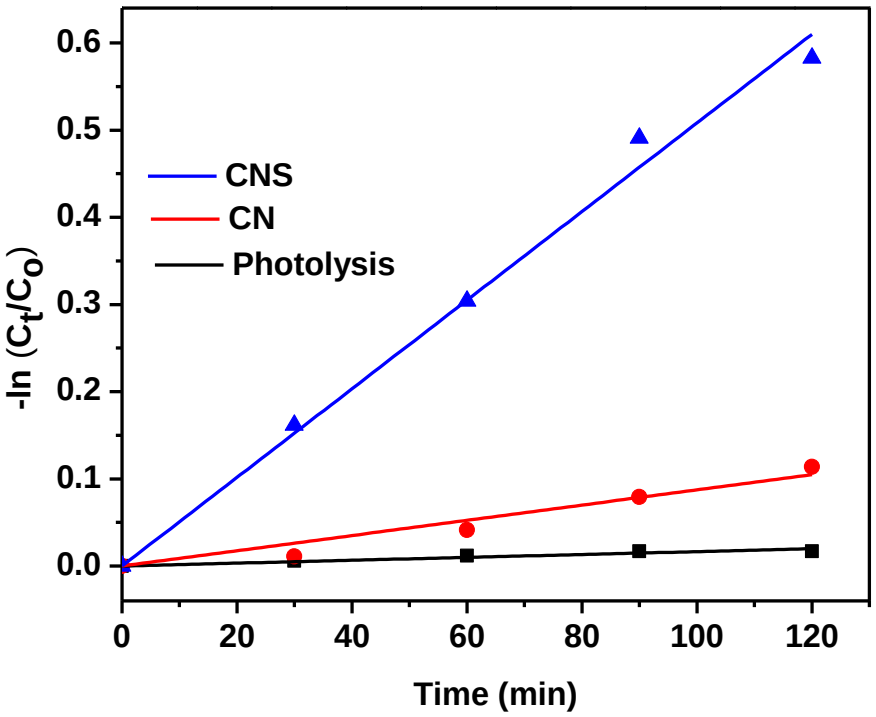

Figure 4.12. Reaction rate constants of CN and CNS.

4.6 Proposed mechanism

The proposed mechanism for transfer and separation of charges during photocatalytic degradation AB-25 is shown with a schematic diagram (Fig.13). To determine the separation of charge, the band edge potentials at the conduction band (CB) and valence band (VB) of CNS and CdS were determined using the equations (3.15) and (3.16).

The CB and VB potentials were -1.07 and 1.55 eV respectively. The obtained CB position of CNS is less negative than the standard redox potential of $^{\bullet}OH/H_2O$ (2.02eV) and $^{\bullet}OH/OH^-$ (+2.69 eV) (20.90), so the h^+ formed react with AB-25 solution directly and take part in photodegradation of AB-25. Furthermore the reduction potential at the CNS CB is more positive than the standard reduction potential of $O_2/^{\bullet}O_2^-$ (0.33 eV), therefore the electrons on the CB could reduce O_2 into $^{\bullet}O_2^-$ and effectively improve the photocatalytic activity [210–212].

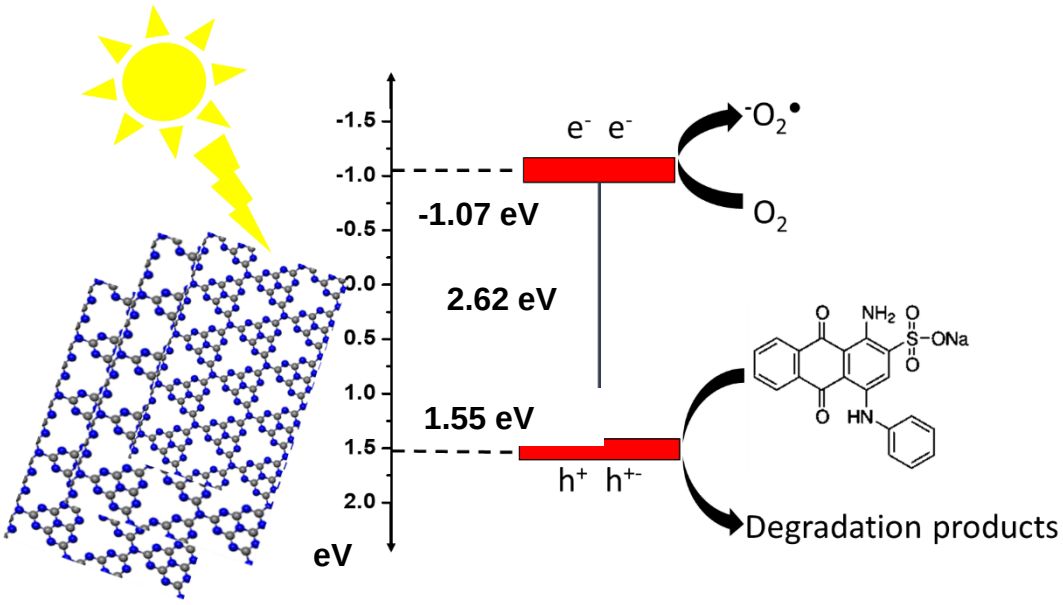

Figure 4.13. Proposed mechanism for CNS photodegradation of AB-25.

4.7 Conclusions

This chapter demonstrated the synthesis of g-C_3N_4 nanosheets through chemical exfoliation of bulk g-C_3N_4. The obtained results showed that the g-C_3N_4 nanosheets displayed superior photocatalytic efficiency compared to bulk g-C_3N_4 and achieved highest removal efficiency of AB-25

References

[1] A. Azizullah, M.N.K. Khattak, P. Richter, D.P. Häder, Water pollution in Pakistan and its impact on public health - A review, Environ. Int. 37 (2011) 479–497. doi:10.1016/j.envint.2010.10.007.

[2] I. Gehrke, A. Somborn-schulz, Innovations in nanotechnology for water treatment, Nanotechnol. Sci. Appl. 8 (2015) 1–17.

[3] C.J.. ; G. Vorösmarty Pamela; ; Salisbury, Joseph; ; Lammers, Richard B., Global Water Resources: Vulnerability from Climate Change and Population Growth, Science (80-.). 289 (2000) 284–288. doi:10.1126/science.289.5477.284.

[4] J. Theron, T.E. Cloete, Emerging Waterborne Infections: Contributing Factors, Agents, and Detection Tools, Crit. Rev. Microbiol. 28 (2008) 1–26. doi:10.1080/1040-840291046669.

[5] K.K. Jain, Nanotechnology and Water, Contemp. Mater. 1 (2012) 26–30. doi:10.7251/122.

[6] F.W. Owa, Water pollution : sources , effects , control and management, Int. Lett. 3 (2014) 1–6.

[7] H. Zhou, D.W. Smith, Advanced technologies in water and wastewater treatment, in: 2002. doi:10.1139/S02-020.

[8] M. Wakil, M. Burhan, L. Ang, K. Choon, Energy-water-environment nexus underpinning future desalination sustainability, Desalination. 413 (2017) 52–64. doi:10.1016/j.desal.2017.03.009.

[9] M. Palaniappan, K. Address, Peak_Water_Talk.Pdf, in: Utah Am. Plan. Assoc. Annu. Conf., 2008: pp. 3–11.

[10] J.K. Bwapwa, Review on Main Issues Causing Deterioration of Water Quality and Water Scarcity: Case Study of South Africa, Environ. Manag. Sustain. Dev. 7 (2018) 14. doi:10.5296/emsd.v7i3.13156.

[11] J. Wang, S. Wang, Removal of pharmaceuticals and personal care products (PPCPs) from wastewater: A review, J. Environ. Manage. 182 (2016) 620–640.

doi:10.1016/j.jenvman.2016.07.049.

[12] G. Boczkaj, A. Fernandes, Wastewater treatment by means of advanced oxidation processes at basic pH conditions : A review, Chem. Eng. J. 320 (2017) 608–633. doi:10.1016/j.cej.2017.03.084.

[13] R. Ananthashankar, Treatment of textile effluent containing Reactive Red 120 dye using advanced oxidation, 2012.

[14] K. Klaus, Pharmaceuticals in the Environment, Annu Rev Env. Resour. 35 (2010) 57–75. doi:10.1146/annurev-environ-052809-161223.

[15] G. Kjosavik, Subtle changes, 2001.

[16] A.B.A. Boxall, M.A. Rudd, B.W. Brooks, D.J. Caldwell, K. Choi, S. Hickmann, E. Innes, K. Ostapyk, J.P. Staveley, T. Verslycke, G.T. Ankley, K.F. Beazley, Review Pharmaceuticals and Personal Care Products in the Environment : What Are the Big Questions ?, 120 (2012) 1221–1229.

[17] G. Li, X. Nie, Y. Gao, T. An, Applied Catalysis B : Environmental Can environmental pharmaceuticals be photocatalytically degraded and completely mineralized in water using g-C_3N_4/TiO_2 under visible light irradiation ?— Implications of persistent toxic intermediates, "Applied Catal. B, Environ. 180 (2016) 726–732. doi:10.1016/j.apcatb.2015.07.014.

[18] B. Hoeger, B. Köllner, D.R. Dietrich, B. Hitzfeld, Water-borne diclofenac affects kidney and gill integrity and selected immune parameters in brown trout (Salmo trutta f. fario), Aquat. Toxicol. 75 (2005) 53–64. doi:10.1016/j.aquatox.2005.07.006.

[19] M. Lillenberg, S. Yurchenko, K. Kipper, K. Herodes, V. Pihl, R. Lõhmus, M. Ivask, A. Kuu, S. Kutti, S. V. Litvin, L. Nei, Presence of fluoroquinolones and sulfonamides in urban sewage sludge and their degradation as a result of composting, Int. J. Environ. Sci. Technol. 7 (2010) 307–312. doi:10.1007/BF03326140.

[20] S.K. Khetan, T.J. Collins, Human pharmaceuticals in the aquatic environment: A challenge to green chemisty, Chem. Rev. 107 (2007) 2319–2364. doi:10.1021/cr020441w.

[21] A.M. Deegan, B. Shaik, K. Nolan, K. Urell, M. Oelgemöller, J. Tobin, A. Morrissey, Treatment options for wastewater effluents from pharmaceutical companies, Int. J. Environ. Sci. Technol. 8 (2011) 649–666. doi:10.1007/BF03326250.

[22] A.J. Ebele, M. Abou-Elwafa Abdallah, S. Harrad, Pharmaceuticals and personal care products (PPCPs) in the freshwater aquatic environment, Emerg. Contam. 3 (2017) 1–16. doi:10.1016/j.emcon.2016.12.004.

[23] B.D. Blair, J.P. Crago, C.J. Hedman, R.D. Klaper, Chemosphere Pharmaceuticals and personal care products found in the Great Lakes above concentrations of environmental concern, Chemosphere. 93 (2013) 2116–2123. doi:10.1016/j.chemosphere.2013.07.057.

[24] C.U. Meteyer, B.A. Rideout, M. Gilbert, H.L. Shivaprasad, L. Oaks, Pathology and proposed pathology of diclofenac poisoning in free living and experimentally exposed oriental white backed vultres (Gypsa bengalensis), P, J. Wildl. Dis. 41 (2005) 707–716.

[25] R. Triebskorn, H. Casper, V. Scheil, J. Schwaiger, Ultrastructural effects of pharmaceuticals (carbamazepine, clofibric acid, metoprolol, diclofenac) in rainbow trout (Oncorhynchus mykiss) and common carp (Cyprinus carpio), Anal. Bioanal. Chem. 387 (2007) 1405–1416. doi:10.1007/s00216-006-1033-x.

[26] J. Schwaiger, H. Ferling, U. Mallow, H. Wintermayr, R.D. Negele, Toxic effects of the non-steroidal anti-inflammatory drug diclofenac. Part I: Histopathological alterations and bioaccumulation in rainbow trout, Aquat. Toxicol. 68 (2004) 141–150. doi:10.1016/j.aquatox.2004.03.014.

[27] A.A.C. and Z.M. Dana Manuela Sirbu, Daniela Curseu, Monica Popa, Environmental Risks of Pharmaceuticals and Personal Care Products in Water, in: Tenth Int. Water Technol. Conf., 2006: pp. 1151–1162.

[28] E. Archer, G.M. Wolfaardt, J.H. van Wyk, Pharmaceutical and personal care products (PPCPs) as endocrine disrupting contaminants (EDCs) in South African surface waters, Water SA. 43 (2017) 684–706. doi:10.4314/wsa.v43i4.16.

[29] O.A.H. Jones, N. Voulvoulis, J.N. Lester, Potential ecological and human health risks associated with the presence of pharmaceutically active compounds in the aquatic environment, Crit. Rev. Toxicol. 34 (2004) 335–350. doi:10.1080/10408440490464697.

[30] A.K. Karen, J.B. Paul, H.M. Kenneth, e P.P. Vinc, E.E. Robert, M.L. James, W.F. Robert, Disrupting Queer Incluslon, Pnas. 104 (2007) 8897–8901. doi:10.1073/pnas.0609568104.

[31] D.J. Caldwell, F. Mastrocco, T.H. Hutchinson, R. Länge, D. Heijerick, C. Janssen, P.D. Anderson, J.P. Sumpter, Derivation of an aquatic predicted no-effect concentration for the synthetic hormone, 17α-ethinyl estradiol, Environ. Sci. Technol. 42 (2008) 7046–7054. doi:10.1021/es800633q.

[32] M.F. Rahman, E.K. Yanful, S.Y. Jasim, Endocrine disrupting compounds (EDCs) and pharmaceuticals and personal care products (PPCPs) in the aquatic environment: Implications for the drinking water industry and global environmental health, J. Water Health. 7 (2009) 224–243. doi:10.2166/wh.2009.021.

[33] B. Lellis, C.Z. Fávaro-polonio, J.A. Pamphile, J.C. Polonio, Effects of textile dyes on health and the environment and bioremediation potential of living organisms, Biotecnol. Res. Innov. 3 (2019) 275–290. doi:10.1016/j.biori.2019.09.001.

[34] R. Paper, Decolorization of mixture of dyes : A critical review, Glob. J. Environ. Sci. Manag. Glob. J. Environ. Sci. Manag. 1 (2015) 71–94. doi:10.7508/gjesm.2015.01.007.

[35] A.M. Deegan, B. Shaik, K. Nolan, K. Urell, J. Tobin, A. Morrissey, Treatment options for wastewater effluents from pharmaceutical companies, 8 (2011) 649–666.

[36] L. Cheng, Q. Xiang, Y. Liao, H. Zhang, CdS-Based photocatalysts, Royal Society of Chemistry, 2018. doi:10.1039/c7ee03640j.

[37] H.L. Lee, A.M. Issam, M. Belmahi, M.B. Assouar, H. Rinnert, M. Alnot, Synthesis and characterizations of bare cds nanocrystals using chemical

precipitation method for photoluminescence application, J. Nanomater. 2009 (2009). doi:10.1155/2009/914501.

[38] S. Kumar, S. Karthikeyan, A.F. Lee, g-C_3N_4-based nanomaterials for visible light-driven photocatalysis, Catalysts. 8 (2018). doi:10.3390/catal8020074.

[39] S. Cao, J. Low, J. Yu, M. Jaroniec, Polymeric Photocatalysts Based on Graphitic Carbon Nitride, Adv. Mater. 27 (2015) 2150–2176. doi:10.1002/adma.201500033.

[40] Q.Y. Liu, Y.L. Qi, Y.F. Zheng, X.C. Song, Synthesis and enhanced photocatalytic activity of g-C_3N_4 hybridized CdS nanoparticles, Bull. Mater. Sci. 40 (2017) 1329–1333. doi:10.1007/s12034-017-1513-y.

[41] R.C. Pawar, V. Khare, C.S. Lee, Hybrid photocatalysts using graphitic carbon nitride/cadmium sulfide/reduced graphene oxide (g-C_3N_4/CdS/RGO) for superior photodegradation of organic pollutants under UV and visible light, Dalt. Trans. 43 (2014) 12514–12527. doi:10.1039/c4dt01278j.

[42] S.W. Cao, Y.P. Yuan, J. Fang, M.M. Shahjamali, F.Y.C. Boey, J. Barber, S.C. Joachim Loo, C. Xue, In-situ growth of CdS quantum dots on g-C_3N_4 nanosheets for highly efficient photocatalytic hydrogen generation under visible light irradiation, Int. J. Hydrogen Energy. 38 (2013) 1258–1266. doi:10.1016/j.ijhydene.2012.10.116.

[43] S. Rasalingam, R. Peng, R.T. Koodali, Removal of hazardous pollutants from wastewaters: Applications of TiO_2-SiO_2 mixed oxide materials, J. Nanomater. 2014 (2014). doi:10.1155/2014/617405.

[44] M.K. Hasan, A. Shahriar, K.U. Jim, Water pollution in Bangladesh and its impact on public health, Heliyon. 5 (2019) e02145. doi:10.1016/j.heliyon.2019.e02145.

[45] S. Rasalingam, R. Peng, R.T. Koodali, 617405.Pdf, 2014 (2014).

[46] U. Tahir, A. Yasmin, U.H. Khan, Phytoremediation: Potential flora for synthetic dyestuff metabolism, J. King Saud Univ. - Sci. 28 (2016) 119–130. doi:10.1016/j.jksus.2015.05.009.

[47] G. Dong, Y. Zhang, Q. Pan, J. Qiu, A fantastic graphitic carbon nitride (g-

C3N4) material: Electronic structure, photocatalytic and photoelectronic properties, J. Photochem. Photobiol. C Photochem. Rev. 20 (2014) 33–50. doi:10.1016/j.jphotochemrev.2014.04.002.

[48] D.A. Yaseen, M. Scholz, Textile dye wastewater characteristics and constituents of synthetic effluents: a critical review, Springer Berlin Heidelberg, 2019. doi:10.1007/s13762-018-2130-z.

[49] T. Robinson, G. McMullan, R. Marchant, P. Nigam, Remediation of dyes in textile effluent: A critical review on current treatment technologies with a proposed alternative, Bioresour. Technol. 77 (2001) 247–255. doi:10.1016/S0960-8524(00)00080-8.

[50] G.S. Gupta, G. Prasad, V.N. Singh, Removal of chrome dye from aqueous solutions by mixed adsorbents: Fly ash and coal, Water Res. 24 (1990) 45–50. doi:10.1016/0043-1354(90)90063-C.

[51] N. Muhd Julkapli, S. Bagheri, S. Bee Abd Hamid, Recent advances in heterogeneous photocatalytic decolorization of synthetic dyes, Sci. World J. 2014 (2014) 25. doi:10.1155/2014/692307.

[52] Y. Fu, T. Viraraghavan, Fungal decolorization of dye wastewaters: A review, Bioresour. Technol. 79 (2001) 251–262. doi:10.1016/S0960-8524(01)00028-1.

[53] V.K. Gupta, S. Khamparia, I. Tyagi, D. Jaspal, A. Malviya, Decolorization of mixture of dyes: A critical review, Glob. J. Environ. Sci. Manag. Glob. J. Environ. Sci. Manag. 1 (2015) 71–94. doi:10.7508/gjesm.2015.01.007.

[54] Z. Aksu, Application of biosorption for the removal of organic pollutants: A review, Process Biochem. 40 (2005) 997–1026. doi:10.1016/j.procbio.2004.04.008.

[55] S. Sumathi, B.S. Manju, Uptake of reactive textile dyes by Aspergillus foetidus, Enzyme Microb. Technol. 27 (2000) 347–355. doi:10.1016/S0141-0229(00)00234-9.

[56] Z. Aksu, S. Tezer, Equilibrium and kinetic modelling of biosorption of Remazol black B by Rhizopus arrhizus in a batch system: Effect of temperature, Process Biochem. 36 (2000) 431–439. doi:10.1016/S0032-9592(00)00233-8.

[57] T. O'Mahony, E. Guibal, J.M. Tobin, Reactive dye biosorption by Rhizopus arrhizus biomass, Enzyme Microb. Technol. 31 (2002) 456–463. doi:10.1016/S0141-0229(02)00110-2.

[58] B. Aruna, R.S. L, E. Shiva, A. Srinu, P. Roja, D. Vijayalakshmi, D.V.R. Prasad, Research Article Biodecolorization of Anthraquinone Textile (Acid Blue 25) Dye By Klebsiella Sp, 6 (2015) 3216–3222.

[59] M. Auta, B.H. Hameed, Preparation of waste tea activated carbon using potassium acetate as an activating agent for adsorption of Acid Blue 25 dye, Chem. Eng. J. 171 (2011) 502–509. doi:10.1016/j.cej.2011.04.017.

[60] C.A. Hsu, T.N. Wen, Y.C. Su, Z.B. Jiang, C.W. Chen, L.F. Shyur, Biological degradation of anthroquinone and azo dyes by a novel laccase from Lentinus sp., Environ. Sci. Technol. 46 (2012) 5109–5117. doi:10.1021/es2047014.

[61] H. hong Li, Y. tao Wang, Y. Wang, H. xia Wang, K. kai Sun, Z. mei Lu, Bacterial degradation of anthraquinone dyes, J. Zhejiang Univ. Sci. B. 20 (2019) 528–540. doi:10.1631/jzus.B1900165.

[62] M.E. Malefane, U. Feleni, A.T. Kuvarega, Tetraphenylporphyrin/WO_3/exfoliated graphite nanocomposite for photocatalytic degradation of an acid dye under visible light irradiation, New J. Chem. 10 (2019) 1–6. doi:10.1039/c9nj02747e.

[63] S. Benkhaya, S. El Harfi, A. El Harfi, Classifications , properties and applications of textile dyes : A review, Appl. J. Environ. Sci. 3 (2018) 311–320.

[64] D. Chakrabortty, S. Sen Gupta, Photo-catalytic decolourisation of toxic dye with N-doped titania: A case study with Acid Blue 25, J. Environ. Sci. (China). 25 (2013) 1034–1043. doi:10.1016/S1001-0742(12)60108-9.

[65] T. Deblonde, C. Cossu-Leguille, P. Hartemann, Emerging pollutants in wastewater: A review of the literature, Int. J. Hyg. Environ. Health. 214 (2011) 442–448. doi:10.1016/j.ijheh.2011.08.002.

[66] M. Clara, G. Windhofer, W. Hartl, K. Braun, M. Simon, O. Gans, C. Scheffknecht, A. Chovanec, Occurrence of phthalates in surface runoff, untreated and treated wastewater and fate during wastewater treatment, Chemosphere. 78 (2010) 1078–1084.

doi:10.1016/j.chemosphere.2009.12.052.

[67] M. la Farré, S. Pérez, L. Kantiani, D. Barceló, Fate and toxicity of emerging pollutants, their metabolites and transformation products in the aquatic environment, TrAC - Trends Anal. Chem. 27 (2008) 991–1007. doi:10.1016/j.trac.2008.09.010.

[68] A. Jennifer, M.A. Abdallah, S. Harrad, Pharmaceuticals and personal care products (PPCPs) in the freshwater aquatic environment, Emerg. Contam. 3 (2017) 1–16. doi:10.1016/j.emcon.2016.12.004.

[69] S.R. Hughes, P. Kay, L.E. Brown, Global synthesis and critical evaluation of pharmaceutical data sets collected from river systems, Environ. Sci. Technol. 47 (2013) 661–677. doi:10.1021/es3030148.

[70] D. Ashton, M. Hilton, K. V. Thomas, Investigating the environmental transport of human pharmaceuticals to streams in the United Kingdom, Sci. Total Environ. 333 (2004) 167–184. doi:10.1016/j.scitotenv.2004.04.062.

[71] S. Wiandt, H.J. Poremski, Selection and prioritisation procedure of hazardous substances for the marine environment within Ospar/Dynamic, Ecotoxicology. 11 (2002) 393–399. doi:10.1023/A:1020569608441.

[72] L. Lonappan, S.K. Brar, R.K. Das, M. Verma, R.Y. Surampalli, Diclofenac and its transformation products: Environmental occurrence and toxicity - A review, Environ. Int. 96 (2016) 127–138. doi:10.1016/j.envint.2016.09.014.

[73] Y. Zhang, S.U. Geißen, C. Gal, Carbamazepine and diclofenac: Removal in wastewater treatment plants and occurrence in water bodies, Chemosphere. 73 (2008) 1151–1161. doi:10.1016/j.chemosphere.2008.07.086.

[74] V. Acuña, A. Ginebreda, J.R. Mor, M. Petrovic, S. Sabater, J. Sumpter, D. Barceló, Balancing the health benefits and environmental risks of pharmaceuticals: Diclofenac as an example, Environ. Int. 85 (2015) 327–333. doi:10.1016/j.envint.2015.09.023.

[75] A.C. Johnson, E. Dumont, R.J. Williams, R. Oldenkamp, I. Cisowska, J.P. Sumpter, Do concentrations of ethinylestradiol, estradiol, and diclofenac in European rivers exceed proposed EU environmental quality standards?,

Environ. Sci. Technol. 47 (2013) 12297–12304. doi:10.1021/es4030035.

[76] A.Y. Shan, T.I.M. Ghazi, S.A. Rashid, Immobilisation of titanium dioxide onto supporting materials in heterogeneous photocatalysis: A review, Appl. Catal. A Gen. 389 (2010) 1–8. doi:10.1016/j.apcata.2010.08.053.

[77] Y. Mehmood, Index Academic Sciences Original Article development and validation of UV-Vis spectrophotometric methods for the estimation of diclofena sodium injections., Int. J. Pharm. Pract. Pharm. Sci. 2 (2015) 1–6.

[78] D. Chen, A.K. Ray, Photodegradation kinetics of 4-nitrophenol in TiO2 suspension, Water Res. 32 (1998) 3223–3234. doi:10.1016/S0043-1354(98)00118-3.

[79] C. Martínez, M. Canle L., M.I. Fernández, J.A. Santaballa, J. Faria, Aqueous degradation of diclofenac by heterogeneous photocatalysis using nanostructured materials, Appl. Catal. B Environ. 107 (2011) 110–118. doi:10.1016/j.apcatb.2011.07.003.

[80] M. Letzel, G. Metzner, T. Letzel, Exposure assessment of the pharmaceutical diclofenac based on long-term measurements of the aquatic input, Environ. Int. 35 (2009) 363–368. doi:10.1016/j.envint.2008.09.002.

[81] C. Hao, R. Clement, P. Yang, Liquid chromatography-tandem mass spectrometry of bioactive pharmaceutical compounds in the aquatic environment-a decade's activities, Anal. Bioanal. Chem. 387 (2007) 1247–1257. doi:10.1007/s00216-006-0956-6.

[82] A.J. Sosiak, T. Hebben, A preliminary survey of pharmaceuticals and endocrine disrupting compounds in treated municipal wastewaters and receiving rivers of Alberta /, 2005. doi:10.5962/bhl.title.113982.

[83] M.J. Benotti, R.A. Trenholm, B.J. Vanderford, J.C. Holady, B.D. Stanford, S.A. Snyder, Pharmaceuticals and endocrine disrupting compounds in U.S. drinking water, Environ. Sci. Technol. 43 (2009) 597–603. doi:10.1021/es801845a.

[84] T. Heberer, Tracking persistent pharmaceutical residues from municipal sewage to drinking water, J. Hydrol. 266 (2002) 175–189. doi:10.1016/S0022-1694(02)00165-8.

[85] F.O. Agunbiade, B. Moodley, Occurrence and distribution pattern of acidic pharmaceuticals in surface water, wastewater, and sediment of the Msunduzi River, Kwazulu-Natal, South Africa, Environ. Toxicol. Chem. 35 (2016) 36–46. doi:10.1002/etc.3144.

[86] M.T. Amin, A.A. Alazba, U. Manzoor, A Review of Removal of Pollutants from Water / Wastewater Using Different Types of Nanomaterials, 2014 (2014).

[87] M.R. Servos, D.T. Bennie, B.K. Burnison, A. Jurkovic, R. McInnis, T. Neheli, A. Schnell, P. Seto, S.A. Smyth, T.A. Ternes, Distribution of estrogens, 17β-estradiol and estrone, in Canadian municipal wastewater treatment plants, Sci. Total Environ. 336 (2005) 155–170. doi:10.1016/j.scitotenv.2004.05.025.

[88] T. Urase, T. Kikuta, Separate estimation of adsorption and degradation of pharmaceutical substances and estrogens in the activated sludge process, Water Res. 39 (2005) 1289–1300. doi:10.1016/j.watres.2005.01.015.

[89] N. Vieno, T. Tuhkanen, L. Kronberg, Removal of pharmaceuticals in drinking water treatment: Effect of chemical coagulation, Environ. Technol. 27 (2006) 183–192. doi:10.1080/09593332708618632.

[90] P. Westerhoff, Y. Yoon, S. Snyder, E. Wert, Fate of endocrine-disruptor, pharmaceutical, and personal care product chemicals during simulated drinking water treatment processes, Environ. Sci. Technol. 39 (2005) 6649–6663. doi:10.1021/es0484799.

[91] M. Petrovic, A. Diaz, F. Ventura, D. Barceló, Occurrence and removal of estrogenic short-chain ethoxy nonylphenolic compounds and their halogenated derivatives during drinking water production, Environ. Sci. Technol. 37 (2003) 4442–4448. doi:10.1021/es034139w.

[92] G. Becher, Drinking Water Chlorination and Health, Acta Hydrochim. Hydrobiol. 27 (1999) 100–102. doi:10.1002/(sici)1521-401x(199902)27:2<100::aid-aheh100>3.3.co;2-1.

[93] N. Bolong, A.F. Ismail, M.R. Salim, T. Matsuura, A review of the effects of emerging contaminants in wastewater and options for their removal, Desalination. 239 (2009) 229–246. doi:10.1016/j.desal.2008.03.020.

[94] Y. Yoon, P. Westerhoff, S.A. Snyder, E.C. Wert, Nanofiltration and ultrafiltration of endocrine disrupting compounds, pharmaceuticals and personal care products, J. Memb. Sci. 270 (2006) 88–100. doi:10.1016/j.memsci.2005.06.045.

[95] L. Braeken, B. Bettens, K. Boussu, P. Van der Meeren, J. Cocquyt, J. Vermant, B. Van der Bruggen, Transport mechanisms of dissolved organic compounds in aqueous solution during nanofiltration, J. Memb. Sci. 279 (2006) 311–319. doi:10.1016/j.memsci.2005.12.024.

[96] J. Lu, T. Zhang, J. Ma, Z. Chen, Evaluation of disinfection by-products formation during chlorination and chloramination of dissolved natural organic matter fractions isolated from a filtered river water, J. Hazard. Mater. 162 (2009) 140–145. doi:10.1016/j.jhazmat.2008.05.058.

[97] M.N. Chong, B. Jin, C.W.K. Chow, C. Saint, Recent developments in photocatalytic water treatment technology: a review., Water Res. 44 (2010) 2997–3027. doi:10.1016/j.watres.2010.02.039.

[98] D.H. Bremner, R. Molina, F. Martínez, J.A. Melero, Y. Segura, Degradation of phenolic aqueous solutions by high frequency sono-Fenton systems (US-Fe_2O_3/SBA-15-H_2O_2), Appl. Catal. B Environ. 90 (2009) 380–388. doi:10.1016/j.apcatb.2009.03.028.

[99] G. Li, Z. Wang, M. Yu, Z. Quan, J. Lin, Fabrication and optical properties of core-shell structured spherical SiO_2@$GdVO_4$:Eu^{3+} phosphors via sol-gel process, J. Solid State Chem. 179 (2006) 2698–2706. doi:10.1016/j.jssc.2006.05.019.

[100] J. Zhang, G. Xiao, F.X. Xiao, B. Liu, Revisiting one-dimensional TiO_2 based hybrid heterostructures for heterogeneous photocatalysis: A critical review, Mater. Chem. Front. 1 (2017) 231–250. doi:10.1039/c6qm00141f.

[101] Y. Cui, In-situ synthesis of C_3N_4/CdS composites with enhanced photocatalytic properties, Cuihua Xuebao/Chinese J. Catal. 36 (2015) 372–379. doi:10.1016/S1872-2067(14)60237-0.

[102] V.S. Kosera, T.M. Cruz, E.S. Chaves, E.R.L. Tiburtius, Journal of

Photochemistry and Photobiology A : Chemistry Triclosan degradation by heterogeneous photocatalysis using ZnO immobilized in biopolymer as catalyst, "Journal Photochem. Photobiol. A Chem. 344 (2017) 184–191. doi:10.1016/j.jphotochem.2017.05.014.

[103] M.R. Hoffmann, S.T. Martin, W. Choi, D.W. Bahnemann, Environmental Applications of Semiconductor Photocatalysis, Chem. Rev. 95 (1995) 69–96. doi:10.1021/cr00033a004.

[104] J.-M. HERRMANN, Water Treatment By Heterogeneous Photocatalysis, in: 1999: pp. 171–194. doi:10.1142/9781848160613_0009.

[105] U.I. Gaya, A.H. Abdullah, Heterogeneous photocatalytic degradation of organic contaminants over titanium dioxide: A review of fundamentals, progress and problems, J. Photochem. Photobiol. C Photochem. Rev. 9 (2008) 1–12. doi:10.1016/j.jphotochemrev.2007.12.003.

[106] M. Ni, M.K.H. Leung, D.Y.C. Leung, K. Sumathy, A review and recent developments in photocatalytic water-splitting using TiO_2 for hydrogen production, Renew. Sustain. Energy Rev. 11 (2007) 401–425. doi:10.1016/j.rser.2005.01.009.

[107] M. Yasmina, K. Mourad, S.H. Mohammed, C. Khaoula, Treatment heterogeneous photocatalysis; Factors influencing the photocatalytic degradation by TiO_2, Energy Procedia. 50 (2014) 559–566. doi:10.1016/j.egypro.2014.06.068.

[108] L. Cheng, Q. Xiang, Y. Liao, Environmental Science, (2018) 4–7. doi:10.1039/c7ee03640j.

[109] M. Wongaree, S. Chiarakorn, S. Chuangchote, Photocatalytic Improvement under Visible Light in TiO_2 Nanoparticles by Carbon Nanotube Incorporation, 2015 (2015).

[110] R.S. Singh, V.K. Rangari, S. Sanagapalli, V. Jayaraman, S. Mahendra, V.P. Singh, Nano-structured CdTe, CdS and TiO_2 for thin film solar cell applications, Sol. Energy Mater. Sol. Cells. 82 (2004) 315–330. doi:10.1016/j.solmat.2004.02.006.

[111] S. Leong, A. Razmjou, K. Wang, K. Hapgood, X. Zhang, H. Wang, TiO_2 based photocatalytic membranes: A review, J. Memb. Sci. 472 (2014) 167–184. doi:10.1016/j.memsci.2014.08.016.

[112] Y. Yu, J.C. Yu, J.G. Yu, Y.C. Kwok, Y.K. Che, J.C. Zhao, L. Ding, W.K. Ge, P.K. Wong, Enhancement of photocatalytic activity of mesoporous TiO_2 by using carbon nanotubes, Appl. Catal. A Gen. 289 (2005) 186–196. doi:10.1016/j.apcata.2005.04.057.

[113] R. Abe, K. Sayama, H. Arakawa, Significant effect of iodide addition on water splitting into H_2 and O_2 over Pt-loaded TiO_2 photocatalyst: Suppression of backward reaction, Chem. Phys. Lett. 371 (2003) 360–364. doi:10.1016/S0009-2614(03)00252-5.

[114] S. Sakthivel, M. V. Shankar, M. Palanichamy, B. Arabindoo, D.W. Bahnemann, V. Murugesan, Enhancement of photocatalytic activity by metal deposition: Characterisation and photonic efficiency of Pt, Au and Pd deposited on TiO_2 catalyst, Water Res. 38 (2004) 3001–3008. doi:10.1016/j.watres.2004.04.046.

[115] E. Szabó-Bárdos, H. Czili, A. Horváth, Photocatalytic oxidation of oxalic acid enhanced by silver deposition on a TiO_2 surface, J. Photochem. Photobiol. A Chem. 154 (2003) 195–201. doi:10.1016/S1010-6030(02)00330-1.

[116] N.L. Wu, M.S. Lee, Enhanced TiO_2 photocatalysis by Cu in hydrogen production from aqueous methanol solution, Int. J. Hydrogen Energy. 29 (2004) 1601–1605. doi:10.1016/j.ijhydene.2004.02.013.

[117] F. Haque, T. Daeneke, K. Kalantar-zadeh, J.Z. Ou, Two-Dimensional Transition Metal Oxide and Chalcogenide-Based Photocatalysts, Nano-Micro Lett. 10 (2018) 1–27. doi:10.1007/s40820-017-0176-y.

[118] A.H. Reshak, S. Auluck, Electronic and optical properties of the 1T phases of TiS_2, $TiSe_2$, and $TiTe_2$, Phys. Rev. B - Condens. Matter Mater. Phys. 68 (2003) 1–7. doi:10.1103/PhysRevB.68.245113.

[119] J.A. Wilson, A.D. Yoffe, The transition metal dichalcogenides discussion and interpretation of the observed optical, electrical and structural properties, Adv. Phys. 18 (1969) 193–335. doi:10.1080/00018736900101307.

[120] L. Nie, Q. Zhang, Recent progress in crystalline metal chalcogenides as efficient photocatalysts for organic pollutant degradation, Inorg. Chem. Front. 4 (2017) 1953–1962. doi:10.1039/c7qi00651a.

[121] F. Li, X. Liu, Q. Zhang, T. Kong, H. Jin, Fabrication and photocatalytic property of CuO nanosheets via a facile solution route, Cryst. Res. Technol. 47 (2012) 1140–1147. doi:10.1002/crat.201200143.

[122] B. Peng, P.K. Ang, K.P. Loh, Two-dimensional dichalcogenides for light-harvesting applications, Nano Today. 10 (2015) 128–137. doi:10.1016/j.nantod.2015.01.007.

[123] D. Ke, S. Liu, K. Dai, J. Zhou, L. Zhang, T. Peng, CdS/regenerated cellulose nanocomposite films for highly efficient photocatalytic H_2 production under visible light irradiation, J. Phys. Chem. C. 113 (2009) 16021–16026. doi:10.1021/jp903378q.

[124] S. Xiong, B. Xi, Y. Qian, CdS hierarchical nanostructures with tunable morphologies: Preparation and photocatalytic properties, J. Phys. Chem. C. 114 (2010) 14029–14035. doi:10.1021/jp1049588.

[125] W.T. Yao, S.H. Yu, S.J. Liu, J.P. Chen, X.M. Liu, F.Q. Li, Architectural control syntheses of CdS and CdSe nanoflowers, branched nanowires, and nanotrees via a solvothermal approach in a mixed solution and their photocatalytic property, J. Phys. Chem. B. 110 (2006) 11704–11710. doi:10.1021/jp060164n.

[126] Q. Shen, J. Xue, A. Mi, H. Jia, X. Liu, B. Xu, The study on properties of CdS photocatalyst with different ratios of zinc-blende and wurtzite structure, RSC Adv. 3 (2013) 20930–20935. doi:10.1039/c3ra42179a.

[127] M. Liu, B. Wang, Y. Zheng, F. Xue, Y. Chen, L. Guo, Transformation of zincblende nanoparticles into wurtzite microrods by a dissolution-regrowth process: An intergrowth homojunction with enhanced photocatalytic activity, Catal. Sci. Technol. 6 (2016) 3371–3377. doi:10.1039/c6cy00298f.

[128] K. Wu, H. Zhu, T. Lian, Ultrafast Exciton Dynamics and Light-Driven H_2 Evolution in Colloidal Semiconductor Nanorods and Pt-Tipped Nanorods, Acc. Chem. Res. 48 (2015) 851–859. doi:10.1021/ar500398g.

[129] J. Yu, Y. Yu, P. Zhou, W. Xiao, B. Cheng, Morphology-dependent photocatalytic H2-production activity of CdS, Appl. Catal. B Environ. 156–157 (2014) 184–191. doi:10.1016/j.apcatb.2014.03.013.

[130] B. Weng, S. Liu, N. Zhang, Z.R. Tang, Y.J. Xu, A simple yet efficient visible-light-driven CdS nanowires-carbon nanotube 1D-1D nanocomposite photocatalyst, J. Catal. 309 (2014) 146–155. doi:10.1016/j.jcat.2013.09.013.

[131] F. Caruso, X. Shi, R.A. Caruso, A. Susha, Hollow titania spheres from layered precursor deposition on sacrificial colloidal core particles, Adv. Mater. 13 (2001) 740–744. doi:10.1002/1521-4095(200105)13:10<740::AID-ADMA740>3.0.CO;2-6.

[132] C. Li, L. Han, R. Liu, H. Li, S. Zhang, G. Zhang, Controlled synthesis of CdS micro/nano leaves with (0001) facets exposed: Enhanced photocatalytic activity toward hydrogen evolution, J. Mater. Chem. 22 (2012) 23815–23820. doi:10.1039/c2jm35415b.

[133] T. Tsuzuki, P.G. McCormick, Synthesis of CdS quantum dots by mechanochemical reaction, Appl. Phys. A Mater. Sci. Process. 65 (1997) 607–609. doi:10.1007/s003390050629.

[134] A. Dumbrava, G. Prodan, D. Berger, M. Bica, Properties of PEG-capped CdS nanopowders synthesized under very mild conditions, Powder Technol. 270 (2015) 197–204. doi:10.1016/j.powtec.2014.10.012.

[135] A. Samadi-maybodi, F. Abbasi, R. Akhoondi, Aqueous synthesis and characterization of CdS quantum dots capped with some amino acids and investigations of their photocatalytic activities, Colloids Surfaces A Physicochem. Eng. Asp. 447 (2014) 111–119. doi:10.1016/j.colsurfa.2014.01.036.

[136] P. Chandran, P. Kumari, S. Sudheer Khan, Photocatalytic activation of CdS NPs under visible light for environmental cleanup and disinfection, Sol. Energy. 105 (2014) 542–547. doi:10.1016/j.solener.2014.04.028.

[137] M. Darwish, A. Mohammadi, N. Assi, Microwave-assisted polyol synthesis and characterization of pvp-capped cds nanoparticles for the photocatalytic

degradation of tartrazine, Mater. Res. Bull. 74 (2016) 387–396. doi:10.1016/j.materresbull.2015.11.002.

[138] R.A. Devi, M. Latha, S. Velumani, G. Oza, P. Reyes-Figueroa, M. Rohini, I.G. Becerril-Juarez, J.-H. Lee, J. Yi, Synthesis and Characterization of Cadmium Sulfide Nanoparticles by Chemical Precipitation Method, J. Nanosci. Nanotechnol. 15 (2015) 8434–8439. doi:10.1166/jnn.2015.11472.

[139] G.C. De, A.M. Roy, S.S. Bhattacharya, Photocatalytic production of hydrogen and concomitant cleavage of industrial waste hydrogen sulphide, Int. J. Hydrogen Energy. 20 (1995) 127–131. doi:10.1016/0360-3199(94)P3692-V.

[140] W. Li, D. Li, Z. Chen, H. Huang, M. Sun, Y. He, X. Fu, High-efficient degradation of dyes by ZnxCd1-xS solid solutions under visible light irradiation, J. Phys. Chem. C. 112 (2008) 14943–14947. doi:10.1021/jp8049075.

[141] F. Yang, N.N. Yan, S. Huang, Q. Sun, L.Z. Zhang, Y. Yu, Zn-doped CdS nanoarchitectures prepared by hydrothermal synthesis: Mechanism for enhanced photocatalytic activity and stability under visible light, J. Phys. Chem. C. 116 (2012) 9078–9084. doi:10.1021/jp300939q.

[142] T.K. Jana, A. Pal, K. Chatterjee, Self assembled flower like CdS-ZnO nanocomposite and its photo catalytic activity, J. Alloys Compd. 583 (2014) 510–515. doi:10.1016/j.jallcom.2013.08.184.

[143] D. Wu, F. Wang, Y. Tan, C. Li, Facile synthesis of NiS/CdS nanocomposites for photocatalytic degradation of quinoline under visible-light irradiation, RSC Adv. 6 (2016) 73522–73526. doi:10.1039/c6ra13439d.

[144] P. Nyamukamba, M.J. Moloto, H. Mungondori, Visible light-active CdS/TiO2 hybrid nanoparticles immobilized on polyacrylonitrile membranes for the photodegradation of dyes in water, J. Nanotechnol. 2019 (2019). doi:10.1155/2019/5135618.

[145] S. Ma, J. Xie, J. Wen, K. He, X. Li, W. Liu, X. Zhang, Constructing 2D layered hybrid CdS nanosheets/MoS_2 heterojunctions for enhanced visible-light photocatalytic H_2 generation, Appl. Surf. Sci. 391 (2017) 580–591. doi:10.1016/j.apsusc.2016.07.067.

[146] Q. Cai, Z. Hu, Q. Zhang, B. Li, Z. Shen, Fullerene (C_{60})/CdS nanocomposite with enhanced photocatalytic activity and stability, Appl. Surf. Sci. 403 (2017) 151–158. doi:10.1016/j.apsusc.2017.01.135.

[147] K.A. Adegoke, M. Iqbal, H. Louis, O.S. Bello, Synthesis, characterization and application of CdS/ZnO nanorod heterostructure for the photodegradation of Rhodamine B dye, Mater. Sci. Energy Technol. 2 (2019) 329–336. doi:10.1016/j.mset.2019.02.008.

[148] S. Cao, J. Yu, G-C_3N_4-based photocatalysts for hydrogen generation, J. Phys. Chem. Lett. 5 (2014) 2101–2107. doi:10.1021/jz500546b.

[149] J. Wen, J. Xie, X. Chen, X. Li, A review on g-C_3N_4 -based photocatalysts, Appl. Surf. Sci. 391 (2017) 72–123. doi:10.1016/j.apsusc.2016.07.030.

[150] E.A. Weiss, Designing the surfaces of semiconductor quantum dots for colloidal photocatalysis, ACS Energy Lett. 2 (2017) 1005–1013. doi:10.1021/acsenergylett.7b00061.

[151] K.R. Reddy, C.V. Reddy, M.N. Nadagouda, N.P. Shetti, S. Jaesool, T.M. Aminabhavi, Polymeric graphitic carbon nitride (g-C_3N_4)-based semiconducting nanostructured materials: Synthesis methods, properties and photocatalytic applications, J. Environ. Manage. 238 (2019) 25–40. doi:10.1016/j.jenvman.2019.02.075.

[152] S. Wang, C. Li, T. Wang, P. Zhang, A. Li, J. Gong, Controllable synthesis of nanotube-type graphitic C_3N_4 and their visible-light photocatalytic and fluorescent properties, J. Mater. Chem. A. 2 (2014) 2885–2890. doi:10.1039/c3ta14576j.

[153] B. Weng, S. Liu, Z. Tang, Y. Xu, RSC Advances One-dimensional nanostructure based materials for versatile photocatalytic applications, (2014) 12685–12700. doi:10.1039/c3ra47910b.

[154] J. Zhang, Y. Chen, X. Wang, Two-dimensional covalent carbon nitride nanosheets: Synthesis, functionalization, and applications, Energy Environ. Sci. 8 (2015) 3092–3108. doi:10.1039/c5ee01895a.

[155] X. Bai, L. Wang, R. Zong, Y. Zhu, Photocatalytic activity enhanced via g-C_3N_4

nanoplates to nanorods, J. Phys. Chem. C. 117 (2013) 9952–9961. doi:10.1021/jp402062d.

[156] Q. Han, B. Wang, J. Gao, Z. Cheng, Y. Zhao, Z. Zhang, L. Qu, Atomically Thin Mesoporous Nanomesh of Graphitic C_3N_4 for High-Efficiency Photocatalytic Hydrogen Evolution, ACS Nano. 10 (2016) 2745–2751. doi:10.1021/acsnano.5b07831.

[157] X. Zhang, X. Xie, H. Wang, J. Zhang, B. Pan, Y. Xie, Enhanced photoresponsive ultrathin graphitic-phase C_3N_4 nanosheets for bioimaging, J. Am. Chem. Soc. 135 (2013) 18–21. doi:10.1021/ja308249k.

[158] J. Senker, K. Schwinghammer, B. V. Lotsch, C. Ziegler, M.B. Mesch, V. Duppel, Crystalline Carbon Nitride Nanosheets for Improved Visible-Light Hydrogen Evolution, J. Am. Chem. Soc. 136 (2014) 1730–1733. doi:10.1021/ja411321s.

[159] B. Luo, G. Liu, L. Wang, Recent advances in 2D materials for photocatalysis, Nanoscale. 8 (2016) 6904–6920. doi:10.1039/c6nr00546b.

[160] P. Niu, L. Zhang, G. Liu, H.M. Cheng, Graphene-like carbon nitride nanosheets for improved photocatalytic activities, Adv. Funct. Mater. 22 (2012) 4763–4770. doi:10.1002/adfm.201200922.

[161] Q. Liu, T. Chen, Y. Guo, Z. Zhang, X. Fang, Ultrathin g-C_3N_4 nanosheets coupled with carbon nanodots as 2D/0D composites for efficient photocatalytic H2 evolution, Appl. Catal. B Environ. 193 (2016) 248–258. doi:10.1016/j.apcatb.2016.04.034.

[162] Y. Xu, S.P. Gao, Band gap of C_3N_4 in the GW approximation, Int. J. Hydrogen Energy. 37 (2012) 11072–11080. doi:10.1016/j.ijhydene.2012.04.138.

[163] K. Maeda, X. Wang, Y. Nishihara, D. Lu, M. Antonietti, K. Domen, Photocatalytic activities of graphitic carbon nitride powder for water reduction and oxidation under visible light, J. Phys. Chem. C. 113 (2009) 4940–4947. doi:10.1021/jp809119m.

[164] A.H. Reshak, AA- and ABA-stacked carbon nitride (C_3N_4): Novel photocatalytic water splitting solar-to-hydrogen energy conversion, Phys. Chem. Chem.

Phys. 20 (2018) 22972–22979. doi:10.1039/c8cp02898b.

[165] A.Y. Liu, M.L. Cohen, Prediction of new low compressibility solids, Science (80-.). 245 (1989) 841–842. doi:10.1126/science.245.4920.841.

[166] B. Jürgens, E. Irran, J. Senker, P. Kroll, H. Müller, W. Schnick, Melem (2,5,8-triamino-tri-s-triazine), an important intermediate during condensation of melamine rings to graphitic carbon nitride: Synthesis, structure determination by x-ray powder diffractometry, solid-state NMR, and theoretical studies, J. Am. Chem. Soc. 125 (2003) 10288–10300. doi:10.1021/ja0357689.

[167] J. Sehnert, K. Baerwinkel, J. Senker, Ab initio calculation of solid-state NMR spectra for different triazine and heptazine based structure proposals of g-C3N4, J. Phys. Chem. B. 111 (2007) 10671–10680. doi:10.1021/jp072001k.

[168] A. Thomas, A. Fischer, F. Goettmann, M. Antonietti, J.O. Müller, R. Schlögl, J.M. Carlsson, Graphitic carbon nitride materials: Variation of structure and morphology and their use as metal-free catalysts, J. Mater. Chem. 18 (2008) 4893–4908. doi:10.1039/b800274f.

[169] Y. Wang, J. Hong, W. Zhang, R. Xu, Carbon nitride nanosheets for photocatalytic hydrogen evolution: Remarkably enhanced activity by dye sensitization, Catal. Sci. Technol. 3 (2013) 1703–1711. doi:10.1039/c3cy20836b.

[170] H. Luo, Z. Zeng, G. Zeng, C. Zhang, R. Xiao, C. Zhou, H. Wang, Y. Zhou, S. Tian, Recent progress on metal-organic frameworks based- and derived-photocatalysts for water splitting, Chem. Eng. J. (2019) 123196. doi:10.1016/j.cej.2019.123196.

[171] D. Zheng, C. Pang, Y. Liu, X. Wang, Shell-engineering of hollow g-C_3N_4 nanospheres via copolymerization for photocatalytic hydrogen evolution , Chem. Commun. 51 (2015) 9706–9709. doi:10.1039/c5cc03143e.

[172] S.W. Bian, Z. Ma, W.G. Song, Preparation and characterization of carbon nitride nanotubes and their applications as catalyst supporter, J. Phys. Chem. C. 113 (2009) 8668–8672. doi:10.1021/jp810630k.

[173] L. Xu, J. Xia, L. Wang, H. Ji, J. Qian, H. Xu, K. Wang, H. Li, Graphitic carbon

nitride nanorods for photoelectrochemical sensing of trace copper(II) ions, Eur. J. Inorg. Chem. (2014) 3665–3673. doi:10.1002/ejic.201402051.

[174] S. Hu, R. Jin, G. Lu, D. Liu, J. Gui, The properties and photocatalytic performance comparison of Fe^{3+}-doped g-C_3N_4 and Fe_2O_3/g-C_3N_4 composite catalysts, RSC Adv. 4 (2014) 24863–24869. doi:10.1039/c4ra03290j.

[175] Y. Wang, Y. Wang, Y. Li, H. Shi, Y. Xu, H. Qin, X. Li, Y. Zuo, S. Kang, L. Cui, Simple synthesis of Zr-doped graphitic carbon nitride towards enhanced photocatalytic performance under simulated solar light irradiation, Catal. Commun. 72 (2015) 24–28. doi:10.1016/j.catcom.2015.08.022.

[176] P. Fageria, R. Nazir, S. Gangopadhyay, H.C. Barshilia, S. Pande, Graphitic-carbon nitride support for the synthesis of shape-dependent ZnO and their application in visible light photocatalysts, RSC Adv. 5 (2015) 80397–80409. doi:10.1039/c5ra12463h.

[177] H. Yu, F. Chen, F. Chen, X. Wang, Applied Surface Science In situ self-transformation synthesis of g-C_3N_4 -modified CdS heterostructure with enhanced photocatalytic activity, Appl. Surf. Sci. 358 (2015) 385–392. doi:10.1016/j.apsusc.2015.06.074.

[178] F. Jiang, T. Yan, H. Chen, A. Sun, C. Xu, X. Wang, Applied Surface Science A g-C_3N_4 – CdS composite catalyst with high visible-light-driven catalytic activity and photostability for methylene blue degradation, Appl. Surf. Sci. 295 (2014) 164–172. doi:10.1016/j.apsusc.2014.01.022.

[179] Y. Guo, J. Wang, Z. Tao, F. Dong, K. Wang, X. Ma, P. Yang, P. Hu, Y. Xu, L. Yang, Facile synthesis of mesoporous CdS nanospheres and their application in photocatalytic degradation and adsorption of organic dyes, Cryst eng comm. 14 (2012) 1185–1188. doi:10.1039/c2ce06172d.

[180] H.M. Xiong, D.G. Shchukin, H. Möhwald, Y. Xu, Y.Y. Xia, Sonochemical synthesis of highly luminescent zinc oxide nanoparticles doped with magnesium(II), Angew. Chemie - Int. Ed. 48 (2009) 2727–2731. doi:10.1002/anie.200805590.

[181] Z.R. Tang, X. Yin, Y. Zhang, Y.J. Xu, Synthesis of titanate nanotube-CdS

nanocomposites with enhanced visible light photocatalytic activity, Inorg. Chem. 52 (2013) 11758–11766. doi:10.1021/ic4010483.

[182] Y. Li, L. Tang, S. Peng, Z. Li, G. Lu, Phosphate-assisted hydrothermal synthesis of hexagonal CdS for efficient photocatalytic hydrogen evolution, Cryst Eng Comm. 14 (2012) 6974–6982. doi:10.1039/c2ce25838b.

[183] M. Salavati-Niasari, M.R. Loghman-Estarki, F. Davar, Controllable synthesis of nanocrystalline CdS with different morphologies by hydrothermal process in the presence of thioglycolic acid, Chem. Eng. J. 145 (2008) 346–350. doi:10.1016/j.cej.2008.08.040.

[184] L.R. Zou, G.F. Huang, D.F. Li, J.H. Liu, A.L. Pan, W.Q. Huang, A facile and rapid route for synthesis of g-C_3N_4 nanosheets with high adsorption capacity and photocatalytic activity, RSC Adv. 6 (2016) 86688–86694. doi:10.1039/c6ra20514c.

[185] N. Chidhambaram, K. Ravichandran, Fabrication of ZnO/g-C_3N_4 nanocomposites for enhanced visible light driven photocatalytic activity Fabrication of ZnO/g-C_3N_4 nanocomposites for enhanced visible light driven photocatalytic activity, (n.d.).

[186] M. Iqbal, A. Ali, N.A. Nahyoon, A. Majeed, R. Pothu, S. Phulpoto, K.H. Thebo, Photocatalytic degradation of organic pollutant with nanosized cadmium sulfide, Mater. Sci. Energy Technol. 2 (2018) 41–45. doi:10.1016/j.mset.2018.09.002.

[187] S. Vadivel, D. Maruthamani, B. Paul, S.S. Dhar, K. Selvam, Facile synthesis of novel $CaFe_2O_4$/g-C_3N_4 nanocomposites for degradation of methylene blue under visible-light irradiation Journal of Colloid and Interface Science Facile synthesis of novel $CaFe_2O_4$/g-C_3N_4 nanocomposites for degradation of methyle, J. Colloid Interface Sci. 480 (2016) 126–136. doi:10.1016/j.jcis.2016.07.012.

[188] Z.X. Han, Z. Zhu, D.D. Wu, J. Wu, Y.R. Liu, Adsorption Kinetics and Thermodynamics of Acid Blue 25 and methylene blue dye solutions on natural sepiolite, Synth. React. Inorganic, Met. Nano-Metal Chem. 44 (2014) 140–147. doi:10.1080/15533174.2013.770755.

[189] S. Kaur, A brief review on photocatalytic activity of ZnS and CQDs nanoparticles, Int. J. Eng. Appl. Sci. Technol. 2 (2017) 75–82. http://www.ijeast.com.

[190] M. Joshi, A. Bhattacharyya, S.W. Ali, Characterization techniques for nanotechnology applications in textiles, Indian J. Fibre Text. Res. 33 (2008) 304–317.

[191] R. Kohli, Methods for Monitoring and Measuring Cleanliness of Surfaces, in: Dev. Surf. Contam. Clean. - Detect. Charact. Anal. Contam., Elsevier, 2012: pp. 107–178. doi:10.1016/B978-1-4377-7883-0.00003-1.

[192] G. ZHANG, Master Thesis, University of Illinois at Urbana-Champaign, 2013, 2013.

[193] P.J. Mafa, A.T. Kuvarega, B.B. Mamba, B. Ntsendwana, Photoelectrocatalytic degradation of sulfamethoxazole on g-C_3N_4/BiOI/EG p-n heterojunction photoanode under visible light irradiation, Appl. Surf. Sci. 483 (2019) 506–520. doi:10.1016/j.apsusc.2019.03.281.

[194] M. Izadifard, G. Achari, C.H. Langford, Application of photocatalysts and LED light sources in drinking water treatment, Catalysts. 3 (2013) 726–743. doi:10.3390/catal3030726.

[195] C.G. Young, an Inductively Coupled Plasma Atomic Emission Spectrometer for the Detection of Nonmetals in the Vacuum Ultraviolet, 2011.

[196] A.M. Sabir, M. Moloy, P.S. Bhasin, Hplc Method Development and Validation: a Review, Int. Res. J. Pharm. 4 (2016) 39–46. doi:10.7897/2230-8407.04407.

[197] F. Jiang, T. Yan, H. Chen, A. Sun, C. Xu, X. Wang, A g-C_3N_4-CdS composite catalyst with high visible-light-driven catalytic activity and photostability for methylene blue degradation, Appl. Surf. Sci. 295 (2014) 164–172. doi:10.1016/j.apsusc.2014.01.022.

[198] Z. Zhang, J. Huang, M. Zhang, Q. Yuan, B. Dong, Ultrathin hexagonal SnS_2 nanosheets coupled with g-C_3N_4 nanosheets as 2D/2D heterojunction photocatalysts toward high photocatalytic activity, Appl. Catal. B Environ. 163 (2015) 298–305. doi:10.1016/j.apcatb.2014.08.013.

[199] A. Akhundi, A. Habibi-yangjeh, Novel magnetically separable g-C_3N_4/AgBr/Fe_3O_4 nanocomposites as visible-light-driven photocatalysts with highly enhanced activities, Ceram. Int. 41 (2015) 5634–5643. doi:10.1016/j.ceramint.2014.12.145.

[200] L.J. Cote, F. Kim, J. Huang, Langmuir-blodgett assembly of graphite oxide single layers, J. Am. Chem. Soc. 131 (2009) 1043–1049. doi:10.1021/ja806262m.

[201] Z. Zhou, J. Wang, J. Yu, Y. Shen, Y. Li, A. Liu, S. Liu, Y. Zhang, Dissolution and liquid crystals phase of 2D polymeric carbon nitride, J. Am. Chem. Soc. 137 (2015) 2179–2182. doi:10.1021/ja512179x.

[202] J. Xu, L. Zhang, R. Shi, Y. Zhu, Chemical exfoliation of graphitic carbon nitride for efficient heterogeneous photocatalysis, J. Mater. Chem. A. 1 (2013) 14766–14772. doi:10.1039/c3ta13188b.

[203] F. Dong, Z. Wang, Y. Sun, W.K. Ho, H. Zhang, Engineering the nanoarchitecture and texture of polymeric carbon nitride semiconductor for enhanced visible light photocatalytic activity, J. Colloid Interface Sci. 401 (2013) 70–79. doi:10.1016/j.jcis.2013.03.034.

[204] C. Li, Z. Sun, W. Huang, S. Zheng, Facile synthesis of g-C_3N_4/montmorillonite composite with enhanced visible light photodegradation of rhodamine B and tetracycline, J. Taiwan Inst. Chem. Eng. 66 (2016) 363–371. doi:10.1016/j.jtice.2016.06.014.

[205] J. Tong, L. Zhang, F. Li, K. Wang, L. Han, S. Cao, Rapid and high-yield production of g-C_3N_4 nanosheets via chemical exfoliation for photocatalytic H_2 evolution, RSC Adv. 5 (2015) 88149–88153. doi:10.1039/c5ra16988g.

[206] J. Zhu, P. Xiao, H. Li, S.A.C. Carabineiro, Graphitic carbon nitride: Synthesis, properties, and applications in catalysis, ACS Appl. Mater. Interfaces. 6 (2014) 16449–16465. doi:10.1021/am502925j.

[207] Y. Chen, X. Wang, Template-Free Synthesis of Hollow G‑C_3N_4 Polymer with Vesicle Structure for Enhanced Photocatalytic Water Splitting, (2018). doi:10.1021/acs.jpcc.7b12496.

[208] H.B. Tao, H. Bin Yang, J. Chen, J. Miao, B. Liu, Biomolecule-assisted synthesis of carbon nitride and sulfur-doped carbon nitride heterojunction nanosheets: An efficient heterojunction photocatalyst for photoelectrochemical applications, Beilstein J. Nanotechnol. 5 (2014) 770–777. doi:10.3762/bjnano.5.89.

[209] J. Tong, L. Zhang, F. Li, K. Wang, L. Han, S. Cao, Rapid and high-yield production of g-C_3N_4 nanosheets via chemical exfoliation for photocatalytic H_2 evolution, RSC Adv. 5 (2015) 88149–88153. doi:10.1039/c5ra16988g.

[210] S. Asadzadeh-khaneghah, A. Habibi-yangjeh, S. Vadivel, Journal of the Taiwan Institute of Chemical Engineers Fabrication of novel g-C_3N_4 nanosheet /carbon dots/$Ag_6Si_2O_7$ nanocomposites with high stability and enhanced visible-light photocatalytic activity, J. Taiwan Inst. Chem. Eng. 103 (2019) 94–109. doi:10.1016/j.jtice.2019.07.018.

[211] G. Mamba, A.K. Mishra, Applied Catalysis B : Environmental Graphitic carbon nitride (g-C_3N_4) nanocomposites : A new and exciting generation of visible light driven photocatalysts for environmental pollution remediation, "Applied Catal. B, Environ. 198 (2016) 347–377. doi:10.1016/j.apcatb.2016.05.052.

[212] J. Jin, J. Yu, G. Liu, P.K. Wong, Single crystal CdS nanowires with high visible-light photocatalytic H_2-production performance, J. Mater. Chem. A. 1 (2013) 10927–10934. doi:10.1039/c3ta12301d.

[213] S. Rengaraj, A. Ferancova, S.H. Jee, S. Venkataraj, Y. Kim, J. Labuda, M. Sillanpää, Physical and electrochemical characterization of CdS hollow microspheres prepared by a novel template free solution phase method, Electrochim. Acta. 56 (2010) 501–509. doi:10.1016/j.electacta.2010.09.019.

[214] J. Fu, B. Chang, Y. Tian, F. Xi, X. Dong, Novel C_3N_4-CdS composite photocatalysts with organic-inorganic heterojunctions: In situ synthesis, exceptional activity, high stability and photocatalytic mechanism, J. Mater. Chem. A. 1 (2013) 3083–3090. doi:10.1039/c2ta00672c.

[215] Q. Li, B. Guo, J. Yu, J. Ran, B. Zhang, H. Yan, J.R. Gong, Highly efficient visible-light-driven photocatalytic hydrogen production of CdS-cluster-decorated graphene nanosheets, J. Am. Chem. Soc. 133 (2011) 10878–

10884. doi:10.1021/ja2025454.

[216] V. Mohanraj, R. Jayaprakash, R. Robert, J. Balavijayalakshmi, S. Gopi, Effect of particle size on optical and electrical properties in mixed CdS and NiS nanoparticles synthesis by ultrasonic wave irradiation method, Mater. Sci. Semicond. Process. 56 (2016) 394–402. doi:10.1016/j.mssp.2016.08.014.

[217] N.H. Patel, M.P. Deshpande, S.H. Chaki, H.R. Keharia, Tuning of optical, thermal and antimicrobial capabilities of CdS nanoparticles with incorporated Mn prepared by chemical method, J. Mater. Sci. Mater. Electron. 28 (2017) 10866–10876. doi:10.1007/s10854-017-6865-y.

[218] A. Modwi, M.A. Ghanem, A.M. Al-Mayouf, A. Houas, Lowering energy band gap and enhancing photocatalytic properties of Cu/ZnO composite decorated by transition metals, J. Mol. Struct. 1173 (2018) 1–6. doi:10.1016/j.molstruc.2018.06.082.

[219] Q. Tang, C. Zhou, X. Yuan, Q. Jing, Y. Mu, A. Du, Facile Synthesis of g-C3N4 Nanosheets/ZnO Nanocomposites with Enhanced Photocatalytic Activity in Reduction of Aqueous Chromium(VI) under Visible Light, Nanomaterials. 6 (2016) 173. doi:10.3390/nano6090173.

[220] D. Wang, Z. Xu, Q. Luo, X. Li, J. An, R. Yin, C. Bao, Preparation and visible-light photocatalytic performances of g-C_3N_4 surface hybridized with a small amount of CdS nanoparticles, J. Mater. Sci. 51 (2016) 893–902. doi:10.1007/s10853-015-9417-y.

[221] A. Kumar, A Review on the Factors Affecting the Photocatalytic Degradation of Hazardous Materials, Mater. Sci. Eng. Int. J. 1 (2017) 1–10. doi:10.15406/mseij.2017.01.00018.

[222] S. Talebi, N. Chaibakhsh, Z. Moradi-Shoeili, Application of nanoscale ZnS/TiO2 composite for optimized photocatalytic decolorization of a textile dye, J. Appl. Res. Technol. 15 (2017) 378–385. doi:10.1016/j.jart.2017.03.007.

[223] Y.S. Al-Degs, M.I. El-Barghouthi, A.H. El-Sheikh, G.M. Walker, Effect of solution pH, ionic strength, and temperature on adsorption behavior of reactive dyes on activated carbon, Dye. Pigment. 77 (2008) 16–23.

doi:10.1016/j.dyepig.2007.03.001.

[224] E.T. Helmy, A. El Nemr, M. Mousa, E. Arafa, S. Eldafrawy, Photocatalytic degradation of organic dyes pollutants in the industrial textile wastewater by using synthesized TiO_2, C-doped TiO_2, S-doped TiO_2 and C,S co-doped TiO_2 nanoparticles, J. Water Environ. Nanotechnol. 3 (2018) 116–127. doi:10.22090/JWENT.2018.02.003.

[225] E. Mugunthan, M.B. Saidutta, P.E. Jagadeeshbabu, Visible light assisted photocatalytic degradation of diclofenac using TiO_2-WO_3 mixed oxide catalysts, Environ. Nanotechnology, Monit. Manag. 10 (2018) 322–330. doi:10.1016/j.enmm.2018.07.012.

[226] S. Iguchi, K. Teramura, S. Hosokawa, T. Tanaka, Effect of the chloride ion as a hole scavenger on the photocatalytic conversion of CO_2 in an aqueous solution over Ni-Al layered double hydroxides, Phys. Chem. Chem. Phys. 17 (2015) 17995–18003. doi:10.1039/c5cp02724a.

[227] L. Das, S.K. Barodia, S. Sengupta, J.K. Basu, Aqueous degradation kinetics of pharmaceutical drug diclofenac by photocatalysis using nanostructured titania–zirconia composite catalyst, Int. J. Environ. Sci. Technol. 12 (2015) 317–326. doi:10.1007/s13762-013-0466-y.

[228] J.M. Monteagudo, H. El-taliawy, A. Durán, G. Caro, K. Bester, Sono-activated persulfate oxidation of diclofenac: Degradation, kinetics, pathway and contribution of the different radicals involved, J. Hazard. Mater. 357 (2018) 457–465. doi:10.1016/j.jhazmat.2018.06.031.

[229] T. Huang, G. Zhang, S. Chong, Y. Liu, N. Zhang, S. Fang, J. Zhu, Effects and mechanism of diclofenac degradation in aqueous solution by US/Zn0, Ultrason. Sonochem. 37 (2017) 676–685. doi:10.1016/j.ultsonch.2017.02.032.

[230] M. V. Bagal, P.R. Gogate, Degradation of diclofenac sodium using combined processes based on hydrodynamic cavitation and heterogeneous photocatalysis, Ultrason. Sonochem. 21 (2014) 1035–1043. doi:10.1016/j.ultsonch.2013.10.020.

[231] P. Sathishkumar, R.A.A. Meena, T. Palanisami, V. Ashokkumar, T. Palvannan,

F.L. Gu, Occurrence, interactive effects and ecological risk of diclofenac in environmental compartments and biota - a review, Sci. Total Environ. 698 (2020) 134057. doi:10.1016/j.scitotenv.2019.134057.

[232] R.R. Giri, H. Ozaki, S. Ota, R. Takanami, S. Taniguchi, Degradation of common pharmaceuticals and personal care products in mixed solutions by advanced oxidation techniques, Int. J. Environ. Sci. Tech. 7 (2010) 251–260. doi:10.1007/BF03326135.

[233] S. Sébastien, Les soignants face à la mort, Rev. Infirm. 1 (2012) 39–41.

[234] H. Xu, L. Wu, L. Jin, K. Wu, Combination Mechanism and Enhanced Visible-Light Photocatalytic Activity and Stability of CdS/g-C_3N_4 Heterojunctions, J. Mater. Sci. Technol. 33 (2017) 30–38. doi:10.1016/j.jmst.2016.04.008.

[235] I.W. As, M.C. Level, P.H. Effects, T. Methods, I. Exchange, R. Osmosis, WQA Technical Fact Sheet: Cadmium Health effects treatment methods Residential Point-of-Entry Point-of-Use, 2013. http://www.epa.gov/safewater/pdfs/factsheets/ioc/cadmium.pdf.

CHAPTER 5
CADMIUM SULFIDE/GRAPHITIC CARBON NITRIDE SYNTHESIS FOR PHOTOCATALYTIC DEGARATION OF AB-25

5.1 Introduction

This chapter discussed the result of the experimental procedure outline in chapter 3, section 3.2, it present the application of CdS and its improved photocatalytic activity by g-C_3N_4 for the photocatalytic degradation of AB-25. The g-C_3N_4 nanosheets (CNS)/CdS composites with varied CNS percentage loadings were prepared via in-situ method of synthesis. Different parameters including effect of catalysts concentration, dye concentrations and pH were considered in this study when performing the AB-25 application studies.

5.2 Results and discussion

5.2.1 X-Ray diffractometer (XRD)

The crystalline phases of (10%, 20% and 30%) CNS/CdS nanocomposites were characterized using XRD analysis (Fig. 5.1). The characteristic peaks of CdS and its composites were identified at 24.8°,26.5°,28.2°,43.8°,47.9° and 52.9º, and were indexed to (100), (002), (101), (110), (103) and (112) planes (PDF card number 41-1487) respectively[187,197,213]. The diffraction peaks at 24.8° and 28.2° indexed to the (100) and (101) planes indicate the existence of hexagonal wurtzite structure of CdS [213]. The diffraction peak at 26.5° for CdS/CdS composites increased with an increase in CNS loading which is attributed to the peak superposition of CNS at 27.5º.

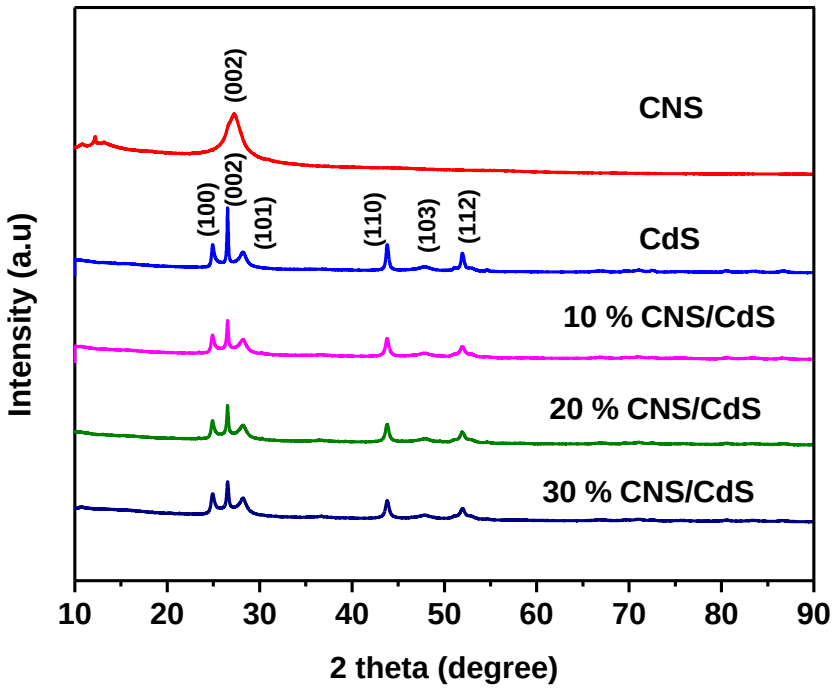

Figure 5.1. XRD pattern of CNS, CdS, 10%, 20% and 30% CNS/CdS.

The crystallite sizes (d) and micro-strain (ε) values of the synthesized materials were determined using Equations (3.6) and (3.7);

The calculated crystallite size and micro-strain values of, CNS, CdS, 10%, 20% 30% CNS/CdS are listed in Table 5.1. It was observed that the crystalline size of CdS decreased with an increase in the amount of CNS added. Furthermore the crystalline structure of CdS changed slightly with increasing CNS however the d spacing of the composite remained the same suggesting the distance between the planes of the composites was the same.

Table 5.1. d spacing, crystalline size, and micro-strain of the as-prepared materials.

Sample	d-spacing (nm)	Crystalline size (nm)	Micro-strain
CNS	0.326	14.985	0.003
CdS	0.358	71.836	0.001
10% CNS/CdS	0.336	58.472	0.001
20% CNS/CdS	0.336	60.243	0.001
30% CNS/CdS	0.336	44.846	0.001

5.2.2 Fourier transformation infra-red (FTIR)

FTIR was used to determine the functional groups of the prepared materials (Fig 5. 2). For CdS four characteristic peaks were observed at 3452, 1641, 1392 and 1117 cm^{-1} respectively. The peaks at 3452 and 1641 cm^{-1} are ascribed to the adsorbed water molecules on the surface of CdS, while the peaks at 1391 and 1117 cm^{-1} were ascribed to the Cd-S band which indicate successful formation of CdS For the composite materials the IR bands characteristic of CNS and CdS were observed, confirming that the composite materials were composed of both CNS and hexagonal CdS [214].

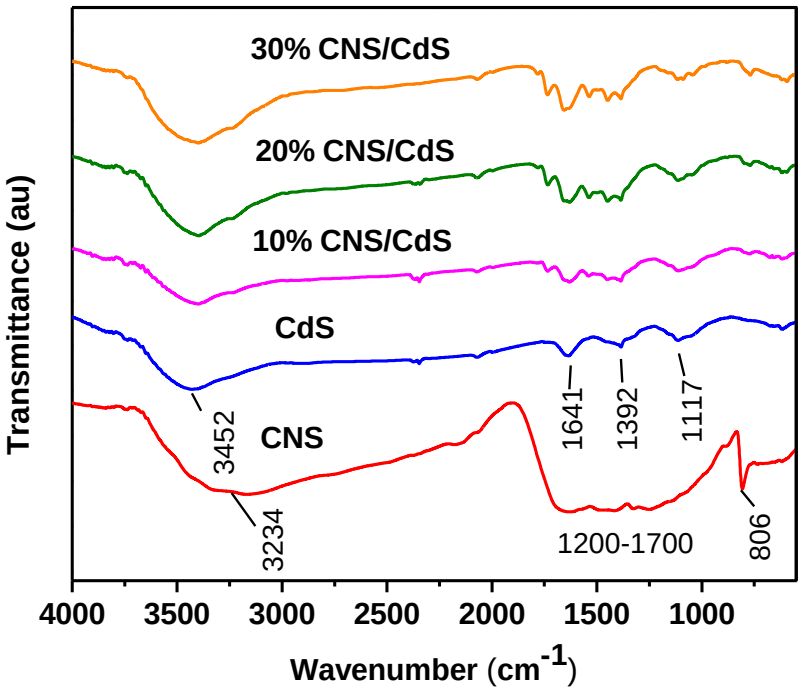

Figure 5.2. HRSEM of CNS, 10%, 20% and 30% CNS/CdS.

5.2.3 Field Emission Scanning Electron Microscope and Energy Dispersive Microscope

The morphology and elemental composition of the materials was studied using FE-SEM (Fig. 5.3). CdS displayed flower like microspheres in the micro range (Fig. 5.3a) [187,202]. The addition of CNS to CdS showed that the CdS microspheres dispersed on the surface of CNS thus proving the interaction between CNS and CdS.

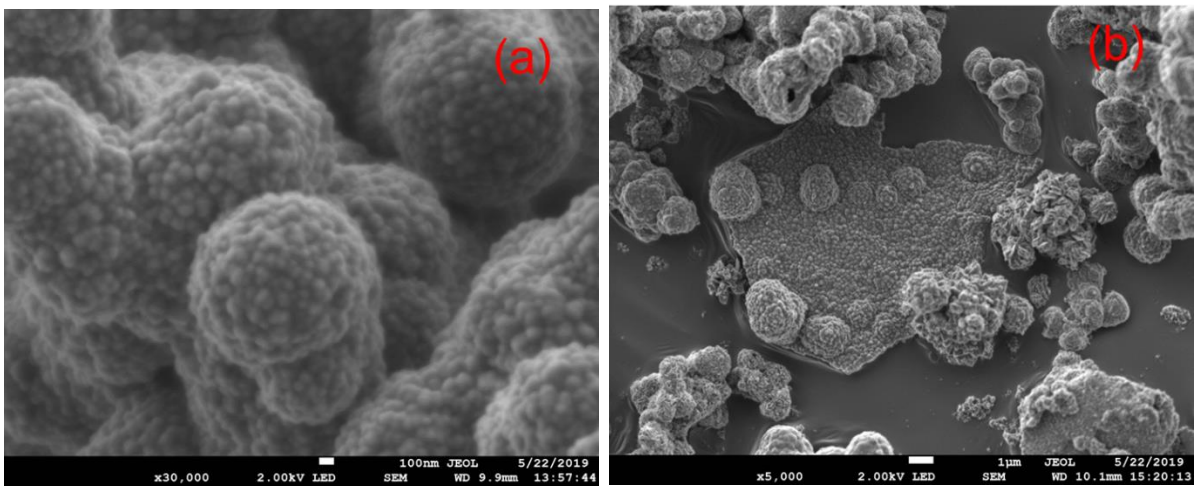

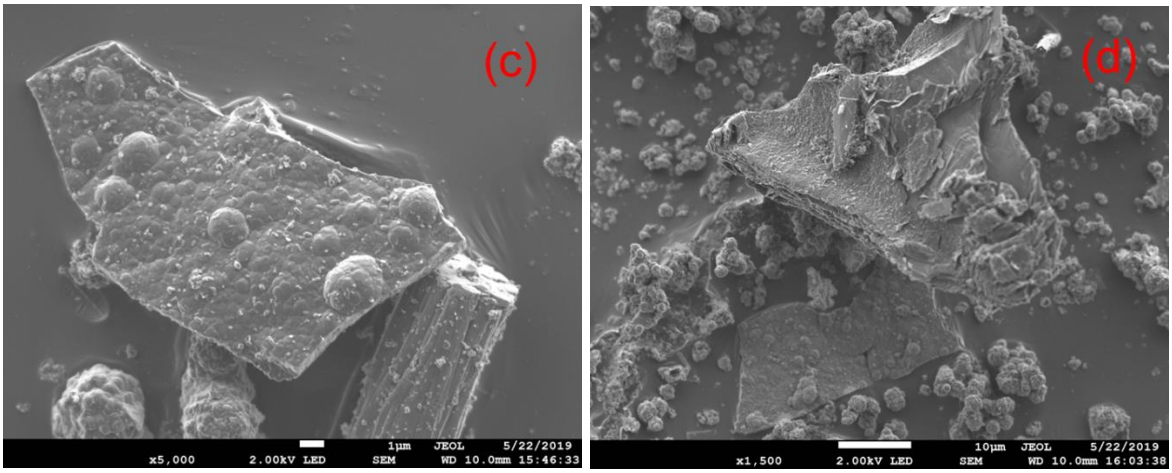

Figure 5.3. FESEM micrograms of 10%, 20% 30% CNS/CdS (a-d).

Energy Dispersive Spectroscopy

The EDS spectrum was used to confirm the elemental analysis of the materials (Fig 5.4). The EDS spectra of CdS confirmed the presence of Cd, S which confirmed the formation of CdS microspheres (Fig. 5.4a). The EDS spectra of the composite materials (10%, 20% and 30% CNS/CdS) are similar, showing the presence of C, O, N, Cd and S, confirming the presence of both CdS and CNS. The C and N peaks were subdued due to the higher amounts of CdS used in the synthesis (Fig. 5.4b-c).

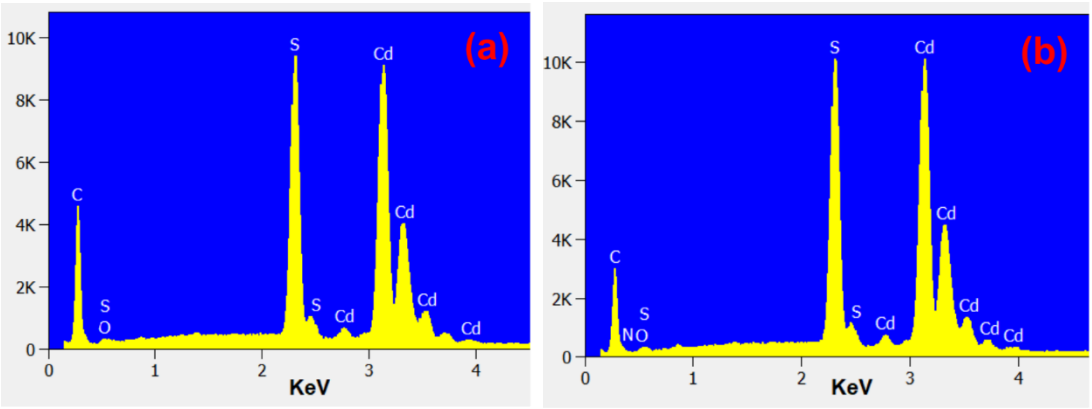

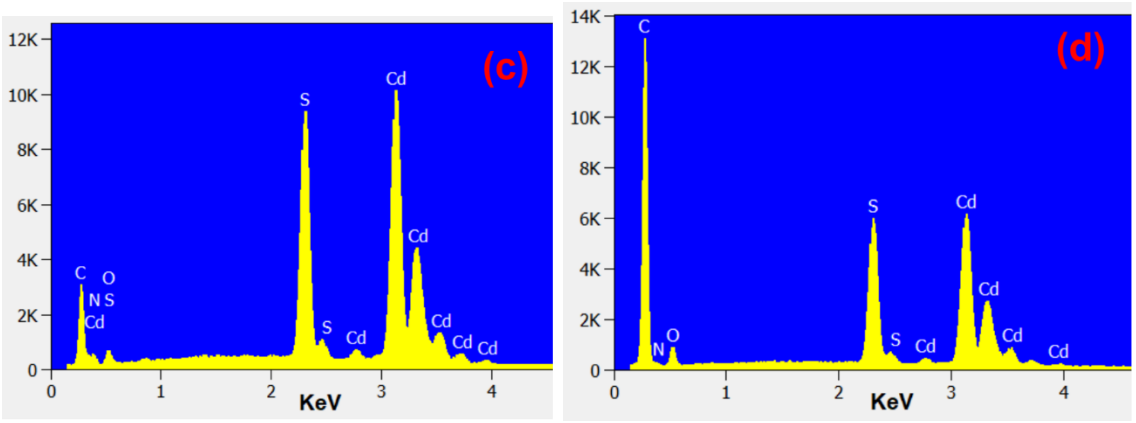

Figure 5.4. EDS analysis of (a) CdS and 10%, 20% and 30%CNS/CdS (b-d).

The EDS mapping was used to confirm the dispersion of Cd on CNS surface (Fig. 5.4a-b). The images showed that CdS microspheres were well dispersed on the surface of CNS as confirmed by SEM observations.

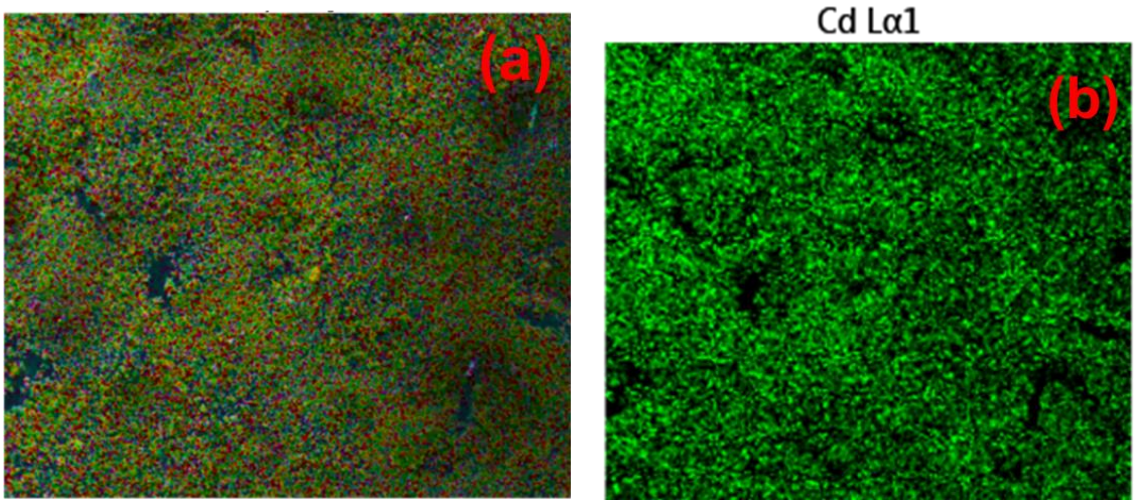

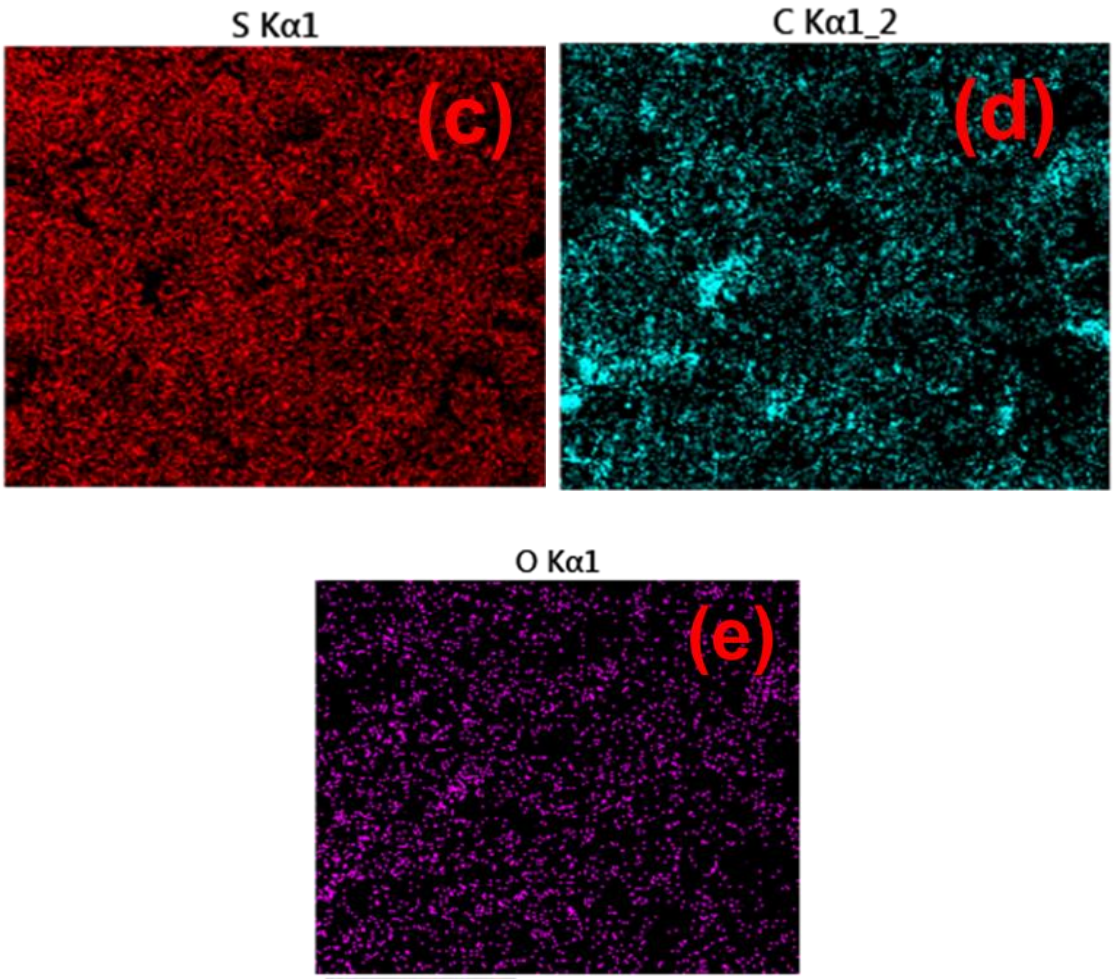

Figure 5.5. EDS mapping images of 10% CNS/CdS (a-d).

5.2.4 Transmission Electron Microscope (TEM)

The morphology of CdS and 10% CNS/CdS (the working composite) are shown on (Fig. 5.6). Fig 5.6a shows a low magnification TEM image of the CdS microspheres, the TEM image of a selected region on the surface of the microspheres showed small CdS particles of certain nanosized range consistent with results obtained on SEM (Fig. 5.6a). The small insert also shows the microspheres particles on the surface consistent SEM images. Furthermore 10% CNS/CdS nanocomposite showed two morphologies, lighter sheet-like structures that are almost transparent which are ascribed to CNS and the darker plate like morphology ascribed to CdS (Fig 5.6b). This confirmed that the CdS microspheres formed an interface with the CNS also confirmed with the interface crystallinity on XRD (Fig 5.1). The SAED

pattern suggest polycrystalline structures and micro spherical structure of CdS (Fig 5.6c).

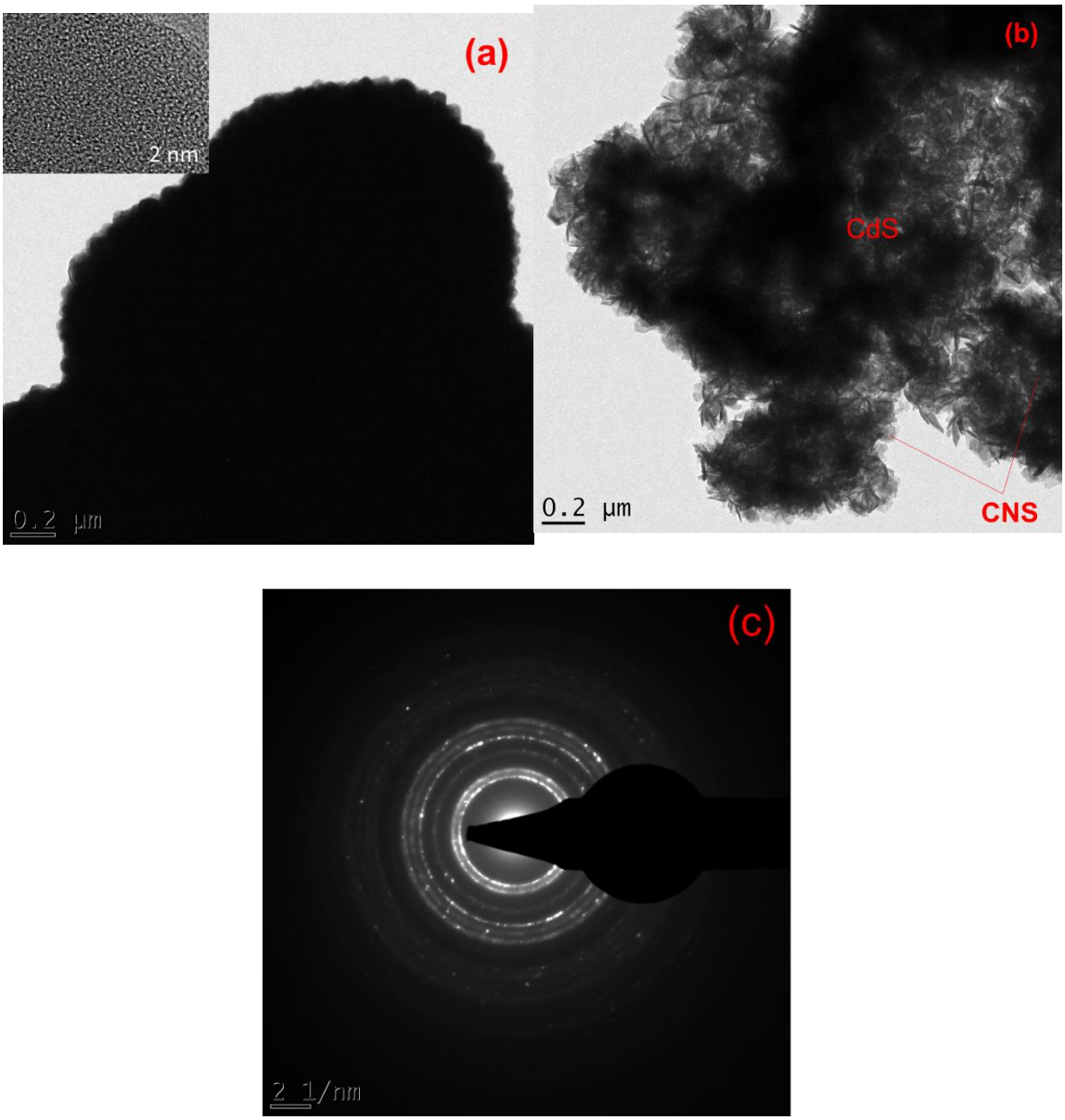

Figure 5.6. TEM analysis of (a) CdS and (b) 10% CNS/CdS and (c) SAED for 10% CNS/CdS.

5.2.5 BET analysis

The pore volume was obtained using the Barrett-Joyner Halenda (BJH) method and the obtained results are highlighted in (Table 5.2). The pore volumes of all the samples are (<2 nm), indicating the presence of microporous structure in the entire sample. Furthermore higher pore volume resulted in increased surface area of the sample, which could lead to enhanced photocatalytic activity.

Table 5.2. Surface area and pore volume of the prepared materials.

Sample	**Surface Area m^2g^{-1}**	**Pore Volume cm^3g^{-1}**
CN	3.04	0.008
CNS	11.02	0.053
CdS	1.11	0.004
10% CNS/CdS	4.40	0.020

The surface area of CdS and 10% CNS/CdS were obtained using the Brunauer-Emmett-Teller (BET) (Fig. 5.7). The hysteresis loops of CdS was type H3, indicating the formation of slit shaped pores with plate-like particles which is consistent with the observed morphology on TEM (Fig. 5.7b) [215]. The BET analysis shows an increase in surface area of CdS from 1.11 to 4.37 m^2g^{-1} after addition CNS. Furthermore high surface area results in high number of the active sites, which make simple transportation of charge carries and thus increase the photocatalytic efficiency.

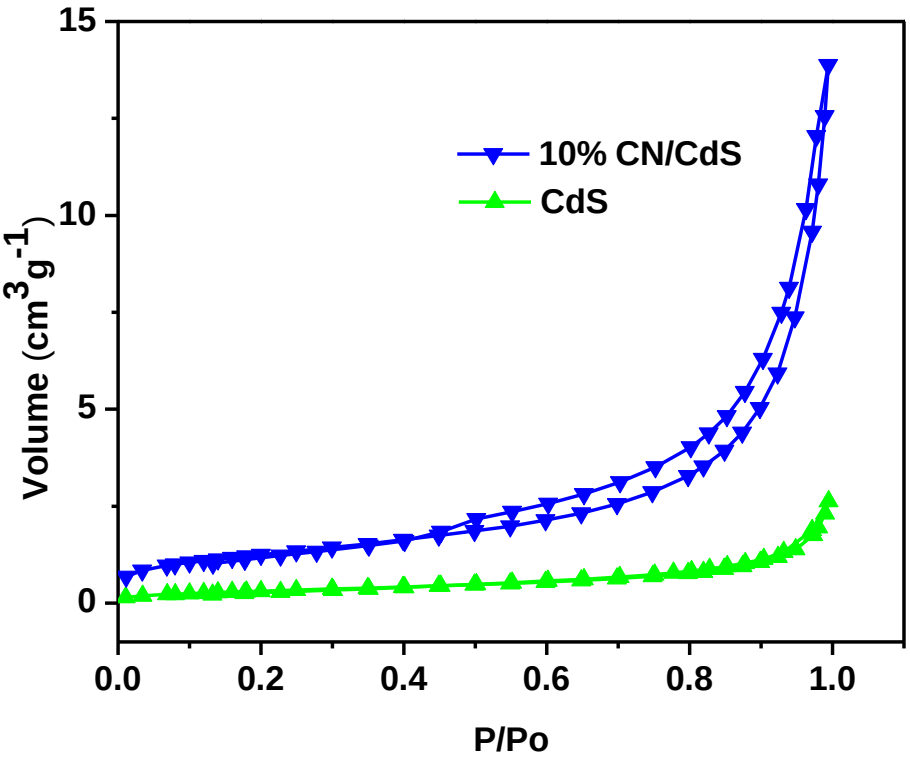

Figure 5.7. BET analysis of CdS and 10% CNS/CdS.

5.2.6 Thermogravimetric Analysis

The thermogravimetric analysis of CdS and 10%, 20% and 30% CNS/CdS nanocomposites was studied at room temperature to 900 ^{o}C under N_2 (Fig. 5.8). Two weight loss stages of CdS, the first was 28.8% between 628-787 ^{o}C The second was at 787-898 ^{o}C and 25.9% was lost and the weight loss above 700 ^{o}C is ascribed to decomposition of hexagonal CdS [216]. Three weight loss stages were observed for the nanocomposites. The firs mass between 254-295 ^{o}C was due to adsorbed moisture on the nanocomposites surface. The increase in CNS amount resulted in more moisture lost. Furthermore the higher the CNS amount, the more CdS weight loss, which suggest that CdS is more stable than CNS incorporated CdS. This may be due to the bond strength variation of Cd-S and CNS-S/Cd [217].Moreover the hexagonal decomposition of CdS decreased with increasing CNS amount.

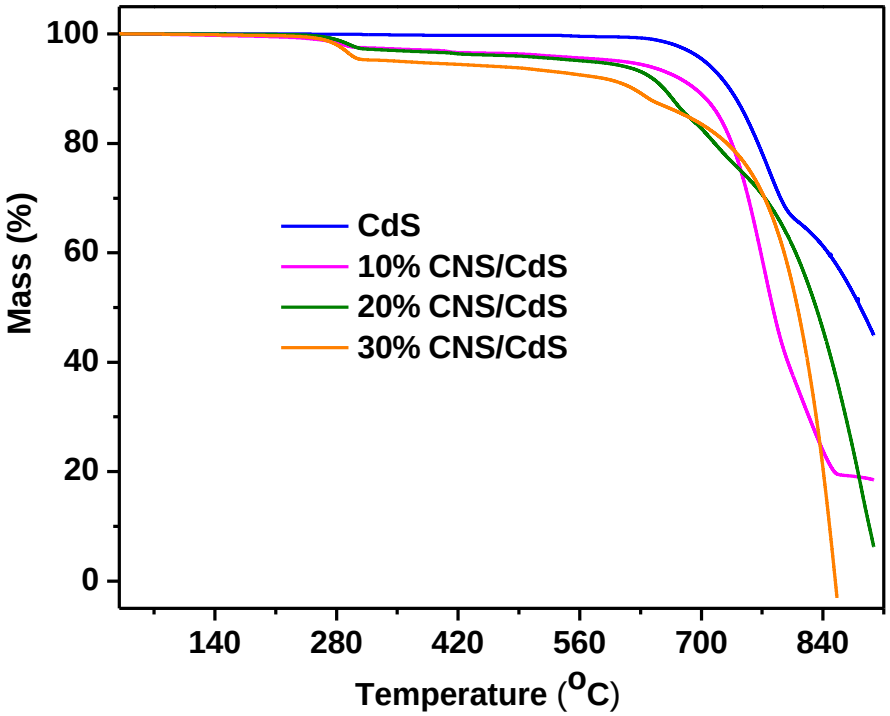

Figure 5.8.TGA analysis of CdS, 10%, 20% and 30% CNS/CdS.

5.3 Optical properties

5.3.1 UV-Vis absorption spectroscopy

The optical properties of the prepared materials were evaluated using UV-Vis spectroscopy (Fig. 5.9a).The absorption of CdS further shifted towards the visible-light region and higher absorption intensities were observed after the addition of CNS. Compared to pure CdS, the adsorption edges of 10%, 20% and 30% CNS/CdS blue-shifted towards the visible range from 509 to 489 nm. The blue shift in absorption edges implies high band gaps and thus more energy is required for photoexcitation of the charge carriers from the valence band to the conduction band of the semiconductor.

The bandgaps of the materials were estimated using the equation (3.11) to (3.13). Fig. 5.9b shows the Tauc plots and the bandgaps of CdS, 10%, 20% and 30% CNS/CdS were estimated to be, 2.21, 2.17, 2.11 and 2.14 eV respectively.

The bandgap of CdS (2.21eV) decreased upon the addition of CNS. The lowest band gap was observed for 10% CNS/CdS (2.17 eV) [218].

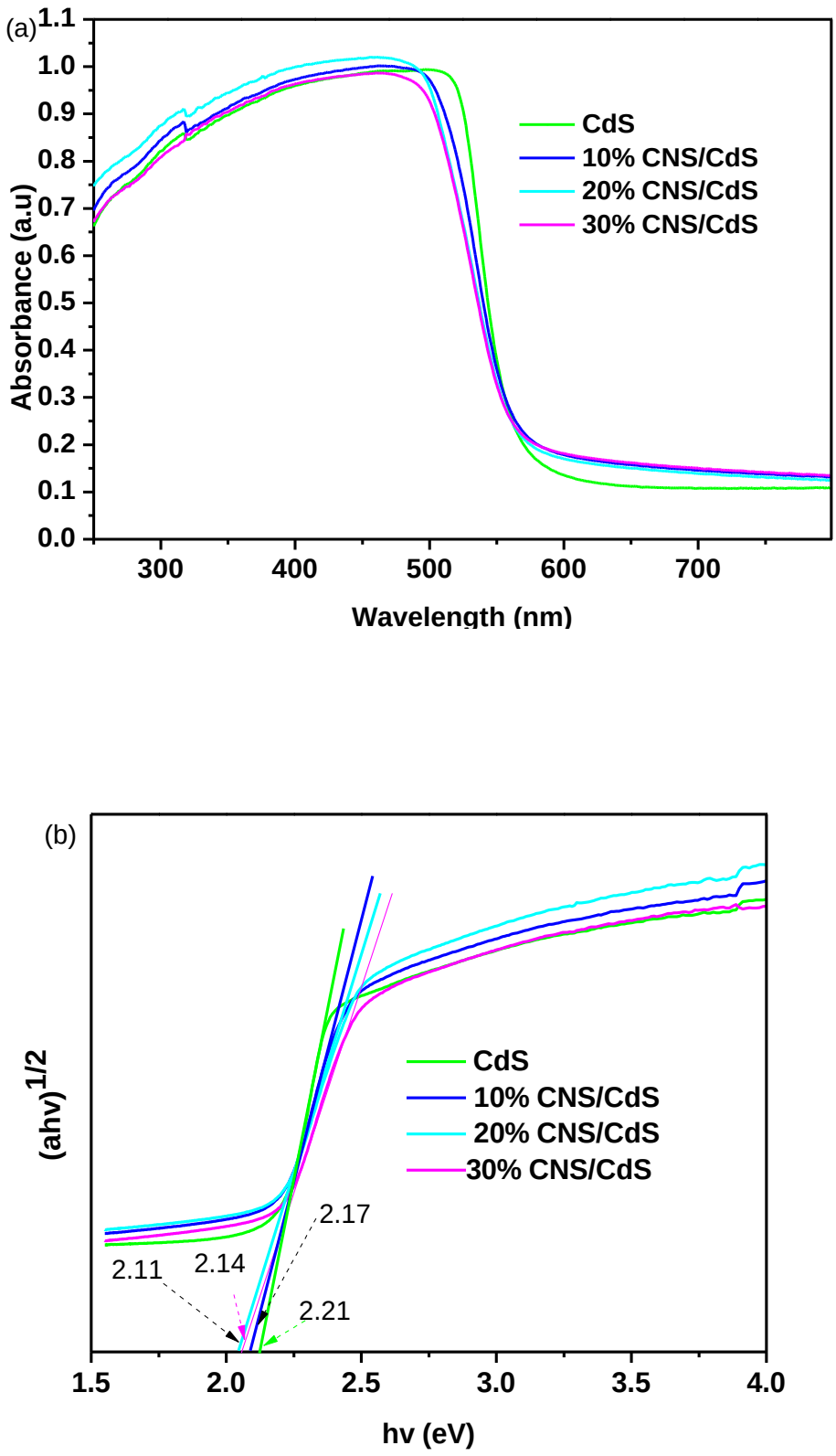

Figure 5.9. (a)UV-Vis spectra and (b) Tauc plots of prepared materials.

5.4 Photocatalytic degradation of AB-25 evaluation

5.4.1 AB-25 Dye degradation absorption

The photocatalytic degradation of AB-25 was monitored over time at the wavelength of maximum absorption of the dye (Fig. 5.10). The absorbance of the dye solution decreased with increasing time. At 180 min, almost no peak observed, showing that the dye solution is completely decolorized by the catalyst.

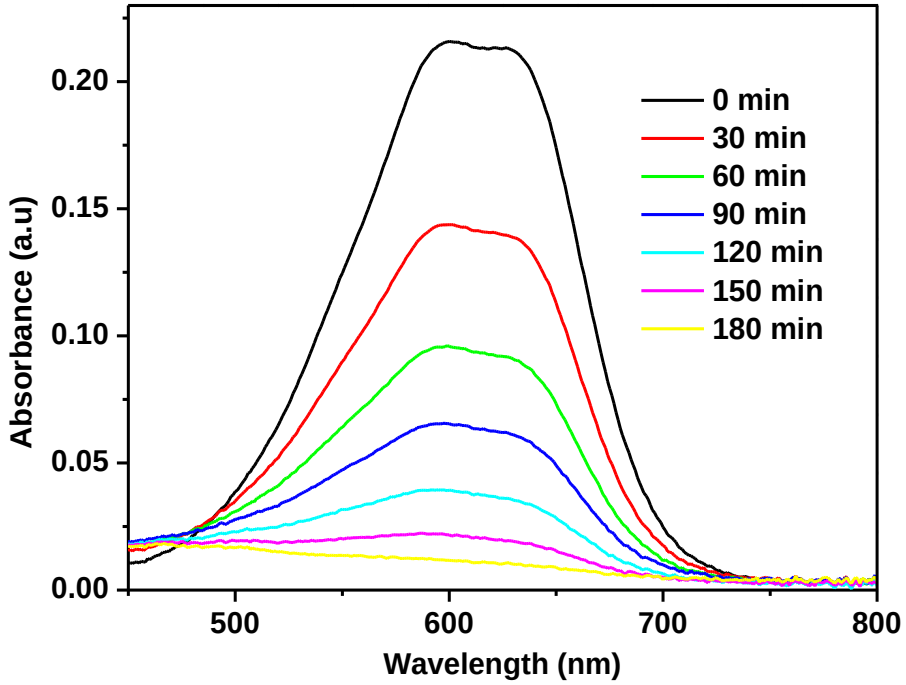

Figure 5.10. UV-Vis absorption spectra for degradation of AB-25.

5.4.2 Effect of CNS/CdS mass ratios on AB degradation efficiency

The effect of CNS on the photo-activity of CdS was evaluated by varying the mass load of CNS (Fig. 5.11). The photocatalytic efficiencies of (CdS, 10%, 20% and 30% CN/CdS) were 89.1%, 99.3, 97.8% and 92% respectively. The photocatalytic efficiency of CdS was significantly enhanced by addition of CNS. Furthermore the 10% CNS/CdS lower loading exhibited much higher photocatalytic efficiency of 99.3% compared to 20% and 30% CNS/CdS nanocomposites and within 60 min visible light irradiation the AB-25 solution was almost colourless (see insert Fig. 5.11). This is due to the high CNS content acting as a recombination centres and block the active sites on the surface of CdS and block from passing through the catalyst therefore reducing the efficiency of charge separation [214,219].

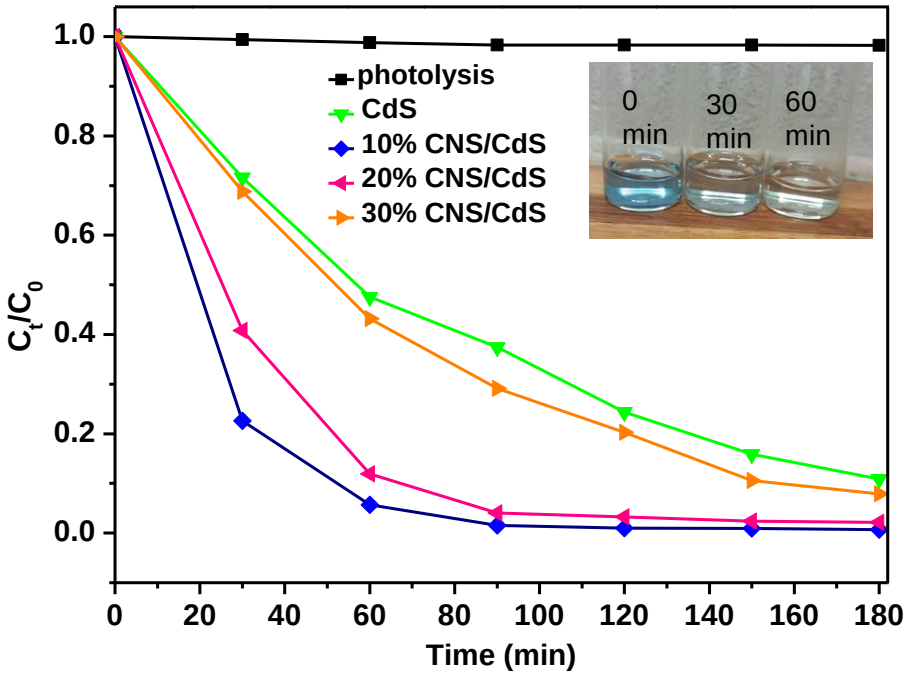

Figure 5.11. Effect of CNS on CdS mass ratios for AB-25 degradation efficiency.

5.4.3 Effect of catalyst dosage

The dosage of 10% CN/CdS was evaluated (Fig. 5.12). The photocatalytic efficiencies of the composite materials for 10, 20 and 40 mg catalyst were 83%, 99% and 66% respectively. The decreased efficiency at lower catalyst loading is due to the small charge carriers generated from the photocatalyst [220]. Furthermore the higher the catalyst dosage the lower the photocatalytic efficiency of the nanocomposite which is attributed to poor light penetration through the slurry solution, thus cause excessive light blockage and scattering by the photocatalyst particles and resulting in the decreasing number of·OH radicals which take part in the decolouration of the dye solution [221].

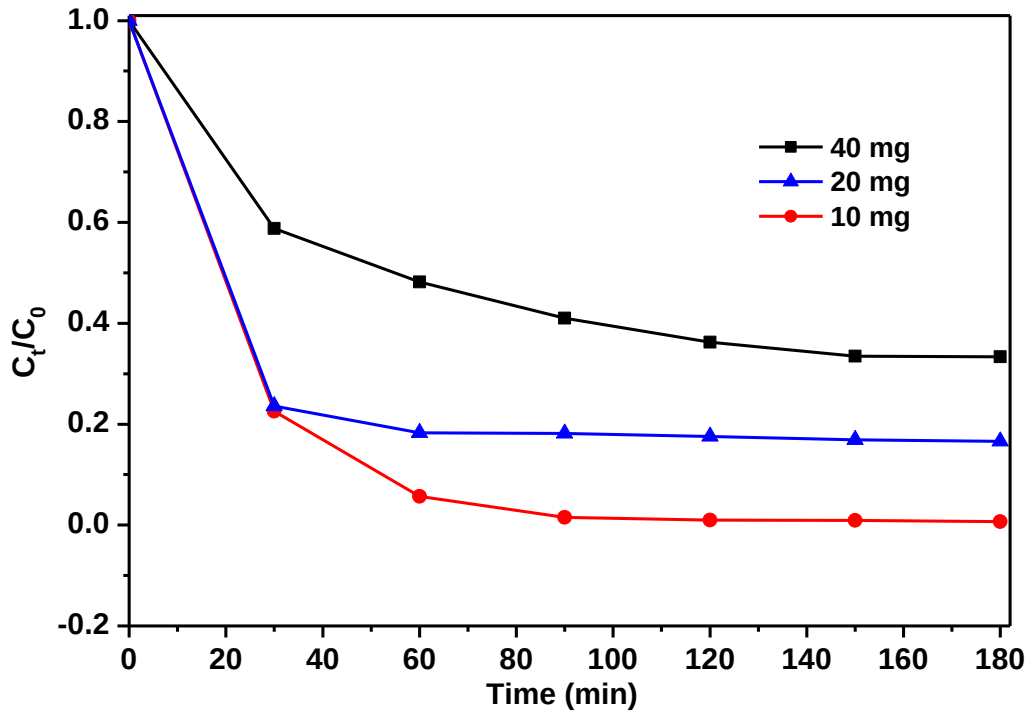

Figure 5.12. Effect of CNS mass ratios on CdS for AB-25 degradation.

5.3.4 Effect of dye concentration

Different concentrations of acid blue 25 dye were selected based on the literature textile dye effluents discharge which are reported in the range 20-50 mg L^{-1}. For initial dye concentrations of 20, 30 and 50 mgL^{-1} the obtained efficiencies were 99.3%, 89.5% and 74.8% respectively (Fig. 5.13). The higher the dye concentration the lower the photocatalytic efficiency, suggesting there are more active sites for adsorption to occur at a fast rate when dye concentration is lower and higher dye concentrations result in lower removal efficiency due to shielding of the photons by the high intensity dye solution [13].

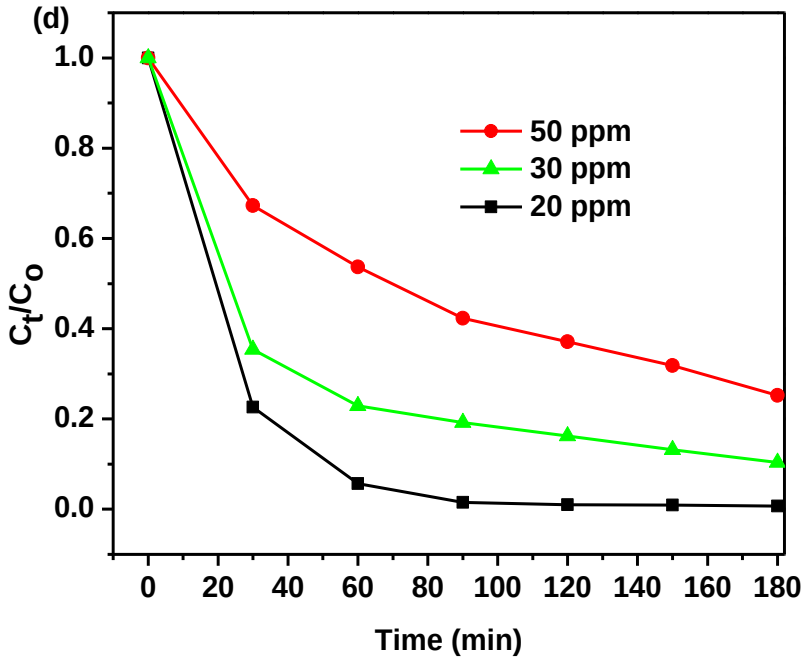

Figure 5.13. The effect of AB-25 concentration.

5.4.4 Effect of pH

The optimum pH of AB-25 was evaluated during photocatalytic degradation (Fig. 5.14) and plays a significant role on the adsorption process of pollutants, as it affects the overall charge on the dye molecules [188]. Different dye pH solutions of 3, 5 and 8 were selected to evaluate the effect of surface charge of the catalyst and the ionic behaviour of AB-25. The dye concentration and photocatalyst dosage were kept constant at 20 ppm and 10 mg respectively. A total volume of 50mL of the dye was used in the studies. The photocatalytic efficiency at pH 3, 5 and 8 were 78.8%, 99.31 and 82.8% respectively. At pH 8 high adsorption of the dye was observed, after the addition of sodium hydroxide, the photocatalytic efficiency of the composite (10% CNS/CdS) decreased to 82.8% which is attributed to the presence of the hydroxide anions and thus competition of the active sites on the surface of the catalyst. At pH 5 the efficiency increased to 99.31% due to the number of hydrogen ions present and making the surface of the catalyst more positive and thus promoting the electrostatic attraction activity between the negatively charged sulfonate anion of the dye and the catalyst [12,222,223].

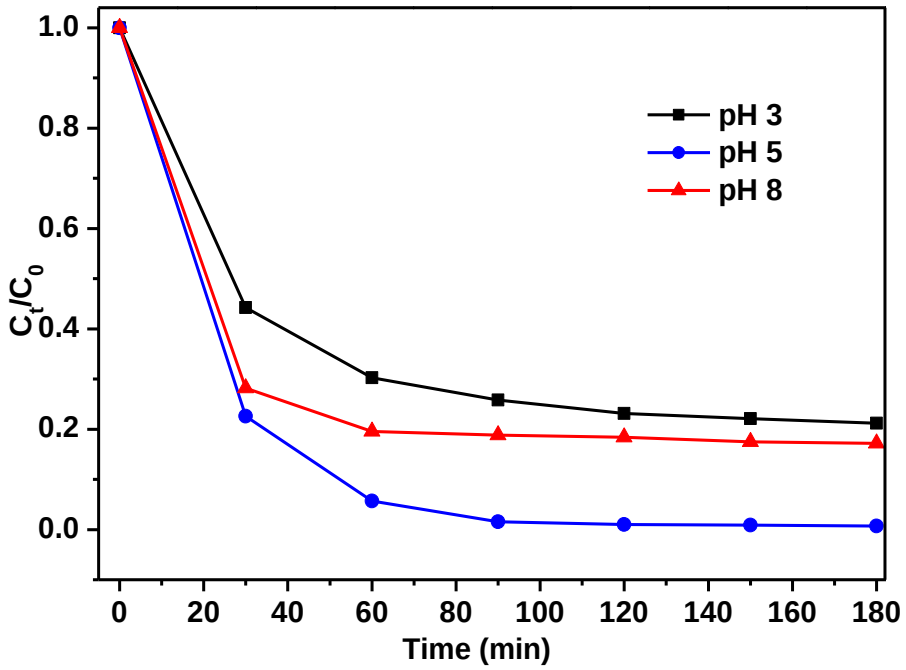

Figure 5.14. The .effect of pH of AB-25.

5.5 Reaction kinetics

The degradation rate of AB-25 was evaluated by modelling the degradation data using the equation (3.13) and (3.14). The Langmuir-Hinshelwood expression was first order [193]. The apparent rate constants at pH 5 for photolysis, CdS, (10, 20 and 30%) CNS/CdS are expressed on (Table 2). The reaction rate resulted in faster reaction rates.

Table 5.3. Reaction rate constants of the prepared materials.

Sample	**Reaction rates min^{-1}**
Photolysis	0.0002
CdS	0.0116
10% CNS/CdS	0.0424
20% CNS/CdS	0.0316

30% CNS/CdS	0.0135

The reaction rate of photolysis was slow. Furthermore the reaction rate of CdS decreased with increasing CN ratios and is ascribed to high recombination of charge carriers. Moreover the enhanced photocatalytic efficiencies are due to formed heterojunction interface of CNS/CdS composites which restrained the recombination of photo induced charge carrier's. Thus the photodegrading of AB-25 followed the pseudo-first order model (Fig. 5.15).

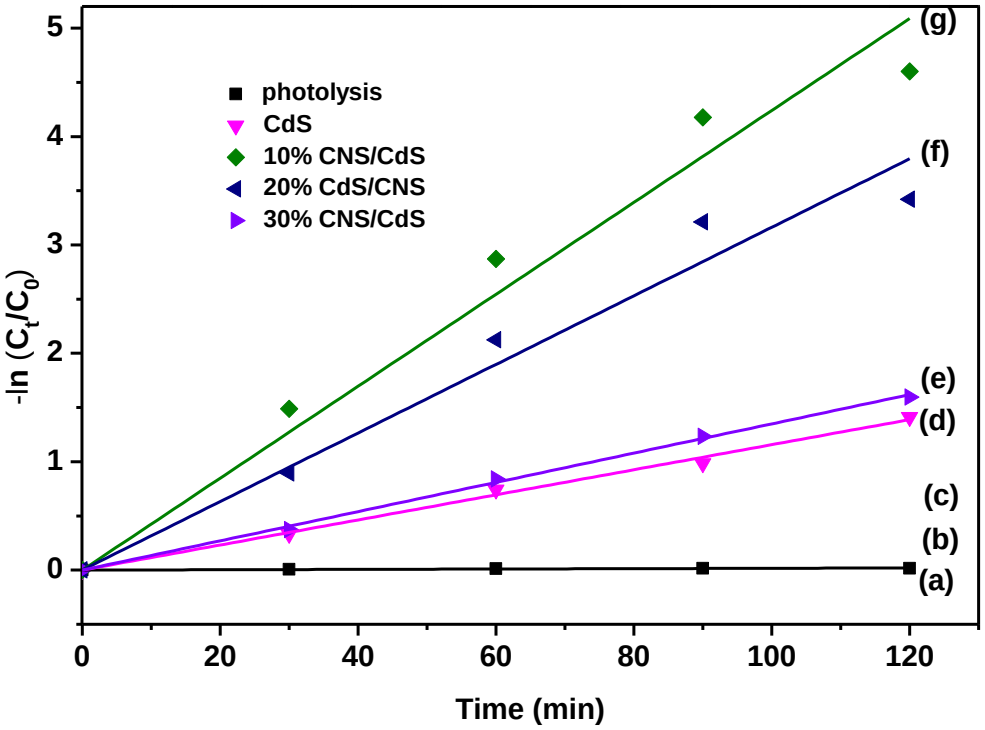

Figure 5.15. Rate Constants for (a) photolysis, (b) CN, (c) CNS, (d) (CdS), (e) 30% CNS/CdS, (f) 20%CNS/CdS and (g) 10%CNS/CdS.

5.6 Photocatalytic stability and reusability

The photocatalytic stability and reusability of the synthesized materials were determined by performing recyclability studies of the optimized AB-25 dye for 4 cycles under the same conditions. After each catalytic cycle, the catalyst slurry was centrifuged, washed and dried at 60 ^{o}C for 6 hours prior to re-use. The photocatalytic efficiencies for the 1st, 2nd, 3rd and 4th catalytic cycles were 99.3%, 97.8%, 94. 60% and 92.0% respectively. The catalyst was still stable after 4 catalytic cycles (Fig.

5.16). The efficiency decreased slightly after 4 cycles and this may be due to the loss of the catalyst during the washing and centrifuging step.

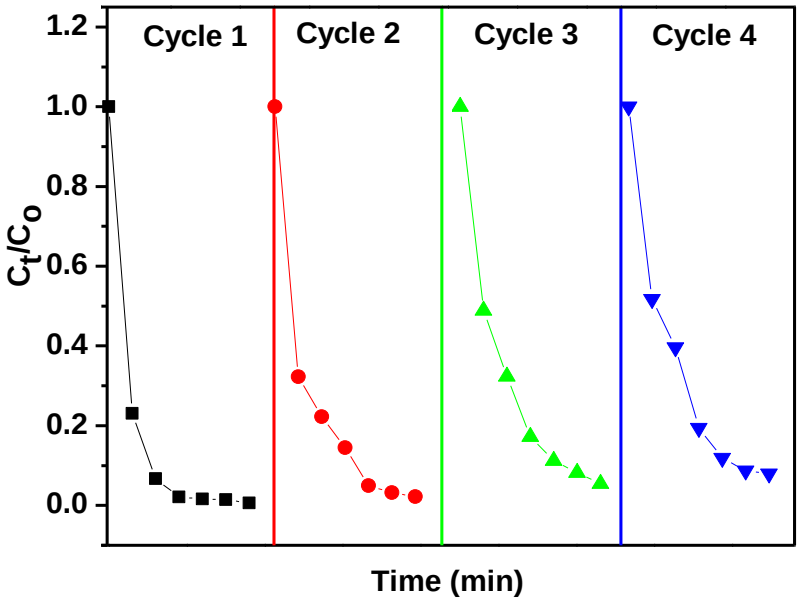

Figure 5.16. Stability of 10% CNS/CdS.

5.7 Reactive species

The charge carrier trapping experiments were conducted to determine the reactive species in the photocatalytic reaction (Fig. 5.17). Benzoquinone (BQ), 2-propanol, and ethylene diamine (EDTA) were used to scavenge superoxide radical anions ($O_2\bullet^-$), hydroxyl radicals and holes (h^+) respectively under optimum conditions (20 mg catalyst, 20 ppm AB-25 (50 mL) at pH 5). The addition of BQ, 2 propanol and EDTA resulted in the reduction in the photocatalytic degradation efficiency of AB-25 to 36.5, 93.5 and 85.6% respectively. The photocatalytic efficiency of the composite reduced slightly with the addition of 2-propanol and EDTA, suggesting that •OH play no major role in the photo-degradation of AB-25. Furthermore the addition of BQ resulted in a significant decrease in the photocatalytic efficiency of the 10% CNS/CdS composite, indicating that $\bullet O_2^-$ is the major species for AB-25 photo-degradation.

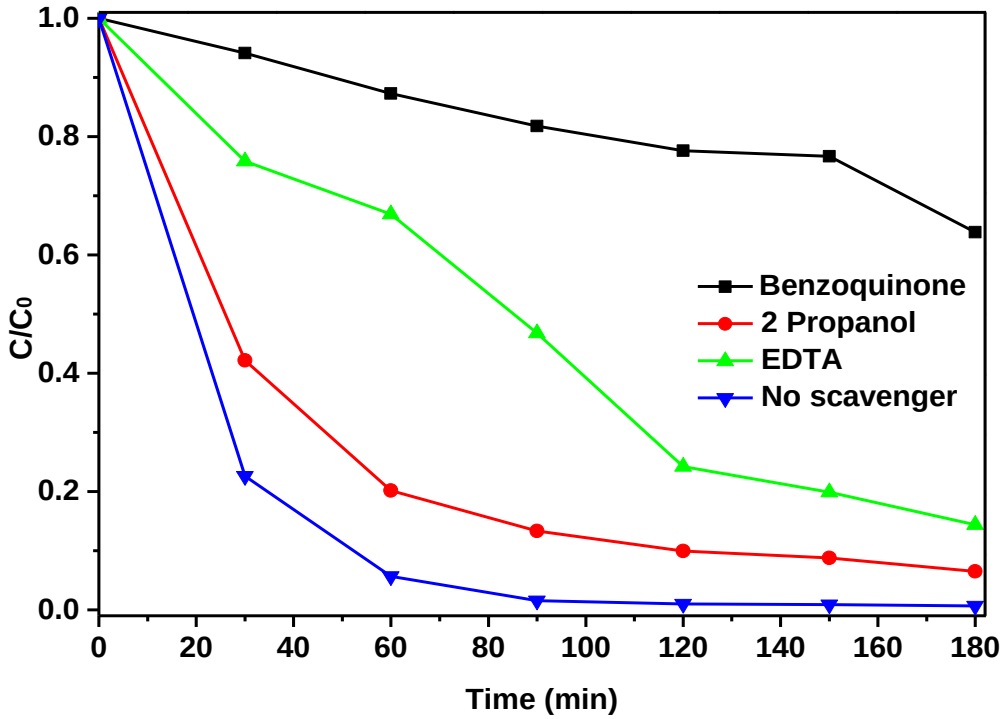

Figure 5.17.Determination of reactive species with different scavengers for photo-degradation of AB-25.

5.8 Proposed photodegradation of AB-25 mechanism

The proposed mechanism for the charge transfer and separation of charges at the interface of the CNS/CdS during photocatalytic degradation AB-25 is shown with a schematic diagram (Fig. 5.18). To determine the separation of charge, the band edge potentials at the conduction band (CB) and valence band (VB) of CNS and CdS were determined using the equations (3.15) and (3.16). The conduction bad (CB) potential of CNS at -1.07 was more negative than the conduction band potential of CdS (-0.32) and the valence band (VB) potential of CdS at 1.70 eV was more positive than the valence band potential of CNS at 1.55 eV. The band potentials of CNS and CdS favour the transfer of photo-generated electrons from the surface of CNS to CdS while the positive holes are transferred from the surface of CdS to CNS. This suggests that the photo-generated electrons and holes move in opposite directions and thus reduce the chances of charge carrier recombination and enhance the charge separation efficiency. Separation of charges promotes generation of reactive hydroxyl and superoxide radicals that participate in oxidative degradation of the dye [193].

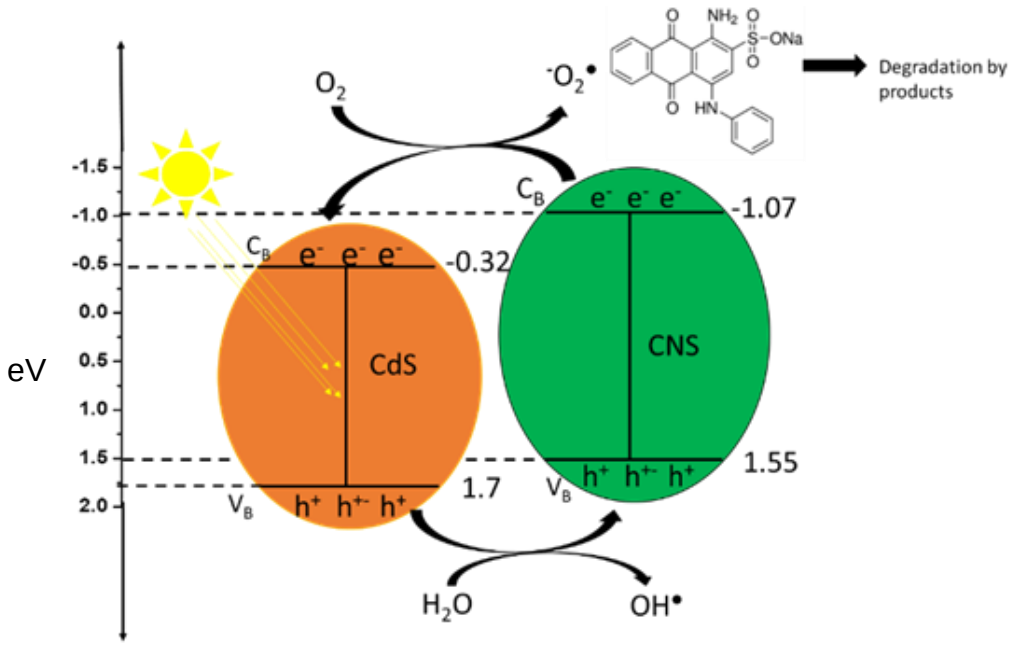

Figure 5.18.The proposed mechanism for photocatalytic degradation of AB-25.

5.9 Conclusions

This chapter demonstrated the in-situ method of cadmium sulphide-graphitic carbon nitride nanosheets (CdS/CNS) with CdS/CNS mass ratios in the range (10-30%) for the photocatalytic degradation of acid blue-25. Increasing the CNS loading decreased the photocatalytic efficiency of CdS and high AB-25 removal was achieved with lower CNS load (10% CNS/CdS).

References

[1] A. Azizullah, M.N.K. Khattak, P. Richter, D.P. Häder, Water pollution in Pakistan and its impact on public health - A review, Environ. Int. 37 (2011) 479–497. doi:10.1016/j.envint.2010.10.007.

[2] I. Gehrke, A. Somborn-schulz, Innovations in nanotechnology for water treatment, Nanotechnol. Sci. Appl. 8 (2015) 1–17.

[3] C.J.. ; G. Vorösmarty Pamela; ; Salisbury, Joseph; ; Lammers, Richard B., Global Water Resources: Vulnerability from Climate Change and Population Growth, Science (80-.). 289 (2000) 284–288. doi:10.1126/science.289.5477.284.

[4] J. Theron, T.E. Cloete, Emerging Waterborne Infections: Contributing Factors, Agents, and Detection Tools, Crit. Rev. Microbiol. 28 (2008) 1–26. doi:10.1080/1040-840291046669.

[5] K.K. Jain, Nanotechnology and Water, Contemp. Mater. 1 (2012) 26–30. doi:10.7251/122.

[6] F.W. Owa, Water pollution : sources , effects , control and management, Int. Lett. 3 (2014) 1–6.

[7] H. Zhou, D.W. Smith, Advanced technologies in water and wastewater treatment, in: 2002. doi:10.1139/S02-020.

[8] M. Wakil, M. Burhan, L. Ang, K. Choon, Energy-water-environment nexus underpinning future desalination sustainability, Desalination. 413 (2017) 52–64. doi:10.1016/j.desal.2017.03.009.

[9] M. Palaniappan, K. Address, Peak_Water_Talk.Pdf, in: Utah Am. Plan. Assoc. Annu. Conf., 2008: pp. 3–11.

[10] J.K. Bwapwa, Review on Main Issues Causing Deterioration of Water Quality and Water Scarcity: Case Study of South Africa, Environ. Manag. Sustain. Dev. 7 (2018) 14. doi:10.5296/emsd.v7i3.13156.

[11] J. Wang, S. Wang, Removal of pharmaceuticals and personal care products

(PPCPs) from wastewater: A review, J. Environ. Manage. 182 (2016) 620–640. doi:10.1016/j.jenvman.2016.07.049.

[12] G. Boczkaj, A. Fernandes, Wastewater treatment by means of advanced oxidation processes at basic pH conditions : A review, Chem. Eng. J. 320 (2017) 608–633. doi:10.1016/j.cej.2017.03.084.

[13] R. Ananthashankar, Treatment of textile effluent containing Reactive Red 120 dye using advanced oxidation, 2012.

[14] K. Klaus, Pharmaceuticals in the Environment, Annu Rev Env. Resour. 35 (2010) 57–75. doi:10.1146/annurev-environ-052809-161223.

[15] G. Kjosavik, Subtle changes, 2001.

[16] A.B.A. Boxall, M.A. Rudd, B.W. Brooks, D.J. Caldwell, K. Choi, S. Hickmann, E. Innes, K. Ostapyk, J.P. Staveley, T. Verslycke, G.T. Ankley, K.F. Beazley, Review Pharmaceuticals and Personal Care Products in the Environment : What Are the Big Questions ?, 120 (2012) 1221–1229.

[17] G. Li, X. Nie, Y. Gao, T. An, Applied Catalysis B : Environmental Can environmental pharmaceuticals be photocatalytically degraded and completely mineralized in water using g-C_3N_4/TiO_2 under visible light irradiation ?— Implications of persistent toxic intermediates, "Applied Catal. B, Environ. 180 (2016) 726–732. doi:10.1016/j.apcatb.2015.07.014.

[18] B. Hoeger, B. Köllner, D.R. Dietrich, B. Hitzfeld, Water-borne diclofenac affects kidney and gill integrity and selected immune parameters in brown trout (Salmo trutta f. fario), Aquat. Toxicol. 75 (2005) 53–64. doi:10.1016/j.aquatox.2005.07.006.

[19] M. Lillenberg, S. Yurchenko, K. Kipper, K. Herodes, V. Pihl, R. Lõhmus, M. Ivask, A. Kuu, S. Kutti, S. V. Litvin, L. Nei, Presence of fluoroquinolones and sulfonamides in urban sewage sludge and their degradation as a result of composting, Int. J. Environ. Sci. Technol. 7 (2010) 307–312. doi:10.1007/BF03326140.

[20] S.K. Khetan, T.J. Collins, Human pharmaceuticals in the aquatic environment:

A challenge to green chemisty, Chem. Rev. 107 (2007) 2319–2364. doi:10.1021/cr020441w.

[21] A.M. Deegan, B. Shaik, K. Nolan, K. Urell, M. Oelgemöller, J. Tobin, A. Morrissey, Treatment options for wastewater effluents from pharmaceutical companies, Int. J. Environ. Sci. Technol. 8 (2011) 649–666. doi:10.1007/BF03326250.

[22] A.J. Ebele, M. Abou-Elwafa Abdallah, S. Harrad, Pharmaceuticals and personal care products (PPCPs) in the freshwater aquatic environment, Emerg. Contam. 3 (2017) 1–16. doi:10.1016/j.emcon.2016.12.004.

[23] B.D. Blair, J.P. Crago, C.J. Hedman, R.D. Klaper, Chemosphere Pharmaceuticals and personal care products found in the Great Lakes above concentrations of environmental concern, Chemosphere. 93 (2013) 2116–2123. doi:10.1016/j.chemosphere.2013 .07.057.

[24] C.U. Meteyer, B.A. Rideout, M. Gilbert, H.L. Shivaprasad, L. Oaks, Pathology and proposed pathophysiology of diclofenac poisoning in free living and experimentally exposed oriental white backed vultures (GYPS BENGALENSIS), J. Wildl. Dis. 41 (2005) 707–716.

[25] R. Triebskorn, H. Casper, V. Scheil, J. Schwaiger, Ultrastructural effects of pharmaceuticals (carbamazepine, clofibric acid, metoprolol, diclofenac) in rainbow trout (Oncorhynchus mykiss) and common carp (Cyprinus carpio), Anal. Bioanal. Chem. 387 (2007) 1405–1416. doi:10.1007/s00216-006-1033-x.

[26] J. Schwaiger, H. Ferling, U. Mallow, H. Wintermayr, R.D. Negele, Toxic effects of the non-steroidal anti-inflammatory drug diclofenac. Part I: Histopathological alterations and bioaccumulation in rainbow trout, Aquat. Toxicol. 68 (2004) 141–150. doi:10.1016/j.aquatox.2004.03.014.

[27] A.A.C. and Z.M. Dana Manuela Sirbu, Daniela Curseu, Monica Popa, Environmental Risks of Pharmaceuticals and Personal Care Products in Water, in: Tenth Int. Water Technol. Conf., 2006: pp. 1151–1162.

[28] E. Archer, G.M. Wolfaardt, J.H. van Wyk, Pharmaceutical and personal care products (PPCPs) as endocrine disrupting contaminants (EDCs) in South

African surface waters, Water SA. 43 (2017) 684–706. doi:10.4314/wsa.v43i4.16.

[29] O.A.H. Jones, N. Voulvoulis, J.N. Lester, Potential ecological and human health risks associated with the presence of pharmaceutically active compounds in the aquatic environment, Crit. Rev. Toxicol. 34 (2004) 335–350. doi:10.1080/10408440490464697.

[30] A.K. Karen, J.B. Paul, H.M. Kenneth, e P.P. Vinc, E.E. Robert, M.L. James, W.F. Robert, Disrupting Queer Incluslon, Pnas. 104 (2007) 8897–8901. doi:10.1073/pnas.0609568104.

[31] D.J. Caldwell, F. Mastrocco, T.H. Hutchinson, R. Länge, D. Heijerick, C. Janssen, P.D. Anderson, J.P. Sumpter, Derivation of an aquatic predicted no-effect concentration for the synthetic hormone, 17α-ethinyl estradiol, Environ. Sci. Technol. 42 (2008) 7046–7054. doi:10.1021/es800633q.

[32] M.F. Rahman, E.K. Yanful, S.Y. Jasim, Endocrine disrupting compounds (EDCs) and pharmaceuticals and personal care products (PPCPs) in the aquatic environment: Implications for the drinking water industry and global environmental health, J. Water Health. 7 (2009) 224–243. doi:10.2166/wh.2009.021.

[33] B. Lellis, C.Z. Fávaro-polonio, J.A. Pamphile, J.C. Polonio, Effects of textile dyes on health and the environment and bioremediation potential of living organisms, Biotecnol. Res. Innov. 3 (2019) 275–290. doi:10.1016/j.biori.2019.09.001.

[34] R. Paper, Decolorization of mixture of dyes : A critical review, Glob. J. Environ. Sci. Manag. Glob. J. Environ. Sci. Manag. 1 (2015) 71–94. doi:10.7508/gjesm.2015.01.007.

[35] A.M. Deegan, B. Shaik, K. Nolan, K. Urell, J. Tobin, A. Morrissey, Treatment options for wastewater effluents from pharmaceutical companies, 8 (2011) 649–666.

[36] L. Cheng, Q. Xiang, Y. Liao, H. Zhang, CdS-Based photocatalysts, Royal Society of Chemistry, 2018. doi:10.1039/c7ee03640j.

[37] H.L. Lee, A.M. Issam, M. Belmahi, M.B. Assouar, H. Rinnert, M. Alnot, Synthesis and characterizations of bare cds nanocrystals using chemical precipitation method for photoluminescence application, J. Nanomater. 2009 (2009). doi:10.1155/2009/914501.

[38] S. Kumar, S. Karthikeyan, A.F. Lee, g-C_3N_4-based nanomaterials for visible light-driven photocatalysis, Catalysts. 8 (2018). doi:10.3390/catal8020074.

[39] S. Cao, J. Low, J. Yu, M. Jaroniec, Polymeric Photocatalysts Based on Graphitic Carbon Nitride, Adv. Mater. 27 (2015) 2150–2176. doi:10.1002/adma.201500033.

[40] Q.Y. Liu, Y.L. Qi, Y.F. Zheng, X.C. Song, Synthesis and enhanced photocatalytic activity of g-C_3N_4 hybridized CdS nanoparticles, Bull. Mater. Sci. 40 (2017) 1329–1333. doi:10.1007/s12034-017-1513-y.

[41] R.C. Pawar, V. Khare, C.S. Lee, Hybrid photocatalysts using graphitic carbon nitride/cadmium sulfide/reduced graphene oxide (g-C_3N_4/CdS/RGO) for superior photodegradation of organic pollutants under UV and visible light, Dalt. Trans. 43 (2014) 12514–12527. doi:10.1039/c4dt01278j.

[42] S.W. Cao, Y.P. Yuan, J. Fang, M.M. Shahjamali, F.Y.C. Boey, J. Barber, S.C. Joachim Loo, C. Xue, In-situ growth of CdS quantum dots on g-C_3N_4 nanosheets for highly efficient photocatalytic hydrogen generation under visible light irradiation, Int. J. Hydrogen Energy. 38 (2013) 1258–1266. doi:10.1016/j.ijhydene.2012.10.116.

[43] S. Rasalingam, R. Peng, R.T. Koodali, Removal of hazardous pollutants from wastewaters: Applications of TiO 2-SiO2 mixed oxide materials, J. Nanomater. 2014 (2014). doi:10.1155/2014/617405.

[44] M.K. Hasan, A. Shahriar, K.U. Jim, Water pollution in Bangladesh and its impact on public health, Heliyon. 5 (2019) e02145. doi:10.1016/j.heliyon.2019.e02145.

[45] S. Rasalingam, R. Peng, R.T. Koodali, Removal of harzadous pollutants from wastewaters: Application of TiO_2-SiO_2, *Review*. (2014).

[46] U. Tahir, A. Yasmin, U.H. Khan,-SiO Phytoremediation: Potential flora for synthetic dyestuff metabolism, J. Kin mixed oxide materials g Saud Univ. - Sci. 28 (2016) 119–130. doi:10.1016/j.jksus.2015.05.009.

[47] G. Dong, Y. Zhang, Q. Pan, J. Qiu, A fantastic graphitic carbon nitride (g-C3N4) material: Electronic structure, photocatalytic and photoelectronic properties, J. Photochem. Photobiol. C Photochem. Rev. 20 (2014) 33–50. doi:10.1016/j.jphotochemrev.2014.04.002.

[48] D.A. Yaseen, M. Scholz, Textile dye wastewater characteristics and constituents of synthetic effluents: a critical review, Springer Berlin Heidelberg, 2019. doi:10.1007/s13762-018-2130-z.

[49] T. Robinson, G. McMullan, R. Marchant, P. Nigam, Remediation of dyes in textile effluent: A critical review on current treatment technologies with a proposed alternative, Bioresour. Technol. 77 (2001) 247–255. doi:10.1016/S0960-8524(00)00080-8.

[50] G.S. Gupta, G. Prasad, V.N. Singh, Removal of chrome dye from aqueous solutions by mixed adsorbents: Fly ash and coal, Water Res. 24 (1990) 45–50. doi:10.1016/0043-1354(90)90063-C.

[51] N. Muhd Julkapli, S. Bagheri, S. Bee Abd Hamid, Recent advances in heterogeneous photocatalytic decolorization of synthetic dyes, Sci. World J. 2014 (2014) 25. doi:10.1155/2014/692307.

[52] Y. Fu, T. Viraraghavan, Fungal decolorization of dye wastewaters: A review, Bioresour. Technol. 79 (2001) 251–262. doi:10.1016/S0960-8524(01)00028-1.

[53] V.K. Gupta, S. Khamparia, I. Tyagi, D. Jaspal, A. Malviya, Decolorization of mixture of dyes: A critical review, Glob. J. Environ. Sci. Manag. Glob. J. Environ. Sci. Manag. 1 (2015) 71–94. doi:10.7508/gjesm.2015.01.007.

[54] Z. Aksu, Application of biosorption for the removal of organic pollutants: A review, Process Biochem. 40 (2005) 997–1026. doi:10.1016/j.procbio.2004.04.008.

[55] S. Sumathi, B.S. Manju, Uptake of reactive textile dyes by Aspergillus foetidus,

Enzyme Microb. Technol. 27 (2000) 347–355. doi:10.1016/S0141-0229(00)00234-9.

[56] Z. Aksu, S. Tezer, Equilibrium and kinetic modelling of biosorption of Remazol black B by Rhizopus arrhizus in a batch system: Effect of temperature, Process Biochem. 36 (2000) 431–439. doi:10.1016/S0032-9592(00)00233-8.

[57] T. O'Mahony, E. Guibal, J.M. Tobin, Reactive dye biosorption by Rhizopus arrhizus biomass, Enzyme Microb. Technol. 31 (2002) 456–463. doi:10.1016/S0141-0229(02)00110-2.

[58] B. Aruna, R.S. L, E. Shiva, A. Srinu, P. Roja, D. Vijayalakshmi, D.V.R. Prasad, Research Article Biodecolorization of Anthraquinone Textile (Acid Blue 25) Dye By Klebsiella Sp, 6 (2015) 3216–3222.

[59] M. Auta, B.H. Hameed, Preparation of waste tea activated carbon using potassium acetate as an activating agent for adsorption of Acid Blue 25 dye, Chem. Eng. J. 171 (2011) 502–509. doi:10.1016/j.cej.2011.04.017.

[60] C.A. Hsu, T.N. Wen, Y.C. Su, Z.B. Jiang, C.W. Chen, L.F. Shyur, Biological degradation of anthroquinone and azo dyes by a novel laccase from Lentinus sp., Environ. Sci. Technol. 46 (2012) 5109–5117. doi:10.1021/es2047014.

[61] H. hong Li, Y. tao Wang, Y. Wang, H. xia Wang, K. kai Sun, Z. mei Lu, Bacterial degradation of anthraquinone dyes, J. Zhejiang Univ. Sci. B. 20 (2019) 528–540. doi:10.1631/jzus.B1900165.

[62] M.E. Malefane, U. Feleni, A.T. Kuvarega, Tetraphenylporphyrin/WO_3/exfoliated graphite nanocomposite for photocatalytic degradation of an acid dye under visible light irradiation, New J. Chem. 10 (2019) 1–6. doi:10.1039/c9nj02747e.

[63] S. Benkhaya, S. El Harfi, A. El Harfi, Classifications , properties and applications of textile dyes : A review, Appl. J. Environ. Sci. 3 (2018) 311–320.

[64] D. Chakrabortty, S. Sen Gupta, Photo-catalytic decolourisation of toxic dye with N-doped titania: A case study with Acid Blue 25, J. Environ. Sci. (China). 25 (2013) 1034–1043. doi:10.1016/S1001-0742(12)60108-9.

[65] T. Deblonde, C. Cossu-Leguille, P. Hartemann, Emerging pollutants in

wastewater: A review of the literature, Int. J. Hyg. Environ. Health. 214 (2011) 442–448. doi:10.1016/j.ijheh.2011.08.002.

[66] M. Clara, G. Windhofer, W. Hartl, K. Braun, M. Simon, O. Gans, C. Scheffknecht, A. Chovanec, Occurrence of phthalates in surface runoff, untreated and treated wastewater and fate during wastewater treatment, Chemosphere. 78 (2010) 1078–1084. doi:10.1016/j.chemosphere.2009.12.052.

[67] M. la Farré, S. Pérez, L. Kantiani, D. Barceló, Fate and toxicity of emerging pollutants, their metabolites and transformation products in the aquatic environment, TrAC - Trends Anal. Chem. 27 (2008) 991–1007. doi:10.1016/j.trac.2008.09.010.

[68] A. Jennifer, M.A. Abdallah, S. Harrad, Pharmaceuticals and personal care products (PPCPs) in the freshwater aquatic environment, Emerg. Contam. 3 (2017) 1–16. doi:10.1016/j.emcon.2016.12.004.

[69] S.R. Hughes, P. Kay, L.E. Brown, Global synthesis and critical evaluation of pharmaceutical data sets collected from river systems, Environ. Sci. Technol. 47 (2013) 661–677. doi:10.1021/es3030148.

[70] D. Ashton, M. Hilton, K. V. Thomas, Investigating the environmental transport of human pharmaceuticals to streams in the United Kingdom, Sci. Total Environ. 333 (2004) 167–184. doi:10.1016/j.scitotenv.2004.04.062.

[71] S. Wiandt, H.J. Poremski, Selection and prioritisation procedure of hazardous substances for the marine environment within Ospar/dynamic, Ecotoxicology. 11 (2002) 393–399. doi:10.1023/A:1020569608441.

[72] L. Lonappan, S.K. Brar, R.K. Das, M. Verma, R.Y. Surampalli, Diclofenac and its transformation products: Environmental occurrence and toxicity - A review, Environ. Int. 96 (2016) 127–138. doi:10.1016/j.envint.2016.09.014.

[73] Y. Zhang, S.U. Geißen, C. Gal, Carbamazepine and diclofenac: Removal in wastewater treatment plants and occurrence in water bodies, Chemosphere. 73 (2008) 1151–1161. doi:10.1016/j.chemosphere.2008.07.086.

[74] V. Acuña, A. Ginebreda, J.R. Mor, M. Petrovic, S. Sabater, J. Sumpter, D. Barceló, Balancing the health benefits and environmental risks of pharmaceuticals: Diclofenac as an example, Environ. Int. 85 (2015) 327–333. doi:10.1016/j.envint.2015.09.023.

[75] A.C. Johnson, E. Dumont, R.J. Williams, R. Oldenkamp, I. Cisowska, J.P. Sumpter, Do concentrations of ethinylestradiol, estradiol, and diclofenac in European rivers exceed proposed EU environmental quality standards?, Environ. Sci. Technol. 47 (2013) 12297–12304. doi:10.1021/es4030035.

[76] A.Y. Shan, T.I.M. Ghazi, S.A. Rashid, Immobilisation of titanium dioxide onto supporting materials in heterogeneous photocatalysis: A review, Appl. Catal. A Gen. 389 (2010) 1–8. doi:10.1016/j.apcata.2010.08.053.

[77] Y. Mehmood, Index Academic Sciences Original Article Development and validation of UV-Vis spectroscophotometric methods for the estimation of diclofenac sodium injections., Int. J. Pharm. Pract. Pharm. Sci. 2 (2015) 1–6.

[78] D. Chen, A.K. Ray, Photodegradation kinetics of 4-nitrophenol in TiO2 suspension, Water Res. 32 (1998) 3223–3234. doi:10.1016/S0043-1354(98)00118-3.

[79] C. Martínez, M. Canle L., M.I. Fernández, J.A. Santaballa, J. Faria, Aqueous degradation of diclofenac by heterogeneous photocatalysis using nanostructured materials, Appl. Catal. B Environ. 107 (2011) 110–118. doi:10.1016/j.apcatb.2011.07.003.

[80] M. Letzel, G. Metzner, T. Letzel, Exposure assessment of the pharmaceutical diclofenac based on long-term measurements of the aquatic input, Environ. Int. 35 (2009) 363–368. doi:10.1016/j.envint.2008.09.002.

[81] C. Hao, R. Clement, P. Yang, Liquid chromatography-tandem mass spectrometry of bioactive pharmaceutical compounds in the aquatic environment-a decade's activities, Anal. Bioanal. Chem. 387 (2007) 1247–1257. doi:10.1007/s00216-006-0956-6.

[82] A.J. Sosiak, T. Hebben, A preliminary survey of pharmaceuticals and endocrine disrupting compounds in treated municipal wastewaters and

receiving rivers of Alberta /, 2005. doi:10.5962/bhl.title.113982.

[83] M.J. Benotti, R.A. Trenholm, B.J. Vanderford, J.C. Holady, B.D. Stanford, S.A. Snyder, Pharmaceuticals and endocrine disrupting compounds in U.S. drinking water, Environ. Sci. Technol. 43 (2009) 597–603. doi:10.1021/es801845a.

[84] T. Heberer, Tracking persistent pharmaceutical residues from municipal sewage to drinking water, J. Hydrol. 266 (2002) 175–189. doi:10.1016/S0022-1694(02)00165-8.

[85] F.O. Agunbiade, B. Moodley, Occurrence and distribution pattern of acidic pharmaceuticals in surface water, wastewater, and sediment of the Msunduzi River, Kwazulu-Natal, South Africa, Environ. Toxicol. Chem. 35 (2016) 36–46. doi:10.1002/etc.3144.

[86] M.T. Amin, A.A. Alazba, U. Manzoor, A Review of Removal of Pollutants from Water / Wastewater Using Different Types of Nanomaterials, 2014 (2014).

[87] M.R. Servos, D.T. Bennie, B.K. Burnison, A. Jurkovic, R. McInnis, T. Neheli, A. Schnell, P. Seto, S.A. Smyth, T.A. Ternes, Distribution of estrogens, 17β-estradiol and estrone, in Canadian municipal wastewater treatment plants, Sci. Total Environ. 336 (2005) 155–170. doi:10.1016/j.scitotenv.2004.05.025.

[88] T. Urase, T. Kikuta, Separate estimation of adsorption and degradation of pharmaceutical substances and estrogens in the activated sludge process, Water Res. 39 (2005) 1289–1300. doi:10.1016/j.watres.2005.01.015.

[89] N. Vieno, T. Tuhkanen, L. Kronberg, Removal of pharmaceuticals in drinking water treatment: Effect of chemical coagulation, Environ. Technol. 27 (2006) 183–192. doi:10.1080/09593332708618632.

[90] P. Westerhoff, Y. Yoon, S. Snyder, E. Wert, Fate of endocrine-disruptor, pharmaceutical, and personal care product chemicals during simulated drinking water treatment processes, Environ. Sci. Technol. 39 (2005) 6649–6663. doi:10.1021/es0484799.

[91] M. Petrovic, A. Diaz, F. Ventura, D. Barceló, Occurrence and removal of estrogenic short-chain ethoxy nonylphenolic compounds and their halogenated

derivatives during drinking water production, Environ. Sci. Technol. 37 (2003) 4442–4448. doi:10.1021/es034139w.

[92] G. Becher, Drinking Water Chlorination and Health, Acta Hydrochim. Hydrobiol. 27 (1999) 100–102. doi:10.1002/(sici)1521-401x(199902)27:2<100::aid-aheh100>3.3.co;2-1.

[93] N. Bolong, A.F. Ismail, M.R. Salim, T. Matsuura, A review of the effects of emerging contaminants in wastewater and options for their removal, Desalination. 239 (2009) 229–246. doi:10.1016/j.desal.2008.03.020.

[94] Y. Yoon, P. Westerhoff, S.A. Snyder, E.C. Wert, Nanofiltration and ultrafiltration of endocrine disrupting compounds, pharmaceuticals and personal care products, J. Memb. Sci. 270 (2006) 88–100. doi:10.1016/j.memsci.2005.06.045.

[95] L. Braeken, B. Bettens, K. Boussu, P. Van der Meeren, J. Cocquyt, J. Vermant, B. Van der Bruggen, Transport mechanisms of dissolved organic compounds in aqueous solution during nanofiltration, J. Memb. Sci. 279 (2006) 311–319. doi:10.1016/j.memsci.2005.12.024.

[96] J. Lu, T. Zhang, J. Ma, Z. Chen, Evaluation of disinfection by-products formation during chlorination and chloramination of dissolved natural organic matter fractions isolated from a filtered river water, J. Hazard. Mater. 162 (2009) 140–145. doi:10.1016/j.jhazmat.2008.05.058.

[97] M.N. Chong, B. Jin, C.W.K. Chow, C. Saint, Recent developments in photocatalytic water treatment technology: a review., Water Res. 44 (2010) 2997–3027. doi:10.1016/j.watres.2010.02.039.

[98] D.H. Bremner, R. Molina, F. Martínez, J.A. Melero, Y. Segura, Degradation of phenolic aqueous solutions by high frequency sono-Fenton systems (US-Fe_2O_3/SBA-15-H_2O_2), Appl. Catal. B Environ. 90 (2009) 380–388. doi:10.1016/j.apcatb.2009.03.028.

[99] G. Li, Z. Wang, M. Yu, Z. Quan, J. Lin, Fabrication and optical properties of core-shell structured spherical SiO_2@$GdVO_4$:Eu^{3+} phosphors via sol-gel process, J. Solid State Chem. 179 (2006) 2698–2706.

doi:10.1016/j.jssc.2006.05.019.

[100] J. Zhang, G. Xiao, F.X. Xiao, B. Liu, Revisiting one-dimensional TiO_2 based hybrid heterostructures for heterogeneous photocatalysis: A critical review, Mater. Chem. Front. 1 (2017) 231–250. doi:10.1039/c6qm00141f.

[101] Y. Cui, In-situ synthesis of C_3N_4/CdS composites with enhanced photocatalytic properties, Cuihua Xuebao/Chinese J. Catal. 36 (2015) 372–379. doi:10.1016/S1872-2067(14)60237-0.

[102] V.S. Kosera, T.M. Cruz, E.S. Chaves, E.R.L. Tiburtius, Journal of Photochemistry and Photobiology A : Chemistry Triclosan degradation by heterogeneous photocatalysis using ZnO immobilized in biopolymer as catalyst, "Journal Photochem. Photobiol. A Chem. 344 (2017) 184–191. doi:10.1016/j.jphotochem.2017.05.014.

[103] M.R. Hoffmann, S.T. Martin, W. Choi, D.W. Bahnemann, Environmental Applications of Semiconductor Photocatalysis, Chem. Rev. 95 (1995) 69–96. doi:10.1021/cr00033a004.

[104] J.-M. Herrmann, Water Treatment By Heterogeneous Photocatalysis, in: 1999: pp. 171–194. doi:10.1142/9781848160613_0009.

[105] U.I. Gaya, A.H. Abdullah, Heterogeneous photocatalytic degradation of organic contaminants over titanium dioxide: A review of fundamentals, progress and problems, J. Photochem. Photobiol. C Photochem. Rev. 9 (2008) 1–12. doi:10.1016/j.jphotochemrev.2007.12.003.

[106] M. Ni, M.K.H. Leung, D.Y.C. Leung, K. Sumathy, A review and recent developments in photocatalytic water-splitting using TiO_2 for hydrogen production, Renew. Sustain. Energy Rev. 11 (2007) 401–425. doi:10.1016/j.rser.2005.01.009.

[107] M. Yasmina, K. Mourad, S.H. Mohammed, C. Khaoula, Treatment heterogeneous photocatalysis; Factors influencing the photocatalytic degradation by TiO_2, Energy Procedia. 50 (2014) 559–566. doi:10.1016/j.egypro.2014.06.068.

[108] L. Cheng, Q. Xiang, Y. Liao, Environmental Science, (2018) 4–7. doi:10.1039/c7ee03640j.

[109] M. Wongaree, S. Chiarakorn, S. Chuangchote, Photocatalytic Improvement under Visible Light in TiO_2 Nanoparticles by Carbon Nanotube Incorporation, 2015 (2015).

[110] R.S. Singh, V.K. Rangari, S. Sanagapalli, V. Jayaraman, S. Mahendra, V.P. Singh, Nano-structured CdTe, CdS and TiO_2 for thin film solar cell applications, Sol. Energy Mater. Sol. Cells. 82 (2004) 315–330. doi:10.1016/j.solmat.2004.02.006.

[111] S. Leong, A. Razmjou, K. Wang, K. Hapgood, X. Zhang, H. Wang, TiO2 based photocatalytic membranes: A review, J. Memb. Sci. 472 (2014) 167–184. doi:10.1016/j.memsci.2014.08.016.

[112] Y. Yu, J.C. Yu, J.G. Yu, Y.C. Kwok, Y.K. Che, J.C. Zhao, L. Ding, W.K. Ge, P.K. Wong, Enhancement of photocatalytic activity of mesoporous TiO_2 by using carbon nanotubes, Appl. Catal. A Gen. 289 (2005) 186–196. doi:10.1016/j.apcata.2005.04.057.

[113] R. Abe, K. Sayama, H. Arakawa, Significant effect of iodide addition on water splitting into H_2 and O_2 over Pt-loaded TiO_2 photocatalyst: Suppression of backward reaction, Chem. Phys. Lett. 371 (2003) 360–364. doi:10.1016/S0009-2614(03)00252-5.

[114] S. Sakthivel, M. V. Shankar, M. Palanichamy, B. Arabindoo, D.W. Bahnemann, V. Murugesan, Enhancement of photocatalytic activity by metal deposition: Characterisation and photonic efficiency of Pt, Au and Pd deposited on TiO_2 catalyst, Water Res. 38 (2004) 3001–3008. doi:10.1016/j.watres.2004.04.046.

[115] E. Szabó-Bárdos, H. Czili, A. Horváth, Photocatalytic oxidation of oxalic acid enhanced by silver deposition on a TiO_2 surface, J. Photochem. Photobiol. A Chem. 154 (2003) 195–201. doi:10.1016/S1010-6030(02)00330-1.

[116] N.L. Wu, M.S. Lee, Enhanced TiO_2 photocatalysis by Cu in hydrogen production from aqueous methanol solution, Int. J. Hydrogen Energy. 29 (2004) 1601–1605. doi:10.1016/j.ijhydene.2004.02.013.

[117] F. Haque, T. Daeneke, K. Kalantar-zadeh, J.Z. Ou, Two-Dimensional Transition Metal Oxide and Chalcogenide-Based Photocatalysts, Nano-Micro Lett. 10 (2018) 1–27. doi:10.1007/s40820-017-0176-y.

[118] A.H. Reshak, S. Auluck, Electronic and optical properties of the 1T phases of TiS2, TiSe2, and TiTe2, Phys. Rev. B - Condens. Matter Mater. Phys. 68 (2003) 1–7. doi:10.1103/PhysRevB.68.245113.

[119] J.A. Wilson, A.D. Yoffe, The transition metal dichalcogenides discussion and interpretation of the observed optical, electrical and structural properties, Adv. Phys. 18 (1969) 193–335. doi:10.1080/00018736900101307.

[120] L. Nie, Q. Zhang, Recent progress in crystalline metal chalcogenides as efficient photocatalysts for organic pollutant degradation, Inorg. Chem. Front. 4 (2017) 1953–1962. doi:10.1039/c7qi00651a.

[121] F. Li, X. Liu, Q. Zhang, T. Kong, H. Jin, Fabrication and photocatalytic property of CuO nanosheets via a facile solution route, Cryst. Res. Technol. 47 (2012) 1140–1147. doi:10.1002/crat.201200143.

[122] B. Peng, P.K. Ang, K.P. Loh, Two-dimensional dichalcogenides for light-harvesting applications, Nano Today. 10 (2015) 128–137. doi:10.1016/j.nantod.2015.01.007.

[123] D. Ke, S. Liu, K. Dai, J. Zhou, L. Zhang, T. Peng, CdS/regenerated cellulose nanocomposite films for highly efficient photocatalytic H_2 production under visible light irradiation, J. Phys. Chem. C. 113 (2009) 16021–16026. doi:10.1021/jp903378q.

[124] S. Xiong, B. Xi, Y. Qian, CdS hierarchical nanostructures with tunable morphologies: Preparation and photocatalytic properties, J. Phys. Chem. C. 114 (2010) 14029–14035. doi:10.1021/jp1049588.

[125] W.T. Yao, S.H. Yu, S.J. Liu, J.P. Chen, X.M. Liu, F.Q. Li, Architectural control syntheses of CdS and CdSe nanoflowers, branched nanowires, and nanotrees via a solvothermal approach in a mixed solution and their photocatalytic property, J. Phys. Chem. B. 110 (2006) 11704–11710. doi:10.1021/jp060164n.

[126] Q. Shen, J. Xue, A. Mi, H. Jia, X. Liu, B. Xu, The study on properties of CdS photocatalyst with different ratios of zinc-blende and wurtzite structure, RSC Adv. 3 (2013) 20930–20935. doi:10.1039/c3ra42179a.

[127] M. Liu, B. Wang, Y. Zheng, F. Xue, Y. Chen, L. Guo, Transformation of zincblende nanoparticles into wurtzite microrods by a dissolution-regrowth process: An intergrowth homojunction with enhanced photocatalytic activity, Catal. Sci. Technol. 6 (2016) 3371–3377. doi:10.1039/c6cy00298f.

[128] K. Wu, H. Zhu, T. Lian, Ultrafast Exciton Dynamics and Light-Driven H2 Evolution in Colloidal Semiconductor Nanorods and Pt-Tipped Nanorods, Acc. Chem. Res. 48 (2015) 851–859. doi:10.1021/ar500398g.

[129] J. Yu, Y. Yu, P. Zhou, W. Xiao, B. Cheng, Morphology-dependent photocatalytic H_2-production activity of CdS, Appl. Catal. B Environ. 156–157 (2014) 184–191. doi:10.1016/j.apcatb.2014.03.013.

[130] B. Weng, S. Liu, N. Zhang, Z.R. Tang, Y.J. Xu, A simple yet efficient visible-light-driven CdS nanowires-carbon nanotube 1D-1D nanocomposite photocatalyst, J. Catal. 309 (2014) 146–155. doi:10.1016/j.jcat.2013.09.013.

[131] F. Caruso, X. Shi, R.A. Caruso, A. Susha, Hollow titania spheres from layered precursor deposition on sacrificial colloidal core particles, Adv. Mater. 13 (2001) 740–744. doi:10.1002/1521-4095(200105)13:10<740::AID-ADMA740>3.0.CO;2-6.

[132] C. Li, L. Han, R. Liu, H. Li, S. Zhang, G. Zhang, Controlled synthesis of CdS micro/nano leaves with (0001) facets exposed: Enhanced photocatalytic activity toward hydrogen evolution, J. Mater. Chem. 22 (2012) 23815–23820. doi:10.1039/c2jm35415b.

[133] T. Tsuzuki, P.G. McCormick, Synthesis of CdS quantum dots by mechanochemical reaction, Appl. Phys. A Mater. Sci. Process. 65 (1997) 607–609. doi:10.1007/s003390050629.

[134] A. Dumbrava, G. Prodan, D. Berger, M. Bica, Properties of PEG-capped CdS nanopowders synthesized under very mild conditions, Powder Technol. 270 (2015) 197–204. doi:10.1016/j.powtec.2014.10.012.

[135] A. Samadi-maybodi, F. Abbasi, R. Akhoondi, Aqueous synthesis and characterization of CdS quantum dots capped with some amino acids and investigations of their photocatalytic activities, Colloids Surfaces A Physicochem. Eng. Asp. 447 (2014) 111–119. doi:10.1016/j.colsurfa.2014.01.036.

[136] P. Chandran, P. Kumari, S. Sudheer Khan, Photocatalytic activation of CdS NPs under visible light for environmental cleanup and disinfection, Sol. Energy. 105 (2014) 542–547. doi:10.1016/j.solener.2014.04.028.

[137] M. Darwish, A. Mohammadi, N. Assi, Microwave-assisted polyol synthesis and characterization of pvp-capped cds nanoparticles for the photocatalytic degradation of tartrazine, Mater. Res. Bull. 74 (2016) 387–396. doi:10.1016/j.materresbull.2015.11.002.

[138] R.A. Devi, M. Latha, S. Velumani, G. Oza, P. Reyes-Figueroa, M. Rohini, I.G. Becerril-Juarez, J.-H. Lee, J. Yi, Synthesis and Characterization of Cadmium Sulfide Nanoparticles by Chemical Precipitation Method, J. Nanosci. Nanotechnol. 15 (2015) 8434–8439. doi:10.1166/jnn.2015.11472.

[139] G.C. De, A.M. Roy, S.S. Bhattacharya, Photocatalytic production of hydrogen and concomitant cleavage of industrial waste hydrogen sulphide, Int. J. Hydrogen Energy. 20 (1995) 127–131. doi:10.1016/0360-3199(94)P3692-V.

[140] W. Li, D. Li, Z. Chen, H. Huang, M. Sun, Y. He, X. Fu, High-efficient degradation of dyes by ZnxCd1-xS solid solutions under visible light irradiation, J. Phys. Chem. C. 112 (2008) 14943–14947. doi:10.1021/jp8049075.

[141] F. Yang, N.N. Yan, S. Huang, Q. Sun, L.Z. Zhang, Y. Yu, Zn-doped CdS nanoarchitectures prepared by hydrothermal synthesis: Mechanism for enhanced photocatalytic activity and stability under visible light, J. Phys. Chem. C. 116 (2012) 9078–9084. doi:10.1021/jp300939q.

[142] T.K. Jana, A. Pal, K. Chatterjee, Self assembled flower like CdS-ZnO nanocomposite and its photo catalytic activity, J. Alloys Compd. 583 (2014) 510–515. doi:10.1016/j.jallcom.2013.08.184.

[143] D. Wu, F. Wang, Y. Tan, C. Li, Facile synthesis of NiS/CdS nanocomposites

for photocatalytic degradation of quinoline under visible-light irradiation, RSC Adv. 6 (2016) 73522–73526. doi:10.1039/c6ra13439d.

[144] P. Nyamukamba, M.J. Moloto, H. Mungondori, Visible light-active CdS/TiO_2 hybrid nanoparticles immobilized on polyacrylonitrile membranes for the photodegradation of dyes in water, J. Nanotechnol. 2019 (2019). doi:10.1155/2019/5135618.

[145] S. Ma, J. Xie, J. Wen, K. He, X. Li, W. Liu, X. Zhang, Constructing 2D layered hybrid CdS nanosheets/MoS_2 heterojunctions for enhanced visible-light photocatalytic H 2 generation, Appl. Surf. Sci. 391 (2017) 580–591. doi:10.1016/j.apsusc.2016.07.067.

[146] Q. Cai, Z. Hu, Q. Zhang, B. Li, Z. Shen, Fullerene (C 60)/CdS nanocomposite with enhanced photocatalytic activity and stability, Appl. Surf. Sci. 403 (2017) 151–158. doi:10.1016/j.apsusc.2017.01.135.

[147] K.A. Adegoke, M. Iqbal, H. Louis, O.S. Bello, Synthesis, characterization and application of CdS/ZnO nanorod heterostructure for the photodegradation of Rhodamine B dye, Mater. Sci. Energy Technol. 2 (2019) 329–336. doi:10.1016/j.mset.2019.02.008.

[148] S. Cao, J. Yu, G-C_3N_4-based photocatalysts for hydrogen generation, J. Phys. Chem. Lett. 5 (2014) 2101–2107. doi:10.1021/jz500546b.

[149] J. Wen, J. Xie, X. Chen, X. Li, A review on g-C_3N_4 -based photocatalysts, Appl. Surf. Sci. 391 (2017) 72–123. doi:10.1016/j.apsusc.2016.07.030.

[150] E.A. Weiss, Designing the surfaces of semiconductor quantum dots for colloidal photocatalysis, ACS Energy Lett. 2 (2017) 1005–1013. doi:10.1021/acsenergylett.7b00061.

[151] K.R. Reddy, C.V. Reddy, M.N. Nadagouda, N.P. Shetti, S. Jaesool, T.M. Aminabhavi, Polymeric graphitic carbon nitride (g-C_3N_4)-based semiconducting nanostructured materials: Synthesis methods, properties and photocatalytic applications, J. Environ. Manage. 238 (2019) 25–40. doi:10.1016/j.jenvman.2019.02.075.

[152] S. Wang, C. Li, T. Wang, P. Zhang, A. Li, J. Gong, Controllable synthesis of nanotube-type graphitic C3N 4 and their visible-light photocatalytic and fluorescent properties, J. Mater. Chem. A. 2 (2014) 2885–2890. doi:10.1039/c3ta14576j.

[153] B. Weng, S. Liu, Z. Tang, Y. Xu, RSC Advances One-dimensional nanostructure based materials for versatile photocatalytic applications, (2014) 12685–12700. doi:10.1039/c3ra47910b.

[154] J. Zhang, Y. Chen, X. Wang, Two-dimensional covalent carbon nitride nanosheets: Synthesis, functionalization, and applications, Energy Environ. Sci. 8 (2015) 3092–3108. doi:10.1039/c5ee01895a.

[155] X. Bai, L. Wang, R. Zong, Y. Zhu, Photocatalytic activity enhanced via g-C_3N_4 nanoplates to nanorods, J. Phys. Chem. C. 117 (2013) 9952–9961. doi:10.1021/jp402062d.

[156] Q. Han, B. Wang, J. Gao, Z. Cheng, Y. Zhao, Z. Zhang, L. Qu, Atomically Thin Mesoporous Nanomesh of Graphitic C_3N_4 for High-Efficiency Photocatalytic Hydrogen Evolution, ACS Nano. 10 (2016) 2745–2751. doi:10.1021/acsnano.5b07831.

[157] X. Zhang, X. Xie, H. Wang, J. Zhang, B. Pan, Y. Xie, Enhanced photoresponsive ultrathin graphitic-phase C_3N_4 nanosheets for bioimaging, J. Am. Chem. Soc. 135 (2013) 18–21. doi:10.1021/ja308249k.

[158] J. Senker, K. Schwinghammer, B. V. Lotsch, C. Ziegler, M.B. Mesch, V. Duppel, Crystalline Carbon Nitride Nanosheets for Improved Visible-Light Hydrogen Evolution, J. Am. Chem. Soc. 136 (2014) 1730–1733. doi:10.1021/ja411321s.

[159] B. Luo, G. Liu, L. Wang, Recent advances in 2D materials for photocatalysis, Nanoscale. 8 (2016) 6904–6920. doi:10.1039/c6nr00546b.

[160] P. Niu, L. Zhang, G. Liu, H.M. Cheng, Graphene-like carbon nitride nanosheets for improved photocatalytic activities, Adv. Funct. Mater. 22 (2012) 4763–4770. doi:10.1002/adfm.201200922.

[161] Q. Liu, T. Chen, Y. Guo, Z. Zhang, X. Fang, Ultrathin g-C_3N_4 nanosheets coupled with carbon nanodots as 2D/0D composites for efficient photocatalytic H2 evolution, Appl. Catal. B Environ. 193 (2016) 248–258. doi:10.1016/j.apcatb.2016.04.034.

[162] Y. Xu, S.P. Gao, Band gap of C_3N_4 in the GW approximation, Int. J. Hydrogen Energy. 37 (2012) 11072–11080. doi:10.1016/j.ijhydene.2012.04.138.

[163] K. Maeda, X. Wang, Y. Nishihara, D. Lu, M. Antonietti, K. Domen, Photocatalytic activities of graphitic carbon nitride powder for water reduction and oxidation under visible light, J. Phys. Chem. C. 113 (2009) 4940–4947. doi:10.1021/jp809119m.

[164] A.H. Reshak, AA- and ABA-stacked carbon nitride (C_3N_4): Novel photocatalytic water splitting solar-to-hydrogen energy conversion, Phys. Chem. Chem. Phys. 20 (2018) 22972–22979. doi:10.1039/c8cp02898b.

[165] A.Y. Liu, M.L. Cohen, Prediction of new low compressibility solids, Science (80-.). 245 (1989) 841–842. doi:10.1126/science.245.4920.841.

[166] B. Jürgens, E. Irran, J. Senker, P. Kroll, H. Müller, W. Schnick, Melem (2,5,8-triamino-tri-s-triazine), an important intermediate during condensation of melamine rings to graphitic carbon nitride: Synthesis, structure determination by x-ray powder diffractometry, solid-state NMR, and theoretical studies, J. Am. Chem. Soc. 125 (2003) 10288–10300. doi:10.1021/ja0357689.

[167] J. Sehnert, K. Baerwinkel, J. Senker, Ab initio calculation of solid-state NMR spectra for different triazine and heptazine based structure proposals of g-C_3N_4, J. Phys. Chem. B. 111 (2007) 10671–10680. doi:10.1021/jp072001k.

[168] A. Thomas, A. Fischer, F. Goettmann, M. Antonietti, J.O. Müller, R. Schlögl, J.M. Carlsson, Graphitic carbon nitride materials: Variation of structure and morphology and their use as metal-free catalysts, J. Mater. Chem. 18 (2008) 4893–4908. doi:10.1039/b800274f.

[169] Y. Wang, J. Hong, W. Zhang, R. Xu, Carbon nitride nanosheets for photocatalytic hydrogen evolution: Remarkably enhanced activity by dye sensitization, Catal. Sci. Technol. 3 (2013) 1703–1711.

doi:10.1039/c3cy20836b.

[170] H. Luo, Z. Zeng, G. Zeng, C. Zhang, R. Xiao, C. Zhou, H. Wang, Y. Zhou, S. Tian, Recent progress on metal-organic frameworks based- and derived-photocatalysts for water splitting, Chem. Eng. J. (2019) 123196. doi:10.1016/j.cej.2019.123196.

[171] D. Zheng, C. Pang, Y. Liu, X. Wang, Shell-engineering of hollow g-C_3N_4 nanospheres via copolymerization for photocatalytic hydrogen evolution , Chem. Commun. 51 (2015) 9706–9709. doi:10.1039/c5cc03143e.

[172] S.W. Bian, Z. Ma, W.G. Song, Preparation and characterization of carbon nitride nanotubes and their applications as catalyst supporter, J. Phys. Chem. C. 113 (2009) 8668–8672. doi:10.1021/jp810630k.

[173] L. Xu, J. Xia, L. Wang, H. Ji, J. Qian, H. Xu, K. Wang, H. Li, Graphitic carbon nitride nanorods for photoelectrochemical sensing of trace copper(II) ions, Eur. J. Inorg. Chem. (2014) 3665–3673. doi:10.1002/ejic.201402051.

[174] S. Hu, R. Jin, G. Lu, D. Liu, J. Gui, The properties and photocatalytic performance comparison of Fe^{3+}-doped g-C_3N_4 and Fe_2O_3/g-C_3N_4 composite catalysts, RSC Adv. 4 (2014) 24863–24869. doi:10.1039/c4ra03290j.

[175] Y. Wang, Y. Wang, Y. Li, H. Shi, Y. Xu, H. Qin, X. Li, Y. Zuo, S. Kang, L. Cui, Simple synthesis of Zr-doped graphitic carbon nitride towards enhanced photocatalytic performance under simulated solar light irradiation, Catal. Commun. 72 (2015) 24–28. doi:10.1016/j.catcom.2015.08.022.

[176] P. Fageria, R. Nazir, S. Gangopadhyay, H.C. Barshilia, S. Pande, Graphitic-carbon nitride support for the synthesis of shape-dependent ZnO and their application in visible light photocatalysts, RSC Adv. 5 (2015) 80397–80409. doi:10.1039/c5ra12463h.

[177] H. Yu, F. Chen, F. Chen, X. Wang, Applied Surface Science In situ self-transformation synthesis of g-C_3N_4 -modified CdS heterostructure with enhanced photocatalytic activity, Appl. Surf. Sci. 358 (2015) 385–392. doi:10.1016/j.apsusc.2015.06.074.

[178] F. Jiang, T. Yan, H. Chen, A. Sun, C. Xu, X. Wang, Applied Surface Science A g-C_3N_4 – CdS composite catalyst with high visible-light-driven catalytic activity and photostability for methylene blue degradation, Appl. Surf. Sci. 295 (2014) 164–172. doi:10.1016/j.apsusc.2014.01.022.

[179] Y. Guo, J. Wang, Z. Tao, F. Dong, K. Wang, X. Ma, P. Yang, P. Hu, Y. Xu, L. Yang, Facile synthesis of mesoporous CdS nanospheres and their application in photocatalytic degradation and adsorption of organic dyes, CrystEngComm. 14 (2012) 1185–1188. doi:10.1039/c2ce06172d.

[180] H.M. Xiong, D.G. Shchukin, H. Möhwald, Y. Xu, Y.Y. Xia, Sonochemical synthesis of highly luminescent zinc oxide nanoparticles doped with magnesium(II), Angew. Chemie - Int. Ed. 48 (2009) 2727–2731. doi:10.1002/anie.200805590.

[181] Z.R. Tang, X. Yin, Y. Zhang, Y.J. Xu, Synthesis of titanate nanotube-CdS nanocomposites with enhanced visible light photocatalytic activity, Inorg. Chem. 52 (2013) 11758–11766. doi:10.1021/ic4010483.

[182] Y. Li, L. Tang, S. Peng, Z. Li, G. Lu, Phosphate-assisted hydrothermal synthesis of hexagonal CdS for efficient photocatalytic hydrogen evolution, Cryst Eng Comm. 14 (2012) 6974–6982. doi:10.1039/c2ce25838b.

[183] M. Salavati-Niasari, M.R. Loghman-Estarki, F. Davar, Controllable synthesis of nanocrystalline CdS with different morphologies by hydrothermal process in the presence of thioglycolic acid, Chem. Eng. J. 145 (2008) 346–350. doi:10.1016/j.cej.2008.08.040.

[184] L.R. Zou, G.F. Huang, D.F. Li, J.H. Liu, A.L. Pan, W.Q. Huang, A facile and rapid route for synthesis of g-C_3N_4 nanosheets with high adsorption capacity and photocatalytic activity, RSC Adv. 6 (2016) 86688–86694. doi:10.1039/c6ra20514c.

[185] N. Chidhambaram, K. Ravichandran, Fabrication of ZnO/g-C_3N_4 nanocomposites for enhanced visible light driven photocatalytic activity Fabrication of ZnO/g-C_3N_4 nanocomposites for enhanced visible light driven photocatalytic activity, (n.d.).

[186] M. Iqbal, A. Ali, N.A. Nahyoon, A. Majeed, R. Pothu, S. Phulpoto, K.H. Thebo, Photocatalytic degradation of organic pollutant with nanosized cadmium sulfide, Mater. Sci. Energy Technol. 2 (2018) 41–45. doi:10.1016/j.mset.2018.09.002.

[187] S. Vadivel, D. Maruthamani, B. Paul, S.S. Dhar, K. Selvam, Facile synthesis of novel $CaFe_2O_4$/g-C_3N_4 nanocomposites for degradation of methylene blue under visible-light irradiation Journal of Colloid and Interface Science Facile synthesis of novel $CaFe_2O_4$/g-C_3N_4 nanocomposites for degradation of methyle, J. Colloid Interface Sci. 480 (2016) 126–136. doi:10.1016/j.jcis.2016.07.012.

[188] Z.X. Han, Z. Zhu, D.D. Wu, J. Wu, Y.R. Liu, Adsorption Kinetics and Thermodynamics of Acid Blue 25 and methylene blue dye solutions on natural sepiolite, Synth. React. Inorganic, Met. Nano-Metal Chem. 44 (2014) 140–147. doi:10.1080/15533174.2013.770755.

[189] S. Kaur, A brief review on photocatalytic activity of ZnS and CQDs nanoparticles, Int. J. Eng. Appl. Sci. Technol. 2 (2017) 75–82. http://www.ijeast.com.

[190] M. Joshi, A. Bhattacharyya, S.W. Ali, Characterization techniques for nanotechnology applications in textiles, Indian J. Fibre Text. Res. 33 (2008) 304–317.

[191] R. Kohli, Methods for Monitoring and Measuring Cleanliness of Surfaces, in: Dev. Surf. Contam. Clean. - Detect. Charact. Anal. Contam., Elsevier, 2012: pp. 107–178. doi:10.1016/B978-1-4377-7883-0.00003-1.

[192] G. ZHANG, Master Thesis, University of Illinois at Urbana-Champaign, 2013, 2013.

[193] P.J. Mafa, A.T. Kuvarega, B.B. Mamba, B. Ntsendwana, Photoelectrocatalytic degradation of sulfamethoxazole on g-C_3N_4/BiOI/EG p-n heterojunction photoanode under visible light irradiation, Appl. Surf. Sci. 483 (2019) 506–520. doi:10.1016/j.apsusc.2019.03.281.

[194] M. Izadifard, G. Achari, C.H. Langford, Application of photocatalysts and LED

light sources in drinking water treatment, Catalysts. 3 (2013) 726–743. doi:10.3390/catal3030726.

[195] C.G. Young, an Inductively Coupled Plasma Atomic Emission Spectrometer for the Detection of Nonmetals in the Vacuum Ultraviolet, 2011.

[196] A.M. Sabir, M. Moloy, P.S. Bhasin, Hplc Method Development and Validation: a Review, Int. Res. J. Pharm. 4 (2016) 39–46. doi:10.7897/2230-8407.04407.

[197] F. Jiang, T. Yan, H. Chen, A. Sun, C. Xu, X. Wang, A g-C_3N_4-CdS composite catalyst with high visible-light-driven catalytic activity and photostability for methylene blue degradation, Appl. Surf. Sci. 295 (2014) 164–172. doi:10.1016/j.apsusc.2014.01.022.

[198] Z. Zhang, J. Huang, M. Zhang, Q. Yuan, B. Dong, Ultrathin hexagonal SnS_2 nanosheets coupled with g-C_3N_4 nanosheets as 2D/2D heterojunction photocatalysts toward high photocatalytic activity, Appl. Catal. B Environ. 163 (2015) 298–305. doi:10.1016/j.apcatb.2014.08.013.

[199] A. Akhundi, A. Habibi-yangjeh, Novel magnetically separable g-C_3N_4/AgBr/ Fe_3O_4 nanocomposites as visible-light-driven photocatalysts with highly enhanced activities, Ceram. Int. 41 (2015) 5634–5643. doi:10.1016/j.ceramint.2014.12.145.

[200] L.J. Cote, F. Kim, J. Huang, Langmuir-blodgett assembly of graphite oxide single layers, J. Am. Chem. Soc. 131 (2009) 1043–1049. doi:10.1021/ja806262m.

[201] Z. Zhou, J. Wang, J. Yu, Y. Shen, Y. Li, A. Liu, S. Liu, Y. Zhang, Dissolution and liquid crystals phase of 2D polymeric carbon nitride, J. Am. Chem. Soc. 137 (2015) 2179–2182. doi:10.1021/ja512179x.

[202] J. Xu, L. Zhang, R. Shi, Y. Zhu, Chemical exfoliation of graphitic carbon nitride for efficient heterogeneous photocatalysis, J. Mater. Chem. A. 1 (2013) 14766–14772. doi:10.1039/c3ta13188b.

[203] F. Dong, Z. Wang, Y. Sun, W.K. Ho, H. Zhang, Engineering the nanoarchitecture and texture of polymeric carbon nitride semiconductor for

enhanced visible light photocatalytic activity, J. Colloid Interface Sci. 401 (2013) 70–79. doi:10.1016/j.jcis.2013.03.034.

[204] C. Li, Z. Sun, W. Huang, S. Zheng, Facile synthesis of g-C_3N_4/montmorillonite composite with enhanced visible light photodegradation of rhodamine B and tetracycline, J. Taiwan Inst. Chem. Eng. 66 (2016) 363–371. doi:10.1016/j.jtice.2016.06.014.

[205] J. Tong, L. Zhang, F. Li, K. Wang, L. Han, S. Cao, Rapid and high-yield production of g-C3N4 nanosheets via chemical exfoliation for photocatalytic H2 evolution, RSC Adv. 5 (2015) 88149–88153. doi:10.1039/c5ra16988g.

[206] J. Zhu, P. Xiao, H. Li, S.A.C. Carabineiro, Graphitic carbon nitride: Synthesis, properties, and applications in catalysis, ACS Appl. Mater. Interfaces. 6 (2014) 16449–16465. doi:10.1021/am502925j.

[207] Y. Chen, X. Wang, Template-Free Synthesis of Hollow G‑C_3N_4 Polymer with Vesicle Structure for Enhanced Photocatalytic Water Splitting, (2018). doi:10.1021/acs.jpcc.7b12496.

[208] H.B. Tao, H. Bin Yang, J. Chen, J. Miao, B. Liu, Biomolecule-assisted synthesis of carbon nitride and sulfur-doped carbon nitride heterojunction nanosheets: An efficient heterojunction photocatalyst for photoelectrochemical applications, Beilstein J. Nanotechnol. 5 (2014) 770–777. doi:10.3762/bjnano.5.89.

[209] J. Tong, L. Zhang, F. Li, K. Wang, L. Han, S. Cao, Rapid and high-yield production of g-C_3N_4 nanosheets via chemical exfoliation for photocatalytic H_2 evolution, RSC Adv. 5 (2015) 88149–88153. doi:10.1039/c5ra16988g.

[210] S. Asadzadeh-khaneghah, A. Habibi-yangjeh, S. Vadivel, Journal of the Taiwan Institute of Chemical Engineers Fabrication of novel g-C_3N_4 nanosheet/carbon dots/$Ag_6Si_2O_7$ nanocomposites with high stability and enhanced visible-light photocatalytic activity, J. Taiwan Inst. Chem. Eng. 103 (2019) 94–109. doi:10.1016/j.jtice.2019.07.018.

[211] G. Mamba, A.K. Mishra, Applied Catalysis B : Environmental Graphitic carbon nitride (g-C_3N_4) nanocomposites : A new and exciting generation of visible

light driven photocatalysts for environmental pollution remediation, "Applied Catal. B, Environ. 198 (2016) 347–377. doi:10.1016/j.apcatb.2016.05.052.

[212] J. Jin, J. Yu, G. Liu, P.K. Wong, Single crystal CdS nanowires with high visible-light photocatalytic H_2-production performance, J. Mater. Chem. A. 1 (2013) 10927–10934. doi:10.1039/c3ta12301d.

[213] S. Rengaraj, A. Ferancova, S.H. Jee, S. Venkataraj, Y. Kim, J. Labuda, M. Sillanpää, Physical and electrochemical characterization of CdS hollow microspheres prepared by a novel template free solution phase method, Electrochim. Acta. 56 (2010) 501–509. doi:10.1016/j.electacta.2010.09.019.

[214] J. Fu, B. Chang, Y. Tian, F. Xi, X. Dong, Novel C_3N_4-CdS composite photocatalysts with organic-inorganic heterojunctions: In situ synthesis, exceptional activity, high stability and photocatalytic mechanism, J. Mater. Chem. A. 1 (2013) 3083–3090. doi:10.1039/c2ta00672c.

[215] Q. Li, B. Guo, J. Yu, J. Ran, B. Zhang, H. Yan, J.R. Gong, Highly efficient visible-light-driven photocatalytic hydrogen production of CdS-cluster-decorated graphene nanosheets, J. Am. Chem. Soc. 133 (2011) 10878–10884. doi:10.1021/ja2025454.

[216] V. Mohanraj, R. Jayaprakash, R. Robert, J. Balavijayalakshmi, S. Gopi, Effect of particle size on optical and electrical properties in mixed CdS and NiS nanoparticles synthesis by ultrasonic wave irradiation method, Mater. Sci. Semicond. Process. 56 (2016) 394–402. doi:10.1016/j.mssp.2016.08.014.

[217] N.H. Patel, M.P. Deshpande, S.H. Chaki, H.R. Keharia, Tuning of optical, thermal and antimicrobial capabilities of CdS nanoparticles with incorporated Mn prepared by chemical method, J. Mater. Sci. Mater. Electron. 28 (2017) 10866–10876. doi:10.1007/s10854-017-6865-y.

[218] A. Modwi, M.A. Ghanem, A.M. Al-Mayouf, A. Houas, Lowering energy band gap and enhancing photocatalytic properties of Cu/ZnO composite decorated by transition metals, J. Mol. Struct. 1173 (2018) 1–6. doi:10.1016/j.molstruc.2018.06.082.

[219] Q. Tang, C. Zhou, X. Yuan, Q. Jing, Y. Mu, A. Du, Facile Synthesis of g-C3N4

Nanosheets/ZnO Nanocomposites with Enhanced Photocatalytic Activity in Reduction of Aqueous Chromium(VI) under Visible Light, Nanomaterials. 6 (2016) 173. doi:10.3390/nano6090173.

[220] D. Wang, Z. Xu, Q. Luo, X. Li, J. An, R. Yin, C. Bao, Preparation and visible-light photocatalytic performances of g-C_3N_4 surface hybridized with a small amount of CdS nanoparticles, J. Mater. Sci. 51 (2016) 893–902. doi:10.1007/s10853-015-9417-y.

[221] A. Kumar, A Review on the Factors Affecting the Photocatalytic Degradation of Hazardous Materials, Mater. Sci. Eng. Int. J. 1 (2017) 1–10. doi:10.15406/mseij.2017.01.00018.

[222] S. Talebi, N. Chaibakhsh, Z. Moradi-Shoeili, Application of nanoscale ZnS/TiO_2 composite for optimized photocatalytic decolorization of a textile dye, J. Appl. Res. Technol. 15 (2017) 378–385. doi:10.1016/j.jart.2017.03.007.

[223] Y.S. Al-Degs, M.I. El-Barghouthi, A.H. El-Sheikh, G.M. Walker, Effect of solution pH, ionic strength, and temperature on adsorption behavior of reactive dyes on activated carbon, Dye. Pigment. 77 (2008) 16–23. doi:10.1016/j.dyepig.2007.03.001.

[224] E.T. Helmy, A. El Nemr, M. Mousa, E. Arafa, S. Eldafrawy, Photocatalytic degradation of organic dyes pollutants in the industrial textile wastewater by using synthesized TiO_2, C-doped TiO_2, S-doped TiO_2 and C,S co-doped TiO_2 nanoparticles, J. Water Environ. Nanotechnol. 3 (2018) 116–127. doi:10.22090/JWENT.2018.02.003.

[225] E. Mugunthan, M.B. Saidutta, P.E. Jagadeeshbabu, Visible light assisted photocatalytic degradation of diclofenac using TiO_2-WO_3 mixed oxide catalysts, Environ. Nanotechnology, Monit. Manag. 10 (2018) 322–330. doi:10.1016/j.enmm.2018.07.012.

[226] S. Iguchi, K. Teramura, S. Hosokawa, T. Tanaka, Effect of the chloride ion as a hole scavenger on the photocatalytic conversion of CO_2 in an aqueous solution over Ni-Al layered double hydroxides, Phys. Chem. Chem. Phys. 17 (2015) 17995–18003. doi:10.1039/c5cp02724a.

[227] L. Das, S.K. Barodia, S. Sengupta, J.K. Basu, Aqueous degradation kinetics of pharmaceutical drug diclofenac by photocatalysis using nanostructured titania–zirconia composite catalyst, Int. J. Environ. Sci. Technol. 12 (2015) 317–326. doi:10.1007/s13762-013-0466-y.

[228] J.M. Monteagudo, H. El-taliawy, A. Durán, G. Caro, K. Bester, Sono-activated persulfate oxidation of diclofenac: Degradation, kinetics, pathway and contribution of the different radicals involved, J. Hazard. Mater. 357 (2018) 457–465. doi:10.1016/j.jhazmat.2018.06.031.

[229] T. Huang, G. Zhang, S. Chong, Y. Liu, N. Zhang, S. Fang, J. Zhu, Effects and mechanism of diclofenac degradation in aqueous solution by US/Zn0, Ultrason. Sonochem. 37 (2017) 676–685. doi:10.1016/j.ultsonch.2017.02.032.

[230] M. V. Bagal, P.R. Gogate, Degradation of diclofenac sodium using combined processes based on hydrodynamic cavitation and heterogeneous photocatalysis, Ultrason. Sonochem. 21 (2014) 1035–1043. doi:10.1016/j.ultsonch.2013.10.020.

[231] P. Sathishkumar, R.A.A. Meena, T. Palanisami, V. Ashokkumar, T. Palvannan, F.L. Gu, Occurrence, interactive effects and ecological risk of diclofenac in environmental compartments and biota - a review, Sci. Total Environ. 698 (2020) 134057. doi:10.1016/j.scitotenv.2019.134057.

[232] R.R. Giri, H. Ozaki, S. Ota, R. Takanami, S. Taniguchi, Degradation of common pharmaceuticals and personal care products in mixed solutions by advanced oxidation techniques, Int. J. Environ. Sci. Tech. 7 (2010) 251–260. doi:10.1007/BF03326135.

[233] A. Fujishima, D.A. Tryk, T.N. Rao, Titanium dioxide photocatalysis, J. of Photochemistry and Photobiology. Rev. 1 (2000) 1-21.

[234] H. Xu, L. Wu, L. Jin, K. Wu, Combination Mechanism and Enhanced Visible-Light Photocatalytic Activity and Stability of CdS/g-C_3N_4 Heterojunctions, J. Mater. Sci. Technol. 33 (2017) 30–38. doi:10.1016/j.jmst.2016.04.008.

[235] I.W. As, M.C. Level, P.H. Effects, T. Methods, I. Exchange, R. Osmosis, WQA Technical Fact Sheet: Cadmium health effectc treatment methods Residential

Point-of-Entry Point-of-Use, 2013.
http://www.epa.gov/safewater/pdfs/factsheets/ioc/cadmium.pdf.

CHAPTER 6

PHOTOCATALYTIC DEGRADATION EVALUTAION OF DICLOFENAC

6.1 Photocatalytic degradation of DFC

The photocatalytic activity of 10% CNS/CdS semiconductor catalyst was evaluated for the photocatalytic degradation of DFC with maximum wavelength (276 nm). The initial concentration, pH and volume were 5 ppm, 6.8 and 50 mL respectively. The reaction was carried under visible light irradiation using the experimental procedure and set up outlined in **section 3.1 (general experiments)**. Different reactive parameters, effect of pH in the range (3-9), catalyst dosage (20-30 mg) and DFC concentrations (5-30 mgL^{-1}) were evaluated. Varying the parameters helps understand the behavior of catalyst and pollutant.

6.1.1 DFC degradation absorption

The absorbance of DFC decreased with increasing time; however DFC was not removed completely removed after 180 min, as the DFC peak at 276 nm was observed after 180 min. Furthermore an increase in absorbance after 90 min in the range 240-280 nm maybe due to the formation of intermediates (Fig 6.1).

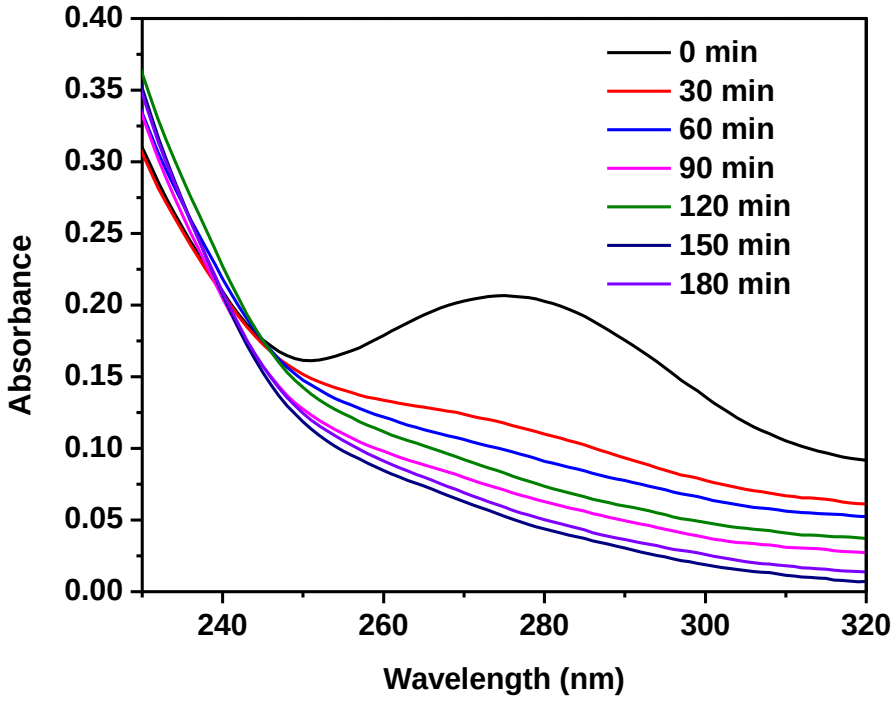

Figure 6.1.UV-Vis absorption spectra of DFC.

6.1.2 Effect of DFC concentration

The effective of concentration of DFC was varied from 5 to 15 ppm (Fig. 6.2). The photocatalytic efficiency decreased with increasing DFC concentrations, achieving 75.0%, 56.3% and 22.5% for 5, 10 and 20 ppm respectively. The photodegradation efficiency decreased with increase in DFC concentration. This was due to the scattering of light by higher concentration of organic substrate and less transformation of light through the pollutant [224]. Furthermore at higher substrate concentration, target molecules occur excessively on the surface of the catalysts and reduce the surface area for photodegradation and this may result in hydroxyl radical formation which affects the photocatalytic efficiency of the catalyst [225]. Moreover inorganic ions such as chlorides, nitrates and carbonates on the DFC structure may have inhibited the surface activity of the photocatalyst and consequently reduced the surface contact between the DFC itself and the photocatalyst and also scavenged both h^+ and •OH and thus reducing the number of •OH on the catalyst surface [221,226].

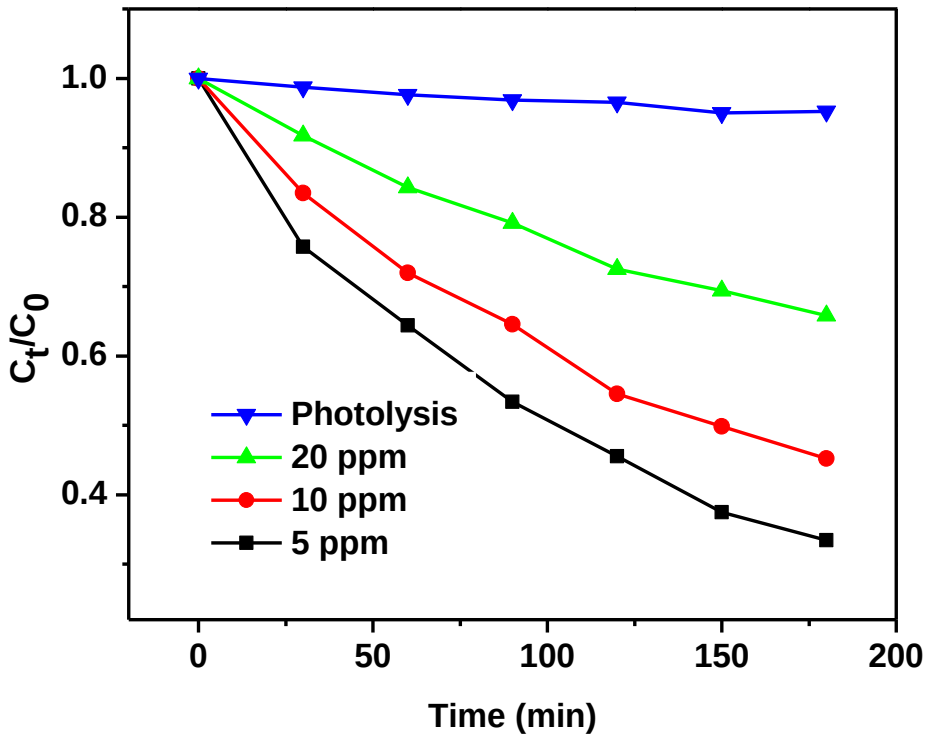

Figure 6.2. The effect of DFC concentration.

6.1.3 Effect of 10% CNS/CdS catalyst dosage

To determine the optimum amount of 10% CNS/CdS for efficient degradation of 5ppm AB-25 at initial pH 6 was studied in the range 10-30 mg (Fig 6.3). The photocatalytic efficiency increased with increasing catalyst amount and the obtained efficiency of 10, 20 and 20 mg catalyst were 42.3%, 65.8% and 85.1% respectively. The increase in catalyst dosage increased the number of active sites available for adsorption of DFC [225,227]. Sufficient light illumination also enhanced excitation of electron-holes and effectively degrading DFC [62].

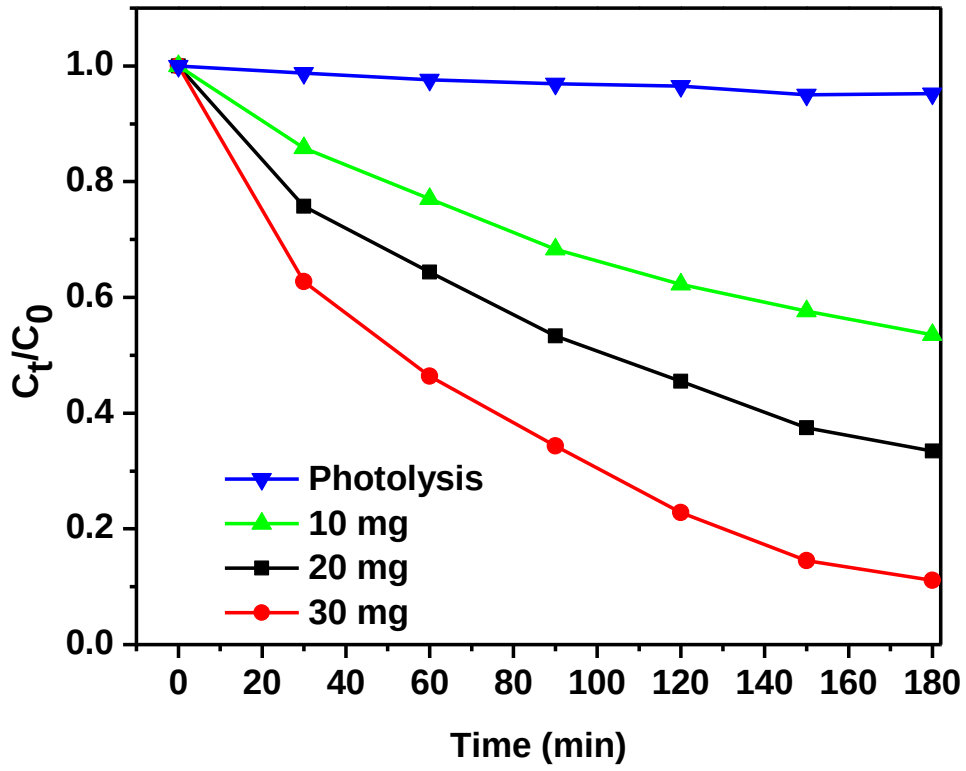

Figure 6.3. Effect of catalysts dosage for DFC degradation.

6.1.4 Effect of pH

The pH of DFC ranging from strong acidic to basic (pH 3 to 9) is shown on (Fig. 6.4). The catalyst dosage 30 mg and DFC concentration 5 mgL^{-1} were used to carry out the effect of pH studies. The removal efficiency at pH 3, 4, 6 and 9 were 77.2%, 82.8%, 65.8% and 46.1% respectively. The highest removal efficiency was achieved at pH 4 showing that DFC removal is higher in acidic medium. This is because DFC generally exist in molecular form at pH's lower than 4.5 (pka =4.5) (57) and at higher pHs, it exists in anionic form [228,229]. Furthermore DFC is hydrophobic in lower pHs (acidic) and hydrophilic at higher pHs (basic or anionic) and at pH value greater than pKa value, DFC deprotonates and make it hydrophilic [230].

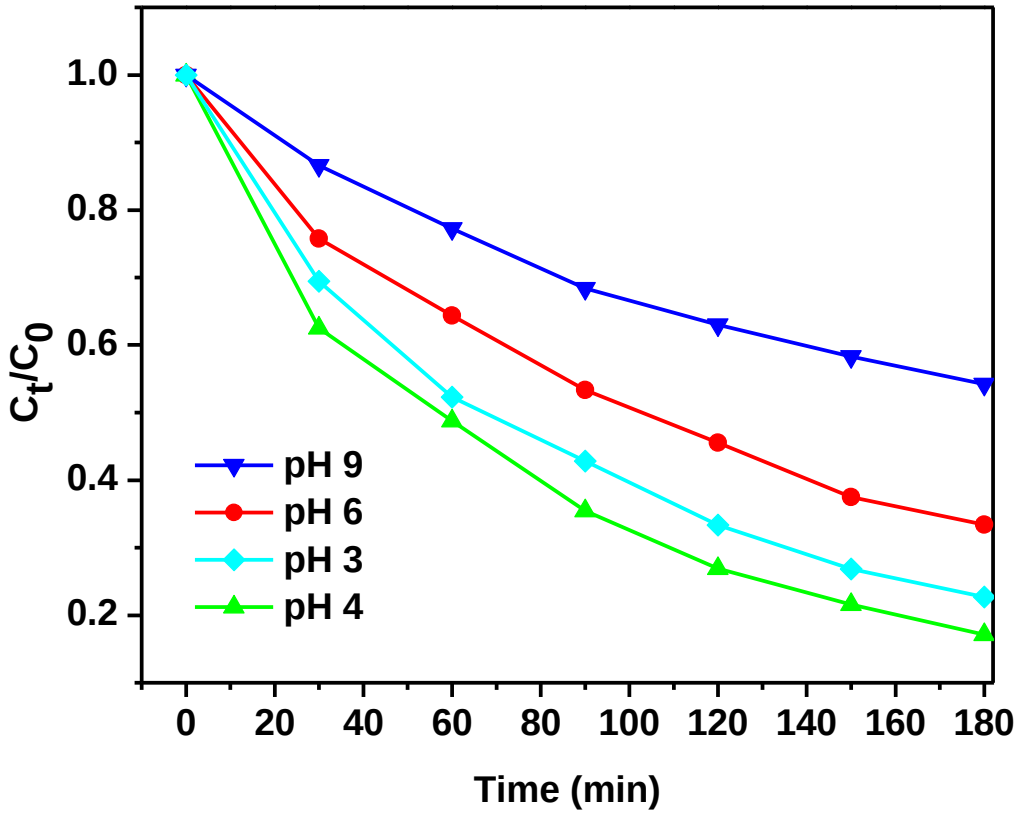

Figure 6.4. Effect of pH on DFC degradation.

6.1.5 Reactive species

The quenching experiments were performed to determine the main reactive species for DFC photocatalytic degradation (Fig 6.5). Benzoquinone (BQ), 2-propanol, and ethylene diamine (EDTA) were added as scavengers for superoxide radical anions ($O_2^{\bullet -}$), hydroxyl radicals and holes (h^+) respectively. The removal efficiency after the addition of EDTA and 2-propanol were 55.1% and 78.9% respectively, suggesting that the h+ when compared to $^{\bullet}OH$ played no important role in the removal of DFC. However the removal efficiency by $^{\bullet}OH$ is high which suggest that they do play some role. Furthermore the addition of (BQ) decreased the efficiency by 28.5% suggesting that the superoxide ions played more important role than the $^{\bullet}OH$ and h+ in removal efficiency of DFC.

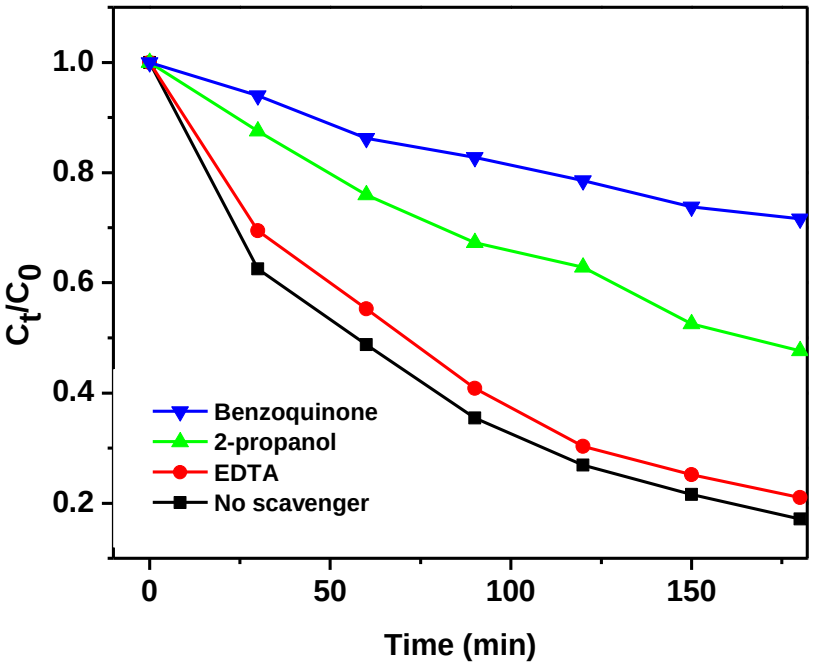

Figure 6.5.Determination of reactive species with different scavengers for photo-degradation of DFC.

6.2 The effect of a mixture of pollutants (AB-25 and DFC)

Typically in a wastewater treatment plant, various types of pollutants from different sources are found, these include pharmaceuticals, dyes, phenols and surfaces. They often interact with each other. Many studies have reported on toxicity of on DFC mixed with other pollutants such as other pharmaceuticals [72]. DFC has groups such as amino, hydroxyl, carbonyls and carboxyl groups in its structure which are active and can form metal complexation [231]. When combined with other pollutants DFC can result in the disruption of total ecological balances of receiving water systems [53,231]. There is little to no studies on the application the photocatalytic degradation of DFC mixed with dyes. The 10% CNS/CdS nanocomposite was studied for the photodegradation of a pollutant mixture of DFC and AB-25. In this section, the effect of 10% CNS/CdS on the degradation of a mixture of DFC and AB-25, Different reactive parameters such the effect of pH in the range (2-9), catalyst dosage (10-30 mg) and effect of AB-25 concentrations on DFC degradation in the (5-20 mgL^{-1}) were evaluated.

6.2.1 DFC and AB-25 absorbance

The photocatalytic activity of 10% CNS/CdS semiconductor photocatalyst was evaluated for the photocatalytic degradation of a mixture of DFC and AB-25 under the conditions, 5 mgL^{-1} (pollutant mixture), 20 mg catalyst and initial pH 6. The absorbance's for both DFC and AB-25 deceased with increasing time and after 180 min almost zero removal of AB-25 was achieved. Furthermore DFC in a reaction mixture was not degraded 180 min (Fig. 6.6). This suggested that the catalyst was more effective at removing AB-25 than DFC. This may be due to the difference in the optimum conditions such as pH and catalysts dosage of the two pollutants. Generally it is difficult to remove different classes of pollutants in one mixture, affecting the removal rate and in a case of dye cocktails degree of decolonization this is because they have different functional groups in different classes of pollutants and thus removal parameters for each of the pollutants in the mixture are critical [53,232].

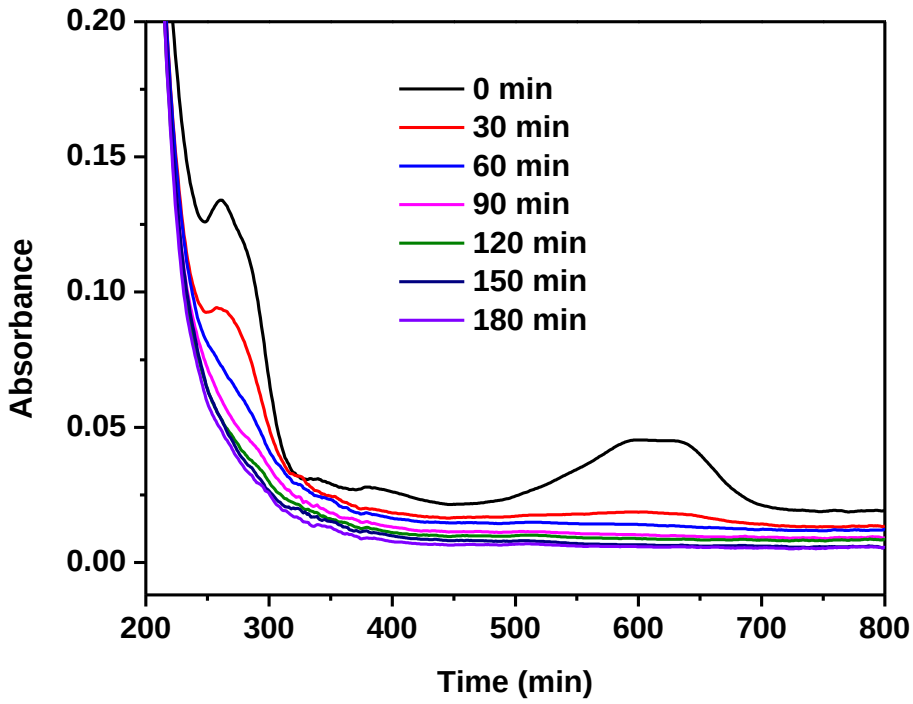

Figure 6.6. UV-Vis absorption spectra of AB-25 and DFC mixture.

6.2.2 The effect of AB-25 on DFC degradation

The effect of AB-25 concentration in the range 5-20 ppm on DFC degradation was studied under the conditions 20 mg catalyst and initial pH 6 (Fig. 6.7). The removal

efficiencies for DFC at 5, 10 and 20 ppm 50.8.7, 35.6 and 28.9% respectively, while the efficiencies for AB-25 at 5, 10 and 20 ppm are 98.3, 97.5 and 75.2% respectively. The results showed that the photocatalytic efficiency for DFC decreased with increasing AB-25 concentration and that DFC was more resistant to degradation than AB-25. The decrease in efficiency at high pollutant concentration maybe due to the pollutants saturating the catalyst surface and thus reduce the photonic efficiency and deactivation of the photocatalyst [221].

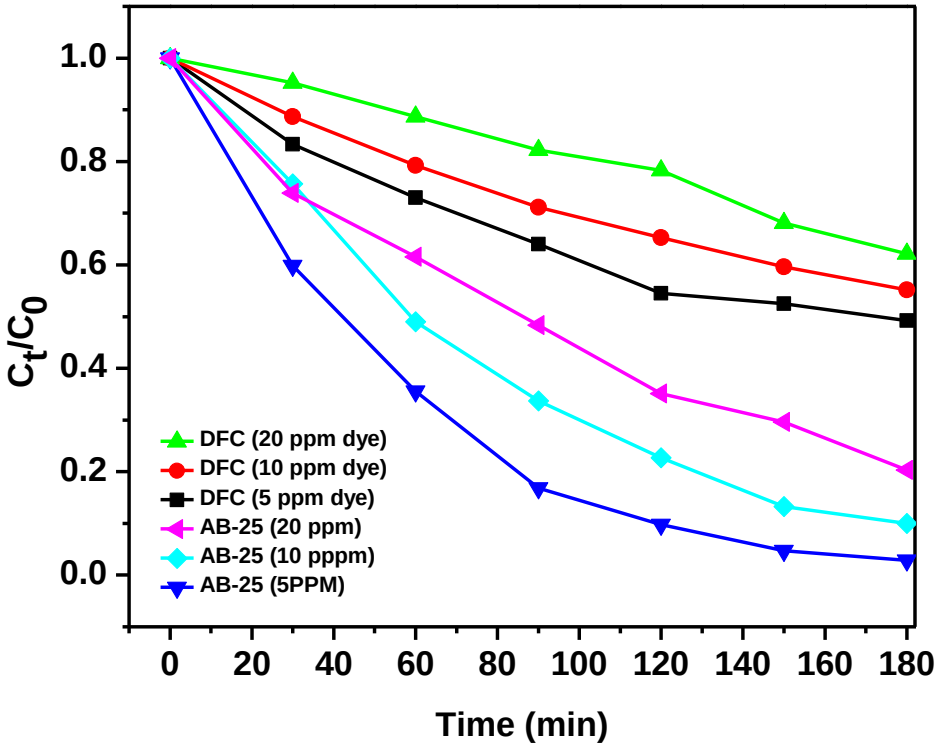

Figure 6.7. Photocatalytic degradation of AB-25 and DFC mixture.

6.2.3 The effect of catalyst dosage

The amount of catalyst was varied from (10-30 mg) and studies for the photocatalytic degradation of a mixture of 5 ppm DFC and AB-25 (Fig. 6.8). The photocatalytic efficiencies of DFC at 10, 20 and 30 mg are 27.6, 50.8 and 68.8% respectively and for AB-25 at 10, 20 and 30 mg are 89.3, 97.2 and 98.7% respectively. The higher the catalysts dosage the higher the photocatalytic efficiency and ascribed to the

complete utilization of incident photons striking on the catalysts surface and the number of active sites available at the catalysts surface.

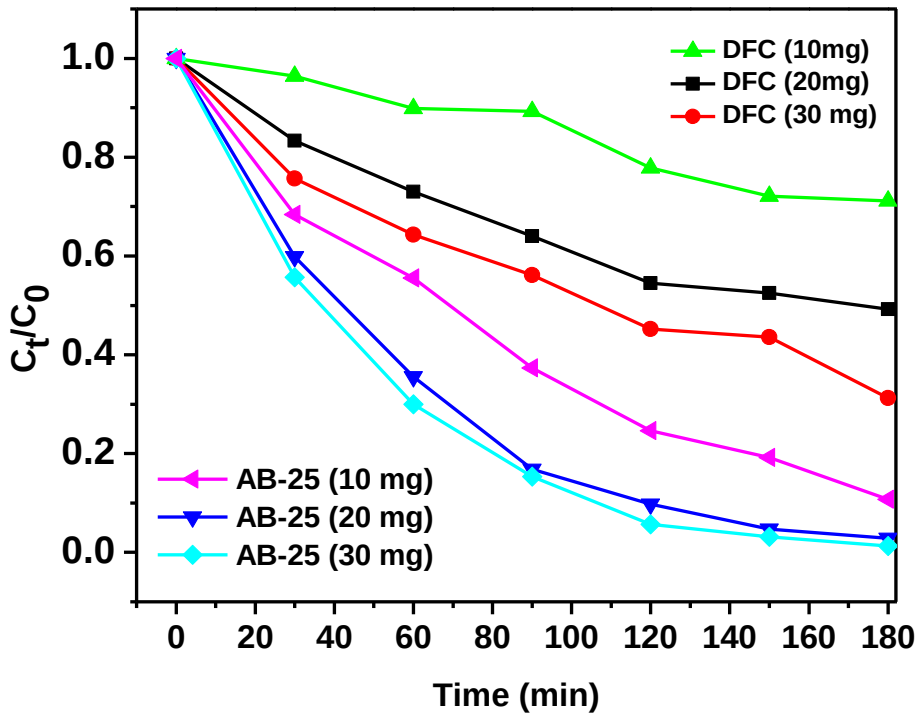

Figure 6.8.The effect of catalyst dosage on degradation of a mixture of DFC and AB-25.

6.2.4 The effect of pH

The pH of the pollutants mixture was studied at the pH range (2-10). The reaction conditions of 40 mg catalyst and 5 ppm pollutant concentration (Fig. 6.9).The removal efficiencies of DFC at pH 2, 6 and 10 were 88.9%, 68.7%, 66.7% and 24.9% respectively and for AB-25 at pH 2, 6 and 10 were 39.7%, 90.4% and 98.6%respectively. DFC is more removed in strong acidic conditions (pH 2) achieved 86.1% removal efficiency, while the efficiency decreased greatly in strong basic conditions, this was also be observed in individual DFC degradation. Furthermore the difference in photocatalytic efficiencies at different pH conditions may be ascribed to the difference in their number of electron pairs which induce electrostatic attractions between their negatively charged molecules and positively charged 10% CNS/CdS nanocomposite at different pH conditions [227].

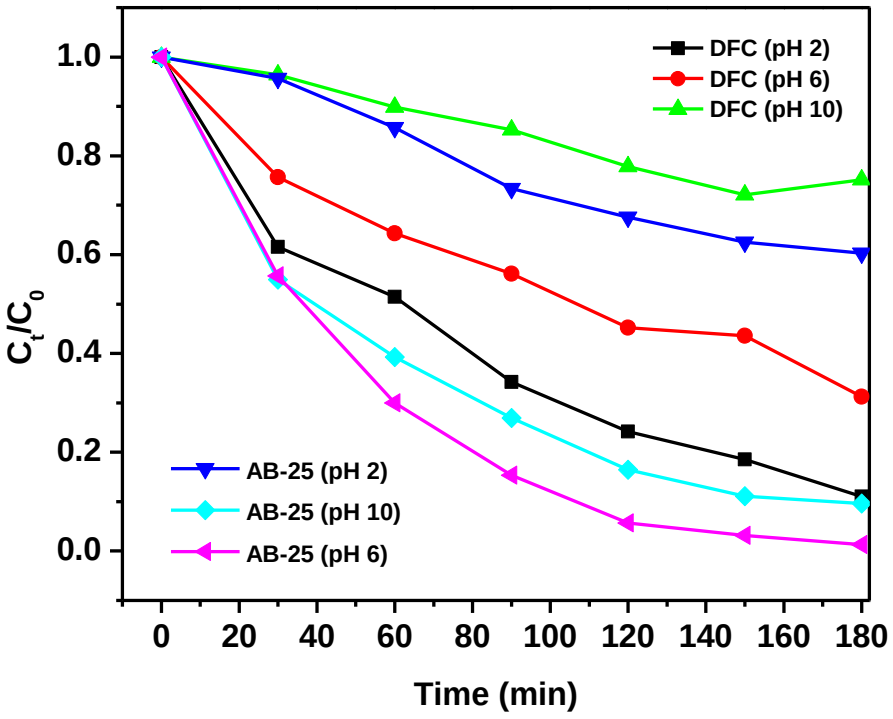

Figure 6.9.The effect of pH on DFC and AB-25 mixture degradation.

6.2.5 Reaction kinetics

To perform a comparison study in the degradation rate of individual DFC and DFC mixed with AB-25, the rate kinetics of 5 ppm DFC at the same pH 6 were evaluated by modelling the degradation data using the Langmuir-Hinshelwood first order kinetics using the expression (3.13 and (3.14). The rate constants for photolysis, individual DFC, DFC (mixture) and AB-25 (mixture are 0.0003, 0.0069, 0.0046 and 0.0198 min^{1}) respectively (Table 1).

Table 6.1. Reaction rate constants of mixture of AB-25 and DFC

Pollutants	**Reaction rates min^{-1}**
Photolysis	0.0003
Individual DFC	0.0069
DFC (mixture)	0.0046
AB-25 (mixture)	0.0198

There rate constant for individual DFC significantly decreased from 0.0069 to 0.0046 min^{-1} and AB-25 had the highest rate constant. This may be ascribed to the strong electron withdrawing groups of AB-25, thus making the catalyst more drawn towards AB-25 than DFC [233] (Fig. 6.10).

Compared to the rate constant of individual AB-25 (Chapter 5), the rate constant of 10% CNS/CdS for AB-25 removal increased in a reaction mixture compared to the individual AB-25 (chapter 5). This difference in rate constants is due to the low initial AB-25 concentrations. The lower the AB-25 concentration, the higher the removal efficiency. Furthermore, though the rate constant slightly decreased, the catalyst was still effective at AB-25 removal even when it is mixed other pollutants.

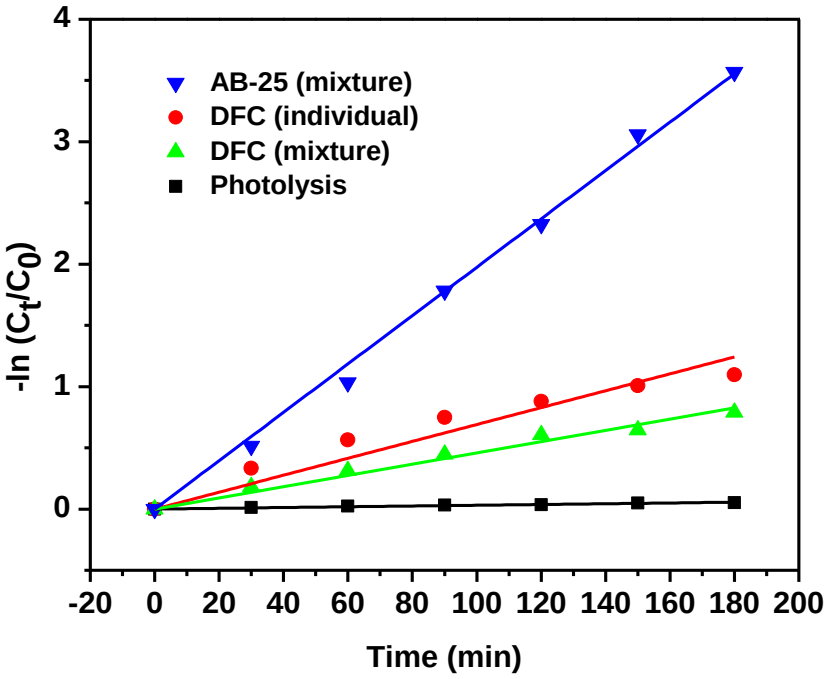

Figure 6.10. Rate Constants for (a) photolysis, (b) DFC (mixture), (c) individuals DFC, (d) AB-25 (mixture).

6.3 Proposed photodegradation of DFC mechanism

The proposed mechanism for the charge transfer and separation of charges at the interface of the CNS/CdS during photocatalytic degradation DFC is shown of schematic diagram (Fig 6.10). In order to determine the separation of charge, the band edge potentials at the conduction band (CB) and valence band (VB) of CNS and CdS were determined using the equations 3.15 and 3.16 [193].

It was established in the previous chapter that the photo-generated electrons and holes move in opposite directions, reducing the chances of charge carrier recombination which resulted in enhanced charge separation efficiency. Furthermore the trapping studies suggest that photocatalytic degradation of DFC was due to the $^{\bullet}O_2^-$ formation.

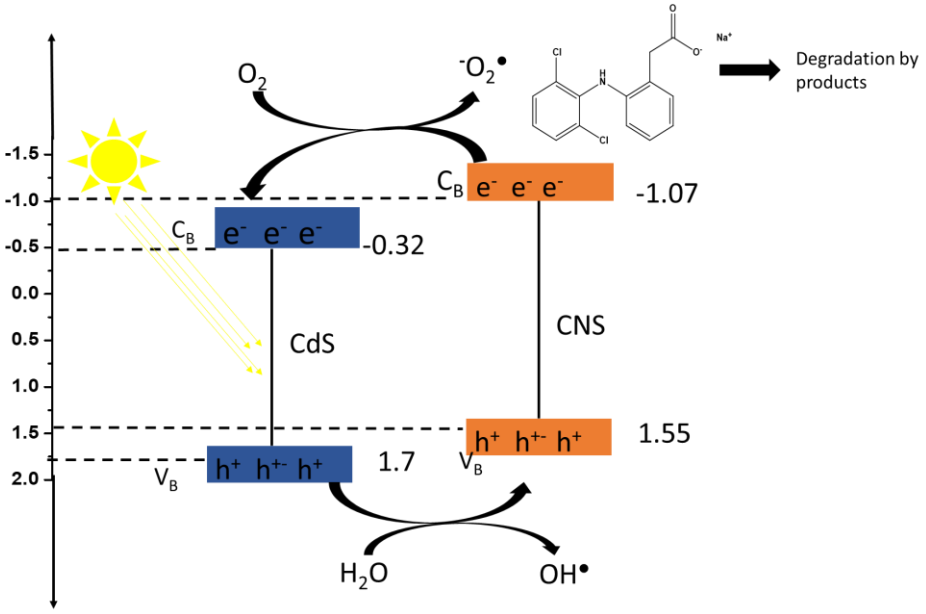

Figure 6.11. The proposed mechanism for photocatalytic degradation of DFC.

6.3.1 Degradation products of DFC

The removal efficiency of DFC was further determined by HPLC-TOF-Ms, to determine the degradation by-products and hypothesize the possible pathway for its degradation (Fig. 6.12a). The results show the decrease in peak intensity of the DFC at 296.12 *m/z* confirming the degradation of DFC with lowest peak intensity after 180 min.

The HPLC results at 0 min (in the dark solution) showed four peaks, a prominent at 296.0241 *m/z* is ascribed to the conjugate base of DFC, with a proton in positive mode, Two peaks at 200.2375 and 130.1591 *m/z* suggesting the presence of intermediates (Fig. 6.11b). The diclofenac sodium peak (318.0064 *m/z*) is barely visible which suggests that the sodium ion reacted with some OH^- that may have been present in the solution when. Furthermore the peaks (200.2375 m/z) and (130.1591 m/z) are still observed after 90 min, suggesting these products remain unconverted. The small peak at 278.013 m/z is ascribed to the protonated molecular ion peak M + $H^{\bullet+}$ of DFC related to the compound (N-2.6-diclorophenyl) indolin-2-one), it may have resulted due to acid treatment of DFC. The peak at 278.0187 disappeared, while peaks with lower molecular weight at 270.3162, 108.519 and 99.512 *m/z*) were observed. A new weak intensity small peak at 75 m/z is observe after 180 min and is ascribed to a ring opening structure (Fig. 11c).

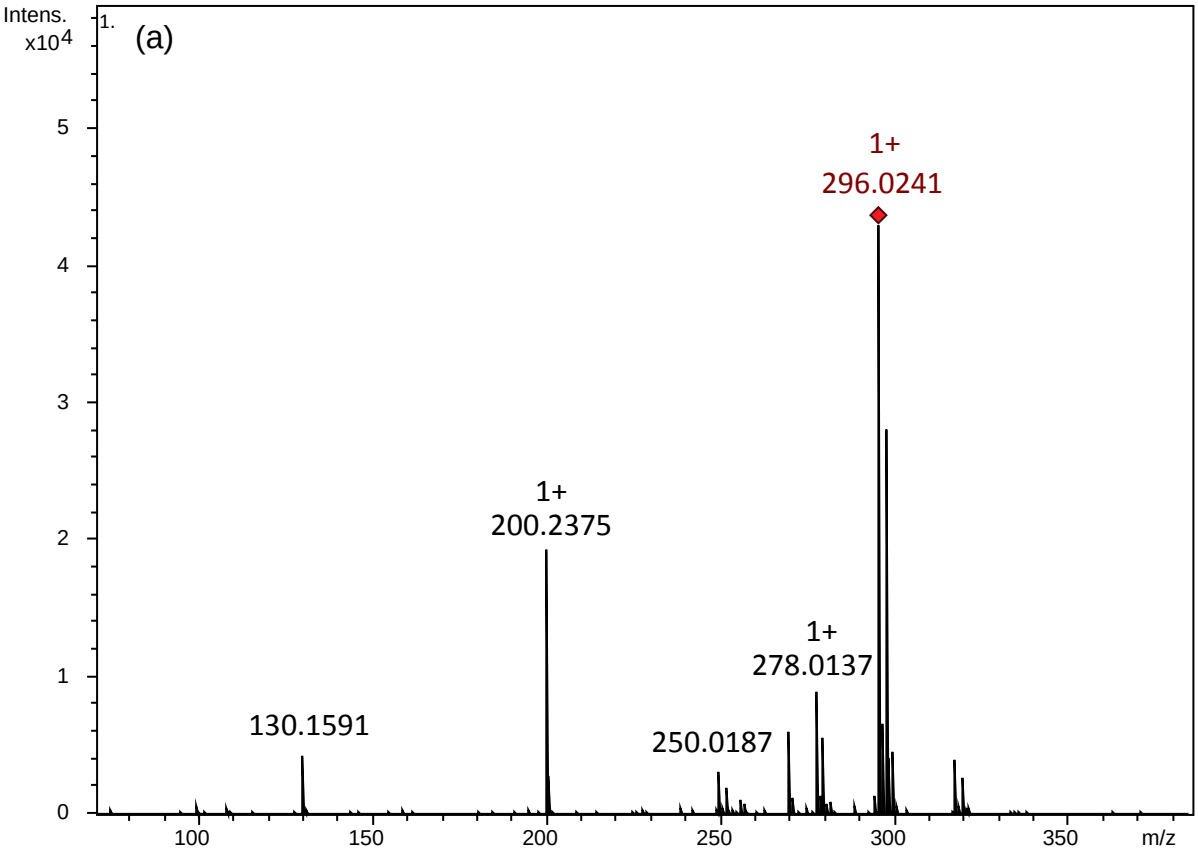
Intens.
x10^4
1.
(a)
5
4
3
2
1
0
1+
296.0241
1+
200.2375
1+
278.0137
130.1591
250.0187
100
150
200
250
300
350
m/z

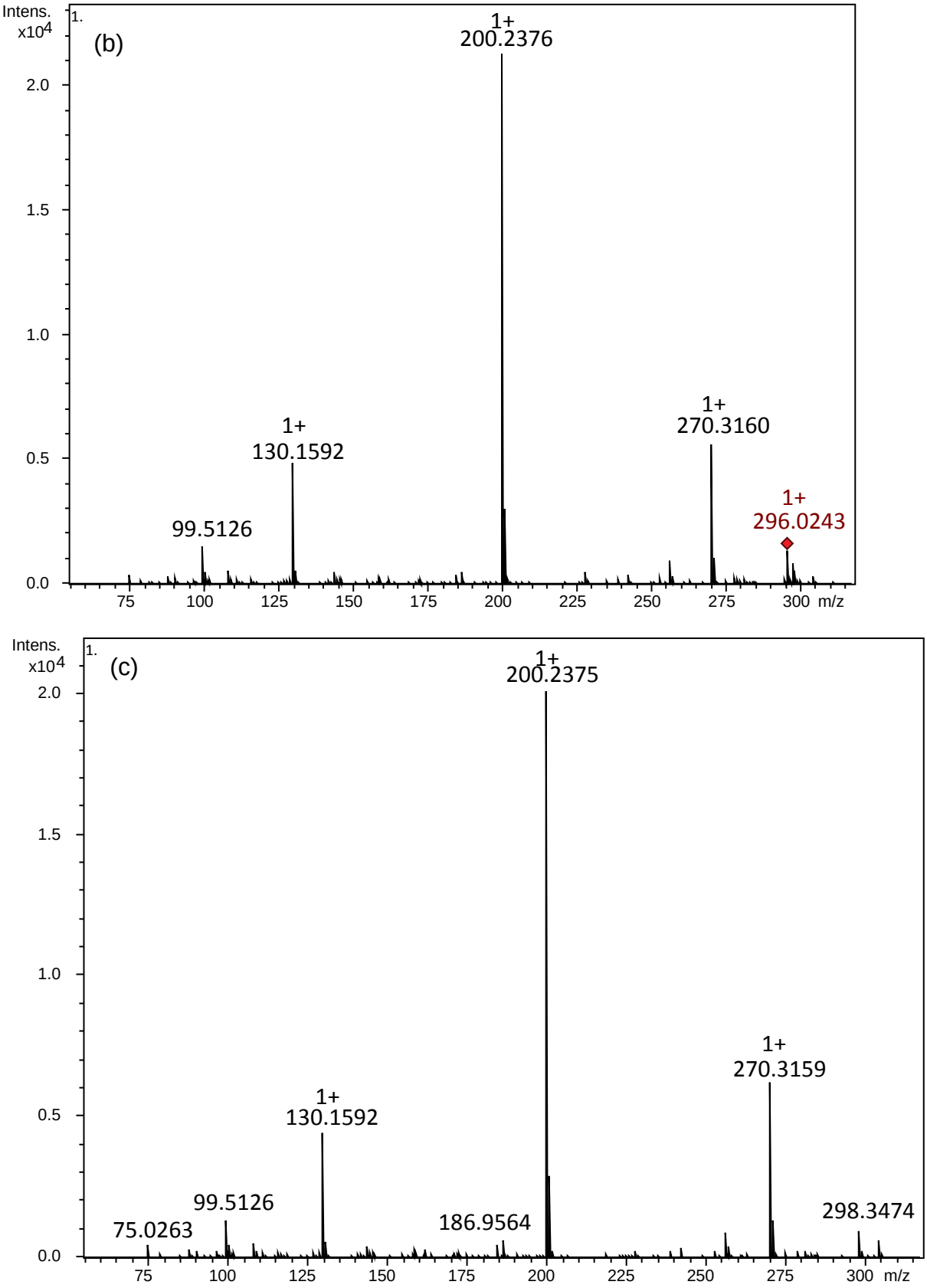

Figure 6.12. Mass spectra of UHPLC TOF-Ms during degradation of DFC at (a) 0 min, (b) 90 min and (c) 180 min.

The degradation of DFC (path1) undergoes dehydration and results in the peak at 278 *m/z* ascribed to 2-2-(2.6-dichlorophenyl) amino) phenyl) acetaldehyde. The intermediate then undergoes decarboxylation, result in the formation of the product with molecular weight (mw=250) ascribed to 2.6-dicloro-(2-methyl phenyl) aniline observed in literature [230]. The peak at 250 m/z undergoes C/N cleavage and results in two low mw intermediated 161 and *108 m/z*, ascribed to (2.6-dichloroaniline) and o-cresol respectively. The intermediates then undergo ring opening and results in peaks at 100 and 74 m/z 3-amino-prop-2-en-1-ol respectively. A similar mechanism is also shown by (Muguntham et al 2018) [225]. Alternatively DFC undergoes decarboxylation and result in intermediate at peak 270 *m/z* ascribed to 2-(2, 6-dichlorophenyl) amino) phenyl) methanol and result in intermediate at 200 *m/z* ascribed to 3-(phenyl amino) phenyl) methanol. The peak at 200 *m/*z then undergoes CN cleavage and result in two low mw peaks at 108 and 92 *m/z* and are ascribed to m-toluedene and toluene respectively. Ring opening of the intermediates resulted in low mw=74 *m/z* butan-1-ol (Fig. 6.13).

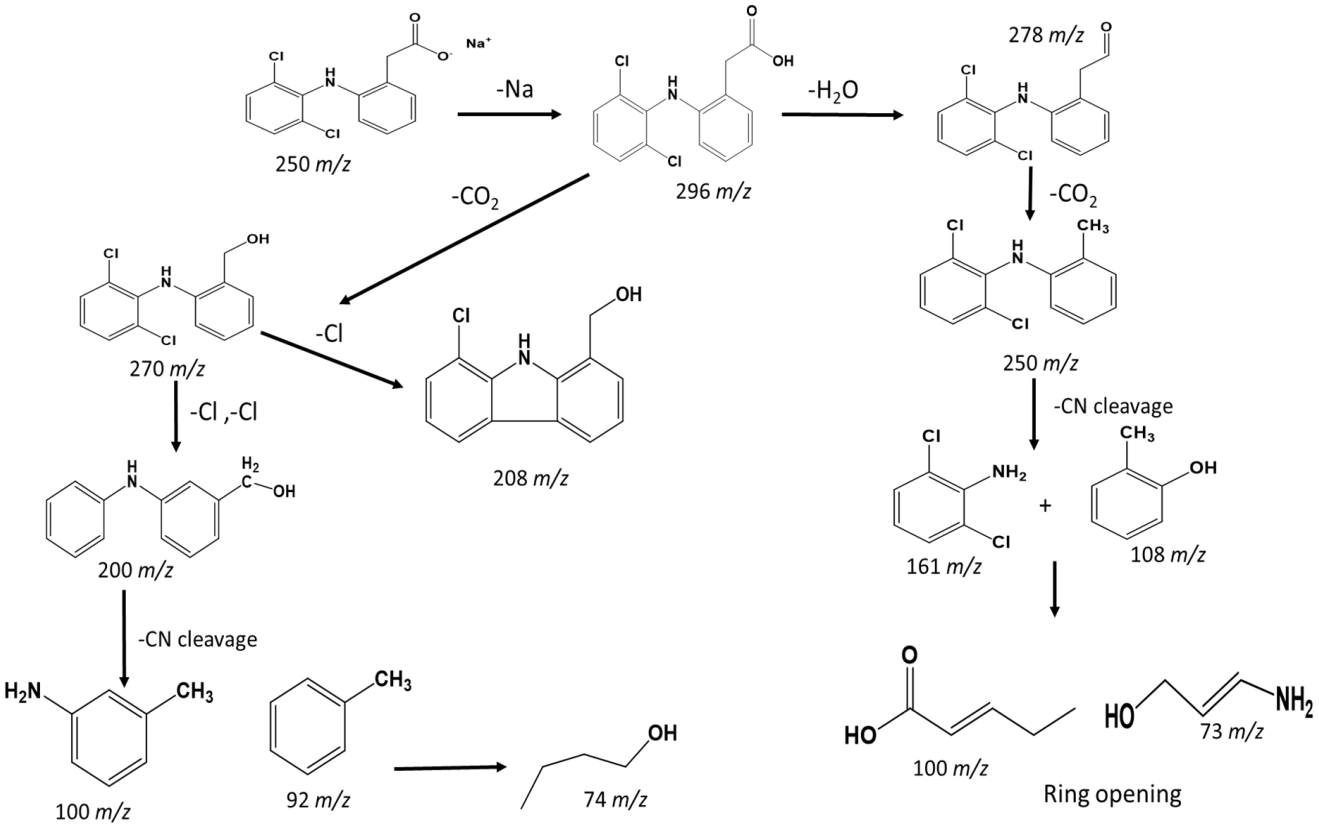

Figure 6.13.Schematic diagram for the photocatalytic degradation pathway of DFC.

6.4 CdS leaching test studies

The leaching of Cd^{2+} during photocatalytic degradation of the pollutants was studies using the ICP=OES (Fig. 6.14). The initial amount of Cd^{2+} in solution for CdS (0.00116 mg/L) increased to 0.00714 after 180 min. This showing that Cd^{2+} in CdS nanoparticles was unstable. Furthermore the cd^{2+} leaching reduced to 0.00442 ppm after coupling with CNS. This may be due to not enough photogenerated electron holes transferred into the DFC solution and not enough holes to cause photo-corrosion of CdS, this also suggest that CNS suppressed photo-corrosion of CdS [146,197]. Another possibility maybe due to the formed heterostructure resulted in effective separation and transfer of photogenerated electron holes and reduced the photo-corrosion of CdS by self-oxidation and improved photo-stability of CdS [234].

According to WHO guidelines the maximum contamination level of cadmium in drinking water is above 0.005 mL^{-1} and the long term exposure to Cd^{2+} concentration above 0.005 mgL^{-1} can result in diarrhoea , muscle cramps, liver damage and renal failure [235]. The amount of Cd^{2+} leached after coupling with CNS is slightly lower than the amount of Cd^{2+} considered to be toxic and we can deduce that the CdS/CNS nanocomposite can be used as alternatives removal of organic pollutants in water without re-contamination with Cd^{2+}.

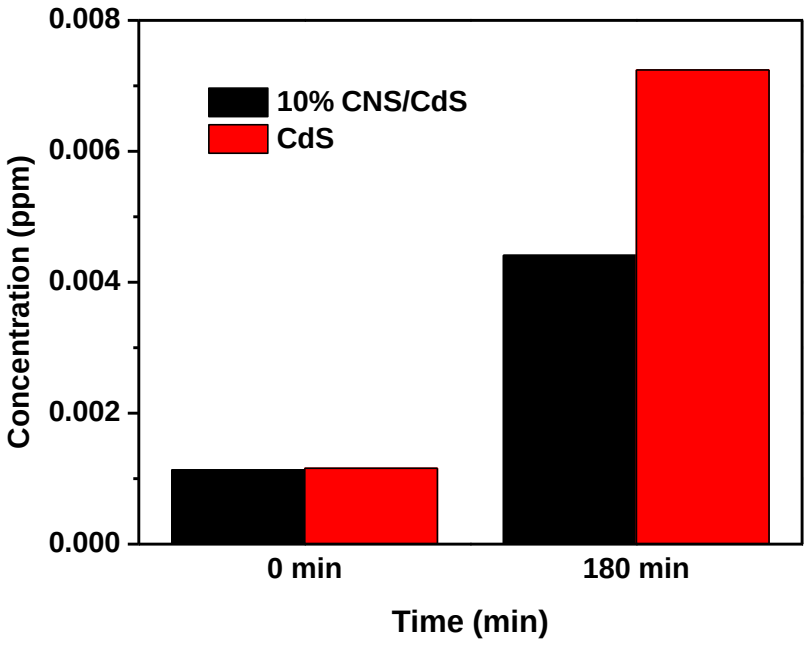

Figure 6.14.Leaching studies of Cd^{2+} of in degradation of DFC at pH 2.

6.5 Conclusion

This chapter demonstrated the photocatalytic degradation of DFC and mixtures of DFC and AB-25 using 10% CNS/CdS. The results showed that the removal efficiency of the nanocomposite reduced for DFC and was not as effective as it was at degrading AB-25. The removal efficiency of DFC in a pollutant mixture of DFC and AB-25 reduced by more than 10% and while for AB-25 reduced by just 2%. Proving that it is difficult for photocatalyst to remove complex mixtures of organic pollutants than it is individual pollutants because of their different optimal conditions. Further studies determined that at lower pH, high photocatalytic efficiencies for DFC degradation can be achieved.

References

[1] A. Azizullah, M.N.K. Khattak, P. Richter, D.P. Häder, Water pollution in Pakistan and its impact on public health - A review, Environ. Int. 37 (2011) 479–497. doi:10.1016/j.envint.2010.10.007.

[2] I. Gehrke, A. Somborn-schulz, Innovations in nanotechnology for water treatment, Nanotechnol. Sci. Appl. 8 (2015) 1–17.

[3] C.J.. ; G. Vorösmarty Pamela; ; Salisbury, Joseph; ; Lammers, Richard B., Global Water Resources: Vulnerability from Climate Change and Population Growth, Science (80-.). 289 (2000) 284–288. doi:10.1126/science.289.5477.284.

[4] J. Theron, T.E. Cloete, Emerging Waterborne Infections: Contributing Factors, Agents, and Detection Tools, Crit. Rev. Microbiol. 28 (2008) 1–26. doi:10.1080/1040-840291046669.

[5] K.K. Jain, Nanotechnology and Water, Contemp. Mater. 1 (2012) 26–30. doi:10.7251/122.

[6] F.W. Owa, Water pollution : sources , effects , control and management, Int. Lett. 3 (2014) 1–6.

[7] H. Zhou, D.W. Smith, Advanced technologies in water and wastewater treatment, in: 2002. doi:10.1139/S02-020.

[8] M. Wakil, M. Burhan, L. Ang, K. Choon, Energy-water-environment nexus underpinning future desalination sustainability, Desalination. 413 (2017) 52–64. doi:10.1016/j.desal.2017.03.009.

[9] M. Palaniappan, K. Address, Peak_Water_Talk.Pdf, in: Utah Am. Plan. Assoc. Annu. Conf., 2008: pp. 3–11.

[10] J.K. Bwapwa, Review on Main Issues Causing Deterioration of Water Quality and Water Scarcity: Case Study of South Africa, Environ. Manag. Sustain. Dev. 7 (2018) 14. doi:10.5296/emsd.v7i3.13156.

[11] J. Wang, S. Wang, Removal of pharmaceuticals and personal care products (PPCPs) from wastewater: A review, J. Environ. Manage. 182 (2016) 620–640.

doi:10.1016/j.jenvman.2016.07.049.

[12] G. Boczkaj, A. Fernandes, Wastewater treatment by means of advanced oxidation processes at basic pH conditions : A review, Chem. Eng. J. 320 (2017) 608–633. doi:10.1016/j.cej.2017.03.084.

[13] R. Ananthashankar, Treatment of textile effluent containing Reactive Red 120 dye using advanced oxidation, 2012.

[14] K. Klaus, Pharmaceuticals in the Environment, Annu Rev Env. Resour. 35 (2010) 57–75. doi:10.1146/annurev-environ-052809-161223.

[15] G. Kjosavik, Subtle changes, 2001.

[16] A.B.A. Boxall, M.A. Rudd, B.W. Brooks, D.J. Caldwell, K. Choi, S. Hickmann, E. Innes, K. Ostapyk, J.P. Staveley, T. Verslycke, G.T. Ankley, K.F. Beazley, Review Pharmaceuticals and Personal Care Products in the Environment : What Are the Big Questions ?, 120 (2012) 1221–1229.

[17] G. Li, X. Nie, Y. Gao, T. An, Applied Catalysis B : Environmental Can environmental pharmaceuticals be photocatalytically degraded and completely mineralized in water using g-C_3N_4/TiO_2 under visible light irradiation ?— Implications of persistent toxic intermediates, "Applied Catal. B, Environ. 180 (2016) 726–732. doi:10.1016/j.apcatb.2015.07.014.

[18] B. Hoeger, B. Köllner, D.R. Dietrich, B. Hitzfeld, Water-borne diclofenac affects kidney and gill integrity and selected immune parameters in brown trout (Salmo trutta f. fario), Aquat. Toxicol. 75 (2005) 53–64. doi:10.1016/j.aquatox.2005.07.006.

[19] M. Lillenberg, S. Yurchenko, K. Kipper, K. Herodes, V. Pihl, R. Lõhmus, M. Ivask, A. Kuu, S. Kutti, S. V. Litvin, L. Nei, Presence of fluoroquinolones and sulfonamides in urban sewage sludge and their degradation as a result of composting, Int. J. Environ. Sci. Technol. 7 (2010) 307–312. doi:10.1007/BF03326140.

[20] S.K. Khetan, T.J. Collins, Human pharmaceuticals in the aquatic environment: A challenge to green chemisty, Chem. Rev. 107 (2007) 2319–2364. doi:10.1021/cr020441w.

[21] A.M. Deegan, B. Shaik, K. Nolan, K. Urell, M. Oelgemöller, J. Tobin, A. Morrissey, Treatment options for wastewater effluents from pharmaceutical companies, Int. J. Environ. Sci. Technol. 8 (2011) 649–666. doi:10.1007/BF03326250.

[22] A.J. Ebele, M. Abou-Elwafa Abdallah, S. Harrad, Pharmaceuticals and personal care products (PPCPs) in the freshwater aquatic environment, Emerg. Contam. 3 (2017) 1–16. doi:10.1016/j.emcon.2016.12.004.

[23] B.D. Blair, J.P. Crago, C.J. Hedman, R.D. Klaper, Chemosphere Pharmaceuticals and personal care products found in the Great Lakes above concentrations of environmental concern, Chemosphere. 93 (2013) 2116–2123. doi:10.1016/j.chemosphere.2013.07.057.

[24] C.U. Meteyer, B.A. Rideout, M. Gilbert, H.L. Shivaprasad, L. Oaks, Pathology and proposed pathophysiology of diclofenac poisoning in the free living and experimentally exposed oriental white-backed vultures (gyps bengalensis), J. Wildl. Dis. 41 (2005) 707–716.

[25] R. Triebskorn, H. Casper, V. Scheil, J. Schwaiger, Ultrastructural effects of pharmaceuticals (carbamazepine, clofibric acid, metoprolol, diclofenac) in rainbow trout (Oncorhynchus mykiss) and common carp (Cyprinus carpio), Anal. Bioanal. Chem. 387 (2007) 1405–1416. doi:10.1007/s00216-006-1033-x.

[26] J. Schwaiger, H. Ferling, U. Mallow, H. Wintermayr, R.D. Negele, Toxic effects of the non-steroidal anti-inflammatory drug diclofenac. Part I: Histopathological alterations and bioaccumulation in rainbow trout, Aquat. Toxicol. 68 (2004) 141–150. doi:10.1016/j.aquatox.2004.03.014.

[27] A.A.C. and Z.M. Dana Manuela Sirbu, Daniela Curseu, Monica Popa, Environmental Risks of Pharmaceuticals and Personal Care Products in Water, in: Tenth Int. Water Technol. Conf., 2006: pp. 1151–1162.

[28] E. Archer, G.M. Wolfaardt, J.H. van Wyk, Pharmaceutical and personal care products (PPCPs) as endocrine disrupting contaminants (EDCs) in South African surface waters, Water SA. 43 (2017) 684–706. doi:10.4314/wsa.v43i4.16.

[29] O.A.H. Jones, N. Voulvoulis, J.N. Lester, Potential ecological and human health risks associated with the presence of pharmaceutically active compounds in the aquatic environment, Crit. Rev. Toxicol. 34 (2004) 335–350. doi:10.1080/10408440490464697.

[30] A.K. Karen, J.B. Paul, H.M. Kenneth, e P.P. Vinc, E.E. Robert, M.L. James, W.F. Robert, Disrupting Queer Incluslon, Pnas. 104 (2007) 8897–8901. doi:10.1073/pnas.0609568104.

[31] D.J. Caldwell, F. Mastrocco, T.H. Hutchinson, R. Länge, D. Heijerick, C. Janssen, P.D. Anderson, J.P. Sumpter, Derivation of an aquatic predicted no-effect concentration for the synthetic hormone, 17α-ethinyl estradiol, Environ. Sci. Technol. 42 (2008) 7046–7054. doi:10.1021/es800633q.

[32] M.F. Rahman, E.K. Yanful, S.Y. Jasim, Endocrine disrupting compounds (EDCs) and pharmaceuticals and personal care products (PPCPs) in the aquatic environment: Implications for the drinking water industry and global environmental health, J. Water Health. 7 (2009) 224–243. doi:10.2166/wh.2009.021.

[33] B. Lellis, C.Z. Fávaro-polonio, J.A. Pamphile, J.C. Polonio, Effects of textile dyes on health and the environment and bioremediation potential of living organisms, Biotecnol. Res. Innov. 3 (2019) 275–290. doi:10.1016/j.biori.2019.09.001.

[34] R. Paper, Decolorization of mixture of dyes : A critical review, Glob. J. Environ. Sci. Manag. Glob. J. Environ. Sci. Manag. 1 (2015) 71–94. doi:10.7508/gjesm.2015.01.007.

[35] A.M. Deegan, B. Shaik, K. Nolan, K. Urell, J. Tobin, A. Morrissey, Treatment options for wastewater effluents from pharmaceutical companies, 8 (2011) 649–666.

[36] L. Cheng, Q. Xiang, Y. Liao, H. Zhang, CdS-Based photocatalysts, Royal Society of Chemistry, 2018. doi:10.1039/c7ee03640j.

[37] H.L. Lee, A.M. Issam, M. Belmahi, M.B. Assouar, H. Rinnert, M. Alnot, Synthesis and characterizations of bare cds nanocrystals using chemical

precipitation method for photoluminescence application, J. Nanomater. 2009 (2009). doi:10.1155/2009/914501.

[38] S. Kumar, S. Karthikeyan, A.F. Lee, g-C_3N_4-based nanomaterials for visible light-driven photocatalysis, Catalysts. 8 (2018). doi:10.3390/catal8020074.

[39] S. Cao, J. Low, J. Yu, M. Jaroniec, Polymeric Photocatalysts Based on Graphitic Carbon Nitride, Adv. Mater. 27 (2015) 2150–2176. doi:10.1002/adma.201500033.

[40] Q.Y. Liu, Y.L. Qi, Y.F. Zheng, X.C. Song, Synthesis and enhanced photocatalytic activity of g-C_3N_4 hybridized CdS nanoparticles, Bull. Mater. Sci. 40 (2017) 1329–1333. doi:10.1007/s12034-017-1513-y.

[41] R.C. Pawar, V. Khare, C.S. Lee, Hybrid photocatalysts using graphitic carbon nitride/cadmium sulfide/reduced graphene oxide (g-C_3N_4/CdS/RGO) for superior photodegradation of organic pollutants under UV and visible light, Dalt. Trans. 43 (2014) 12514–12527. doi:10.1039/c4dt01278j.

[42] S.W. Cao, Y.P. Yuan, J. Fang, M.M. Shahjamali, F.Y.C. Boey, J. Barber, S.C. Joachim Loo, C. Xue, In-situ growth of CdS quantum dots on g-C_3N_4 nanosheets for highly efficient photocatalytic hydrogen generation under visible light irradiation, Int. J. Hydrogen Energy. 38 (2013) 1258–1266. doi:10.1016/j.ijhydene.2012.10.116.

[43] S. Rasalingam, R. Peng, R.T. Koodali, Removal of hazardous pollutants from wastewaters: Applications of TiO_2-SiO_2 mixed oxide materials, J. Nanomater. 2014 (2014). doi:10.1155/2014/617405.

[44] M.K. Hasan, A. Shahriar, K.U. Jim, Water pollution in Bangladesh and its impact on public health, Heliyon. 5 (2019) e02145. doi:10.1016/j.heliyon.2019.e02145.

[45] S. Rasalingam, R. Peng, R.T. Koodali, 617405.Pdf, 2014 (2014).

[46] U. Tahir, A. Yasmin, U.H. Khan, Phytoremediation: Potential flora for synthetic dyestuff metabolism, J. King Saud Univ. - Sci. 28 (2016) 119–130. doi:10.1016/j.jksus.2015.05.009.

[47] G. Dong, Y. Zhang, Q. Pan, J. Qiu, A fantastic graphitic carbon nitride (g-C_3N_4)

material: Electronic structure, photocatalytic and photoelectronic properties, J. Photochem. Photobiol. C Photochem. Rev. 20 (2014) 33–50. doi:10.1016/j.jphotochemrev.2014.04.002.

[48] D.A. Yaseen, M. Scholz, Textile dye wastewater characteristics and constituents of synthetic effluents: a critical review, Springer Berlin Heidelberg, 2019. doi:10.1007/s13762-018-2130-z.

[49] T. Robinson, G. McMullan, R. Marchant, P. Nigam, Remediation of dyes in textile effluent: A critical review on current treatment technologies with a proposed alternative, Bioresour. Technol. 77 (2001) 247–255. doi:10.1016/S0960-8524(00)00080-8.

[50] G.S. Gupta, G. Prasad, V.N. Singh, Removal of chrome dye from aqueous solutions by mixed adsorbents: Fly ash and coal, Water Res. 24 (1990) 45–50. doi:10.1016/0043-1354(90)90063-C.

[51] N. Muhd Julkapli, S. Bagheri, S. Bee Abd Hamid, Recent advances in heterogeneous photocatalytic decolorization of synthetic dyes, Sci. World J. 2014 (2014) 25. doi:10.1155/2014/692307.

[52] Y. Fu, T. Viraraghavan, Fungal decolorization of dye wastewaters: A review, Bioresour. Technol. 79 (2001) 251–262. doi:10.1016/S0960-8524(01)00028-1.

[53] V.K. Gupta, S. Khamparia, I. Tyagi, D. Jaspal, A. Malviya, Decolorization of mixture of dyes: A critical review, Glob. J. Environ. Sci. Manag. Glob. J. Environ. Sci. Manag. 1 (2015) 71–94. doi:10.7508/gjesm.2015.01.007.

[54] Z. Aksu, Application of biosorption for the removal of organic pollutants: A review, Process Biochem. 40 (2005) 997–1026. doi:10.1016/j.procbio.2004.04.008.

[55] S. Sumathi, B.S. Manju, Uptake of reactive textile dyes by Aspergillus foetidus, Enzyme Microb. Technol. 27 (2000) 347–355. doi:10.1016/S0141-0229(00)00234-9.

[56] Z. Aksu, S. Tezer, Equilibrium and kinetic modelling of biosorption of Remazol black B by Rhizopus arrhizus in a batch system: Effect of temperature, Process Biochem. 36 (2000) 431–439. doi:10.1016/S0032-9592(00)00233-8.

[57] T. O'Mahony, E. Guibal, J.M. Tobin, Reactive dye biosorption by Rhizopus arrhizus biomass, Enzyme Microb. Technol. 31 (2002) 456–463. doi:10.1016/S0141-0229(02)00110-2.

[58] B. Aruna, R.S. L, E. Shiva, A. Srinu, P. Roja, D. Vijayalakshmi, D.V.R. Prasad, Research Article Biodecolorization of Anthraquinone Textile (Acid Blue 25) Dye By Klebsiella Sp, 6 (2015) 3216–3222.

[59] M. Auta, B.H. Hameed, Preparation of waste tea activated carbon using potassium acetate as an activating agent for adsorption of Acid Blue 25 dye, Chem. Eng. J. 171 (2011) 502–509. doi:10.1016/j.cej.2011.04.017.

[60] C.A. Hsu, T.N. Wen, Y.C. Su, Z.B. Jiang, C.W. Chen, L.F. Shyur, Biological degradation of anthroquinone and azo dyes by a novel laccase from Lentinus sp., Environ. Sci. Technol. 46 (2012) 5109–5117. doi:10.1021/es2047014.

[61] H. hong Li, Y. tao Wang, Y. Wang, H. xia Wang, K. kai Sun, Z. mei Lu, Bacterial degradation of anthraquinone dyes, J. Zhejiang Univ. Sci. B. 20 (2019) 528–540. doi:10.1631/jzus.B1900165.

[62] M.E. Malefane, U. Feleni, A.T. Kuvarega, Tetraphenylporphyrin/WO_3/exfoliated graphite nanocomposite for photocatalytic degradation of an acid dye under visible light irradiation, New J. Chem. 10 (2019) 1–6. doi:10.1039/c9nj02747e.

[63] S. Benkhaya, S. El Harfi, A. El Harfi, Classifications , properties and applications of textile dyes : A review, Appl. J. Environ. Sci. 3 (2018) 311–320.

[64] D. Chakrabortty, S. Sen Gupta, Photo-catalytic decolourisation of toxic dye with N-doped titania: A case study with Acid Blue 25, J. Environ. Sci. (China). 25 (2013) 1034–1043. doi:10.1016/S1001-0742(12)60108-9.

[65] T. Deblonde, C. Cossu-Leguille, P. Hartemann, Emerging pollutants in wastewater: A review of the literature, Int. J. Hyg. Environ. Health. 214 (2011) 442–448. doi:10.1016/j.ijheh.2011.08.002.

[66] M. Clara, G. Windhofer, W. Hartl, K. Braun, M. Simon, O. Gans, C. Scheffknecht, A. Chovanec, Occurrence of phthalates in surface runoff, untreated and treated wastewater and fate during wastewater treatment, Chemosphere. 78 (2010) 1078–1084.

doi:10.1016/j.chemosphere.2009.12.052.

[67] M. la Farré, S. Pérez, L. Kantiani, D. Barceló, Fate and toxicity of emerging pollutants, their metabolites and transformation products in the aquatic environment, TrAC - Trends Anal. Chem. 27 (2008) 991–1007. doi:10.1016/j.trac.2008.09.010.

[68] A. Jennifer, M.A. Abdallah, S. Harrad, Pharmaceuticals and personal care products (PPCPs) in the freshwater aquatic environment, Emerg. Contam. 3 (2017) 1–16. doi:10.1016/j.emcon.2016.12.004.

[69] S.R. Hughes, P. Kay, L.E. Brown, Global synthesis and critical evaluation of pharmaceutical data sets collected from river systems, Environ. Sci. Technol. 47 (2013) 661–677. doi:10.1021/es3030148.

[70] D. Ashton, M. Hilton, K. V. Thomas, Investigating the environmental transport of human pharmaceuticals to streams in the United Kingdom, Sci. Total Environ. 333 (2004) 167–184. doi:10.1016/j.scitotenv.2004.04.062.

[71] S. Wiandt, H.J. Poremski, Selection and prioritisation procedure of hazardous substances for the marine environment within Ospar/dynamic, Ecotoxicology. 11 (2002) 393–399. doi:10.1023/A:1020569608441.

[72] L. Lonappan, S.K. Brar, R.K. Das, M. Verma, R.Y. Surampalli, Diclofenac and its transformation products: Environmental occurrence and toxicity - A review, Environ. Int. 96 (2016) 127–138. doi:10.1016/j.envint.2016.09.014.

[73] Y. Zhang, S.U. Geißen, C. Gal, Carbamazepine and diclofenac: Removal in wastewater treatment plants and occurrence in water bodies, Chemosphere. 73 (2008) 1151–1161. doi:10.1016/j.chemosphere.2008.07.086.

[74] V. Acuña, A. Ginebreda, J.R. Mor, M. Petrovic, S. Sabater, J. Sumpter, D. Barceló, Balancing the health benefits and environmental risks of pharmaceuticals: Diclofenac as an example, Environ. Int. 85 (2015) 327–333. doi:10.1016/j.envint.2015.09.023.

[75] A.C. Johnson, E. Dumont, R.J. Williams, R. Oldenkamp, I. Cisowska, J.P. Sumpter, Do concentrations of ethinylestradiol, estradiol, and diclofenac in European rivers exceed proposed EU environmental quality standards?,

Environ. Sci. Technol. 47 (2013) 12297–12304. doi:10.1021/es4030035.

[76] A.Y. Shan, T.I.M. Ghazi, S.A. Rashid, Immobilisation of titanium dioxide onto supporting materials in heterogeneous photocatalysis: A review, Appl. Catal. A Gen. 389 (2010) 1–8. doi:10.1016/j.apcata.2010.08.053.

[77] Y. Mehmood, Index Academic Sciences Original Article development and validation of UV-Vis spectrophotometric method for the estimation of diclofenac sodium injections., Int. J. Pharm. Pract. Pharm. Sci. 2 (2015) 1–6.

[78] D. Chen, A.K. Ray, Photodegradation kinetics of 4-nitrophenol in TiO_2 suspension, Water Res. 32 (1998) 3223–3234. doi:10.1016/S0043-1354(98)00118-3.

[79] C. Martínez, M. Canle L., M.I. Fernández, J.A. Santaballa, J. Faria, Aqueous degradation of diclofenac by heterogeneous photocatalysis using nanostructured materials, Appl. Catal. B Environ. 107 (2011) 110–118. doi:10.1016/j.apcatb.2011.07.003.

[80] M. Letzel, G. Metzner, T. Letzel, Exposure assessment of the pharmaceutical diclofenac based on long-term measurements of the aquatic input, Environ. Int. 35 (2009) 363–368. doi:10.1016/j.envint.2008.09.002.

[81] C. Hao, R. Clement, P. Yang, Liquid chromatography-tandem mass spectrometry of bioactive pharmaceutical compounds in the aquatic environment-a decade's activities, Anal. Bioanal. Chem. 387 (2007) 1247–1257. doi:10.1007/s00216-006-0956-6.

[82] A.J. Sosiak, T. Hebben, A preliminary survey of pharmaceuticals and endocrine disrupting compounds in treated municipal wastewaters and receiving rivers of Alberta /, 2005. doi:10.5962/bhl.title.113982.

[83] M.J. Benotti, R.A. Trenholm, B.J. Vanderford, J.C. Holady, B.D. Stanford, S.A. Snyder, Pharmaceuticals and endocrine disrupting compounds in U.S. drinking water, Environ. Sci. Technol. 43 (2009) 597–603. doi:10.1021/es801845a.

[84] T. Heberer, Tracking persistent pharmaceutical residues from municipal sewage to drinking water, J. Hydrol. 266 (2002) 175–189. doi:10.1016/S0022-1694(02)00165-8.

[85] F.O. Agunbiade, B. Moodley, Occurrence and distribution pattern of acidic pharmaceuticals in surface water, wastewater, and sediment of the Msunduzi River, Kwazulu-Natal, South Africa, Environ. Toxicol. Chem. 35 (2016) 36–46. doi:10.1002/etc.3144.

[86] M.T. Amin, A.A. Alazba, U. Manzoor, A Review of Removal of Pollutants from Water / Wastewater Using Different Types of Nanomaterials, 2014 (2014).

[87] M.R. Servos, D.T. Bennie, B.K. Burnison, A. Jurkovic, R. McInnis, T. Neheli, A. Schnell, P. Seto, S.A. Smyth, T.A. Ternes, Distribution of estrogens, 17β-estradiol and estrone, in Canadian municipal wastewater treatment plants, Sci. Total Environ. 336 (2005) 155–170. doi:10.1016/j.scitotenv.2004.05.025.

[88] T. Urase, T. Kikuta, Separate estimation of adsorption and degradation of pharmaceutical substances and estrogens in the activated sludge process, Water Res. 39 (2005) 1289–1300. doi:10.1016/j.watres.2005.01.015.

[89] N. Vieno, T. Tuhkanen, L. Kronberg, Removal of pharmaceuticals in drinking water treatment: Effect of chemical coagulation, Environ. Technol. 27 (2006) 183–192. doi:10.1080/09593332708618632.

[90] P. Westerhoff, Y. Yoon, S. Snyder, E. Wert, Fate of endocrine-disruptor, pharmaceutical, and personal care product chemicals during simulated drinking water treatment processes, Environ. Sci. Technol. 39 (2005) 6649–6663. doi:10.1021/es0484799.

[91] M. Petrovic, A. Diaz, F. Ventura, D. Barceló, Occurrence and removal of estrogenic short-chain ethoxy nonylphenolic compounds and their halogenated derivatives during drinking water production, Environ. Sci. Technol. 37 (2003) 4442–4448. doi:10.1021/es034139w.

[92] G. Becher, Drinking Water Chlorination and Health, Acta Hydrochim. Hydrobiol. 27 (1999) 100–102. doi:10.1002/(sici)1521-401x(199902)27:2<100::aid-aheh100>3.3.co;2-1.

[93] N. Bolong, A.F. Ismail, M.R. Salim, T. Matsuura, A review of the effects of emerging contaminants in wastewater and options for their removal, Desalination. 239 (2009) 229–246. doi:10.1016/j.desal.2008.03.020.

[94] Y. Yoon, P. Westerhoff, S.A. Snyder, E.C. Wert, Nanofiltration and ultrafiltration of endocrine disrupting compounds, pharmaceuticals and personal care products, J. Memb. Sci. 270 (2006) 88–100. doi:10.1016/j.memsci.2005.06.045.

[95] L. Braeken, B. Bettens, K. Boussu, P. Van der Meeren, J. Cocquyt, J. Vermant, B. Van der Bruggen, Transport mechanisms of dissolved organic compounds in aqueous solution during nanofiltration, J. Memb. Sci. 279 (2006) 311–319. doi:10.1016/j.memsci.2005.12.024.

[96] J. Lu, T. Zhang, J. Ma, Z. Chen, Evaluation of disinfection by-products formation during chlorination and chloramination of dissolved natural organic matter fractions isolated from a filtered river water, J. Hazard. Mater. 162 (2009) 140–145. doi:10.1016/j.jhazmat.2008.05.058.

[97] M.N. Chong, B. Jin, C.W.K. Chow, C. Saint, Recent developments in photocatalytic water treatment technology: a review., Water Res. 44 (2010) 2997–3027. doi:10.1016/j.watres.2010.02.039.

[98] D.H. Bremner, R. Molina, F. Martínez, J.A. Melero, Y. Segura, Degradation of phenolic aqueous solutions by high frequency sono-Fenton systems (US-Fe_2O_3/SBA-15-H_2O_2), Appl. Catal. B Environ. 90 (2009) 380–388. doi:10.1016/j.apcatb.2009.03.028.

[99] G. Li, Z. Wang, M. Yu, Z. Quan, J. Lin, Fabrication and optical properties of core-shell structured spherical SiO_2@$GdVO_4$:Eu^{3+} phosphors via sol-gel process, J. Solid State Chem. 179 (2006) 2698–2706. doi:10.1016/j.jssc.2006.05.019.

[100] J. Zhang, G. Xiao, F.X. Xiao, B. Liu, Revisiting one-dimensional TiO_2 based hybrid heterostructures for heterogeneous photocatalysis: A critical review, Mater. Chem. Front. 1 (2017) 231–250. doi:10.1039/c6qm00141f.

[101] Y. Cui, In-situ synthesis of C_3N_4/CdS composites with enhanced photocatalytic properties, Cuihua Xuebao/Chinese J. Catal. 36 (2015) 372–379. doi:10.1016/S1872-2067(14)60237-0.

[102] V.S. Kosera, T.M. Cruz, E.S. Chaves, E.R.L. Tiburtius, Journal of

Photochemistry and Photobiology A : Chemistry Triclosan degradation by heterogeneous photocatalysis using ZnO immobilized in biopolymer as catalyst, "Journal Photochem. Photobiol. A Chem. 344 (2017) 184–191. doi:10.1016/j.jphotochem.2017.05.014.

[103] M.R. Hoffmann, S.T. Martin, W. Choi, D.W. Bahnemann, Environmental Applications of Semiconductor Photocatalysis, Chem. Rev. 95 (1995) 69–96. doi:10.1021/cr00033a004.

[104] J.-M. Herrmann, Water Treatment By Heterogeneous Photocatalysis, in: 1999: pp. 171–194. doi:10.1142/9781848160613_0009.

[105] U.I. Gaya, A.H. Abdullah, Heterogeneous photocatalytic degradation of organic contaminants over titanium dioxide: A review of fundamentals, progress and problems, J. Photochem. Photobiol. C Photochem. Rev. 9 (2008) 1–12. doi:10.1016/j.jphotochemrev.2007.12.003.

[106] M. Ni, M.K.H. Leung, D.Y.C. Leung, K. Sumathy, A review and recent developments in photocatalytic water-splitting using TiO_2 for hydrogen production, Renew. Sustain. Energy Rev. 11 (2007) 401–425. doi:10.1016/j.rser.2005.01.009.

[107] M. Yasmina, K. Mourad, S.H. Mohammed, C. Khaoula, Treatment heterogeneous photocatalysis; Factors influencing the photocatalytic degradation by TiO_2, Energy Procedia. 50 (2014) 559–566. doi:10.1016/j.egypro.2014.06.068.

[108] L. Cheng, Q. Xiang, Y. Liao, Cd based photocatalysis, Environmental Science, (2018) 4–7. doi:10.1039/c7ee03640j.

[109] M. Wongaree, S. Chiarakorn, S. Chuangchote, Photocatalytic Improvement under Visible Light in TiO_2 Nanoparticles by Carbon Nanotube Incorporation, 2015 (2015).

[110] R.S. Singh, V.K. Rangari, S. Sanagapalli, V. Jayaraman, S. Mahendra, V.P. Singh, Nano-structured CdTe, CdS and TiO_2 for thin film solar cell applications, Sol. Energy Mater. Sol. Cells. 82 (2004) 315–330. doi:10.1016/j.solmat.2004.02.006.

[111] S. Leong, A. Razmjou, K. Wang, K. Hapgood, X. Zhang, H. Wang, TiO_2 based photocatalytic membranes: A review, J. Memb. Sci. 472 (2014) 167–184. doi:10.1016/j.memsci.2014.08.016.

[112] Y. Yu, J.C. Yu, J.G. Yu, Y.C. Kwok, Y.K. Che, J.C. Zhao, L. Ding, W.K. Ge, P.K. Wong, Enhancement of photocatalytic activity of mesoporous TiO_2 by using carbon nanotubes, Appl. Catal. A Gen. 289 (2005) 186–196. doi:10.1016/j.apcata.2005.04.057.

[113] R. Abe, K. Sayama, H. Arakawa, Significant effect of iodide addition on water splitting into H_2 and O_2 over Pt-loaded TiO_2 photocatalyst: Suppression of backward reaction, Chem. Phys. Lett. 371 (2003) 360–364. doi:10.1016/S0009-2614(03)00252-5.

[114] S. Sakthivel, M. V. Shankar, M. Palanichamy, B. Arabindoo, D.W. Bahnemann, V. Murugesan, Enhancement of photocatalytic activity by metal deposition: Characterisation and photonic efficiency of Pt, Au and Pd deposited on TiO_2 catalyst, Water Res. 38 (2004) 3001–3008. doi:10.1016/j.watres.2004.04.046.

[115] E. Szabó-Bárdos, H. Czili, A. Horváth, Photocatalytic oxidation of oxalic acid enhanced by silver deposition on a TiO_2 surface, J. Photochem. Photobiol. A Chem. 154 (2003) 195–201. doi:10.1016/S1010-6030(02)00330-1.

[116] N.L. Wu, M.S. Lee, Enhanced TiO_2 photocatalysis by Cu in hydrogen production from aqueous methanol solution, Int. J. Hydrogen Energy. 29 (2004) 1601–1605. doi:10.1016/j.ijhydene.2004.02.013.

[117] F. Haque, T. Daeneke, K. Kalantar-zadeh, J.Z. Ou, Two-Dimensional Transition Metal Oxide and Chalcogenide-Based Photocatalysts, Nano-Micro Lett. 10 (2018) 1–27. doi:10.1007/s40820-017-0176-y.

[118] A.H. Reshak, S. Auluck, Electronic and optical properties of the 1T phases of TiS_2, $TiSe_2$, and $TiTe_2$, Phys. Rev. B - Condens. Matter Mater. Phys. 68 (2003) 1–7. doi:10.1103/PhysRevB.68.245113.

[119] J.A. Wilson, A.D. Yoffe, The transition metal dichalcogenides discussion and interpretation of the observed optical, electrical and structural properties, Adv. Phys. 18 (1969) 193–335. doi:10.1080/00018736900101307.

[120] L. Nie, Q. Zhang, Recent progress in crystalline metal chalcogenides as efficient photocatalysts for organic pollutant degradation, Inorg. Chem. Front. 4 (2017) 1953–1962. doi:10.1039/c7qi00651a.

[121] F. Li, X. Liu, Q. Zhang, T. Kong, H. Jin, Fabrication and photocatalytic property of CuO nanosheets via a facile solution route, Cryst. Res. Technol. 47 (2012) 1140–1147. doi:10.1002/crat.201200143.

[122] B. Peng, P.K. Ang, K.P. Loh, Two-dimensional dichalcogenides for light-harvesting applications, Nano Today. 10 (2015) 128–137. doi:10.1016/j.nantod.2015.01.007.

[123] D. Ke, S. Liu, K. Dai, J. Zhou, L. Zhang, T. Peng, CdS/regenerated cellulose nanocomposite films for highly efficient photocatalytic H_2 production under visible light irradiation, J. Phys. Chem. C. 113 (2009) 16021–16026. doi:10.1021/jp903378q.

[124] S. Xiong, B. Xi, Y. Qian, CdS hierarchical nanostructures with tunable morphologies: Preparation and photocatalytic properties, J. Phys. Chem. C. 114 (2010) 14029–14035. doi:10.1021/jp1049588.

[125] W.T. Yao, S.H. Yu, S.J. Liu, J.P. Chen, X.M. Liu, F.Q. Li, Architectural control syntheses of CdS and CdSe nanoflowers, branched nanowires, and nanotrees via a solvothermal approach in a mixed solution and their photocatalytic property, J. Phys. Chem. B. 110 (2006) 11704–11710. doi:10.1021/jp060164n.

[126] Q. Shen, J. Xue, A. Mi, H. Jia, X. Liu, B. Xu, The study on properties of CdS photocatalyst with different ratios of zinc-blende and wurtzite structure, RSC Adv. 3 (2013) 20930–20935. doi:10.1039/c3ra42179a.

[127] M. Liu, B. Wang, Y. Zheng, F. Xue, Y. Chen, L. Guo, Transformation of zincblende nanoparticles into wurtzite microrods by a dissolution-regrowth process: An intergrowth homojunction with enhanced photocatalytic activity, Catal. Sci. Technol. 6 (2016) 3371–3377. doi:10.1039/c6cy00298f.

[128] K. Wu, H. Zhu, T. Lian, Ultrafast Exciton Dynamics and Light-Driven H_2 Evolution in Colloidal Semiconductor Nanorods and Pt-Tipped Nanorods, Acc. Chem. Res. 48 (2015) 851–859. doi:10.1021/ar500398g.

[129] J. Yu, Y. Yu, P. Zhou, W. Xiao, B. Cheng, Morphology-dependent photocatalytic H_2-production activity of CdS, Appl. Catal. B Environ. 156–157 (2014) 184–191. doi:10.1016/j.apcatb.2014.03.013.

[130] B. Weng, S. Liu, N. Zhang, Z.R. Tang, Y.J. Xu, A simple yet efficient visible-light-driven CdS nanowires-carbon nanotube 1D-1D nanocomposite photocatalyst, J. Catal. 309 (2014) 146–155. doi:10.1016/j.jcat.2013.09.013.

[131] F. Caruso, X. Shi, R.A. Caruso, A. Susha, Hollow titania spheres from layered precursor deposition on sacrificial colloidal core particles, Adv. Mater. 13 (2001) 740–744. doi:10.1002/1521-4095(200105)13:10<740::AID-ADMA740>3.0.CO;2-6.

[132] C. Li, L. Han, R. Liu, H. Li, S. Zhang, G. Zhang, Controlled synthesis of CdS micro/nano leaves with (0001) facets exposed: Enhanced photocatalytic activity toward hydrogen evolution, J. Mater. Chem. 22 (2012) 23815–23820. doi:10.1039/c2jm35415b.

[133] T. Tsuzuki, P.G. McCormick, Synthesis of CdS quantum dots by mechanochemical reaction, Appl. Phys. A Mater. Sci. Process. 65 (1997) 607–609. doi:10.1007/s003390050629.

[134] A. Dumbrava, G. Prodan, D. Berger, M. Bica, Properties of PEG-capped CdS nanopowders synthesized under very mild conditions, Powder Technol. 270 (2015) 197–204. doi:10.1016/j.powtec.2014.10.012.

[135] A. Samadi-maybodi, F. Abbasi, R. Akhoondi, Aqueous synthesis and characterization of CdS quantum dots capped with some amino acids and investigations of their photocatalytic activities, Colloids Surfaces A Physicochem. Eng. Asp. 447 (2014) 111–119. doi:10.1016/j.colsurfa.2014.01.036.

[136] P. Chandran, P. Kumari, S. Sudheer Khan, Photocatalytic activation of CdS NPs under visible light for environmental cleanup and disinfection, Sol. Energy. 105 (2014) 542–547. doi:10.1016/j.solener.2014.04.028.

[137] M. Darwish, A. Mohammadi, N. Assi, Microwave-assisted polyol synthesis and characterization of pvp-capped cds nanoparticles for the photocatalytic

degradation of tartrazine, Mater. Res. Bull. 74 (2016) 387–396. doi:10.1016/j.materresbull.2015.11.002.

[138] R.A. Devi, M. Latha, S. Velumani, G. Oza, P. Reyes-Figueroa, M. Rohini, I.G. Becerril-Juarez, J.-H. Lee, J. Yi, Synthesis and Characterization of Cadmium Sulfide Nanoparticles by Chemical Precipitation Method, J. Nanosci. Nanotechnol. 15 (2015) 8434–8439. doi:10.1166/jnn.2015.11472.

[139] G.C. De, A.M. Roy, S.S. Bhattacharya, Photocatalytic production of hydrogen and concomitant cleavage of industrial waste hydrogen sulphide, Int. J. Hydrogen Energy. 20 (1995) 127–131. doi:10.1016/0360-3199(94)P3692-V.

[140] W. Li, D. Li, Z. Chen, H. Huang, M. Sun, Y. He, X. Fu, High-efficient degradation of dyes by ZnxCd1-xS solid solutions under visible light irradiation, J. Phys. Chem. C. 112 (2008) 14943–14947. doi:10.1021/jp8049075.

[141] F. Yang, N.N. Yan, S. Huang, Q. Sun, L.Z. Zhang, Y. Yu, Zn-doped CdS nanoarchitectures prepared by hydrothermal synthesis: Mechanism for enhanced photocatalytic activity and stability under visible light, J. Phys. Chem. C. 116 (2012) 9078–9084. doi:10.1021/jp300939q.

[142] T.K. Jana, A. Pal, K. Chatterjee, Self assembled flower like CdS-ZnO nanocomposite and its photo catalytic activity, J. Alloys Compd. 583 (2014) 510–515. doi:10.1016/j.jallcom.2013.08.184.

[143] D. Wu, F. Wang, Y. Tan, C. Li, Facile synthesis of NiS/CdS nanocomposites for photocatalytic degradation of quinoline under visible-light irradiation, RSC Adv. 6 (2016) 73522–73526. doi:10.1039/c6ra13439d.

[144] P. Nyamukamba, M.J. Moloto, H. Mungondori, Visible light-active CdS/TiO_2 hybrid nanoparticles immobilized on polyacrylonitrile membranes for the photodegradation of dyes in water, J. Nanotechnol. 2019 (2019). doi:10.1155/2019/5135618.

[145] S. Ma, J. Xie, J. Wen, K. He, X. Li, W. Liu, X. Zhang, Constructing 2D layered hybrid CdS nanosheets/MoS_2 heterojunctions for enhanced visible-light photocatalytic H_2 generation, Appl. Surf. Sci. 391 (2017) 580–591. doi:10.1016/j.apsusc.2016.07.067.

[146] Q. Cai, Z. Hu, Q. Zhang, B. Li, Z. Shen, Fullerene (C_{60})/CdS nanocomposite with enhanced photocatalytic activity and stability, Appl. Surf. Sci. 403 (2017) 151–158. doi:10.1016/j.apsusc.2017.01.135.

[147] K.A. Adegoke, M. Iqbal, H. Louis, O.S. Bello, Synthesis, characterization and application of CdS/ZnO nanorod heterostructure for the photodegradation of Rhodamine B dye, Mater. Sci. Energy Technol. 2 (2019) 329–336. doi:10.1016/j.mset.2019.02.008.

[148] S. Cao, J. Yu, G-C_3N_4-based photocatalysts for hydrogen generation, J. Phys. Chem. Lett. 5 (2014) 2101–2107. doi:10.1021/jz500546b.

[149] J. Wen, J. Xie, X. Chen, X. Li, A review on g-C_3N_4 -based photocatalysts, Appl. Surf. Sci. 391 (2017) 72–123. doi:10.1016/j.apsusc.2016.07.030.

[150] E.A. Weiss, Designing the surfaces of semiconductor quantum dots for colloidal photocatalysis, ACS Energy Lett. 2 (2017) 1005–1013. doi:10.1021/acsenergylett.7b00061.

[151] K.R. Reddy, C.V. Reddy, M.N. Nadagouda, N.P. Shetti, S. Jaesool, T.M. Aminabhavi, Polymeric graphitic carbon nitride (g-C_3N_4)-based semiconducting nanostructured materials: Synthesis methods, properties and photocatalytic applications, J. Environ. Manage. 238 (2019) 25–40. doi:10.1016/j.jenvman.2019.02.075.

[152] S. Wang, C. Li, T. Wang, P. Zhang, A. Li, J. Gong, Controllable synthesis of nanotube-type graphitic C_3N_4 and their visible-light photocatalytic and fluorescent properties, J. Mater. Chem. A. 2 (2014) 2885–2890. doi:10.1039/c3ta14576j.

[153] B. Weng, S. Liu, Z. Tang, Y. Xu, RSC Advances One-dimensional nanostructure based materials for versatile photocatalytic applications, (2014) 12685–12700. doi:10.1039/c3ra47910b.

[154] J. Zhang, Y. Chen, X. Wang, Two-dimensional covalent carbon nitride nanosheets: Synthesis, functionalization, and applications, Energy Environ. Sci. 8 (2015) 3092–3108. doi:10.1039/c5ee01895a.

[155] X. Bai, L. Wang, R. Zong, Y. Zhu, Photocatalytic activity enhanced via g-C_3N_4

nanoplates to nanorods, J. Phys. Chem. C. 117 (2013) 9952–9961. doi:10.1021/jp402062d.

[156] Q. Han, B. Wang, J. Gao, Z. Cheng, Y. Zhao, Z. Zhang, L. Qu, Atomically Thin Mesoporous Nanomesh of Graphitic C_3N_4 for High-Efficiency Photocatalytic Hydrogen Evolution, ACS Nano. 10 (2016) 2745–2751. doi:10.1021/acsnano.5b07831.

[157] X. Zhang, X. Xie, H. Wang, J. Zhang, B. Pan, Y. Xie, Enhanced photoresponsive ultrathin graphitic-phase C_3N_4 nanosheets for bioimaging, J. Am. Chem. Soc. 135 (2013) 18–21. doi:10.1021/ja308249k.

[158] J. Senker, K. Schwinghammer, B. V. Lotsch, C. Ziegler, M.B. Mesch, V. Duppel, Crystalline Carbon Nitride Nanosheets for Improved Visible-Light Hydrogen Evolution, J. Am. Chem. Soc. 136 (2014) 1730–1733. doi:10.1021/ja411321s.

[159] B. Luo, G. Liu, L. Wang, Recent advances in 2D materials for photocatalysis, Nanoscale. 8 (2016) 6904–6920. doi:10.1039/c6nr00546b.

[160] P. Niu, L. Zhang, G. Liu, H.M. Cheng, Graphene-like carbon nitride nanosheets for improved photocatalytic activities, Adv. Funct. Mater. 22 (2012) 4763–4770. doi:10.1002/adfm.201200922.

[161] Q. Liu, T. Chen, Y. Guo, Z. Zhang, X. Fang, Ultrathin g-C_3N_4 nanosheets coupled with carbon nanodots as 2D/0D composites for efficient photocatalytic H2 evolution, Appl. Catal. B Environ. 193 (2016) 248–258. doi:10.1016/j.apcatb.2016.04.034.

[162] Y. Xu, S.P. Gao, Band gap of C_3N_4 in the GW approximation, Int. J. Hydrogen Energy. 37 (2012) 11072–11080. doi:10.1016/j.ijhydene.2012.04.138.

[163] K. Maeda, X. Wang, Y. Nishihara, D. Lu, M. Antonietti, K. Domen, Photocatalytic activities of graphitic carbon nitride powder for water reduction and oxidation under visible light, J. Phys. Chem. C. 113 (2009) 4940–4947. doi:10.1021/jp809119m.

[164] A.H. Reshak, AA- and ABA-stacked carbon nitride (C_3N_4): Novel photocatalytic water splitting solar-to-hydrogen energy conversion, Phys. Chem. Chem.

Phys. 20 (2018) 22972–22979. doi:10.1039/c8cp02898b.

[165] A.Y. Liu, M.L. Cohen, Prediction of new low compressibility solids, Science (80-.). 245 (1989) 841–842. doi:10.1126/science.245.4920.841.

[166] B. Jürgens, E. Irran, J. Senker, P. Kroll, H. Müller, W. Schnick, Melem (2,5,8-triamino-tri-s-triazine), an important intermediate during condensation of melamine rings to graphitic carbon nitride: Synthesis, structure determination by x-ray powder diffractometry, solid-state NMR, and theoretical studies, J. Am. Chem. Soc. 125 (2003) 10288–10300. doi:10.1021/ja0357689.

[167] J. Sehnert, K. Baerwinkel, J. Senker, Ab initio calculation of solid-state NMR spectra for different triazine and heptazine based structure proposals of g-C3N4, J. Phys. Chem. B. 111 (2007) 10671–10680. doi:10.1021/jp072001k.

[168] A. Thomas, A. Fischer, F. Goettmann, M. Antonietti, J.O. Müller, R. Schlögl, J.M. Carlsson, Graphitic carbon nitride materials: Variation of structure and morphology and their use as metal-free catalysts, J. Mater. Chem. 18 (2008) 4893–4908. doi:10.1039/b800274f.

[169] Y. Wang, J. Hong, W. Zhang, R. Xu, Carbon nitride nanosheets for photocatalytic hydrogen evolution: Remarkably enhanced activity by dye sensitization, Catal. Sci. Technol. 3 (2013) 1703–1711. doi:10.1039/c3cy20836b.

[170] H. Luo, Z. Zeng, G. Zeng, C. Zhang, R. Xiao, C. Zhou, H. Wang, Y. Zhou, S. Tian, Recent progress on metal-organic frameworks based- and derived-photocatalysts for water splitting, Chem. Eng. J. (2019) 123196. doi:10.1016/j.cej.2019.123196.

[171] D. Zheng, C. Pang, Y. Liu, X. Wang, Shell-engineering of hollow g-C_3N_4 nanospheres via copolymerization for photocatalytic hydrogen evolution , Chem. Commun. 51 (2015) 9706–9709. doi:10.1039/c5cc03143e.

[172] S.W. Bian, Z. Ma, W.G. Song, Preparation and characterization of carbon nitride nanotubes and their applications as catalyst supporter, J. Phys. Chem. C. 113 (2009) 8668–8672. doi:10.1021/jp810630k.

[173] L. Xu, J. Xia, L. Wang, H. Ji, J. Qian, H. Xu, K. Wang, H. Li, Graphitic carbon

nitride nanorods for photoelectrochemical sensing of trace copper(II) ions, Eur. J. Inorg. Chem. (2014) 3665–3673. doi:10.1002/ejic.201402051.

[174] S. Hu, R. Jin, G. Lu, D. Liu, J. Gui, The properties and photocatalytic performance comparison of Fe^{3+}-doped g-C_3N_4 and Fe_2O_3/g-C_3N_4 composite catalysts, RSC Adv. 4 (2014) 24863–24869. doi:10.1039/c4ra03290j.

[175] Y. Wang, Y. Wang, Y. Li, H. Shi, Y. Xu, H. Qin, X. Li, Y. Zuo, S. Kang, L. Cui, Simple synthesis of Zr-doped graphitic carbon nitride towards enhanced photocatalytic performance under simulated solar light irradiation, Catal. Commun. 72 (2015) 24–28. doi:10.1016/j.catcom.2015.08.022.

[176] P. Fageria, R. Nazir, S. Gangopadhyay, H.C. Barshilia, S. Pande, Graphitic-carbon nitride support for the synthesis of shape-dependent ZnO and their application in visible light photocatalysts, RSC Adv. 5 (2015) 80397–80409. doi:10.1039/c5ra12463h.

[177] H. Yu, F. Chen, F. Chen, X. Wang, Applied Surface Science In situ self-transformation synthesis of g-C_3N_4 -modified CdS heterostructure with enhanced photocatalytic activity, Appl. Surf. Sci. 358 (2015) 385–392. doi:10.1016/j.apsusc.2015.06.074.

[178] F. Jiang, T. Yan, H. Chen, A. Sun, C. Xu, X. Wang, Applied Surface Science A g-C_3N_4 – CdS composite catalyst with high visible-light-driven catalytic activity and photostability for methylene blue degradation, Appl. Surf. Sci. 295 (2014) 164–172. doi:10.1016/j.apsusc.2014.01.022.

[179] Y. Guo, J. Wang, Z. Tao, F. Dong, K. Wang, X. Ma, P. Yang, P. Hu, Y. Xu, L. Yang, Facile synthesis of mesoporous CdS nanospheres and their application in photocatalytic degradation and adsorption of organic dyes, CrystEngComm. 14 (2012) 1185–1188. doi:10.1039/c2ce06172d.

[180] H.M. Xiong, D.G. Shchukin, H. Möhwald, Y. Xu, Y.Y. Xia, Sonochemical synthesis of highly luminescent zinc oxide nanoparticles doped with magnesium(II), Angew. Chemie - Int. Ed. 48 (2009) 2727–2731. doi:10.1002/anie.200805590.

[181] Z.R. Tang, X. Yin, Y. Zhang, Y.J. Xu, Synthesis of titanate nanotube-CdS

nanocomposites with enhanced visible light photocatalytic activity, Inorg. Chem. 52 (2013) 11758–11766. doi:10.1021/ic4010483.

[182] Y. Li, L. Tang, S. Peng, Z. Li, G. Lu, Phosphate-assisted hydrothermal synthesis of hexagonal CdS for efficient photocatalytic hydrogen evolution, CrystEngComm. 14 (2012) 6974–6982. doi:10.1039/c2ce25838b.

[183] M. Salavati-Niasari, M.R. Loghman-Estarki, F. Davar, Controllable synthesis of nanocrystalline CdS with different morphologies by hydrothermal process in the presence of thioglycolic acid, Chem. Eng. J. 145 (2008) 346–350. doi:10.1016/j.cej.2008.08.040.

[184] L.R. Zou, G.F. Huang, D.F. Li, J.H. Liu, A.L. Pan, W.Q. Huang, A facile and rapid route for synthesis of g-C_3N_4 nanosheets with high adsorption capacity and photocatalytic activity, RSC Adv. 6 (2016) 86688–86694. doi:10.1039/c6ra20514c.

[185] N. Chidhambaram, K. Ravichandran, Fabrication of ZnO/g-C_3N_4 nanocomposites for enhanced visible light driven photocatalytic activity Fabrication of ZnO/g-C_3N_4 nanocomposites for enhanced visible light driven photocatalytic activity, (n.d.).

[186] M. Iqbal, A. Ali, N.A. Nahyoon, A. Majeed, R. Pothu, S. Phulpoto, K.H. Thebo, Photocatalytic degradation of organic pollutant with nanosized cadmium sulfide, Mater. Sci. Energy Technol. 2 (2018) 41–45. doi:10.1016/j.mset.2018.09.002.

[187] S. Vadivel, D. Maruthamani, B. Paul, S.S. Dhar, K. Selvam, Facile synthesis of novel $CaFe_2O_4$/g-C_3N_4 nanocomposites for degradation of methylene blue under visible-light irradiation Journal of Colloid and Interface Science Facile synthesis of novel $CaFe_2O_4$/g-C_3N_4 nanocomposites for degradation of methyle, J. Colloid Interface Sci. 480 (2016) 126–136. doi:10.1016/j.jcis.2016.07.012.

[188] Z.X. Han, Z. Zhu, D.D. Wu, J. Wu, Y.R. Liu, Adsorption Kinetics and Thermodynamics of Acid Blue 25 and methylene blue dye solutions on natural sepiolite, Synth. React. Inorganic, Met. Nano-Metal Chem. 44 (2014) 140–147. doi:10.1080/15533174.2013.770755.

[189] S. Kaur, A brief review on photocatalytic activity of ZnS and CQDs nanoparticles, Int. J. Eng. Appl. Sci. Technol. 2 (2017) 75–82. http://www.ijeast.com.

[190] M. Joshi, A. Bhattacharyya, S.W. Ali, Characterization techniques for nanotechnology applications in textiles, Indian J. Fibre Text. Res. 33 (2008) 304–317.

[191] R. Kohli, Methods for Monitoring and Measuring Cleanliness of Surfaces, in: Dev. Surf. Contam. Clean. - Detect. Charact. Anal. Contam., Elsevier, 2012: pp. 107–178. doi:10.1016/B978-1-4377-7883-0.00003-1.

[192] G. Zhang, Master Thesis, University of Illinois at Urbana-Champaign, 2013, 2013.

[193] P.J. Mafa, A.T. Kuvarega, B.B. Mamba, B. Ntsendwana, Photoelectrocatalytic degradation of sulfamethoxazole on g-C 3 N 4 /BiOI/EG p-n heterojunction photoanode under visible light irradiation, Appl. Surf. Sci. 483 (2019) 506–520. doi:10.1016/j.apsusc.2019.03.281.

[194] M. Izadifard, G. Achari, C.H. Langford, Application of photocatalysts and LED light sources in drinking water treatment, Catalysts. 3 (2013) 726–743. doi:10.3390/catal3030726.

[195] C.G. Young, an Inductively Coupled Plasma Atomic Emission Spectrometer for the Detection of Nonmetals in the Vacuum Ultraviolet, 2011.

[196] A.M. Sabir, M. Moloy, P.S. Bhasin, Hplc Method Development and Validation: a Review, Int. Res. J. Pharm. 4 (2016) 39–46. doi:10.7897/2230-8407.04407.

[197] F. Jiang, T. Yan, H. Chen, A. Sun, C. Xu, X. Wang, A g-C_3N_4-CdS composite catalyst with high visible-light-driven catalytic activity and photostability for methylene blue degradation, Appl. Surf. Sci. 295 (2014) 164–172. doi:10.1016/j.apsusc.2014.01.022.

[198] Z. Zhang, J. Huang, M. Zhang, Q. Yuan, B. Dong, Ultrathin hexagonal SnS2 nanosheets coupled with g-C_3N_4 nanosheets as 2D/2D heterojunction photocatalysts toward high photocatalytic activity, Appl. Catal. B Environ. 163 (2015) 298–305. doi:10.1016/j.apcatb.2014.08.013.

[199] A. Akhundi, A. Habibi-yangjeh, Novel magnetically separable g-C_3N_4/AgBr/Fe_3O_4 nanocomposites as visible-light-driven photocatalysts with highly enhanced activities, Ceram. Int. 41 (2015) 5634–5643. doi:10.1016/j.ceramint.2014.12.145.

[200] L.J. Cote, F. Kim, J. Huang, Langmuir-blodgett assembly of graphite oxide single layers, J. Am. Chem. Soc. 131 (2009) 1043–1049. doi:10.1021/ja806262m.

[201] Z. Zhou, J. Wang, J. Yu, Y. Shen, Y. Li, A. Liu, S. Liu, Y. Zhang, Dissolution and liquid crystals phase of 2D polymeric carbon nitride, J. Am. Chem. Soc. 137 (2015) 2179–2182. doi:10.1021/ja512179x.

[202] J. Xu, L. Zhang, R. Shi, Y. Zhu, Chemical exfoliation of graphitic carbon nitride for efficient heterogeneous photocatalysis, J. Mater. Chem. A. 1 (2013) 14766–14772. doi:10.1039/c3ta13188b.

[203] F. Dong, Z. Wang, Y. Sun, W.K. Ho, H. Zhang, Engineering the nanoarchitecture and texture of polymeric carbon nitride semiconductor for enhanced visible light photocatalytic activity, J. Colloid Interface Sci. 401 (2013) 70–79. doi:10.1016/j.jcis.2013.03.034.

[204] C. Li, Z. Sun, W. Huang, S. Zheng, Facile synthesis of g-C_3N_4/montmorillonite composite with enhanced visible light photodegradation of rhodamine B and tetracycline, J. Taiwan Inst. Chem. Eng. 66 (2016) 363–371. doi:10.1016/j.jtice.2016.06.014.

[205] J. Tong, L. Zhang, F. Li, K. Wang, L. Han, S. Cao, Rapid and high-yield production of g-C_3N_4 nanosheets via chemical exfoliation for photocatalytic H2 evolution, RSC Adv. 5 (2015) 88149–88153. doi:10.1039/c5ra16988g.

[206] J. Zhu, P. Xiao, H. Li, S.A.C. Carabineiro, Graphitic carbon nitride: Synthesis, properties, and applications in catalysis, ACS Appl. Mater. Interfaces. 6 (2014) 16449–16465. doi:10.1021/am502925j.

[207] Y. Chen, X. Wang, Template-Free Synthesis of Hollow G‑C_3N_4 Polymer with Vesicle Structure for Enhanced Photocatalytic Water Splitting, (2018). doi:10.1021/acs.jpcc.7b12496.

[208] H.B. Tao, H. Bin Yang, J. Chen, J. Miao, B. Liu, Biomolecule-assisted synthesis of carbon nitride and sulfur-doped carbon nitride heterojunction nanosheets: An efficient heterojunction photocatalyst for photoelectrochemical applications, Beilstein J. Nanotechnol. 5 (2014) 770–777. doi:10.3762/bjnano.5.89.

[209] J. Tong, L. Zhang, F. Li, K. Wang, L. Han, S. Cao, Rapid and high-yield production of g-C_3N_4 nanosheets via chemical exfoliation for photocatalytic H_2 evolution, RSC Adv. 5 (2015) 88149–88153. doi:10.1039/c5ra16988g.

[210] S. Asadzadeh-khaneghah, A. Habibi-yangjeh, S. Vadivel, Journal of the Taiwan Institute of Chemical Engineers Fabrication of novel g-C_3N_4 nanosheet / carbon dots / $Ag_6Si_2O_7$ nanocomposites with high stability and enhanced visible-light photocatalytic activity, J. Taiwan Inst. Chem. Eng. 103 (2019) 94–109. doi:10.1016/j.jtice.2019.07.018.

[211] G. Mamba, A.K. Mishra, Applied Catalysis B : Environmental Graphitic carbon nitride (g-C_3N_4) nanocomposites : A new and exciting generation of visible light driven photocatalysts for environmental pollution remediation, "Applied Catal. B, Environ. 198 (2016) 347–377. doi:10.1016/j.apcatb.2016.05.052.

[212] J. Jin, J. Yu, G. Liu, P.K. Wong, Single crystal CdS nanowires with high visible-light photocatalytic H_2-production performance, J. Mater. Chem. A. 1 (2013) 10927–10934. doi:10.1039/c3ta12301d.

[213] S. Rengaraj, A. Ferancova, S.H. Jee, S. Venkataraj, Y. Kim, J. Labuda, M. Sillanpää, Physical and electrochemical characterization of CdS hollow microspheres prepared by a novel template free solution phase method, Electrochim. Acta. 56 (2010) 501–509. doi:10.1016/j.electacta.2010.09.019.

[214] J. Fu, B. Chang, Y. Tian, F. Xi, X. Dong, Novel C_3N_4-CdS composite photocatalysts with organic-inorganic heterojunctions: In situ synthesis, exceptional activity, high stability and photocatalytic mechanism, J. Mater. Chem. A. 1 (2013) 3083–3090. doi:10.1039/c2ta00672c.

[215] Q. Li, B. Guo, J. Yu, J. Ran, B. Zhang, H. Yan, J.R. Gong, Highly efficient visible-light-driven photocatalytic hydrogen production of CdS-cluster-decorated graphene nanosheets, J. Am. Chem. Soc. 133 (2011) 10878–

10884. doi:10.1021/ja2025454.

[216] V. Mohanraj, R. Jayaprakash, R. Robert, J. Balavijayalakshmi, S. Gopi, Effect of particle size on optical and electrical properties in mixed CdS and NiS nanoparticles synthesis by ultrasonic wave irradiation method, Mater. Sci. Semicond. Process. 56 (2016) 394–402. doi:10.1016/j.mssp.2016.08.014.

[217] N.H. Patel, M.P. Deshpande, S.H. Chaki, H.R. Keharia, Tuning of optical, thermal and antimicrobial capabilities of CdS nanoparticles with incorporated Mn prepared by chemical method, J. Mater. Sci. Mater. Electron. 28 (2017) 10866–10876. doi:10.1007/s10854-017-6865-y.

[218] A. Modwi, M.A. Ghanem, A.M. Al-Mayouf, A. Houas, Lowering energy band gap and enhancing photocatalytic properties of Cu/ZnO composite decorated by transition metals, J. Mol. Struct. 1173 (2018) 1–6. doi:10.1016/j.molstruc.2018.06.082.

[219] Q. Tang, C. Zhou, X. Yuan, Q. Jing, Y. Mu, A. Du, Facile Synthesis of g-C_3N_4 Nanosheets/ZnO Nanocomposites with Enhanced Photocatalytic Activity in Reduction of Aqueous Chromium(VI) under Visible Light, Nanomaterials. 6 (2016) 173. doi:10.3390/nano6090173.

[220] D. Wang, Z. Xu, Q. Luo, X. Li, J. An, R. Yin, C. Bao, Preparation and visible-light photocatalytic performances of g-C_3N_4 surface hybridized with a small amount of CdS nanoparticles, J. Mater. Sci. 51 (2016) 893–902. doi:10.1007/s10853-015-9417-y.

[221] A. Kumar, A Review on the Factors Affecting the Photocatalytic Degradation of Hazardous Materials, Mater. Sci. Eng. Int. J. 1 (2017) 1–10. doi:10.15406/mseij.2017.01.00018.

[222] S. Talebi, N. Chaibakhsh, Z. Moradi-Shoeili, Application of nanoscale ZnS/TiO_2 composite for optimized photocatalytic decolorization of a textile dye, J. Appl. Res. Technol. 15 (2017) 378–385. doi:10.1016/j.jart.2017.03.007.

[223] Y.S. Al-Degs, M.I. El-Barghouthi, A.H. El-Sheikh, G.M. Walker, Effect of solution pH, ionic strength, and temperature on adsorption behavior of reactive dyes on activated carbon, Dye. Pigment. 77 (2008) 16–23.

doi:10.1016/j.dyepig.2007.03.001.

[224] E.T. Helmy, A. El Nemr, M. Mousa, E. Arafa, S. Eldafrawy, Photocatalytic degradation of organic dyes pollutants in the industrial textile wastewater by using synthesized TiO_2, C-doped TiO_2, S-doped TiO_2 and C,S co-doped TiO_2 nanoparticles, J. Water Environ. Nanotechnol. 3 (2018) 116–127. doi:10.22090/JWENT.2018.02.003.

[225] E. Mugunthan, M.B. Saidutta, P.E. Jagadeeshbabu, Visible light assisted photocatalytic degradation of diclofenac using TiO_2-WO_3 mixed oxide catalysts, Environ. Nanotechnology, Monit. Manag. 10 (2018) 322–330. doi:10.1016/j.enmm.2018.07.012.

[226] S. Iguchi, K. Teramura, S. Hosokawa, T. Tanaka, Effect of the chloride ion as a hole scavenger on the photocatalytic conversion of CO_2 in an aqueous solution over Ni-Al layered double hydroxides, Phys. Chem. Chem. Phys. 17 (2015) 17995–18003. doi:10.1039/c5cp02724a.

[227] L. Das, S.K. Barodia, S. Sengupta, J.K. Basu, Aqueous degradation kinetics of pharmaceutical drug diclofenac by photocatalysis using nanostructured titania–zirconia composite catalyst, Int. J. Environ. Sci. Technol. 12 (2015) 317–326. doi:10.1007/s13762-013-0466-y.

[228] J.M. Monteagudo, H. El-taliawy, A. Durán, G. Caro, K. Bester, Sono-activated persulfate oxidation of diclofenac: Degradation, kinetics, pathway and contribution of the different radicals involved, J. Hazard. Mater. 357 (2018) 457–465. doi:10.1016/j.jhazmat.2018.06.031.

[229] T. Huang, G. Zhang, S. Chong, Y. Liu, N. Zhang, S. Fang, J. Zhu, Effects and mechanism of diclofenac degradation in aqueous solution by US/Zn0, Ultrason. Sonochem. 37 (2017) 676–685. doi:10.1016/j.ultsonch.2017.02.032.

[230] M. V. Bagal, P.R. Gogate, Degradation of diclofenac sodium using combined processes based on hydrodynamic cavitation and heterogeneous photocatalysis, Ultrason. Sonochem. 21 (2014) 1035–1043. doi:10.1016/j.ultsonch.2013.10.020.

[231] P. Sathishkumar, R.A.A. Meena, T. Palanisami, V. Ashokkumar, T. Palvannan,

F.L. Gu, Occurrence, interactive effects and ecological risk of diclofenac in environmental compartments and biota - a review, Sci. Total Environ. 698 (2020) 134057. doi:10.1016/j.scitotenv.2019.134057.

[232] R.R. Giri, H. Ozaki, S. Ota, R. Takanami, S. Taniguchi, Degradation of common pharmaceuticals and personal care products in mixed solutions by advanced oxidation techniques, Int. J. Environ. Sci. Tech. 7 (2010) 251–260. doi:10.1007/BF03326135.

[233] S. Sébastien, Les soignants face à la mort, Rev. Infirm. 1 (2012) 39–41.

[234] H. Xu, L. Wu, L. Jin, K. Wu, Combination Mechanism and Enhanced Visible-Light Photocatalytic Activity and Stability of CdS/g-C_3N_4 Heterojunctions, J. Mater. Sci. Technol. 33 (2017) 30–38. doi:10.1016/j.jmst.2016.04.008.

[235] I.W. As, M.C. Level, P.H. Effects, T. Methods, I. Exchange, R. Osmosis, WQA Technical Fact Sheet: Cadmium health effects treatment methods Residential Point-of-Entry Point-of-Use, 2013. http://www.epa.gov/safewater/pdfs/factsheets/ioc/cadmium.pdf.

CHAPTER 7
CONCLSUION AND RECOMEMDATIONS

7.1 Conclusion

This study successfully set the objectives and the following conclusions be drawn from the results that come from this work.

- The g-C_3N_4 nanosheets were successfully prepared via chemical exfoliation method. CdS microspheres were successfully synthesized using the hydrothermal method and the Cd/g-C_3N_4 heterojunction nanocomposite was successfully coupled using the *in-situ* hydrothermal method.
- The SEM, TEM and EDS confirmed the synthesis of the nanosheets and the nanoparticles. They also confirmed successful coupling of CdS and CNS.
- The XRD analysis confirmed no change in the crystallinity of CN after chemical exfoliation. The slight increase in the highest peak intensity of CdS (27 ^oC), confirmed the presence of both CNS and CdS thus successful formation of CNS/CdS nanocomposite, which resulted in the increase in surface area of CdS (1.11 m^2g) and the nanocomposite (10% CNS/CdS 4.37 m^2g).
- UV-Vis and PL analysis confirmed that CNS improved that optical properties of CdS confirmed by the red shift in the visible light absorption.
- The photocatalyst with 10% CNS/CdS exhibited the highest photodegradation efficiency achieving 99.3% removal of 20 ppm AB-25 at pH 5.
- The 10% CNS/CdS was used for photodegradation of DFC and 65% removal of DFC was achieved at pH 5.
- In a sample solution containing the mixture of AB-25 and DFC, the catalyst was more efficient in dye removal than it was for DFC. This confirmed that DFC is harder to degrade in a mixture because of its size which may hinder favourable adsorption on the catalyst surface.

Recommendations

- The photodegradation of AB-25 was a success with respect to the UV-Vis analysis. But it is recommended that TOC is used after degradation of the

samples to determine the total organic carbon of the pollutants and determine extend of the degradation.

- The CNS/CdS nanocomposites should be used on other pollutants to evaluate how viable the material is in photodegradation of other pollutants.
- It is also recommended to test the photocatalytic efficacy of CNS/CdS nanocomposite for photocatalytic degradation of real waste water.